

iscte

INSTITUTO
UNIVERSITÁRIO
DE LISBOA

Exploring ILP and heuristic formulations for planning multiband optical networks

Margarida Isabel Carreto Vaz

Master degree in Telecommunications and Computer Engineering,

Supervisor:

PhD, Luís Gonçalo Lecoq Vences e Costa Cancela, Assistant Professor
Iscte-Instituto Universitário de Lisboa

Co-Supervisor:

PhD, João Lopes Rebola, Associate Professor
Iscte-Instituto Universitário de Lisboa

November, 2022



TECNOLOGIAS
E ARQUITETURA

Department of Information Science and Technology

Exploring ILP and heuristic formulations for planning multiband optical networks

Margarida Isabel Carreto Vaz

Master degree in Telecommunications and Computer Engineering,

Supervisor:

PhD, Luís Gonçalo Lecoq Vences e Costa Cancela, Assistant Professor
Iscte-Instituto Universitário de Lisboa

Co-Supervisor:

PhD, João Lopes Rebola, Associate Professor
Iscte-Instituto Universitário de Lisboa

November, 2022

Família

Acknowledgment

I am so thankful to Iscte-Instituto Universitário de Lisboa, for all the experiences and the knowledge I earned this past five years, and for making them much more enjoyable. I am also grateful to all the teachers, staff, and colleges that were always ready to help. Special thanks to the Instituto de Telecomunicações for the support to complete this dissertation. I would like to express my deepest gratitude to my supervisors Professor Luís Cancela and Professor João Rebola for the constant support, guidance, and time throughout all these months, and without whom I would not have been able to complete this dissertation.

I would like to thank my parents and friends for being supportive, patient, and for the constant encouragement throughout my years of studies and during this work. Lastly, I'd like to mention my brother for always assisting me in my studies.

Resumo

Para responder ao crescimento do número de pedidos de tráfego nas atuais redes de telecomunicações óticas, são necessárias soluções como a multibanda e grelha flexível para melhorar a eficiência na utilização do espectro e a capacidade de transmissão. Esta dissertação foca-se no planeamento do encaminhamento e da atribuição de comprimentos de onda (RWA) em redes multibanda utilizando soluções heurísticas e de programação inteira linear (ILP), para otimizar a alocação de espectro.

Desenvolveram-se ferramentas de planeamento de redes multibanda C+L para resolver o problema RWA em redes estáticas, utilizando grelhas flexíveis e fixas, explorando diferentes métricas de encaminhamento, como a distância e relação sinal-ruído ótica. Primeiro, comparou-se o desempenho de ferramentas RWA, uma heurística e outra ILP numa grelha fixa, em relação ao número de comprimentos de onda e tempo de computação, para diferentes topologias de rede. Depois, adaptou-se a ferramenta RWA heurística para suportar a grelha flexível, considerando, as limitações da camada física, para resolver problemas de encaminhamento, atribuição de formato de modulação e espectro (RMSA).

Concluiu-se que o RWA ILP atinge o número ótimo de comprimentos de onda, quando um pedido tem vários caminhos candidatos, contudo requer mais tempo de computação que a ferramenta heurística. Nos problemas RMSA, o número de intervalos de frequência (FSs) atribuídos depende da taxa de erro de bit (BER). Em redes com ligações mais curtas, são necessários mais FSs com a diminuição da BER. As redes com ligações mais longas requerem menos FSs com a diminuição da BER, pois os pedidos bloqueados aumentam.

Palavras-Chave: Limitações da camada física; programação inteira linear; encaminhamento, atribuição de formato de modulação e espectro; transmissão multibanda; planeamento de redes óticas.

Abstract

To keep up with the growth in traffic demands in nowadays optical telecommunications networks, solutions such as multiband and flexible grid are needed to improve spectrum efficiency and transmission capacity. This dissertation focuses on planning the routing and wavelength assignment (RWA) in multiband networks using both heuristic and integer linear programming (ILP) solutions to optimize the spectrum allocation.

We develop C+L multiband network planning tools to solve the RWA problem in static networks, using flexible and fixed grids, exploring different routing metrics, such as distance and optical signal-to-noise ratio. First, we compare the performance of two RWA tools, a heuristic and an ILP, considering a fixed grid, in terms of the number of wavelengths and computation time, for different network topologies. Then, we extend our RWA heuristic tool to deal with the flexible grid and be aware of the physical layer impairments, to be capable of solving routing, modulation format and spectrum assignment (RMSA) problems.

We have concluded that our RWA ILP achieves the optimum number of wavelengths, when it uses more than one candidate path per demand but requires more computing time than the RWA heuristic tool. In RMSA problems, the number of allocated frequency slots (FSs) is dependent on the bit error rate (BER). Networks with shorter links require more FSs as the BER decreases. Networks with longer links require less FSs as the BER decreases, since the blocked demands increase.

Keywords: Physical layer impairments; integer linear programming; routing, modulation format and spectrum assignment; multiband transmission; optical networks planning.

Contents

Acknowledgment	iii
Resumo	v
Abstract	vii
List of Figures	xi
List of Tables	xiii
List of Acronyms	xvii
List of Symbols	xix
Chapter 1. Introduction	1
1.1. Motivation and context	1
1.2. Goals	2
1.3. Dissertation organization	2
1.4. Main contributions	3
Chapter 2. A Literature Review on ILP and Heuristic Algorithms for Solving the RWA Problem	5
2.1. Introduction	5
2.2. Integer Linear Programming formulations	5
2.2.1. Link-Path formulation	5
2.2.2. Node-Link formulation	13
2.2.3. Restoration design problem	17
2.2.4. RWA problem	21
2.3. Heuristic algorithms	29
2.3.1. Routing algorithms	29
2.3.2. Wavelength assignment algorithms	30
2.4. Heuristic algorithms and ILP formulations applied in a real network scenario	31
2.5. Conclusion	33
Chapter 3. Physical Layer Impairments in C+L Multiband Optical Networks	35
3.1. Introduction	35
3.2. C+L multiband spectrum	35
3.3. ASE noise accumulation	36
3.4. Nonlinear interference and stimulated Raman scattering	41
3.5. Other physical layer impairments	49
3.6. Conclusion	51

Contents

Chapter 4. C+L Multiband Network Design Considering Physical Layer Impairments	53
4.1. Introduction	53
4.2. RWA problem with ILP and heuristic solutions	53
4.3. Multiband optical network simulator	57
4.4. Results and discussion	59
4.5. Conclusion	68
Chapter 5. Conclusions and Future Work	69
5.1. Final conclusions	69
5.2. Future work	70
References	71
Appendix A. Matlab scripts used in Chapter 2	75
A.1. Example 1	75
A.2. Example 3	76
A.3. Example 4	76
A.4. Example 7	77
A.5. Examples 8 and 9	79
A.6. Example 10	82
A.7. Examples 11 and 12	84
A.8. Example 13	87
A.9. ILP formulations applied in the portuguese backbone networked	90
Appendix B. OSNR path calculation details in Chapter 3	95
Appendix C. Complementary material used in Chapter 4	97
C.1. Real network topologies	97
C.2. First Fit and Most Used algorithms	98
C.3. ILP solution for RWA	102
C.4. Paths used to solve the RWA problem	105
C.5. Multiband optical network simulator	105
C.6. ASE and NLI noise power in the COST 239 network	116
C.7. RMSA solution	116
Appendix D. Scientific contributions	133
Appendices	75

List of Figures

2.1	Physical topology of a 4-node network and its corresponding logical topology. . .	6
2.2	Physical topology used for the network Examples 1 and 2 and the corresponding candidate paths for each demand.	8
2.3	Physical topology used in Examples 3 and 4 and the corresponding candidate paths for each demand.	11
2.4	Physical topology of an example network with six arcs.	14
2.5	Flow of demand between nodes for demands \hat{h}_{12} , \hat{h}_{13} and \hat{h}_{23} in the network represented in Figure 2.4.	14
2.6	Logical and physical topology of the network considered in Example 6.	16
2.7	Physical topology considered for the network Example 7, for the failure states $s=1$ and $s=2$ and the corresponding candidate paths that can be used for each demand and state.	18
2.8	Physical topology used for the network Examples 8 and 9 and the corresponding normal and backup paths for each demand.	20
2.9	Physical topology used for the network Example 8, considering state $s=1$, and Example 9, considering state $s=5$, with the corresponding normal and backup paths for each demand.	21
2.10	Physical topology used for the network Example 10, considering state $s=0$ with two available colors $c=2$	24
2.11	Physical topology 6-node example network.	24
2.12	Physical topology used for the network in Example 11, considering state $s=0$ with five available colors $c=5$	25
2.13	Physical topology used for the network in Example 12, considering state $s=0$ with six available colors $c=6$	27
2.14	Physical topology 5-node example network.	28
2.15	Physical topology used for the network in Example 13, considering state $s=0$ with five available colors $c=2$	29
2.16	Physical topology used for the network in Example 14, considering state $s=0$ with five available colors $c=1$	29
2.17	Physical topology of a 12-node portuguese backbone network.	31
2.18	Link capacity of the portuguese backbone network represented in Figure 2.17 obtained with a heuristic and an ILP solution.	33
3.1	C and L band spectrum and corresponding frequencies according with the ITU-T grid.	36
3.2	Schematic of an optical amplified generic link i between two network nodes. . .	37
3.3	COST 239 optical network, with 11 nodes, 26 links represented by e_i (where $i=1$... 26), and corresponding link distances.	38

List of Figures

3.4	NLI coefficient as a function of the channel frequency without SRS and with SRS, considering both coherent and incoherent scenarios with the parameters of Table 3.8.	43
3.5	NLI coefficient as a function of the number of spans without SRS and with SRS, considering $f=-4$ THz and several modulation formats.	47
3.6	NLI coefficient as a function of the number of spans without SRS and with SRS, considering $f=0$ THz and several modulation formats.	47
4.1	Link capacity obtained with heuristic solution and ILP with four candidate paths per demand for COST 239 network.	56
4.2	Flowchart of the Matlab simulator used to solve the RMSA problem in a flexible grid C+L multiband network aware of the PLIs.	58
4.3	FSs allocated in the different links for the different demands in the COST 239 network for $BER=4\times 10^{-2}$	60
4.4	FSs allocated in the different links for the different demands in the COST 239 network for $BER=10^{-3}$	64
4.5	Blocked demands percentage and allocated FSs percentage for three BERs, 4×10^{-2} , 10^{-2} , and 10^{-3}	66
C1	Optical network COST 239 physical topology.	97
C2	Optical network NSFNET physical topology.	98
C3	Optical network UBN physical topology.	98
C4	Optical network CONUS 30 physical topology.	99

List of Tables

2.1	Unit cost per link.	7
2.2	Demand volume for each demand.	7
2.3	Candidate paths for each demand.	7
2.4	Link-path relations.	8
2.5	Variables used in Link-Path formulation.	9
2.6	Possible solution for Example 1.	10
2.7	Unit path cost of each candidate path for Example 4.	13
2.8	Candidate paths for each demand in Examples 5 and 6.	16
2.9	Unit path cost of each candidate path in Example 6.	16
2.10	Link capacity solution for each one of the six states of Example 7.	19
2.11	Link-path relations for the backup paths represented in Figure 2.8.	20
2.12	Variables used in RWA problem based on the Link-Path formulation.	22
2.13	Number of the variables and constraints needed to solve the RWA problem in Example 10.	23
2.14	Solution of Example 10.	23
2.15	List of candidate paths for each demand.	24
2.16	Number of the variables and constraints need to solve the RWA problem in Example 11.	25
2.17	Solution of Example 11.	25
2.18	Candidate paths for each demand for Example 12.	26
2.19	Number of the variables and constraints need to solve the WA problem in Example 12.	26
2.20	Solution of Example 12.	27
2.21	Demand pairs for Example 13.	28
2.22	Candidate paths list for each demand in Example 13.	28
2.23	Number of the variables and constraints need to solve the WA problem in Example 13.	28
2.24	Traffic Matrix in VC-3.	32
2.25	Link Capacity for Dijkstra algorithm and ILP.	33
3.1	Fixed grid with $\Delta_{ch}=50$ GHz and flexible grid with FS=12.5 GHz for C, L, and C+L bands.	36
3.2	Demand pairs for demands 1 to 4 in COST 239 network.	39
3.3	WDM system parameters used to calculate the OSNR for demands 1 to 4 in COST 239 network.	39
3.4	Candidate paths for the four demands considered in the COST 239 network.	39

List of Tables

3.5	Number of in-line amplifiers needed in link e_i , gain of each pre and in-line amplifier and corresponding noise figure for each optical link, and total ASE noise power of the links belonging to the candidate paths used in the four demands in COST 239 network.	40
3.6	OSNRs for the candidate paths for the four demands considered in COST 239 network.	40
3.7	Optical paths with highest OSNR for the four demands considered in COST 239 network.	40
3.8	Parameters used to obtain Figure 3.4.	42
3.9	WDM system parameters used to calculate the OSNR with NLI and SRS for the four demands considered in COST 239 network.	43
3.10	Number of spans needed in each link, NLI coefficient and noise power at the end of each link used by the candidate path for the four demands considered in the COST 239 network.	44
3.11	OSNR considering only the NLI noise for the candidate paths of the four demands considered in COST 239 network.	44
3.12	Total OSNR with ASE and NLI noises for the candidate paths for the four demands considered in COST 239 network.	45
3.13	Optical paths with highest OSNR for the four demands considered in COST 239 network.	45
3.14	Modulation formats and corresponding excess kurtosis.	46
3.15	Link spans lengths, correction factor and NLI noise power.	48
3.16	Total OSNR for the candidate paths for the four demands considered in COST 239 network for the QPSK modulation.	48
3.17	Modulation formats with corresponding theoretical ROSNRs and practical ROSNRs for $BER=10^{-3}$	49
3.18	Optical paths with best OSNR for the four demands considered in COST 239 network for QPSK modulation.	49
3.19	Total OSNR for the candidate paths for the four demands considered in COST 239 network for 16-QAM modulation.	49
3.20	Optical paths with best OSNR for the four demands considered in COST 239 network with the respective modulation format.	50
3.21	Number of nodes and amplifiers, safety margin and residual margin of the optical paths for the four demands considered in the COST 239 network.	50
3.22	Modulation formats with corresponding theoretical ROSNRs and practical ROSNRs for $BER=4\times 10^{-2}$	51
3.23	Optical paths with best OSNR for the four demands considered in COST 239 network with the respective modulation format for $BER=4\times 10^{-2}$	51
4.1	Physical and logical features for the network topologies considered.	53
4.2	Total number of wavelengths obtained for the different network topologies with the WA heuristic algorithms, FF and MU, for different ordering strategies.	54
4.3	Total number of wavelengths used in the different network topologies obtained with the ILP formulation, given in equation (4.1), as well as the respective computation time.	55

List of Tables

4.4	System parameters used to solve the RMSA problem.	59
4.5	System parameters used to calculate the OSNR of each path.	59
4.6	RMSA solution for the COST 239 optical network with $BER=4\times 10^{-2}$	61
4.7	RMSA solution for the COST 239 optical network with $BER=10^{-3}$	63
4.8	RMSA solution for the real network topologies COST 239, NSFNET, UBN, and CONUS 30, for three different BERs - Part 1.	65
4.9	RMSA solution for the real network topologies COST 239, NSFNET, UBN, and CONUS 30, for three different BERs - Part 2.	67
A.1	Matlab results for Example 2	76
A.2	Matlab results for Example 3	76
A.3	Matlab results for Example 4	77
A.4	Comparison between RWA ILP formulation parameters and alternative RWA formulation parameters.	87
B.1	Total OSNR with ASE noise for the candidate paths for demands 1 to 4 with $G_{max}=23$ dB for network COST 239.	95
B.2	Total OSNR with ASE noise for the candidate paths for demands 1 to 4 with $P_m=1.46$ dBm for network COST 239.	95
B.3	Total OSNR with NLI noise for the candidate paths for demands 1 to 4 with $P_m=1.46$ dBm for network COST 239.	95
C.1	Path list used to obtain Figure 4.1	106
C.2	NLI and ASE noise powers at the end of each link in the COST 239 optical network for the modulation formats 64-QAM, 16-QAM and QPSK.	117
C.3	Modulation formats with corresponding theoretical ROSNRs and practical ROSNRs for $BER=10^{-3}$	117
C.4	RMSA solution for the COST 239 optical network with $BER=10^{-2}$	118
C.5	RMSA solution for the NSFNET optical network with $BER=4\times 10^{-2}$	119
C.6	Blocked demands in the RMSA solution for the NSFNET optical network with $BER=4\times 10^{-2}$	119
C.7	RMSA solution for the NSFNET optical network with $BER=10^{-2}$	120
C.8	Blocked demands in the RMSA solution for the NSFNET optical network with $BER=10^{-2}$	120
C.9	RMSA solution for the NSFNET optical network with $BER=10^{-3}$	120
C.10	Blocked demands in the RMSA solution for the NSFNET optical network with $BER=10^{-3}$	121
C.11	RMSA solution for the UBN optical network with $BER=4\times 10^{-2}$	123
C.12	Blocked demands in the RMSA solution for the UBN optical network with $BER=4\times 10^{-2}$	123
C.13	RMSA solution for the UBN optical network with $BER=10^{-2}$	124
C.14	Blocked demands in the RMSA solution for the UBN optical network with $BER=10^{-2}$	125
C.15	RMSA solution for the UBN optical network with $BER=10^{-3}$	125
C.16	Blocked demands in the RMSA solution for the UBN optical network with $BER=10^{-3}$	125

List of Tables

C.17	RMSA solution for the CONUS 30 optical network with $\text{BER}=4\times 10^{-2}$	128
C.18	Blocked demands in the RMSA solution for the CONUS 30 optical network with $\text{BER}=4\times 10^{-2}$	128
C.19	RMSA solution for the CONUS 30 optical network with $\text{BER}=10^{-2}$	130
C.20	Blocked demands in the RMSA solution for the CONUS 30 optical network with $\text{BER}=10^{-2}$	130
C.21	RMSA solution for the CONUS 30 optical network with $\text{BER}=10^{-3}$	131
C.22	Blocked demands in the RMSA solution for the CONUS 30 optical network with $\text{BER}=10^{-3}$	132

List of Acronyms

ASE: Amplified Spontaneous Emission
BER: Bit Error Rate
COI: Channel Of Interest
DVU: Demand Volume Units
EDFA: Erbium-Doped Fiber Amplifiers
FAR: Fixed Alternate Routing
FEC: Forward Error-Correction
FF: First-Fit
FR: Fixed-Path Routing
FS: Frequency Slot
HD: Hard-Decision
ILP: Integer Linear Programming
ITU-T: International Telecommunication Union
LCU: Link Capacity Unit
LPF: Longest Path First
MU: Most Used
NLI: Nonlinear Interference
OSNR: Optical Signal-To-Noise Ratio
OTU: Optical Transport Network
OXC: Optical Cross-Connect
PDM: Polarization-Division Multiplexing
PLIs: Physical Layer Impairments
QAM: Quadrature Amplitude Modulation
QoS: Quality of Service
QPSK: Quadrature Phase-Shift Keying
R: Random Path policy
RMSA: Routing, Modulation Format and Spectrum Assignment
ROADM: Reconfigurable Optical Add/Drop Multiplexer
ROSNR: Required Optical Signal-To-Noise Ratio.
RP: Random Path Ordering
RWA: Routing and Wavelength Assignment
SD: Soft-Decision

List of Symbols

SMF: Single Mode Fibers

SNR: Signal-to-Noise Ratio

SPF: Shortest Path First

SPM: Self-Phase Modulation

SRS: Stimulated Raman Scattering

WA: Wavelength Assignment

WDM: Wavelength Division Multiplexing

WSS: Wavelength Selective Switch

XPM: Cross-Phase Modulation

List of Symbols

α	Fiber attenuation coefficient
α_{es}	Link availability
β_2	Group velocity dispersion parameter
β_3	Third order dispersion parameter
β_{edpq}	Back-up path link relations
Δ_f	Channel frequency separation
Δ_{ch}	Channel spacing
δ_{edp}	Link relations
η_{GN}	NLI coefficient
η_{SPM}	Closed- form NLI parameter of the SPM contribution
η_{XPM}	Closed-form NLI parameter of the XPM contribution
η_{corr}	NLI parameter correction factor
γ	Nonlinear coefficient
\hat{c}_{arc}	Capacity of arc in the Node-Path formulation
\hat{h}_d	Demand volume in the Node-Path formulation
λ_0	Reference wavelength
ν_0	Optical frequency of a WDM channel
ω_{dps}	Binary availability coefficient of backup path (d, q) in situation s
$\bar{\alpha}$	Generic attenuation parameter
\bar{n}_2	Nonlinear refractive index
Φ	Excess kurtosis
ϕ	Phase mismatch term
F	Objective function
θ_{dps}	Binary availability coefficient of path (d, p) in situation s
$\tilde{x}_{d,p}$	Flow in demand d through path p in the Node-Path formulation
y_e	Load on link e
ε	Coherence factor
ξ_e	Unit cost of link e
ξ_{arc}	Unit cost of the arc
ζ_{dp}	Unit cost of path p
A_{eff}	Fiber effective area
B_0	Optical bandwidth
B_k	Bandwidth of k -th interfering channel
B_m	COI channel bandwidth
B_{FS}	Frequency slots bandwidth
C	Total number of colors of the network
c	Specific color in the network

List of Symbols

c_e	Capacity of link e for capacitated problems
C_r	Raman gain slope
c_{light}	Speed of light
C_{WSS}	Number of cascaded WSSs
D	Total number of demands in the network
d	Specific demand in the network
$D_{\lambda 0}$	Dispersion
E	Total number of links in the network
e	Link
e_i	Specific link i in the network
f_k	Frequency of the k -th interfering channel
f_m	Frequency of the center channel
F_n	Noise figure
$f_{n,in,i,j}$	In-line amplifier noise figure
$f_{n,pos,i}$	Post-amplifier noise figure
$f_{n,pre,i}$	Pre-amplifier noise figure
$g_{in,i,j}$	In-line amplifier gain
G_{max}	EDFA maximum gain
$g_{pos,i}$	Post-amplifier gain
$g_{pre,i}$	Pre-amplifier gain
h	Planck constant
h_d	Volume of demand d
h_{ds}	Volume of demand d to be realized in situation s , expressed in number of light-paths
k_{paths}	Number of candidate paths
L_{sec}	Length of the link
L_{span}	Span length
M	Modulation format
m	Central channel
N_v	Number of nodes
N_a	Total number of optical amplifiers
N_{ch}	Total number of channels
$N_{in,i}$	Number of in-line amplifiers
N_{spans}	Number of spans
$osnr_{in,i,j}$	In-line amplifier OSNR
$osnr_{pos,i}$	Post-amplifier OSNR
$osnr_{pre,i}$	Pre-amplifier OSNR
$OSNR_{tot,m}$	Total OSNR in channel m
p	Candidate path
P_d	Total number of candidate paths in the demand d
P_m	Average launch signal power per channel
p_{ASE}	ASE noise power
P_{dp}	Specific candidate path p for demand d
P_{filt}	Filtering penalty

p_{NLI}	NLI power
P_{tot}	Total transmitted optical power
P_{xtalk}	Crosstalk penalty
q	Backup path
Q_{dpq}	Backup path for specific demand
$R_{b,i}$	Information bit rate
$R_{b,l}$	Line bit rate
$R_{s,l}$	Symbol rate
RM_m	Residual margin
s	Failure state
S_0	Dispersion slope
SM_m	Safety margin
u_{dpq}	Binary variable corresponding to flow x_{dpq0}
V	Total number of nodes in the network
v	Specific node in the network
x_{dpc}	Flow (number of light-paths) realizing demand d in color c on path p
x_{dpq0}	Normal flow of demand d allocated to pair (P_{dp}, Q_{dpq})
x_{dps}	Flow in demand d through path p for failure state s
x_{dp}	Flow allocated to path p of demand d
y_e	Capacity of link e for uncapacitated problems
z_{ce}	Number of times the color c is used in link e

Introduction

1.1. Motivation and context

The increased use of the Internet in everyday life has triggered a worldwide huge growth of data traffic in optical telecommunication networks. New technologies like 5G, Internet of Things, virtual reality, and the different social media platforms require new technical solutions to provide the large capacity needed to satisfy all traffic requests [1]. To accommodate such traffic growth, one solution is to expand the transmission beyond the C-band while maintaining the operation of the current optical fibers, which is known as the multiband solution [2]. This solution allows using the currently existing and deployed optical fibers, single mode fibers (SMF) with low-water peak G.652.D [3], and increase the available bandwidth/wavelengths by using the additional O-, E-, S-, and L-bands [1]. The current wavelengths range typically supported in installed SMF is from 1530 nm to 1565 nm, corresponding to the available C-band bandwidth of 35 nm [4]. By adding the L-band, as in recent deployed optical fiber links, whose bandwidth is 60 nm (1565-1625 nm), the multiband solution C+L spectrum achieves a much wider enhanced range of 95 nm [4].

Another solution considered to accommodate the traffic growth is to use a flexible grid instead of a fixed grid. With the fixed grid, the same bandwidth is allocated to each wavelength division multiplexing (WDM) channel, in order to accommodate a specific symbol rate. Typically, the channel width used in WDM channels with fixed grid is 50 GHz [5]. On the other hand, with a flexible grid, the optical spectrum is divided into smaller frequency slots (FSs) of 12.5 GHz, a solution that allows to increase the WDM bandwidth efficiency in SMFs [1]. The FSs are now going to be attributed depending on the demands bit rate [1], avoiding the waste of unused spectrum that occurs in the fixed grid solution. Hence, the flexible grid solution allows to spare network resources and to improve transmission capacity when comparing with the fixed grid.

In this scenario where the capacity of the optical network is increased, by using multiband solutions with the flexible grid, the efficiency in using the network resources is crucial, and, so well designed planning tools are of paramount importance. These tools determine how the network accommodates the traffic, and solve how the different demands are routed, protected, groomed (traffic aggregation), select the modulation formats used, and which wavelengths should be assigned, depending on the grid used [6]. The planning problems can be described using integer linear programming (ILP) and heuristic solutions. With the heuristic algorithms, the solution obtained may not be optimal, but it leads to satisfactory results in a reasonable amount of time [6]. On the other hand, with the ILP formalism, the solution reached is optimal, however, as the number of demands and the size of the network increases, the running time required to reach the optimal solution becomes significantly longer [6], becoming difficult to apply the ILP to solve the planning problem in larger networks with many nodes [7].

With the multiband solution, the network planning is more challenging, since there is more spectrum available to be assigned and there are also more pronounced physical layer impairments

(PLIs) in comparison with the ones considered in C-band only transmission [1]. So, in this dissertation we will develop and analyze planning tools to solve routing, modulation format and spectrum assignment (RMSA) problems for multiband static networks with a flexible grid, aware of PLIs, considering different quadrature amplitude modulation (QAM) formats for different bit error rates (BERs).

1.2. Goals

The main goal of this dissertation is to develop a planning tool to route the demands in static C+L multiband networks. First, we developed a two-step RWA planning tool for a fixed grid optical network, based on a heuristic approach, using well-known algorithms such as the Dijkstra algorithm for routing, and First-Fit, Most-Used, and Random algorithms for WA. Then, we implement a single-step RWA planning tool based on an ILP formalism, and compare its performance with the one obtained with the two-step RWA heuristic tool. Finally, we improve the heuristic RWA planning tool to be aware of the PLIs, to select the modulation format and FSs assigned targeting the efficient use of the spectrum and the improvement of the performance in a multiband network with a flexible grid, hence, becoming a RMSA problem. The PLIs considered are the amplified spontaneous emission (ASE) noise, nonlinear interference (NLI) noise, stimulated Raman scattering (SRS) effect, crosstalk, filtering effects, and system aging. The impact of the PLIs is assessed through the computation of the optical signal-to-noise ratio (OSNR) of each link belonging to a particular optical path and the OSNR is used as a metric to perform the network optimization.

1.3. Dissertation organization

This dissertation is organized in five chapters.

In Chapter 2, we review routing and wavelength assignment algorithms based on ILP formulations and heuristic algorithms. The ILP formulations studied for routing are the Link-Path and Node-Link formulations. Based on the Link-Path formulation, we studied two restoration design problems, and an ILP formulation for solving the RWA problem in wavelength division multiplexing (WDM) transparent optical networks. The heuristic algorithms studied for routing are the Dijkstra algorithm and the Yen's k -shortest path algorithm, and the First-Fit, Most-Used, and Random algorithms are used for WA.

Chapter 3 is focused on the path OSNR degradation induced by the PLIs in a C+L optical network. The PLIs studied are the ASE noise power, the NLI noise power and SRS effect using closed-form formulas based on a Gaussian model that can incorporate or not the modulation format effect, the crosstalk, the filtering effects, and the system aging. We studied the PLIs effects with different amplifiers maximum gain, channel launch powers and BERs.

In Chapter 4, we solve and analyze the RWA and RMSA problems for different real network topologies. First, we solve the RWA problem with heuristic algorithms using different ordering strategies in a two-step approach, where the routing problem is solved first, and then, the WA is performed, and with a ILP formulation, where the RWA problem is solved in only one-step for a path list with various candidate paths. Then, we present the simulator developed to solve the RMSA problem in the C+L multiband considering the PLIs, and apply the simulator to four real network topologies.

Chapter 5 is dedicated to the final conclusions of this work, and some future work proposals are presented.

1.4. Main contributions

This dissertation has the following main contributions:

- Study and compare the common two-step RWA heuristic solution (based on the Dijkstra, First-Fit, and Most Used algorithms) with a single-step RWA ILP solution for several network topologies. The study is focused on the number of wavelengths assigned and the required computation time as a function of the number of candidate paths.
- Implementation of a PLI-aware simulator to solve the RMSA problem in a C+L multi-band network, considering several real network topologies. The path OSNR is used as a routing metric with the aim of minimizing the number of FSs allocated in a static network scenario with a flexible grid.
- Study the allocation of FSs and the blocking of demands in several optical networks as a function of the BER.

A Literature Review on ILP and Heuristic Algorithms for Solving the RWA Problem

2.1. Introduction

Routing and wavelength assignment is an important task in wavelength division multiplexing optical networks. RWA selects a path between the source and the destination node (routing) and reserves for each link that constitutes that path the most suitable wavelength (wavelength assignment), establishing a light-path to serve a given traffic demand [8].

The RWA problem can be solved using a one-step process, or a two-step process [6]. The two-step RWA process starts by selecting the route, and then, by assigning the same wavelength to each link [6]. The one-step RWA treats the routing problem and the wavelength assignment problem at the same time. Using this method under heavy load conditions provides an improvement in network performance in comparison with the two-step RWA [6].

RWA problems can be solved using exact procedures that find the optimal solution or heuristic approaches that may not find the optimal solution. The heuristic algorithms are preferable for solving the RWA problem in large networks [8]. The exact procedure, e.g. based on an integer linear programming problem, is more suitable for smaller networks and with static traffic [8].

This chapter reviews some typical ILP formulations in Section 2.2 and heuristic approaches in Section 2.3 for solving the RWA problem in optical networks. Subsections 2.2.1 and 2.2.2 present two different formulations to solve network dimensioning problems with ILP formulations, respectively, the Link-Path formulation and the Node-Link formulation. The restoration design problem and the RWA problem are addressed, respectively, in subsections 2.2.3 and 2.2.4. Section 2.3 presents the most used heuristics algorithms for routing, in subsection 2.3.1, and wavelength assignment, in subsection 2.3.2. This chapter concludes with Section 2.4 that presents a real network scenario designed with both an exact algorithm based on a ILP formulation and the usual heuristics algorithms.

2.2. Integer Linear Programming formulations

An integer linear programming (ILP) formulation is a mathematical formulation of an optimization problem in which variables are restricted to integers [8]. This formulation allows obtaining optimal solutions for network design problems [8]. In this section we will introduce two common ILP formulations, the Link-Path and Node-Link formulations, and we will use the Link-Path formulation to solve a restoration design problem and a RWA problem.

2.2.1. Link-Path formulation

The formulation presented in this subsection that describes network dimensioning problems is called link-demand-path-identifier-based formulation, or shortly, Link-Path formulation [7].

In Figure 2.1, it is represented the physical and logical topologies of a four-node network, used to explain the Link-Path formulation and related network concepts. The physical topology of the network example consists of four nodes (vertices), designated with notation $v=1, \dots, 4$, (where V represents the total number of nodes of the physical topology, in this scenario $V=4$), and five undirected links (edges) denoted as e_i with $i=1, \dots, 5$ (where E represents the total number of links, in this scenario $E=5$). The corresponding network logical topology consists of three nodes ($V=3$) and three demands, $d=1, \dots, 3$ (where D denotes the total number of demands in a network, in this scenario $D=3$). A demand corresponds to a flow of information between a pair of nodes and can be undirected (bi-directional), $v-v'$ or directed (uni-directional), $v \rightarrow v'$.

In this network, only three of the four nodes generate demands, the fourth node ($v=4$) is a transit node. Transit nodes do not generate any demand. However, nodes that originate demands can also be transit nodes when they are intermediate nodes along the path of other demands.

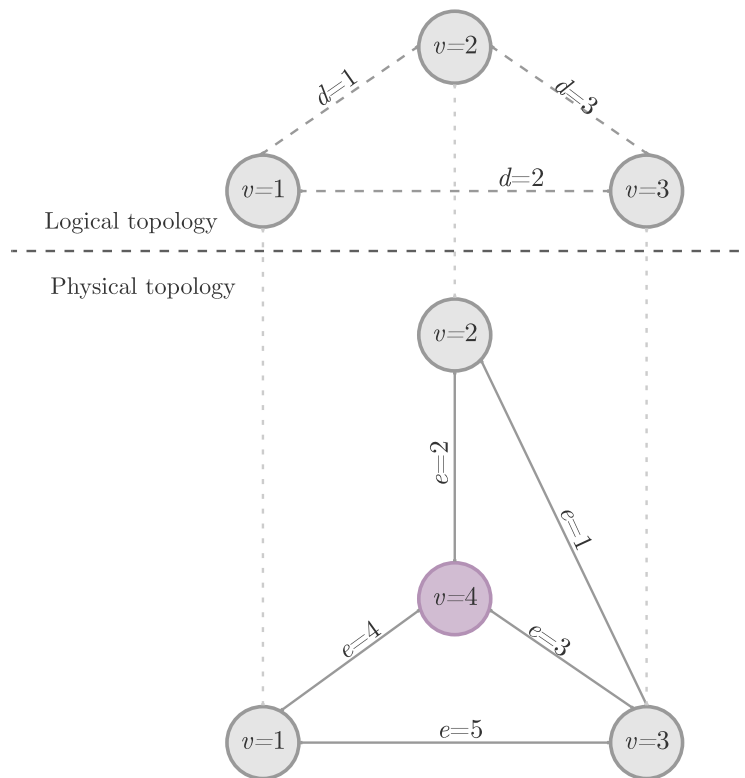


Figure 2.1. Physical topology of a 4-node network and its corresponding logical topology.

Each demand d is characterized by a demand volume h_d . Each demand volume is quantified in demand volume units (DVU). The capacity of a link is characterized using the link capacity unit (LCU). The unit cost per link e , $\xi_e \geq 0$, is quantified in LCUs. The LCU and DVU must be consistent with each other. As an example, the unit used in this section is Mbps.

Table 2.1 indicates the considered links unit cost for the network example shown in Figure 2.1 and Table 2.2 shows the demand volume considered for each demand.

There are two different types of dimensioning problems, uncapacitated problems where the capacity of each link e is a variable of the problem and is represented by y_e , and capacitated

Link e	Unit Cost per Link ξ_e
$e=1$	$\xi_1 = 2$
$e=2$	$\xi_2 = 1$
$e=3$	$\xi_3 = 1$
$e=4$	$\xi_4 = 3$
$e=5$	$\xi_5 = 1$

Table 2.1. Unit cost per link.

Demand d	Demand Volume h_d
$d=1$	$h_1 = 15$
$d=2$	$h_2 = 20$
$d=3$	$h_3 = 10$

Table 2.2. Demand volume for each demand.

problems where the capacity of each link e is known and represented by c_e . Next some examples of these dimensioning problems are presented.

The first example, named Example 1, corresponds to an uncapacitated problem, considering the network topology and demands shown in Figure 2.1. From the several paths available for the different demand volumes to be routed, as can be seen in Table 2.3 the only candidate path for $d=1$ is represented by P_{d1} where $d=1$ and $p=1$ and uses links $e=2$ and $e=4$. For $d=2$ there are two candidate paths, represented by P_{21} and P_{22} , where P_{21} uses only link $e=5$ and P_{22} uses links $e=3$ and $e=4$. Finally, for $d=3$ there are also two candidate paths, represented by P_{31} and P_{32} , where P_{31} uses only link $e=1$ and P_{32} uses links $e=2$ and $e=3$.

Demand d	Candidate paths P_{dp}
$d=1$	$P_{11} = \{2, 4\}$
$d=2$	$P_{21} = \{5\}$ $P_{22} = \{3, 4\}$
$d=3$	$P_{31} = \{1\}$ $P_{32} = \{2, 3\}$

Table 2.3. Candidate paths for each demand.

Each path will have a corresponding flow variable that is represented by x_{dp} , with d defining the demand and p the candidate path. The paths can be $p=1, \dots, P_d$, where P_d represents the total number of candidate paths for demand d .

The demand volume h_d is obtained by summing the flows corresponding to each candidate path. The following demand equations correspond to the demands in the network shown in Figure 2.1.

$$x_{11} = h_1 \quad (2.1a)$$

$$x_{21} + x_{22} = h_2 \quad (2.1b)$$

$$x_{31} + x_{32} = h_3 \quad (2.1c)$$

These equations can be generalized for any demand d . The demand equation in a compact form is:

$$\sum_p x_{pd} = h_d, \quad d = 1, 2, \dots, D \quad (2.2)$$

The link capacity y_e must also be taken into consideration, and the sum of all the flows that pass through each link has to be equal or inferior to y_e . The following inequations show the capacity inequalities corresponding to the five links of the network shown in Figure 2.1, considering the candidate paths shown in Table 2.3.

$$x_{31} \leq y_1 \quad (2.3a)$$

$$x_{11} + x_{32} \leq y_2 \quad (2.3b)$$

$$x_{22} + x_{32} \leq y_3 \quad (2.3c)$$

$$x_{11} + x_{22} \leq y_4 \quad (2.3d)$$

$$x_{21} \leq y_5 \quad (2.3e)$$

The right side of the inequalities corresponds to the total link capacity, and the left side represents the link loads y_e , that correspond to the sum of the flows that pass through a link e . The link loads must be inferior or equal to the link capacity $y_e \leq c_e$. To write the capacity inequalities in a more compact notation, the relation between the links, demands, and candidate paths can be written as shown in Table 2.4. The relation between candidate paths p , demands d and links e are typically known as link-path relations [7].

Link e \ Path P_{dp}	$P_{11} = \{2, 4\}$	$P_{21} = \{5\}$	$P_{22} = \{3, 4\}$	$P_{31} = \{1\}$	$P_{32} = \{2, 3\}$
$e=1$	0	0	0	1	0
$e=2$	1	0	0	0	1
$e=3$	0	0	1	0	1
$e=4$	1	0	1	0	0
$e=5$	0	1	0	0	0

Table 2.4. Link-path relations.

In Table 2.4, if the path passes through the link, the entry is 1, and if it does not pass, the entry is 0. To write the link-path relations more compactly, the variable δ_{edp} is defined. If the candidate path p for demand d , uses link e , then $\delta_{edp} = 1$ otherwise, $\delta_{edp} = 0$. Using this variable, the capacity inequalities (2.3) can be written in a more general compact form as

$$\sum_d \sum_p \delta_{edp} x_{pd} \leq y_e, \quad e = 1, 2, \dots, E; \quad d = 1, 2, \dots, D; \quad p = 1, 2, \dots, P_d. \quad (2.4)$$

Knowing the demand equations (2.2) and the capacity inequalities (2.4), the dimensioning problem consists in finding the “best way” (i.e. the best paths) to route the demands across the network. This problem can lead to many possible solutions, so it is necessary to create goals to find the solution of best interest. Different goals can be defined, such as minimizing the total routing cost, minimize the capacity cost, or minimizing the congestion of the most congested link in the network. The goal of the dimensioning problem is represented by the objective function **F**.

The goal chosen for Example 1 is to minimize the capacity cost of the network represented in Figure 2.2.

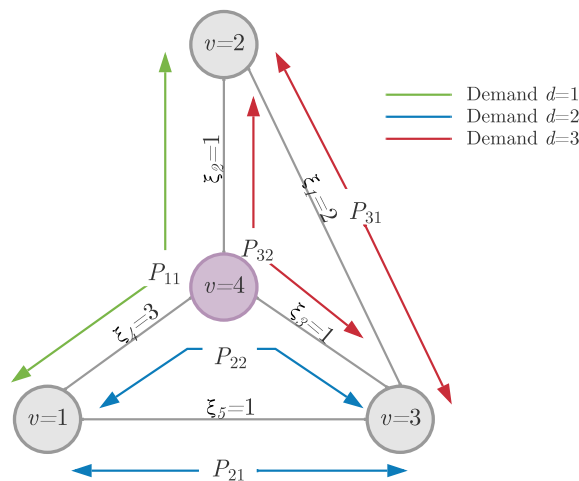


Figure 2.2. Physical topology used for the network Examples 1 and 2 and the corresponding candidate paths for each demand.

The objective function \mathbf{F} for this uncapacitated problem is the sum of the product of each link capacity by the unit cost of each link given in Table 2.1, as:

$$\begin{aligned}\mathbf{F} &= \xi_1 y_1 + \xi_2 y_2 + \xi_3 y_3 + \xi_4 y_4 + \xi_5 y_5 \\ &= 2y_1 + y_2 + y_3 + 3y_4 + y_5\end{aligned}\quad (2.5)$$

The objective function \mathbf{F} , given by (2.5) for uncapacitated dimensioning problems can also be written in a compact form as:

$$\mathbf{F} = \sum_{e=1}^E \xi_e y_e = \sum_e \xi_e y_e \quad (2.6)$$

For a generic network, this dimensioning uncapacitated problem can be written as:

$$\begin{aligned}\text{minimize: } \mathbf{F} &= \sum_e \xi_e y_e \\ \text{subject to: } \sum_p x_{pd} &= h_d, \quad d = 1, 2, \dots, D \\ \sum_d \sum_p \delta_{edp} x_{pd} &= y_e, \quad e = 1, 2, \dots, E; \quad d = 1, 2, \dots, D; \quad p = 1, 2, \dots, P_d. \\ x &\geq 0, \quad y \geq 0\end{aligned}\quad (2.7)$$

Table 2.5 shows all the variables used in the Link-Path formulation.

Variable	Description
V	Total number of nodes of the network
v	$v=1, \dots, V$ denotes a specific node in the network
E	Total number of links of the network
e	$e=1, \dots, E$ denotes a specific link in the network
D	Total number of demands of the network
d	$d=1, \dots, D$ denotes a specific demand in the network
h_d	Demand volume of demand d
ξ_e	Unit cost of link e
ζ_{dp}	Unit path cost for demand d with assigned path p
c_e	Capacity of link e for capacitated problems
y_e	Capacity of link e for uncapacitated problems
P_d	Total number of candidate paths for demand d
p	$p=1, \dots, P_d$ denotes a candidate path for demand d
P_{dp}	Candidate path p for demand d
x_{dp}	Flow for demand d through path p
\underline{y}_e	Link load for link e
δ_{edp}	$\delta_{edp}=1$, if candidate path p for demand d uses link e ; otherwise, $\delta_{edp}=0$
\mathbf{F}	Objective function

Table 2.5. Variables used in Link-Path formulation.

For the network given in Figure 2.2, considering the values in Tables 2.1, 2.2 and 2.3, equations (2.7), and the variables described in Table 2.5 the ILP formulation for Example 1 can be written as in the equations and inequalities (2.8).

All the equations and inequalities (2.8) described will be used to reach the optimal solution for this uncapacitated dimensioning problem, corresponding to the network example of Figure 2.2. To obtain the optimal solution of minimizing the link capacity y_e , each link capacity must be fully used, meaning that the capacity inequalities (2.3) of link load and link capacity will become equalities, so $\underline{y}_e = y_e$. One non-optimal solution for this uncapacitated problem is represented in Table 2.6 [7].

$$\begin{aligned}
 \text{minimize: } \mathbf{F} &= 2y_1 + y_2 + y_3 + 3y_4 + y_5 \\
 x_{11} &= 15 \\
 x_{21} + x_{22} &= 20 \\
 x_{31} + x_{32} &= 10 \\
 \text{subject to: } x_{31} &\leq y_1 \\
 x_{11} + x_{32} &\leq y_2 \\
 x_{22} + x_{32} &\leq y_3 \\
 x_{11} + x_{22} &\leq y_4 \\
 x_{21} &\leq y_5 \\
 x_{11}, x_{21}, x_{22}, x_{31}, x_{32} &\geq 0, \quad y_1, y_2, y_3, y_4, y_5 \geq 0.
 \end{aligned} \tag{2.8}$$

Link Capacity y_e	Flow x_{dp}
$y_1 = 5$	$x_{11}=15$
$y_2 = 20$	$x_{21}=15$
$y_3 = 10$	$x_{22}=5$
$y_4 = 20$	$x_{31}=5$
$y_5 = 15$	$x_{32} = 5$

Table 2.6. Possible solution for Example 1.

With this solution [7], the objective function is $\mathbf{F} = 115$. This solution is not optimal since it does not minimize the capacity cost. To clarify this point, consider that the unit path cost (ζ_{dp}) is the total cost of the candidate path, given by:

$$\zeta_{dp} = \sum_e \delta_{edp} \xi_e \quad d = 1, 2, \dots, D \quad p = 1, 2, \dots, P_d. \tag{2.9}$$

In the solution given in Table 2.6, the second candidate path for the second demand $P_{22} = \{3, 4\}$ has five units of flows ($x_{22} = 5$) attributed. The unit path cost for this path is $\zeta_{22} = \xi_3 + \xi_4 = 1 + 3 = 4$. The first path ($P_{21} = \{5\}$) for this demand has a unit path cost of one ($\zeta_{21} = \xi_5 = 1$). So, in Example 1, if the flow from path P_{22} is moved to path P_{21} , the cost saved will be $\zeta_{22} - \zeta_{21} = 4 - 1 = 3$ per unit of flow, saving fifteen LCUs in total ($x_{22}(\zeta_{22} - \zeta_{21}) = 15$). Since demand $d=1$ only has one candidate path, this demand is optimized. In demand $d=3$, both path costs are the same ($\zeta_{31} = \zeta_{32} = 2$), and any division of the flow through the two paths is not going to affect the final cost; therefore, demand $d=3$ is also optimized.

In conclusion, moving all the flow from P_{22} to P_{21} will minimize the capacity cost in this problem and consequently the objective function \mathbf{F} . With the new allocation of flow in demand $d=2$, the solution to minimize the capacity cost gives $\mathbf{F}^{opt}=100$ [7], which is optimal as denoted by the superscript *opt*. The flow and capacities solution for this dimensioning problem, which is optimal since it minimizes the cost function, are as follows:

$$\begin{aligned}
 x_{11}^{opt} &= 15 \\
 x_{21}^{opt} &= 20, \quad x_{22}^{opt} = 0 \\
 x_{31}^{opt} &= 10 - a, \quad x_{32}^{opt} = a, \quad \text{for any } 0 \leq a \leq 10 \\
 y_1^{opt} &= 10 - a, \quad y_2^{opt} = 15 + a, \quad y_3^{opt} = a, \quad y_4^{opt} = 15, \quad y_5^{opt} = 20
 \end{aligned}$$

where a represents a number between 0 and 10, and for any integer number in this interval, the dimensioning problem solutions will be optimal. The optimal solution for Example 1 with $a=0$ was confirmed with Matlab using function `linprog`. The corresponding Matlab code and results are shown in Appendix A.1.

Another example of an uncapacitated problem is given in the following, which is called Example 2. For this example problem, a restriction in the flows is imposed. Each demand can only use one candidate path to satisfy all the demand volume, using one flow per demand, which is a typical scenario in optical networks. Example 2 considers the network topology described in Figure 2.2, the candidate paths are the same as described in Table 2.3, and the goal for the objective function is also to minimize the capacity cost.

The restriction in the flows modifies the flow allocation for demands $d=2$ and $d=3$. With this restriction, the variable, a can only be 0 or 10. The optimal objective function is still $\mathbf{F}^{opt}=100$ and the dimensioning problem solution is given by:

$$\begin{aligned} x_{11}^{opt} &= 15 \\ x_{21}^{opt} &= 20, x_{22}^{opt} = 0 \\ x_{31}^{opt} &= a, x_{32}^{opt} = 10 - a, \quad \text{for } a = 0 \text{ or } a = 10 \\ y_1^{opt} &= 10 - a, y_2^{opt} = 15 + a, y_3^{opt} = a, y_4^{opt} = 15, y_5^{opt} = 20 \end{aligned}$$

Consider now Example 3. In this example, another candidate path for demand $d=1$ described in Table 2.3 is added. The flow restrictions in Example 2 are not considered for this example. The paths considered in Example 3 are represented in Figure 2.3.

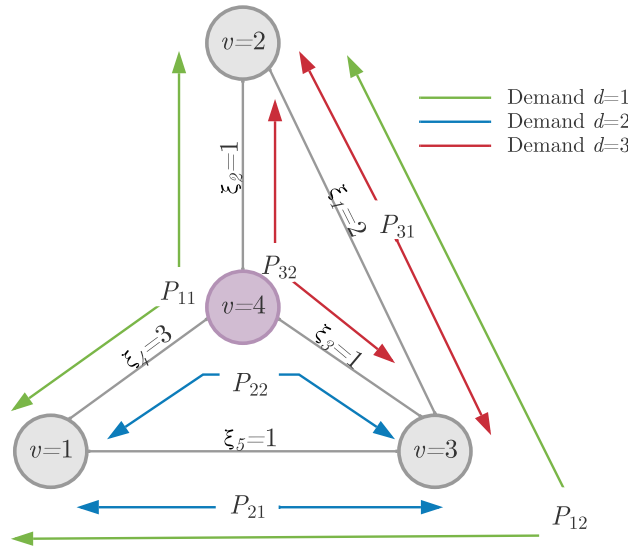


Figure 2.3. Physical topology used in Examples 3 and 4 and the corresponding candidate paths for each demand.

The addition of path $P_{12} = \{1, 5\}$, changes equation (2.1a) for the demand $d=1$ and the capacity inequality (2.3) corresponding to the link capacities that this new path uses, y_1 and y_5 as:

$$\begin{aligned} x_{11} + x_{12} &= 15 \\ x_{12} + x_{31} &\leq y_1 \\ x_{12} + x_{21} &\leq y_5 \end{aligned} \tag{2.10}$$

For Example 3, the problem of minimizing the capacity cost can be written as:

$$\begin{aligned}
 & \textbf{minimize: } \mathbf{F} = 2y_1 + y_2 + y_3 + 3y_4 + y_5 \\
 & \quad x_{11} + x_{12} \quad \quad \quad = 15 \\
 & \quad \quad \quad x_{21} + x_{22} \quad \quad = 20 \\
 & \quad \quad \quad \quad \quad x_{31} + x_{32} = 10 \\
 & \textbf{subject to: } \quad x_{12} \quad \quad + x_{31} \quad \leq y_1 \\
 & \quad x_{11} \quad \quad \quad + x_{32} \leq y_2 \\
 & \quad \quad \quad x_{22} \quad + x_{32} \leq y_3 \\
 & \quad x_{11} \quad \quad + x_{22} \quad \leq y_4 \\
 & \quad \quad \quad x_{12} + x_{21} \quad \leq y_5 \\
 & \quad x_{11}, x_{12}, x_{21}, x_{22}, x_{31}, x_{32} \geq 0, \quad y_1, y_2, y_3, y_4, y_5 \geq 0.
 \end{aligned} \tag{2.11}$$

The unit path cost for the first candidate path for demand $d=1$ is $\zeta_{11} = 1 + 3 = 4$ ($P_{11} = \{2, 4\}$) and the unit path cost for the new added path is $\zeta_{12} = 2 + 1 = 3$. Knowing the new cost, the solution for this example that minimizes the objective function, for demand $d=1$, is $x_{11}^{opt} = 0$ and $x_{12}^{opt} = 15$. So, the dimensioning problem solution is given by:

$$\begin{aligned}
 x_{11}^{opt} &= 0, \quad x_{12}^{opt} = 15 \\
 x_{21}^{opt} &= 20, \quad x_{22}^{opt} = 0 \\
 x_{31}^{opt} &= 10 - a, \quad x_{32}^{opt} = a \quad \text{for any } 0 \leq a \leq 10 \\
 y_1^{opt} &= 15 + (10 - a), \quad y_2^{opt} = a, \quad y_3^{opt} = a, \quad y_4^{opt} = 0, \quad y_5^{opt} = 35
 \end{aligned}$$

The new optimal capacity cost for this example is $\mathbf{F}^{opt}=85$, decreasing the cost by 15 LCUs, in comparison with the previous example. The solution of Example 3 shows how important it is to choose the path list to obtain an optimal solution. A brute force strategy, which results also in an optimal solution, is to consider all the possible paths, although it can be time consuming for large networks with many demands. Example 3 was also solved in Matlab using function `linprog`, as shown in Appendix A.2.

Now, let us consider Example 4 which is a capacitated problem. The network physical topology, and the candidate paths are represented in Figure 2.3. For this example, the capacity of each link is known, and is represented by c_e . Capacitated problems equations can be written in a compact generic form by:

$$\begin{aligned}
 \sum_p x_{pd} &= h_d, \quad d = 1, 2, \dots, D \\
 \sum_d \sum_p \delta_{edp} x_{pd} &= c_e, \quad e = 1, 2, \dots, E; \quad d = 1, 2, \dots, D; \quad p = 1, 2, \dots, P_d. \\
 x_{pd} &\geq 0,
 \end{aligned} \tag{2.12}$$

The capacity of each link, considered in Example 4 is $c_e = (c_1, c_2, c_3, c_4, c_5) = (10, 15, 5, 15, 30)$. The goal for the objective function \mathbf{F} for this example is to minimize the total routing cost,

$$\mathbf{F} = \zeta_{11}x_{11} + \zeta_{12}x_{12} + \zeta_{21}x_{21} + \zeta_{22}x_{22} + \zeta_{31}x_{31} + \zeta_{32}x_{32} \tag{2.13}$$

Table 2.7 has the path cost of each candidate path.

Candidate Paths P_{dp}	Unit Path Cost ζ_{dp}
$P_{11} = \{2, 4\}$	$\zeta_{11} = 4$
$P_{12} = \{1, 5\}$	$\zeta_{12} = 3$
$P_{21} = \{5\}$	$\zeta_{21} = 1$
$P_{22} = \{3, 4\}$	$\zeta_{22} = 4$
$P_{31} = \{1\}$	$\zeta_{31} = 2$
$P_{32} = \{2, 3\}$	$\zeta_{32} = 2$

Table 2.7. Unit path cost of each candidate path for Example 4.

So, the capacitated problem for Example 4 can be written as:

$$\begin{aligned}
 \text{minimize: } & \mathbf{F} = 4x_{11} + 3x_{12} + x_{21} + 4x_{22} + 2x_{31} + 2x_{32} \\
 & x_{11} + x_{12} = 15 \\
 & \quad \quad \quad x_{21} + x_{22} = 20 \\
 & \quad \quad \quad \quad \quad x_{31} + x_{32} = 10 \\
 \text{subject to: } & \quad \quad \quad x_{12} \quad \quad \quad + x_{31} \leq 10 \\
 & x_{11} \quad \quad \quad \quad \quad + x_{32} \leq 15 \\
 & \quad \quad \quad \quad \quad x_{22} \quad \quad \quad + x_{32} \leq 5 \\
 & x_{11} \quad \quad \quad + x_{22} \leq 15 \\
 & \quad \quad \quad x_{12} + x_{21} \leq 30 \\
 & x_{11}, x_{12}, x_{21}, x_{22}, x_{31}, x_{32} \geq 0,
 \end{aligned} \tag{2.14}$$

The optimal solution for Example 4, obtained using Matlab function `linprog` is:

$$\begin{aligned}
 x_{11}^{opt} &= 10, x_{12}^{opt} = 5 \\
 x_{21}^{opt} &= 20, x_{22}^{opt} = 0 \\
 x_{31}^{opt} &= 5, x_{32}^{opt} = 5 \\
 \mathbf{F}^{opt} &= 95
 \end{aligned}$$

The Matlab script for Example 4 is shown in Appendix A.3.

2.2.2. Node-Link formulation

Another formulation that can be used for dimensioning problems is the Node-Link formulation [7]. In this formulation, the links and demands are considered to be directed. Each node has a flow conservation law, meaning that if a node is the source for the demand in consideration, the out coming flow minus the incoming flow is equal to that demand volume, so flows entering the node are negative and flows exiting the node are positive.

The network topology represented in Figure 2.4 is a three-node ($V=3$) network with three links ($E=3$). Each undirected link in this notation is composed by two directed links, also known as arcs. For example, the undirected link 1-2 is now represented by two arcs, $1 \rightarrow 2$ and $2 \rightarrow 1$.

All three demands ($D=3$) are now directed. In this case, it is enough to choose only one direction for the flow to pass through. Considering demand volume \hat{h}_{12} , between nodes $v=1$ and $v=2$ with origin in $v=1$ and destination $v=2$, the directed demand is represented by $\langle 1 : 2 \rangle$. From the node 1 ($v=1$) perspective, there are two possibilities to provision the demand volume from the source node, arc $1 \rightarrow 2$ for flow allocated $\tilde{x}_{12,12}$ ($\tilde{x}_{d,p}$ where p is the candidate path for the directed demand d) and arcs $1 \rightarrow 3$ and $3 \rightarrow 2$ for flow allocated vector $\tilde{x}_{13,12}$ and $\tilde{x}_{32,12}$. In this formulation, for the flow allocation, the first subscript pair represents the arc and the

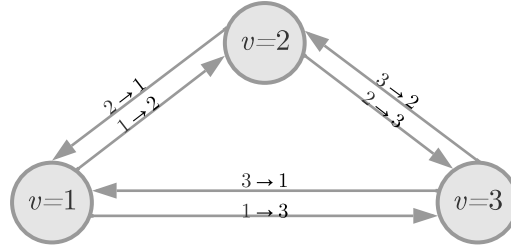


Figure 2.4. Physical topology of an example network with six arcs.

second refers to the directed demand pair. Figure 2.5 shows the candidate paths for the directed demands $\langle 1 : 2 \rangle$, $\langle 1 : 3 \rangle$ and $\langle 2 : 3 \rangle$, respectively. In this formulation, it is added a “tilde” (\sim) to the flow and a “hat” ($\hat{}$) to the demand volume to differentiate the Node-Link notation from the Link-Path formulation.

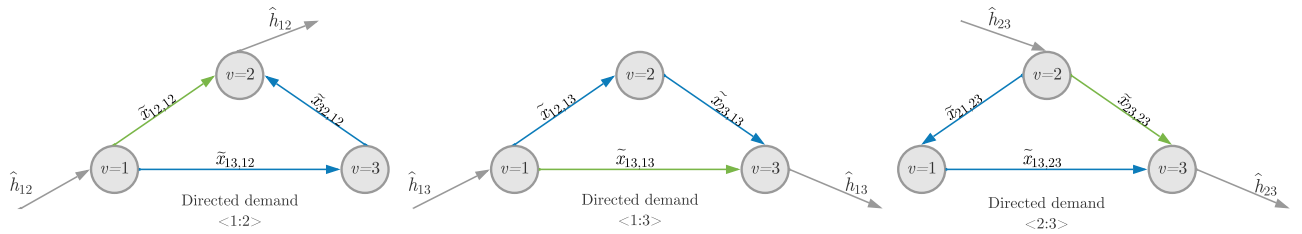


Figure 2.5. Flow of demand between nodes for demands \hat{h}_{12} , \hat{h}_{13} and \hat{h}_{23} in the network represented in Figure 2.4.

For demand $\langle 1 : 2 \rangle$, knowing that the nodes must obey the flow conservation law, the demand equations for nodes 1 (source node), 3 (transit node) and 2 (destination node) are given, respectively, by:

$$-\hat{h}_{12} - \tilde{x}_{21,12} - \tilde{x}_{31,12} + \tilde{x}_{12,12} + \tilde{x}_{13,12} = 0. \quad (2.15a)$$

$$-\tilde{x}_{13,12} - \tilde{x}_{23,12} + \tilde{x}_{31,12} + \tilde{x}_{32,12} = 0. \quad (2.15b)$$

$$-\tilde{x}_{12,12} - \tilde{x}_{32,12} + \hat{h}_{12} + \tilde{x}_{21,12} + \tilde{x}_{23,12} = 0. \quad (2.15c)$$

In this case, as shown in Figure 2.5, in each directed arc, the flow only goes through one direction so, the flow allocated to vectors $\tilde{x}_{21,12}$, $\tilde{x}_{31,12}$ and $\tilde{x}_{23,12}$ is zero. With this, the following flow conservation equations for demand $\langle 1 : 2 \rangle$ can be obtained:

$$\begin{aligned} \tilde{x}_{12,12} + \tilde{x}_{13,12} &= \hat{h}_{12} \\ -\tilde{x}_{13,12} + \tilde{x}_{32,12} &= 0 \\ -\tilde{x}_{12,12} - \tilde{x}_{32,12} &= -\hat{h}_{12} \end{aligned} \quad (2.16)$$

For demand $\langle 1 : 3 \rangle$, considering the representation of the flows and demand volumes for each node represented in Figure 2.5, the flow conservation equations for demand $\langle 1 : 3 \rangle$ are given by

$$\begin{aligned}
 \tilde{x}_{12,13} + \tilde{x}_{13,13} &= \hat{h}_{13} \\
 -\tilde{x}_{12,13} + \tilde{x}_{23,13} &= 0 \\
 -\tilde{x}_{13,13} - \tilde{x}_{23,13} &= -\hat{h}_{13}
 \end{aligned} \tag{2.17}$$

For demand $\langle 2 : 3 \rangle$, following the same reasoning, the demand equations are given by:

$$\begin{aligned}
 \tilde{x}_{21,23} + \tilde{x}_{23,23} &= \hat{h}_{23} \\
 \tilde{x}_{13,23} - \tilde{x}_{21,23} &= 0 \\
 -\tilde{x}_{13,23} - \tilde{x}_{23,23} &= -\hat{h}_{23}
 \end{aligned} \tag{2.18}$$

The inequalities for the link capacity concerning arcs $1 \rightarrow 2$ and $2 \rightarrow 1$ are given by:

$$\tilde{x}_{12,12} + \tilde{x}_{12,13} \leq \hat{c}_{12}. \tag{2.19}$$

$$\tilde{x}_{21,23} \leq \hat{c}_{21}. \tag{2.20}$$

For arcs $2 \rightarrow 3$ and $3 \rightarrow 2$ the inequalities are:

$$\tilde{x}_{23,13} + \tilde{x}_{23,23} \leq \hat{c}_{23}. \tag{2.21}$$

$$\tilde{x}_{32,12} \leq \hat{c}_{32}. \tag{2.22}$$

And for arc $1 \rightarrow 3$ the inequality is:

$$\tilde{x}_{13,12} + \tilde{x}_{13,13} + \tilde{x}_{13,23} \leq \hat{c}_{13}. \tag{2.23}$$

As arc $3 \rightarrow 1$ does not have any incoming or out coming flow, $\hat{c}_{31}=0$.

Considering now the capacitated problem described in the following example, named Example 5. The network topology used is the one represented in Figure 2.4. The goal of this capacitated problem is to minimize the total routing cost, assuming that the unit cost of every arc is one, $\xi_{arc} = 1$.

With the capacity link inequalities (2.16) - (2.18) and demand equations (2.19) - (2.23), the problem to minimize the total routing cost can be written as:

$$\mathbf{minimize:} \quad \mathbf{F} = \tilde{x}_{12,12} + \tilde{x}_{13,12} + \tilde{x}_{32,12} + \tilde{x}_{12,13} + \tilde{x}_{13,13} + \tilde{x}_{23,13} + \tilde{x}_{21,23} + \tilde{x}_{13,23} + \tilde{x}_{23,23}$$

subject to

$$\begin{aligned}
 \tilde{x}_{12,12} + \tilde{x}_{13,12} &= \hat{h}_{12} \\
 -\tilde{x}_{13,12} + \tilde{x}_{32,12} &= 0 \\
 -\tilde{x}_{12,12} - \tilde{x}_{32,12} &= -\hat{h}_{12} \\
 \tilde{x}_{12,13} + \tilde{x}_{13,13} &= \hat{h}_{13} \\
 -\tilde{x}_{12,13} + \tilde{x}_{23,13} &= 0 \\
 -\tilde{x}_{13,13} - \tilde{x}_{23,13} &= -\hat{h}_{13} \\
 \tilde{x}_{21,23} + \tilde{x}_{23,23} &= \hat{h}_{23} \\
 -\tilde{x}_{21,23} + \tilde{x}_{13,23} &= 0 \\
 -\tilde{x}_{13,23} - \tilde{x}_{23,23} &= -\hat{h}_{23} \\
 \tilde{x}_{12,12} + \tilde{x}_{12,13} &\leq \hat{c}_{12} \\
 \tilde{x}_{21,23} &\leq \hat{c}_{21} \\
 \tilde{x}_{13,12} + \tilde{x}_{13,13} + \tilde{x}_{13,23} &\leq \hat{c}_{13} \\
 \tilde{x}_{23,13} + \tilde{x}_{23,23} &\leq \hat{c}_{23} \\
 \tilde{x}_{32,12} &\leq \hat{c}_{32}
 \end{aligned} \tag{2.24}$$

The candidate paths used in Example 5 are represented in Figure 2.5. The capacity considered for each arc is $\hat{c}_{arc} = (\hat{c}_{12}, \hat{c}_{21}, \hat{c}_{13}, \hat{c}_{31}, \hat{c}_{23}, \hat{c}_{32}) = (10, 10, 10, 10, 15, 15)$, and the demand volume considered for each directed demand is $\hat{h}_d = (\hat{h}_{12}, \hat{h}_{13}, \hat{h}_{23}) = (5, 7, 8)$.

The optimal solution for Example 5, is to route the flow for each directed demand through the direct arc from the source node to the destination node, as follows,

$$\begin{aligned} \hat{x}_{12,12}^{opt} &= 5, \hat{x}_{13,12}^{opt} = 0, \hat{x}_{32,12}^{opt} = 0 \\ \hat{x}_{13,13}^{opt} &= 7, \hat{x}_{21,13}^{opt} = 0, \hat{x}_{32,13}^{opt} = 0 \\ \hat{x}_{23,23}^{opt} &= 8, \hat{x}_{21,23}^{opt} = 0, \hat{x}_{13,23}^{opt} = 0 \\ \mathbf{F}^{opt} &= 20 \end{aligned}$$

In order to compare the Node-Link and Link-Path formulations, the same problem is represented for the Link-Path formulation in example. Figure 2.6 represents the physical and logical topologies for this Example 6. This network consists of three nodes ($V=3$) and three undirected links ($E=3$).

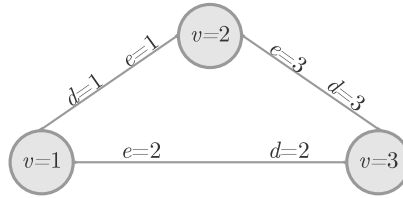


Figure 2.6. Logical and physical topology of the network considered in Example 6.

The variables demand volume and link capacity are the same as considered for Example 5, but adapted to the Link-Path formulation, i.e., $h_d = (h_1, h_2, h_3) = (5, 7, 8)$ $c_e = (c_1, c_2, c_3) = (10, 10, 15)$. The candidate paths used in this example are represented in Table 2.8.

Demand d	Candidate Path P_{dp}
$d = 1$	$P_{11} = \{1\}$ $P_{12} = \{2, 3\}$
$d = 2$	$P_{21} = \{2\}$ $P_{22} = \{1, 3\}$
$d = 3$	$P_{31} = \{3\}$ $P_{32} = \{2, 1\}$

Table 2.8. Candidate paths for each demand in Examples 5 and 6.

The objective function goal is the same as Example 5, to minimize the total routing cost. In Example 6 the unit link cost for every link is also one, $\xi_e = 1$. The unit path cost of each candidate path is represented in Table 2.9.

Candidate Paths P_{dp}	Unit Path Cost ζ_{dp}
$P_{11} = \{1\}$	$\zeta_{11} = 1$
$P_{12} = \{2, 3\}$	$\zeta_{12} = 2$
$P_{21} = \{2\}$	$\zeta_{21} = 1$
$P_{22} = \{1, 3\}$	$\zeta_{22} = 2$
$P_{31} = \{3\}$	$\zeta_{31} = 1$
$P_{32} = \{2, 1\}$	$\zeta_{32} = 2$

Table 2.9. Unit path cost of each candidate path in Example 6.

By considering the candidate paths shown in Table 2.8, the minimization problem can be written using the Link-Path formulation as:

$$\begin{aligned}
\text{minimize: } \mathbf{F} &= x_{11} + 2x_{12} + x_{21} + 2x_{22} + x_{31} + 2x_{32} \\
& x_{11} + x_{12} & & = 5 \\
& & x_{21} + x_{22} & = 7 \\
& & & x_{31} + x_{32} = 8 \\
\text{subject to: } & x_{11} & + x_{22} & + x_{32} \leq 10 \\
& & x_{12} + x_{21} & + x_{32} \leq 10 \\
& & x_{12} & + x_{22} + x_{31} \leq 15 \\
& x_{11}, x_{12}, x_{21}, x_{22}, x_{31}, x_{32} & \geq 0.
\end{aligned} \tag{2.25}$$

The optimal solution for Example 6 is $\mathbf{F}^{opt}=20$, and the flow allocation for each demand is:

$$\begin{aligned}
x_{11}^{opt} &= 5, x_{12}^{opt} = 0 \\
x_{21}^{opt} &= 7, x_{22}^{opt} = 0 \\
x_{31}^{opt} &= 8, x_{32}^{opt} = 0
\end{aligned}$$

In conclusion, the same results are obtained with both formulations with this objective function goal and network topology.

As a final remark regarding the Link-Path and Node-Link formulations it should be noted that the Link-Path formulation requires pre-processing of the candidate paths, whereas the Node-Link formulation does not required this action, since all the possible paths are considered. In order to ensure the optimal solution the Node-Link formulation should always be used, however, in particular in large networks this formalism can be very time consuming. For networks where the best paths can be easily found the Link-Path formulation could be used as it requires less computing [7]. In this dissertation we are going to use the Link-Path formulation presented in subsection 2.2.1, since the choice of the candidate paths is easily done.

2.2.3. Restoration design problem

Having mechanisms of protection or restoration that re-establish resources in case of failure is very important to improve network resilience [7]. In a protection mechanism the restoration of connections happens before the failure, in contrast, restoration only addresses the failure after it happen [7]. With a dedicated protection mechanism link capacity is reserved for set failures and this capacity can not be used in the normal state, assuring the automatic switch over for the protection path. The backup path is a path disjoint from the normal path, meaning these two paths do not share any links. In terms of capacity design problems studied in this work, there is no difference between the formulations when protection or restoration is used.

In the following, we consider a restoration design problem, where link failures are taken into account for the optimization problem [7]. Concerning the network topology of Figure 2.1 and that only one link can be unavailable at a time, there are five possible failure states, denoted by $s=1, \dots, 5$. Each failure state corresponds to a failure in a specific link, hence, $s \equiv e$. When all links are available, in the normal operation state, $s=0$.

The restoration design problem is explained through an example, Example 7. The goal for this example is to minimize the link capacity with the demand volume fully realized for all five failure states and normal operation state. The candidate paths considered for this example are the ones represented in Figure 2.3.

In this example, to introduce the failure states in the Link-Path formulation, the demand equations are changed introducing the dependence on the failure states s . The generalized demand equation for the restoration design problem is [7]:

$$\sum_p x_{dps} = h_d, \quad p = 1, 2, \dots, P_d \quad s = 0, 1, \dots, S \quad d = 1, 2, \dots, D. \quad (2.26)$$

The capacity inequalities must also be modified to consider the state of the different links by introducing one more inequality representing the six states of the network (the normal state and the five failure states). A working link e is represented by $\alpha_{es}=1$ (when $s \neq e$), while $\alpha_{es}=0$ (when $s=e$) characterizes a link e in failure. The generalized capacity inequality for the restoration design problem is [7]:

$$\sum_d \sum_p \delta_{edp} x_{pds} \leq \alpha_{es} y_e, \quad s = 0, 1, \dots, S \quad e = 1, 2, \dots, E. \quad (2.27)$$

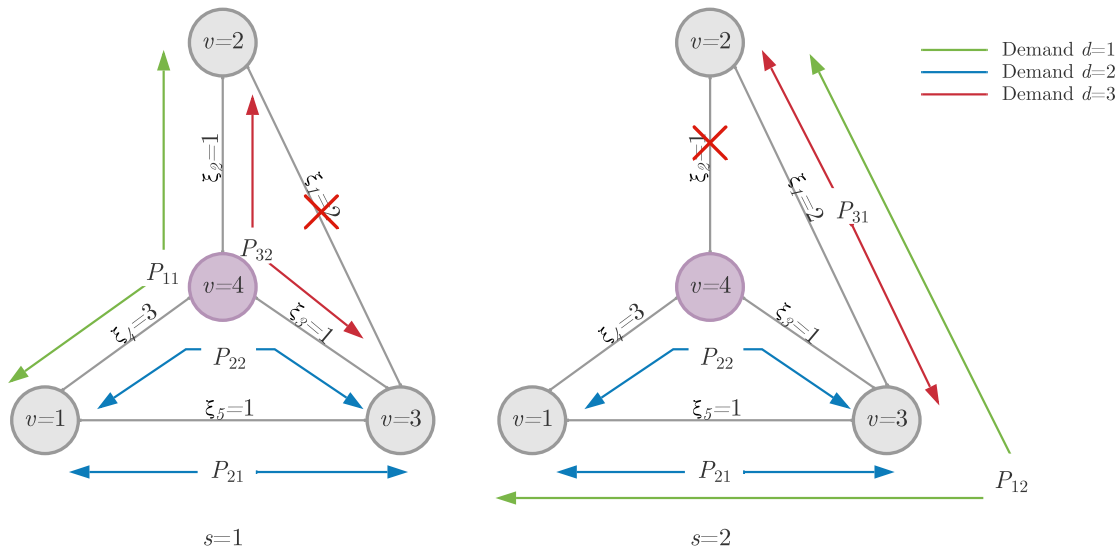


Figure 2.7. Physical topology considered for the network Example 7, for the failure states $s=1$ and $s=2$ and the corresponding candidate paths that can be used for each demand and state.

The objective function goal is to minimize the link capacity ensuring that, for every state failure, the network has the capacity to fully transport all three demands. Figure 2.7 represents two possible failure states $s=1$ and $s=2$. When link $e=1$ fails, the candidate paths P_{12} and P_{31} cannot be used. So, the demands $d=1$ and $d=3$ have to be fully realized by the paths P_{11} and P_{32} . If the failure is in link $e=2$, the paths that cannot be used are P_{11} and P_{32} .

In this example, it is necessary to solve the problem for every failure state and normal state to minimize the cost function of the network, leading to a different flow distribution in each failure state. The solution for the six states is:

$$s = 0 : \quad x_{110}^{opt} = 0 \quad x_{120}^{opt} = 15 \quad x_{210}^{opt} = 20 \quad x_{220}^{opt} = 0 \quad x_{310}^{opt} = 0 \quad x_{320}^{opt} = 10 \quad (2.28a)$$

$$s = 1 : x_{111}^{opt} = 15 \quad x_{121}^{opt} = 0 \quad x_{211}^{opt} = 20 \quad x_{221}^{opt} = 0 \quad x_{311}^{opt} = 0 \quad x_{321}^{opt} = 10 \quad (2.28b)$$

$$s = 2 : x_{112}^{opt} = 0 \quad x_{122}^{opt} = 15 \quad x_{212}^{opt} = 20 \quad x_{222}^{opt} = 0 \quad x_{312}^{opt} = 10 \quad x_{322}^{opt} = 0 \quad (2.28c)$$

$$s = 3 : x_{113}^{opt} = 0 \quad x_{123}^{opt} = 15 \quad x_{213}^{opt} = 20 \quad x_{223}^{opt} = 0 \quad x_{313}^{opt} = 10 \quad x_{323}^{opt} = 0 \quad (2.28d)$$

$$s = 4 : x_{114}^{opt} = 0 \quad x_{124}^{opt} = 15 \quad x_{214}^{opt} = 20 \quad x_{224}^{opt} = 0 \quad x_{314}^{opt} = 0 \quad x_{324}^{opt} = 10 \quad (2.28e)$$

$$s = 5 : x_{115}^{opt} = 15 \quad x_{125}^{opt} = 0 \quad x_{215}^{opt} = 0 \quad x_{225}^{opt} = 20 \quad x_{315}^{opt} = 0 \quad x_{325}^{opt} = 10 \quad (2.28f)$$

From the solutions for every state given by equation (2.28), the link capacity changes depending on the state, resulting in the capacities presented in Table 2.10.

$s=0$	$y_1 = 15$	$y_2 = 10$	$y_3 = 10$	$y_4 = 0$	$y_5 = 35$	$\mathbf{F}=85$
$s=1$	$y_1 = 0$	$y_2 = 25$	$y_3 = 10$	$y_4 = 15$	$y_5 = 20$	$\mathbf{F}=100$
$s=2$	$y_1 = 25$	$y_2 = 0$	$y_3 = 0$	$y_4 = 0$	$y_5 = 35$	$\mathbf{F}=85$
$s=3$	$y_1 = 25$	$y_2 = 0$	$y_3 = 0$	$y_4 = 0$	$y_5 = 35$	$\mathbf{F}=85$
$s=4$	$y_1 = 15$	$y_2 = 10$	$y_3 = 10$	$y_4 = 0$	$y_5 = 35$	$\mathbf{F}=85$
$s=5$	$y_1 = 0$	$y_2 = 25$	$y_3 = 30$	$y_4 = 35$	$y_5 = 0$	$\mathbf{F}=160$

Table 2.10. Link capacity solution for each one of the six states of Example 7.

Analyzing the link capacity solution for each state given in Table 2.10, the maximized link capacity of each link is:

$$y_1^{opt} = 25 \quad y_2^{opt} = 25 \quad y_3^{opt} = 30 \quad y_4^{opt} = 35 \quad y_5^{opt} = 35 \quad (2.29)$$

The optimal cost for this example calculated with equation (2.6) is $\mathbf{F}^{opt}=245$ [7]. The result of this example shows that when restoration design is considered, assuming that the demand volumes are fully realized for all network states, the network cost becomes much higher when compared with Example 3, where there was no protection, giving $\mathbf{F}^{opt}=85$. The Matlab script used to solve this problem is presented in Appendix A.4

Another restoration design problem is the restoration design problem with single backup paths. In this restoration problem the path that has a failure link moves to the designated single backup path to solve the failure situation [7]. The difference between this method and the one presented earlier in this subsection is that the traffic, in a normal scenario, cannot be bifurcated between the normal and backup paths, meaning that the backup path is used only when the normal path is unavailable. Furthermore, the backup path cannot share any links with the normal path, i.e. is a disjoint path. To distinguish the normal path P_{dp} from the backup path, the backup paths are represented by Q_{dpq} , where d represents the demand, $p=1, \dots, P_d$ labels the normal path, and $q=1, \dots, Q_{dpq}$ is the label for the possible backup paths.

The following examples, Examples 8 and 9, consider path restoration with single backup paths using the network described in Figure 2.3. Figure 2.8 represents the normal and backup paths considered for these examples. The normal path corresponds to the lowest cost path, while the backup path is a disjoint path.

As observed in Figure 2.8 the normal paths P_{dp} are disjointed from the backup paths Q_{dpq} . The availability of the normal path P_{dp} for the state s is represented by the binary variable θ_{dps} and the corresponding representation for the backup path availability is ω_{dps} . These two binary variables are related by $\omega_{dps}=1 - \theta_{dps}$. The binary variable θ_{dps} depends on the availability of the link α_{es} , meaning that when the normal path uses link e and this link has failed, $\alpha_{es}=0$, then $\theta_{dps}=0$ and $\omega_{dps}=1$.

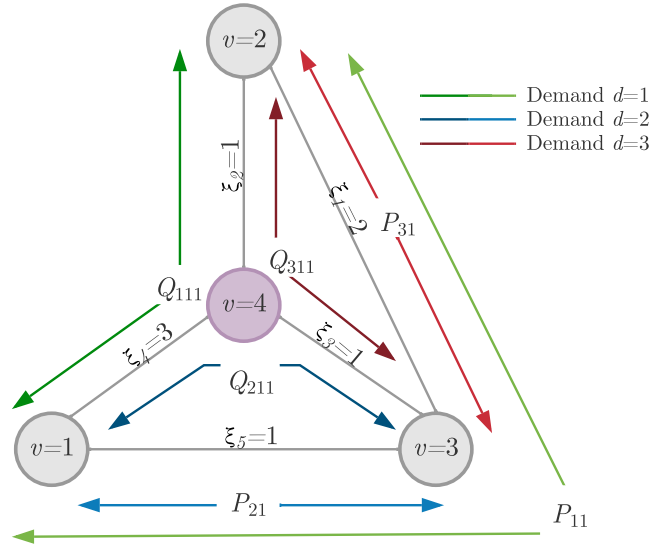


Figure 2.8. Physical topology used for the network Examples 8 and 9 and the corresponding normal and backup paths for each demand.

The link path relation represented in Table 2.4 is identified by δ_{edp} for the normal path, with P_{11} , P_{21} and P_{31} denoting the normal paths, and β_{edpq} is the link path relation for the backup path and is represented in Table 2.11.

Link e	Backup Path Q_{dpq}	$Q_{111} = \{2, 4\}$	$Q_{211} = \{3, 4\}$	$Q_{311} = \{2, 3\}$
$e=1$		0	0	0
$e=2$		1	0	1
$e=3$		0	1	1
$e=4$		1	1	0
$e=5$		0	0	0

Table 2.11. Link-path relations for the backup paths represented in Figure 2.8.

The normal flow for the pair (P_{dp}, Q_{dpq}) is represented by x_{dpq0} . The binary variable u_{dpq} corresponds to the normal flow when set to 1.

The path restoration with single backup paths modifies the capacity and demand constraints shown in Section 2.2.1 to [7]:

$$\sum_p \sum_q x_{dpq0} = h_d, \quad d = 1, 2, \dots, D. \quad (2.30a)$$

$$\sum_q u_{dpq} \leq 1, \quad d = 1, 2, \dots, D \quad p = 1, 2, \dots, P_d. \quad (2.30b)$$

$$x_{dpq0} \leq h_d u_{dpq}, \quad d = 1, 2, \dots, D \quad p = 1, 2, \dots, P_d \quad q = 1, 2, \dots, Q_{dp} \quad (2.30c)$$

$$\sum_d \sum_p \sum_q (\delta_{edp} \theta_{dps} + \beta_{edpq} \omega_{dps}) x_{dpq0} \leq \alpha_{es} y_e, \quad e = 1, 2, \dots, E \quad s = 1, 2, \dots, S. \quad (2.30d)$$

Equation (2.30b) imposes that only one path is going to be used as a backup, and equation (2.30c) imposes that only that pair normal-backup path can transport the demand volume h_d . The new capacity inequality is shown in (2.30d). This inequality considers that if the normal path or the backup path use link e (depending on the value of δ_{edp} and β_{edp}), with

availability depending on the network state (θ_{dps} and ω_{dps}), then, the capacity of this link has to accommodate the demand volume of this path.

For Example 8, as shown in Figure 2.9, the link $e=1$ has failed, the normal paths P_{11} and P_{31} are not available and so, the backup paths Q_{111} and Q_{211} are used.

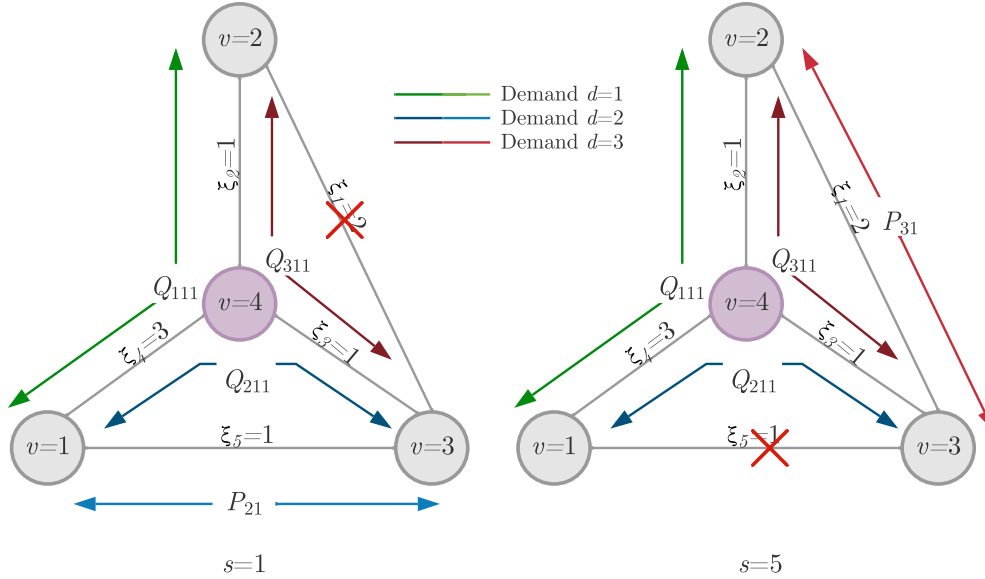


Figure 2.9. Physical topology used for the network Example 8, considering state $s=1$, and Example 9, considering state $s=5$, with the corresponding normal and backup paths for each demand.

The solution for minimizing the capacities in Example 8 has been obtained using Matlab and gives $\mathbf{F}^{opt} = 100$ and the following link capacities,

$$y_1^{opt} = 0 \quad y_2^{opt} = 25 \quad y_3^{opt} = 10 \quad y_4^{opt} = 15 \quad y_5^{opt} = 20. \quad (2.31)$$

Example 9 has link $e=5$ down, affecting the normal paths for demands $d=1$ and $d=2$, P_{11} and P_{21} , which are replaced, respectively by, Q_{111} and Q_{211} , as shown in Figure 2.9. For this example, the solution is $\mathbf{F}^{opt} = 160$, obtained with Matlab and the link capacities are:

$$y_1^{opt} = 10 \quad y_2^{opt} = 15 \quad y_3^{opt} = 20 \quad y_4^{opt} = 35 \quad y_5^{opt} = 0. \quad (2.32)$$

The Matlab script used to solve Examples 8 and 9 is presented in Appendix A.5.

The single path backup allows for the demands to be fully realized, if any of the links fail and the cost objective function is lower compared with the one obtained first in this subsection. In the restoration design problem, since there are no designated backup paths to ensure that the demand volume is fully realized for any of the failure states, it is necessary to have a much higher link capacity, and consequently, the optimum cost function is higher than when a designated disjoint backup path is calculated. However with this mechanism, the links always have the capacity to restore connections. In conclusion, when using single path backup protection, the cost function is lower and guarantees the full realization of every demand volume.

2.2.4. RWA problem

This subsection describes the ILP formulation for solving the RWA problem in wavelength division multiplexing (WDM) transparent optical networks [7]. The nodes used in transparent

WDM networks are called optical cross-connects (OXC) [7]. In this dissertation we assume that there is no wavelength conversion inside these nodes, so the wavelength has to be the same in all links belonging to a path.

In WDM networks, the DVUs and LCUs described in subsection 2.2.1 now correspond to wavelengths and optical fibers, respectively [7]. Each wavelength can, typically, carry 10 Gbps (1 DVU = 10 Gbps) and one optical fiber can transport 100 different wavelengths (1 LCU = 100 DVUs) [7]. The wavelengths can also be called by *colors*.

The variables represented in Table 2.5 have to be adapted to include the wavelengths represented by $c=1,\dots,C$ (where C represents the total number of wavelengths). Table 2.12 summarizes the variables and constraints used in the ILP formulation for WDM networks. The total number of colors used in a optical fiber is represented by z_{ce} with c defining the color and e the link. The flow variable is now denoted by x_{dpc} for demand d , path p and color c since the flow picked includes the color used to satisfy the demand, which ensures the usage of the same color throughout the path, meaning no wavelength conversion is performed. The variable y_e is the capacity of link e expressed in number of fibers and the volume of demand d to be realized in situation s , expressed in number of light-paths is represent by h_{ds} .

Variable	Description
C	Total number of colors of the network
c	$c=1,\dots, C$ denotes a specific color in the network
z_{ce}	Number of times color c is used in link e
h_{ds}	Volume of demand d to be realized in situation s , expressed in number of light-paths
y_e	Capacity of link e expressed in the number of fibers
x_{dpc}	Flow for demand d through path p for color c

Table 2.12. Variables used in RWA problem based on the Link-Path formulation.

To calculate which flow realizes the demand volume for the situation s , the following constraint is used:

$$\sum_p \theta_{dps} \sum_c x_{dpc} \geq h_{ds} \quad d = 1, 2, \dots, D \quad s = 1, 2, \dots, S. \quad (2.33)$$

In this formulation the number of times color c is used in the link e is evaluated by another constraint, given by:

$$\sum_d \sum_p \delta_{edp} x_{dpc} = z_{ce} \quad c = 1, 2, \dots, C \quad e = 1, 2, \dots, E. \quad (2.34)$$

This constraint checks if the path uses link e and if that flow is using color c . The last constraint guarantees that the optical fibers assigned to each link e satisfy all demands for each color c , and is given by:

$$y_e \leq z_{ce} \quad c = 1, 2, \dots, C \quad e = 1, 2, \dots, E. \quad (2.35)$$

Next, we will present three examples using three small network topologies where we will solve the RWA problem using this ILP formulation. In the first example, Example 10, the physical network topology and the candidate paths are described in Figure 2.3. The demand volume for the three demands in the normal situation ($s=0$) is 1, $h_{d0}=1$ and two available colors ($C=2$) are considered. The objective is to minimize the capacity cost. This ILP problem can be written as:

$$\begin{aligned}
 & \mathbf{minimize:} \quad \mathbf{F} = \sum_e \xi_e y_e \\
 & \mathbf{subject\ to:} \quad \sum_p \theta_{dps} \sum_c x_{dpc} \geq h_{ds} \quad d = 1, 2 \quad s = 0 \\
 & \quad \quad \quad \sum_d \sum_p \delta_{edp} x_{dpc} = z_{ce} \quad c = 1, 2 \quad e = 1, 2, \dots, 5 \\
 & \quad \quad \quad y_e \leq z_{ce} \quad c = 1, 2 \quad e = 1, 2, \dots, 5.
 \end{aligned} \tag{2.36}$$

The number of variables and constraints used in (2.36) to solve this RWA problem is described in Table 2.13.

Variable/Constraints	Number
Demand d	3
Candidate paths P_{dp} per demand d	2
Total P_{dp}	6
Flow x_{dpc}	$C \times P_{dp} = 12$
Links e	5
Total number of color c available	2
Number of times color c is used in the link e z_{ce}	1
z_{ce}	$e \times C \times z_{ce} = 10$
Capacity per link y_e	5
Function objective \mathbf{F}	$x_{dpc} + z_{ce} + y_e = 27$

Table 2.13. Number of the variables and constraints needed to solve the RWA problem in Example 10.

The solution obtained for this RWA problem obtained with Matlab is described in Table 2.14 and Figure 2.10.

Demand	Path	Color	Flow
$d=1$	P_{12}	$c=2$	x_{122}
$d=2$	P_{21}	$c=1$	x_{211}
$d=3$	P_{31}	$c=1$	x_{311}

Table 2.14. Solution of Example 10.

The objective function reached in this problem is $\mathbf{F}=3$, meaning that are needed two optical fibers for the two links in use ($e=1,5$) ($\mathbf{F}=\delta_1 e_1 + \delta_5 e_5 = 2 \times 1 + 1 \times 1$). This problem was solved with Matlab script presented in Appendix A.6.

In the next example, Example 11, the physical topology of the network used is described in Figure 2.11. The physical topology for this network consists of six nodes ($V=6$) and eight links ($E=8$). The figure also shows the distance between the nodes in km. The logical topology for this network is a full mesh consisting of fifteen demands ($D=15$).

The objective of this example is to minimize the capacity cost in the normal state ($s=0$). The demand volume considered for all demands in this example is one ($h_{ds}=1$), there are five colors available ($C=5$), and the cost of each link is one ($\xi_e = 1$). The candidate paths for each demand are represented in Table 2.15.

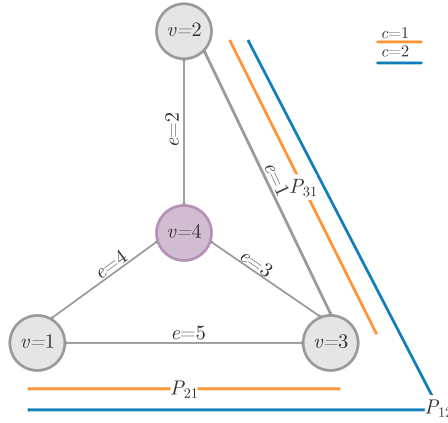


Figure 2.10. Physical topology used for the network Example 10, considering state $s=0$ with two available colors $c=2$.

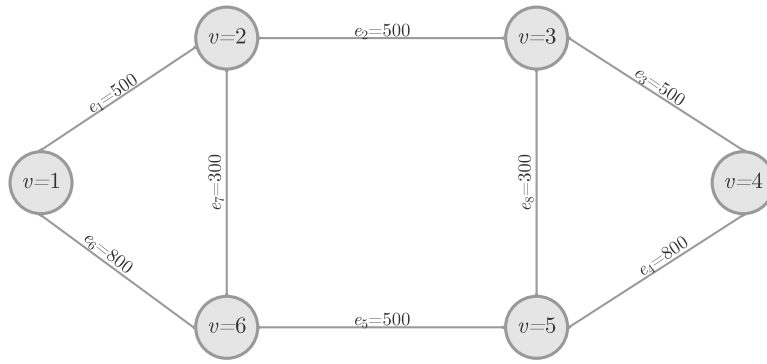


Figure 2.11. Physical topology 6-node example network.

Demand d	Candidate paths P_{dp}
$d=1$	$P_{11} = \{1\}$ $P_{12} = \{6, 7\}$
$d=2$	$P_{21} = \{1, 2\}$ $P_{22} = \{6, 5, 8\}$
$d=3$	$P_{31} = \{1, 2, 3\}$ $P_{32} = \{6, 5, 4\}$
$d=4$	$P_{41} = \{1, 2, 8\}$ $P_{42} = \{6, 5\}$
$d=5$	$P_{51} = \{6\}$ $P_{52} = \{1, 7\}$
$d=6$	$P_{61} = \{2\}$ $P_{62} = \{7, 5, 8\}$
$d=7$	$P_{71} = \{2, 3\}$ $P_{72} = \{7, 5, 4\}$
$d=8$	$P_{81} = \{2, 8\}$ $P_{82} = \{7, 5\}$
$d=9$	$P_{91} = \{7\}$ $P_{92} = \{1, 6\}$
$d=10$	$P_{101} = \{3\}$ $P_{102} = \{8, 4\}$
$d=11$	$P_{111} = \{8\}$ $P_{112} = \{3, 4\}$
$d=12$	$P_{121} = \{2, 7\}$ $P_{122} = \{8, 5\}$
$d=13$	$P_{131} = \{3, 8\}$ $P_{132} = \{4\}$
$d=14$	$P_{141} = \{3, 2, 7\}$ $P_{142} = \{4, 5\}$
$d=15$	$P_{151} = \{5\}$ $P_{152} = \{8, 2, 7\}$

Table 2.15. List of candidate paths for each demand.

The number of variables and constraints needed to solve this example using equations (2.33) to (2.35) is described in Table 2.16.

The solution of the paths used for each demand and the respective color obtained with Matlab is described in Table 2.20 and Figure 2.13.

Variable/Constraints	Number
Demand d	15
Candidate paths P_{dp} per demand d	2
Total P_{dp}	30
Flow x_{dpc}	$C \times P_{dp} = 150$
Links e	8
Number of times color c is used in the link e z_{ce}	1
z_{ce}	$e \times C \times z_{ce} = 40$
Capacity per link y_e	8
Function objective \mathbf{F}	$x_{dpc} + z_{ce} + y_e = 198$

Table 2.16. Number of the variables and constraints need to solve the RWA problem in Example 11.

Demand	Path	Color	Flow
$d=1$	P_{12}	$c=2$	x_{122}
$d=2$	P_{22}	$c=5$	x_{225}
$d=3$	P_{32}	$c=3$	x_{323}
$d=4$	P_{42}	$c=1$	x_{421}
$d=5$	P_{51}	$c=4$	x_{514}
$d=6$	P_{61}	$c=4$	x_{614}
$d=7$	P_{72}	$c=4$	x_{724}
$d=8$	P_{81}	$c=2$	x_{812}
$d=9$	P_{91}	$c=5$	x_{915}
$d=10$	P_{102}	$c=1$	x_{1021}
$d=11$	P_{111}	$c=4$	x_{1114}
$d=12$	P_{121}	$c=1$	x_{1211}
$d=13$	P_{132}	$c=5$	x_{1325}
$d=14$	P_{142}	$c=2$	x_{1422}
$d=15$	P_{152}	$c=3$	x_{1523}

Table 2.17. Solution of Example 11.

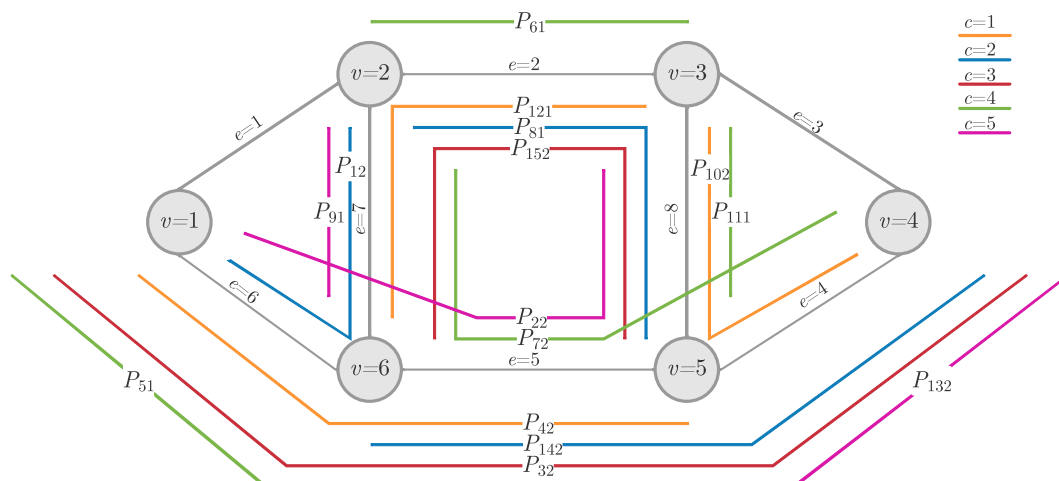


Figure 2.12. Physical topology used for the network in Example 11, considering state $s=0$ with five available colors $c=5$.

The optimal solution found for this example is $\mathbf{F}=6$, so six optical fibers are needed on every link except for links $e=1$ and $e=3$. These links are not utilized by the paths used in the solution.

In the following example, the network considered is still the one shown in Figure 2.11, but instead of solving a RWA problem only the wavelength assignment problem (WA) is solved. The objective of this problem is also to minimize the capacity cost. The paths used were decided using the Link-Path formulation and are represented in Table 2.21.

Demand d	Candidate paths P_{dp}
$d=1$	$P_{11} = \{1\}$
$d=2$	$P_{21} = \{1, 2\}$
$d=3$	$P_{31} = \{6, 5, 4\}$
$d=4$	$P_{42} = \{6, 5\}$
$d=5$	$P_{51} = \{6\}$
$d=6$	$P_{61} = \{2\}$
$d=7$	$P_{71} = \{2, 3\}$
$d=8$	$P_{81} = \{7, 5\}$
$d=9$	$P_{91} = \{7\}$
$d=10$	$P_{101} = \{3\}$
$d=11$	$P_{111} = \{8\}$
$d=12$	$P_{121} = \{8, 5\}$
$d=13$	$P_{131} = \{4\}$
$d=14$	$P_{141} = \{4, 5\}$
$d=15$	$P_{151} = \{5\}$

Table 2.18. Candidate paths for each demand for Example 12.

In Example 12 six colors ($C=6$) are considered and the demand volume considered is one ($h_{ds}=1$) in the normal state ($s=0$). The number of the constraints and variables for this problem used in equations 2.33 to 2.35 are represented in Table 2.23.

Variable/Constraints	Number
Demand d	15
Candidate paths P_{dp} per demand d	1
Total P_{dp}	15
Flow x_{dpc}	$C \times P_{dp} = 90$
Links e	8
Number of times color c is used in the link e z_{ce}	1
z_{ce}	$e \times C \times z_{ce} = 48$
Capacity per link y_e	8
Function objective \mathbf{F}	$x_{dpc} + z_{ce} + y_e = 146$

Table 2.19. Number of the variables and constraints need to solve the WA problem in Example 12.

The solution for the color used in each demand obtained with Matlab for this example is described in Table 2.20 and Figure 2.13.

The optimal solution for Example 12 is $\mathbf{F}=8$, this means that to solve this problem eight optical fibers are needed, one for each link.

Comparing Example 11, which solves a RWA problem, and Example 12, a WA problem, it can be concluded that to obtain the optimal solution in Example 12 one more color and one more optical fiber are needed to satisfy all demand requests. However, since it only has one path available for each demand fewer variables and constraints are needed to solve the problem. Example 11, even though it uses fewer colors, more constraints and variables are needed. For

Demand	Color	Flow
$d=1$	$c=5$	x_{115}
$d=2$	$c=4$	x_{214}
$d=3$	$c=3$	x_{313}
$d=4$	$c=2$	x_{412}
$d=5$	$c=4$	x_{514}
$d=6$	$c=6$	x_{616}
$d=7$	$c=5$	x_{715}
$d=8$	$c=4$	x_{814}
$d=9$	$c=6$	x_{916}
$d=10$	$c=6$	x_{1016}
$d=11$	$c=6$	x_{1116}
$d=12$	$c=5$	x_{1215}
$d=13$	$c=2$	x_{1312}
$d=14$	$c=6$	x_{1416}
$d=15$	$c=1$	x_{1511}

Table 2.20. Solution of Example 12.

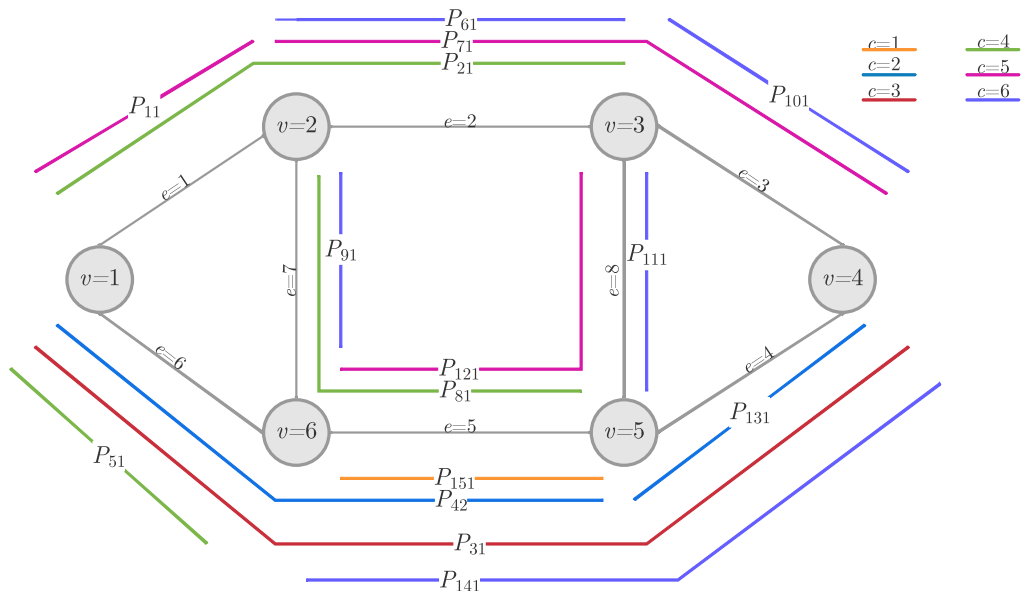


Figure 2.13. Physical topology used for the network in Example 12, considering state $s=0$ with six available colors $c=6$.

networks with more nodes solving the RWA problem can increase the time to find the optimal solution with an ILP solver. The script used in Matlab to solve these problems is available in Appendix A.7.

To validate the RWA formulation presented in [7] we will use the physical network topology shown in Figure 2.14. A comparison between the RWA formulation and the one presented in [9] is done in Appendix A.8

The physical network represented in Figure 2.14, consists of five nodes ($V=5$) and seven undirected links ($E=7$). The logical network consists of eight demands $D=8$. The demands considered for this Example 13 are given in Table 2.21. Table 2.22 shows the candidate paths used for the eight demands, and Table 2.23 shows the variables used to solve the example represented in Figure 2.16.

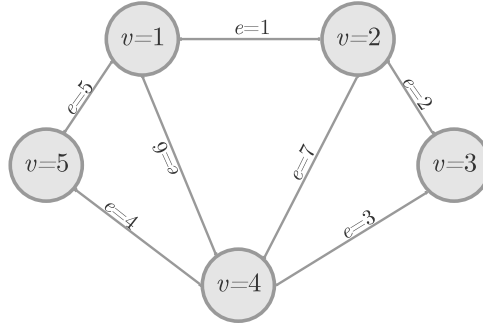


Figure 2.14. Physical topology 5-node example network.

Demand d	Demand pair
$d=1$	[1-3]
$d=2$	[2-4]
$d=3$	[3-1]
$d=4$	[3-5]
$d=5$	[4-2]
$d=6$	[4-5]
$d=7$	[5-3]
$d=8$	[5-4]

Table 2.21. Demand pairs for Example 13.

Demand d	Candidate paths P_{dp}
$d=1$	$P_{11} = \{1, 2\}$ $P_{12} = \{6, 3\}$
$d=2$	$P_{21} = \{7\}$ $P_{22} = \{1, 7\}$
$d=3$	$P_{31} = \{2, 1\}$ $P_{32} = \{3, 6\}$
$d=4$	$P_{41} = \{3, 4\}$ $P_{42} = \{2, 1, 5\}$
$d=5$	$P_{51} = \{7\}$ $P_{52} = \{3, 2\}$
$d=6$	$P_{61} = \{4\}$ $P_{62} = \{6, 5\}$
$d=7$	$P_{71} = \{4, 3\}$ $P_{72} = \{5, 1, 2\}$
$d=8$	$P_{81} = \{4\}$ $P_{82} = \{5, 6\}$

Table 2.22. Candidate paths list for each demand in Example 13.

Variable/Constraints	Count
Demand d	8
Candidate paths P_{dp} per demand d	2
Total P_{dp}	16
Flow x_{dpc}	$C \times P_{dp} = 32$
Links e	14 (undirected)
Number of times color c is used in the link e z_{ce}	1
Total z_{ce}	$e \times C \times z_{ce} = 28$
Total capacity per link y_e	8
Function objective \mathbf{F}	$x_{dpc} + z_{ce} + y_e = 68$

Table 2.23. Number of the variables and constraints need to solve the WA problem in Example 13.

We have solved the RWA problem considering two colors ($C=2$) and one color ($C=1$) and the result is shown in Figures 2.15 ($C=2$) and Figure 2.16 ($C=1$). The value of the objective \mathbf{F} is 12 and 14, respectively for $C=2$ and $C=1$. These results are in agreement with the ones

reported in [9] for the same network scenario and the Matlab code that implements this problem is in Appendix A.8.

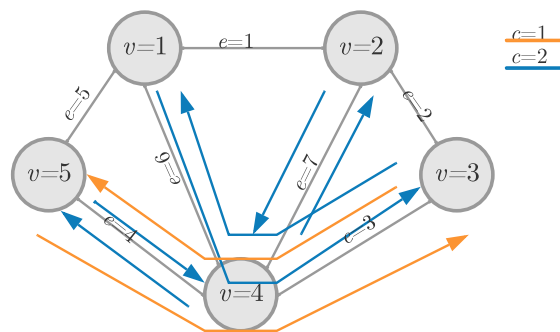


Figure 2.15. Physical topology used for the network in Example 13, considering state $s=0$ with five available colors $c=2$.

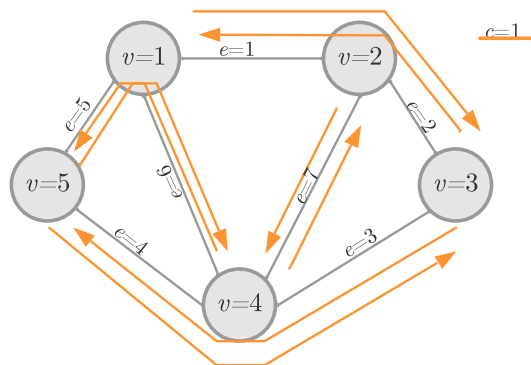


Figure 2.16. Physical topology used for the network in Example 14, considering state $s=0$ with five available colors $c=1$.

2.3. Heuristic algorithms

Heuristic algorithms are powerful tools for solving network design problems in a reasonable amount of time, despite the optimal solution can not be obtained in several scenarios. In this section, we review some of the most common routing and wavelength assignment heuristics used in optical networks [8].

2.3.1. Routing algorithms

Each traffic demand between a source node and a destination node has many candidate paths suitable to satisfy the request. Routing is the process of selecting the most appropriate path for the demand [10]. For a network's physical topology and a given traffic matrix, the goal of the routing algorithm is to find a route for each traffic demand. The traffic matrix can be static or dynamic, dynamic traffic means that the traffic matrix changes over time [8].

With multiple paths available between a source and destination node, the routing algorithm chooses the most appropriate route for each traffic demand based on one or more metrics. The metrics chosen define various paths depending on the goals for the network such as delay-oriented, quality of service (QoS), or utilization-oriented [8]. Some of the most common metrics are: minimize the number of hops in a path, minimize the path distance, or maximize the OSNR of the path [6].

When the traffic matrix is static, the node pairs are always known and static routing algorithms are used. The path configuration can be done manually or using a management system [11]. When the traffic matrix is dynamic, the node pairs change over time, and demand requests between a pair of nodes arrive in different time instants. In this case, a dynamic routing algorithm is used. This algorithm is configured by the control plane [11].

Fixed-Path Routing (FR) is the simplest algorithm to route the demands [6]. In this strategy, all calculations are performed before any traffic is added to the network. A set of candidate paths is generated before the network starts to route demands. From the list of candidate paths, the more suitable is chosen for the source/destination pair, and this path is the only one used to route all demand requests for this pair [6]. Fixed-Path Routing is used with the shortest path algorithm to calculate the shortest path for all demand requests. Some shortest path algorithms used by FR are the Dijkstra algorithm and Yen's k -shortest path algorithm [10].

Another routing algorithm is Fixed Alternate Routing (FAR), which is an updated version of Fixed-Path Routing [10]. In FAR, a set of candidate paths is generated before any demand is added to the network. In this strategy, not just one candidate path is attributed to each source/destination pair. Some M paths are narrowed down from the set of candidate paths, and when there is a new demand request for the source/destination pair, one of the M paths is selected to route the demand request [6].

Using the FAR adds more computational complexity but allows some adaptation to the network state, solving some of the blocking and congestion of the network [10]. However, this algorithm may not find all possible routes between a source/destination pair, therefore, in terms of call blocking, this algorithm is not optimum [10].

2.3.2. Wavelength assignment algorithms

Wavelength Assignment (WA) is an integral part of the network planning process. After the routing algorithm selects the path, determining which links are going to be used, the WA algorithm selects a feasible wavelength for the path from the available wavelengths. Whenever two different paths use the same link, they cannot share the same wavelength [6]. The wavelengths can be assigned to the paths as they arrive, one at a time, after the routing process or in parallel with the routing selection [6].

There are wavelength assignment algorithms for both static and dynamic traffic. In static cases, the goal is to minimize the number of wavelengths in use, and in WA dynamic algorithms the goal is to minimize the network blocking [8].

Some common heuristics solutions used are First-Fit (FF), Most Used (MU), and Random algorithm (R) policies [6].

With the First-Fit policy, the wavelengths are indexed from 1 to W , where W is the maximum wavelength supported on the fiber [8]. The index for this scheme in static networks is fixed and can be ordered with the following strategies: shortest path first (SPF), longest path first (LPF), and random path (RP) ordering [11]. The search for wavelength starts with the lowest index, and the first free wavelength found is assigned to the light-path. Therefore, the higher indexes wavelengths are left unused for future demands. Using this scheme does not require global information of the network [10]. FF performs well in dynamic networks regarding blocking probability and fairness and has lower computational complexity and small overhead [8].

In the Most Used scheme, whenever a new wavelength is required, a new wavelength order is established from most used to least used. The search for an available wavelength proceeds like

in the policy FF. This scheme permits wavelengths already in use to be the first ones considered. This policy at the cost of more information is more adaptive than FF [8]. MU requires global network information and centralized control. It also has longer overheads [8].

With the Random algorithm policy, each available wavelength is listed, and indexed like in the FF scheme [10]. Random algorithm will search all available wavelengths for the route request. From the available wavelengths, one is randomly selected to the light-path. The probability for an available wavelength to be chosen is uniform [8]. This policy does not require global information on the network. The Random algorithm has a higher computation time than the FF policy. This algorithm is also more computationally complex [8].

2.4. Heuristic algorithms and ILP formulations applied in a real network scenario

In this section, the link capacity of an example of a portuguese network topology is studied considering an ILP and a heuristic method for solving the routing problem. The routing algorithm used for the heuristic solution is the Dijkstra algorithm based on the shortest path in distance, and for the ILP solution is a formulation based on the Link-Path formulation considering two candidate paths for each demand.

Figure 2.17 describes the physical topology of an example of a portuguese backbone network [9]. The physical topology of this network consists of 12 nodes ($V=12$) and 18 links ($E=18$). The longest link is between nodes $v=1$ and $v=12$ with 1050 km and the shortest is 47 km between $v=7$ and $v=8$.

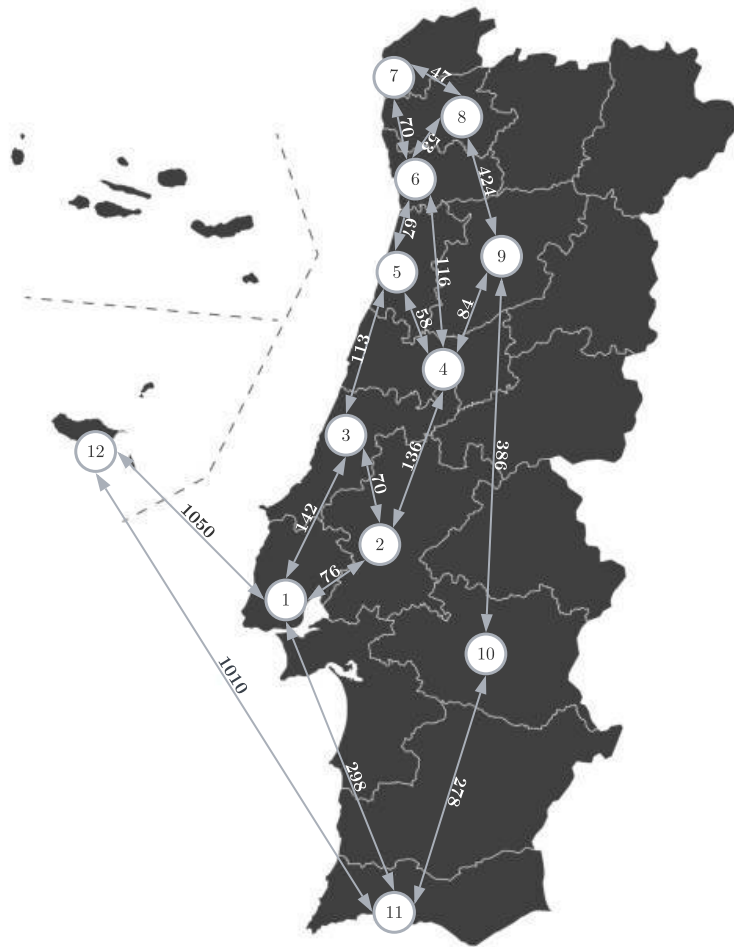


Figure 2.17. Physical topology of a 12-node portuguese backbone network.

The logical topology for the network is a full mesh, so there are demands between all nodes (D=132). The demand volume for each demand is represented in Table 2.24 considering the VC-3 as the traffic unit.

	1	2	3	4	5	6	7	8	9	10	11	12
1	0	104	137	104	207	3322	21	104	91	104	203	75
2	104	0	21	104	21	21	104	21	75	21	21	21
3	137	21	0	104	21	21	125	21	21	63	42	21
4	104	104	104	0	89	21	53	21	21	21	21	21
5	207	21	21	89	0	42	63	21	83	21	42	87
6	3322	21	21	21	42	0	83	42	42	21	21	21
7	21	104	125	53	63	83	0	116	53	42	145	42
8	104	21	21	21	21	42	116	0	21	21	21	21
9	91	75	21	21	83	42	53	21	0	42	21	21
10	104	21	63	21	21	21	42	21	42	0	68	42
11	203	21	42	21	42	21	145	21	21	68	0	21
12	75	21	21	21	87	21	42	21	21	42	21	0

Table 2.24. Traffic Matrix in VC-3.

In the heuristic solution, the Dijkstra algorithm was used for calculate the shortest path for every demand, so only one path for each demand is used. This algorithm finds the path that minimizes the distance between nodes, represented in Figure 2.17 in km.

For the ILP solution, we have considered two paths for each demand. The first path, was also found with the Dijkstra algorithm to minimize the distance between the nodes. The second path considered is the one with fewer hops between nodes, different from the first path.

This problem is solved with equation (2.37). The uncapacitated demand equations, and capacity inequalities are the same described in subsection 2.2.1: Link-Path formulation equation (2.2), and inequality (2.4). The goal for the objective function \mathbf{F} in this problem is to minimize the link capacity with the highest capacity. So, to solve this problem the objective function changes while assigning the paths to each demand, so the link with the highest capacity is always the one being minimized.

$$\begin{aligned}
 & \mathbf{minimize:} \quad \mathbf{F} = \max\{y_e\} \\
 & \mathbf{subject\ to:} \quad \sum_p x_{pd} = h_d, \quad d = 1, 2, \dots, D \\
 & \sum_d \sum_p \delta_{edp} x_{pd} = y_e, \quad e = 1, 2, \dots, E; \quad d = 1, 2, \dots, D; \quad p = 1, 2, \dots, P_d. \\
 & x \geq 0, y \geq 0
 \end{aligned} \tag{2.37}$$

The link capacity for each link obtained with the heuristic and the ILP solution is shown in Table 2.25 and Figure 2.18. Both these solutions were obtained using Matlab, the ILP script is in Appendix A.9.

As observed in Table 2.25 and Figure 2.18, the link capacity in the heuristic solution is not evenly spread. The capacity of the most used links, $e=[1,3]$, $e=[3,5]$, and $e=[5,6]$ is higher than 4000 VC-3, whereas in any other links the average capacity is 339 VC-3. In Figure 2.18, it is shown that for the ILP solution the capacity of the links is better distributed among them. In the ILP solution the highest link capacity used is 2583 VC-3 in links $e=[1,2]$, $e=[2,4]$, and $e=[4,6]$, which is about half of the capacity of the most used link in the heuristic solution ($e=[3,5]$). The capacity decreases around 56%.

Link	Dijkstra	ILP
[1,2]	425	2583
[1,3]	4254	2227
[1,11]	641	730
[1,12]	330	372
[2,3]	188	408
[2,4]	479	2583
[3,5]	4597	2582
[4,5]	381	961
[4,6]	295	2583
[4,9]	659	748
[5,6]	4157	1848
[6,7]	731	752
[6,8]	314	314
[7,8]	116	116
[8,9]	0	0
[9,10]	252	341
[10,11]	214	125
[11,12]	63	21

Table 2.25. Link Capacity for Dijkstra algorithm and ILP.

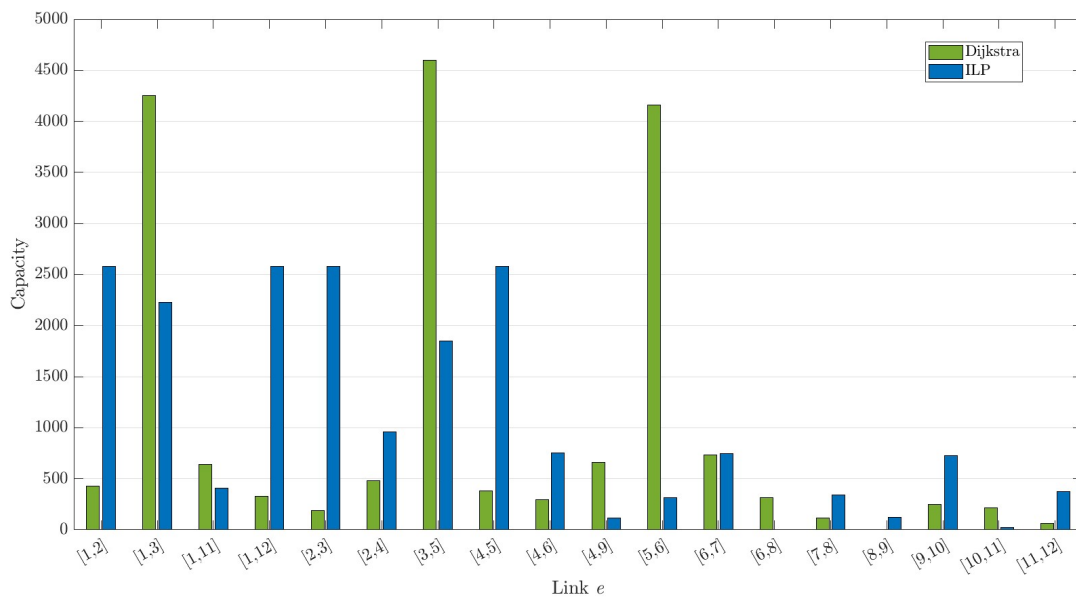


Figure 2.18. Link capacity of the portugese backbone network represented in Figure 2.17 obtained with a heuristic and an ILP solution.

2.5. Conclusion

In this chapter, we review two methods to solve the RWA problem. The first one is the heuristic solution which may not find the optimal solution but solves it in a reasonable amount of time. The second one is the ILP solution that uses a mathematical formulation to optimize the problem to find the optimal solution. For this method two formulations were considered to solve the routing part of the problem, the Link-Path and Node-Link and several examples were presented.

Considering the Link-Path formulation two restoration design problems were presented. The first restoration design problem is a protection problem, therefore the links have enough capacity to ensure that every demand is satisfied even if a link fails. With the restoration design problem with single backup paths the failure is solved only for the specific link after it has failed.

This chapter also presented an ILP formulation to solve the RWA in WDM networks based on the Link-Path formulation.

Considering the solution with heuristic algorithms the RWA problem is solved in two-steps, first the routing and after the wavelength assignment. The routing algorithm chooses the path with the most appropriate route based on the chosen metric. With the Fixed-Path Routing the path list only has one path per demand. In contrast, with the Fixed Alternate Routing the path list can have multiple paths per demand. For the wavelength assignment three heuristic algorithms were considered, First-Fit, Most Used, and Random algorithm.

To end this chapter, the heuristic and ILP solutions for the routing problem were compared in a real network. Our results show that with the ILP solution, the link capacity is distributed more evenly throughout the links than with the heuristic solution.

Physical Layer Impairments in C+L Multiband Optical Networks

3.1. Introduction

The optical signal-to-noise ratio (OSNR) of a light-path can be used as routing metric in a C+L multiband optical network [6]. In this scenario, it is necessary to assess the performance degradation induced by the physical layer impairments (PLIs) along the optical path. The PLIs that most impair the performance of C+L multiband networks are the amplified spontaneous emission (ASE) noise originating in the optical amplifiers, the nonlinear interference (NLI) caused by the Kerr effect, the passband narrowing due to filtering effects, in-band crosstalk due to filtering imperfections and out-band crosstalk due to channels spectrum proximity. Also in these optical networks, the stimulated Raman scattering (SRS) becomes more pronounced due to the larger spectrum used in C+L multiband networks, so this impairment must be taken into account, when assessing the path OSNR, in such systems.

Section 3.2 presents the C+L multiband spectrum organization for both the fixed and flexible grid solutions. In Section 3.3, the impact of the accumulation of ASE noise in a C+L multiband optical network is evaluated. Section 3.4 assesses the impact of the NLI on the OSNR in a C+L multiband optical network, considering first a model based on a Gaussian modulation and, then, a model that takes into account the modulation format. Section 3.5 briefly describe the impact of other PLIs, like the filtering effect and crosstalk. Finally, Section 3.6 concludes the chapter highlighting the chapter main results.

3.2. C+L multiband spectrum

With the C+L multiband solution the spectrum range increases from the 35 nm of the C-band to 90 nm, as illustrated in Figure 3.1, where the nominal central frequencies of the optical channels are defined accordingly with the Telecommunication Standardization Sector of International Telecommunication Union (ITU-T) grid [12]. It is considered a 5 nm gap of unused spectrum between the C and L bands to avoid interferences between the bands [13]. The central frequency in the C band is 193.75 THz and in the L band is 187.75 THz. The first frequency attributed in the whole spectrum is 195.90 THz and the last available frequency is 184.50 THz.

Inside the C+L band, the optical channels can be spaced using a fixed or a flexible grid [1]. With the fixed grid, the same channel bandwidth is allocated to each demand, typically 50 GHz [5]. On the other hand, with a flexible grid, the optical spectrum is divided in smaller frequency slots (FSs) with a spacing of 12.5 GHz [1]. This solution allows to improve transmission capacity and save network resources when comparing to the fixed grid [1]. Accordingly with the ITU-T recommendation (G.694.1), the central frequencies of the FSs allowed for the flexible grid are given by [12]:

$$f_i = 193.1 + n_i \times 0.00625 \quad [\text{THz}] \quad (3.1)$$

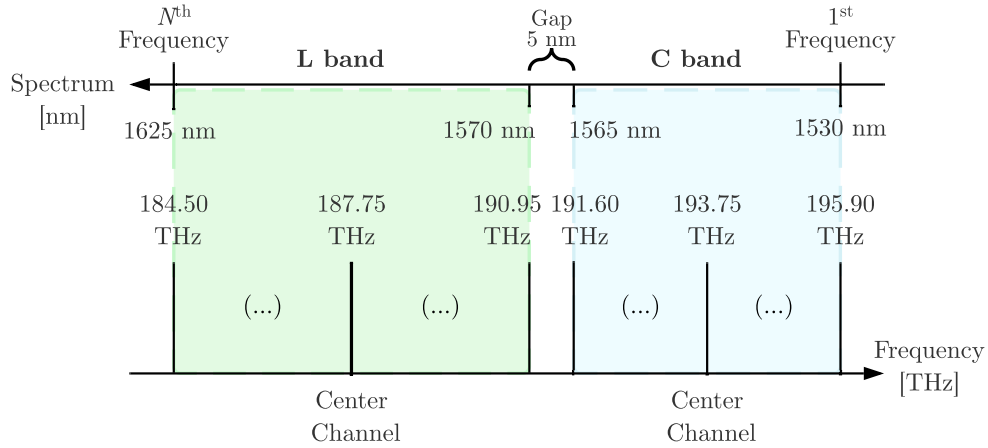


Figure 3.1. C and L band spectrum and corresponding frequencies according with the ITU-T grid.

with the nominal central frequency granularity in THz given by 0.00625 and where n_i is an integer. The frequency slots width (B_{FS}) is given by [12]:

$$B_{FS} = 12.5 \times s_i \quad [\text{GHz}] \quad (3.2)$$

where the slot width granularity is 12.5 GHz and s_i is a positive integer.

In Table 3.1, it is shown the number of channels and the central channel, respectively, for the fixed (ITU-T 50 GHz) and flexible grid (ITU-T 12.5 GHz) scenarios, considering the C-band, L-band and C+L band cases. In the C-band using the fixed grid, there are 87 channels available, whereas with the flexible grid, there are 345 slots available. For the multiband solution considering a 5 nm gap between bands, the flexible grid has 862 frequency slots available, and the fixed grid has 217 channels.

Band	Spectrum [nm]	Range [nm]	Number of channels	Central channel	Number of FSs	Central FSs
C	1530-1565	35	87	44	345	173
L	1565-1625	60	131	66	521	261
C+L	1530-1565 1570-1625	90	217	109	862	431

Table 3.1. Fixed grid with $\Delta_{ch}=50$ GHz and flexible grid with FS=12.5 GHz for C, L, and C+L bands.

3.3. ASE noise accumulation

Erbium-Doped Fiber Amplifiers (EDFA) are used to compensate the optical node and fiber losses, extending the transmission reach to hundreds or thousands of kms. Figure 3.2 represents an optical amplified link with N spans between two nodes, and it shows that EDFAs can be used as a post, in-line, and pre-amplifiers. The post-amplifier compensates for the node losses and boosts the signal that leaves the source node. In-line and pre-amplifiers are used to compensate the fiber attenuation along the optical path.

In this work, the gain of the pre-amplifier G_{pre} is set to compensate exactly the previous links losses,

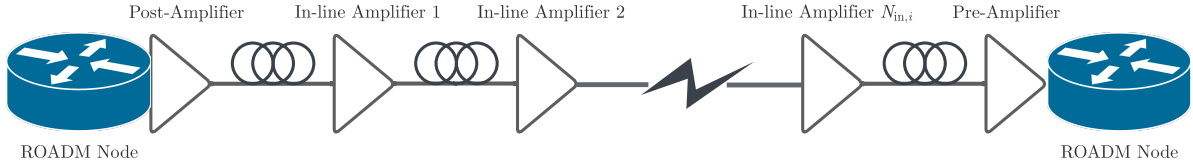


Figure 3.2. Schematic of an optical amplified generic link i between two network nodes.

$$G_{pre} = L_{sec} \times \alpha \quad (3.3)$$

where the link's length is represented by L_{sec} and α is the fiber attenuation coefficient, which is assumed, to also include the losses of splices and connectors. The amplifier's gain for the pre-amplifier has to satisfy the maximum gain G_{max} of the EDFA. If the gain of the pre-amplifier calculated using equation (3.3) exceeds the maximum gain G_{max} , then in-line amplifiers have to be added to that specific fiber link, ensuring that the EDFAs can fully compensate the link losses. The number of in-line amplifiers used in generic link i is, then, calculated by:

$$N_{in,i} = \left\lceil \frac{G_{pre}}{G_{max}} \right\rceil - 1 \quad (3.4)$$

When using in-line amplification, the gain of the in-line amplifiers and pre-amplifier is assumed equal and is obtained with:

$$G_{in} = \left\lceil \frac{G_{pre}}{N_{in,i} + 1} \right\rceil - 1 \quad (3.5)$$

Furthermore, we assume that all the other characteristics of the in-line amplifiers are the same as the ones of the pre-amplifier, namely the noise figure, f_n , and optical bandwidth, B_0 . The post-amplifier gain is considered to be the same for every link, $G_{pos,i}=18$ dB [14], assuming that a route and select architecture is used for the ROADM nodes [14].

Knowing the amplifiers gain required to compensate for the overall losses, the power of the ASE noise per polarization generated by a pre, in-line, and post-amplifier must be calculated. The ASE noise power of the pre and post-amplifiers depends on the link i , and the ASE noise power of the in-line amplifier depends on the link i , and span j , and are given, respectively, by [15]:

$$p_{ASE,pre,i} = \frac{f_{n,pre,i}}{2} (g_{pre,i} - 1) h \nu_0 B_0 \quad (3.6)$$

$$p_{ASE,pos,i} = \frac{f_{n,pos,i}}{2} (g_{pos,i} - 1) h \nu_0 B_0 \quad (3.7)$$

$$p_{ASE,in,i,j} = \frac{f_{n,in,i,j}}{2} (g_{in,i,j} - 1) h \nu_0 B_0 \quad (3.8)$$

where the pre-amplifiers gain $g_{pre,i}$ is set to be the equal to the in-line amplifiers gain $g_{in,i,j}$, and $g_{pos,i}$ is the post-amplifiers gain. The Planck constant is $h = 6.626 \times 10^{-34}$ J/s, ν_0 represents the optical frequency of a WDM channel (which in the following studies is considered to be the WDM central channel frequency), and B_0 the optical bandwidth, which in coherent detection systems is equal to the symbol rate $R_{s,l}$. The noise figures represented by $f_{n,pre,i}$, $f_{n,in,i,j}$ and $f_{n,pos,i}$ depend on the type of amplifier and on the post, in-line and pre-amplifier gains. Considering that the noise figure is 5 dB for the maximum amplifier gain of 25 dB and 7 dB for a gain of 15 dB [14], the noise figure of each amplifier is calculated, in dB, with:

$$F_n = -0.2G_k + 10 \quad \text{where } k = \textit{pos} \textit{ or } \textit{in} \textit{ or } \textit{pre}. \quad (3.9)$$

The total $\text{OSNR}_{tot,m}$ is used to quantify the impact of the ASE noise generated by all the amplifiers along an optical path composed of several links n_{links} , in channel m , as the one depicted in Figure 3.2, and is calculated using [14]:

$$\frac{1}{\text{OSNR}_{tot,m}} = \sum_{i=1}^{n_{links}} \left(\frac{1}{\text{OSNR}_{pos,i}} + \frac{1}{\text{OSNR}_{pre,i}} + \sum_{j=1}^{N_{in,i}} \frac{1}{\text{OSNR}_{in,i,j}} \right) \quad (3.10)$$

where $\text{OSNR}_{pos,i}$, $\text{OSNR}_{pre,i}$ and $\text{OSNR}_{in,i,j}$ correspond, respectively, to the OSNRs originated at the output of each post, in-line and pre-amplifiers, which are obtained by:

$$\text{OSNR}_k = \frac{p_m}{2 \times p_{ASE,k}} \quad \text{where } k = \textit{pre}, \textit{i}, \textit{ or } \textit{pos}, \textit{i}, \textit{ or } \textit{in}, \textit{i}, \textit{j}. \quad (3.11)$$

where p_m is the power of the channel m and $p_{ASE,k}$ is the ASE noise power of each amplifier calculated with equations (3.6)-(3.8).

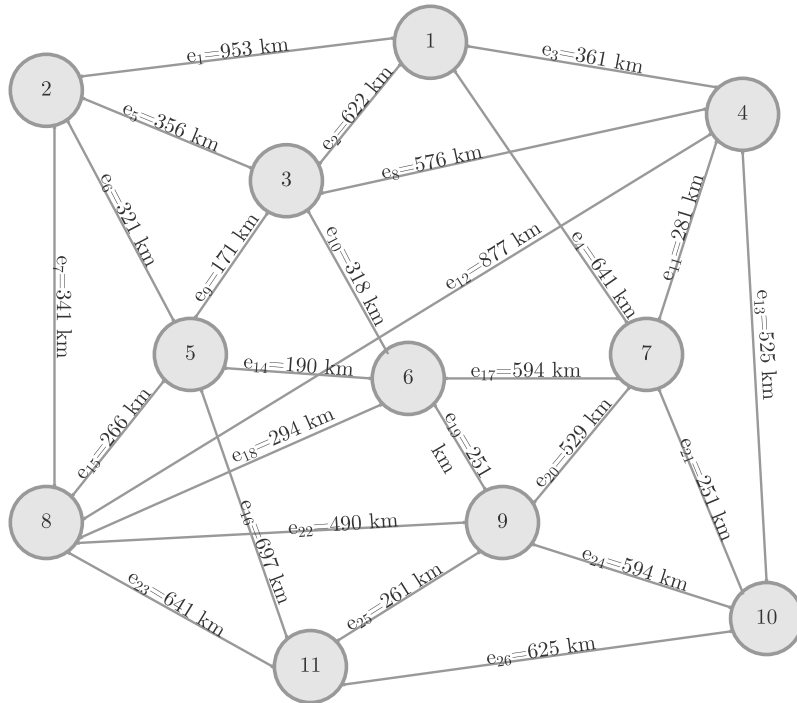


Figure 3.3. COST 239 optical network, with 11 nodes, 26 links represented by e_i (where $i=1 \dots 26$), and corresponding link distances.

In the following, an example of the $\text{OSNR}_{tot,m}$ calculation in the C-band (the wavelength ranges from 1530 to 1565 nm, and the frequency span is 195.9-191.6 THz) with the channel spacing of 50 GHz for the optical network COST 239 [16], represented in Figure 3.3, is performed. The physical topology of the network represented in Figure 3.3 consists of eleven nodes ($V=11$) and twenty-six links ($E=26$). The longest link in this topology is e_1 with 953 km and the shortest link is e_9 between nodes $v=3$ and $v=5$ with 171 km. In this example, only four demands $d=1, \dots, 4$ are considered as represented in Table 3.2, and the OSNR of each path is calculated at the receiver input using the system parameters shown in Table 3.3.

For each demand, five candidate paths are considered, as represented in Table 3.4. The shortest candidate path is the first one P_{d1} , and the longest in the list is the fifth path P_{d5} . Considering all demands, the shortest is path P_{31} with 361 km, and the longest is P_{35} with 1815

Demand d	Demand pair
$d = 1$	[1-2]
$d = 2$	[1-3]
$d = 3$	[1-4]
$d = 4$	[1-5]

Table 3.2. Demand pairs for demands 1 to 4 in COST 239 network.

Parameters	Values
Channel Spacing Δ_{ch}	50 GHz
Total number of channels N_{ch}	87
Frequency of the central channel ν_0	193.70 THz
Fiber attenuation coefficient α	0.25 dB/km
Symbol rate $R_{s,l}$	32 Gbaud
Average launch signal power per channel P_m	0 dBm
Amplifier maximum gain G_{max}	25 dB

Table 3.3. WDM system parameters used to calculate the OSNR for demands 1 to 4 in COST 239 network.

Demand d	Candidate Paths P_{dp}
$d = 1$	$P_{11} = \{1\}$ $P_{12} = \{2, 5\}$ $P_{13} = \{2, 9, 6\}$ $P_{14} = \{3, 8, 5\}$ $P_{15} = \{2, 9, 15, 7\}$
$d = 2$	$P_{21} = \{2\}$ $P_{22} = \{3, 8\}$ $P_{23} = \{1, 5\}$ $P_{24} = \{1, 6, 9\}$ $P_{25} = \{4, 11, 8\}$
$d = 3$	$P_{31} = \{3\}$ $P_{32} = \{4, 11\}$ $P_{33} = \{2, 8\}$ $P_{34} = \{4, 21, 13\}$ $P_{35} = \{2, 10, 17, 11\}$
$d = 4$	$P_{41} = \{2, 9\}$ $P_{42} = \{3, 8, 9\}$ $P_{43} = \{2, 10, 14\}$ $P_{44} = \{1, 6\}$ $P_{45} = \{2, 5, 6\}$

Table 3.4. Candidate paths for the four demands considered in the COST 239 network.

km. Consequently, the shortest and the longest paths are the ones that have a lower and higher number of amplifiers, respectively. Path P_{31} uses five amplifiers (one pre-amplifier, one post amplifier, and three in-line amplifiers), while path P_{35} has 24 amplifiers, (four pre-amplifiers, four post-amplifiers, and sixteen in-line amplifiers). The maximum number of nodes in the candidate path is five nodes, in paths P_{15} and P_{35} , and the lower number of nodes is two, in the direct paths P_{11} , P_{21} and P_{31} .

To calculate the ASE noise power at the output of each amplifier used in each path, first, it is necessary to find the number of in-line amplifiers in each link, using equations (3.3) and (3.4). The noise figure for the amplifiers depends on these gains and is calculated with equation (3.9). The number of in-line amplifiers, the respective gains of each in-line and pre-amplifier, and noise figures are shown in Table 3.5, for the optical links belonging to the candidate paths shown in Table 3.4. The post-amplifier gain and noise figure are the same in all links. For this example, we have considered $G_{pos}=18$ dB [14] and, so, $F_{n,pos}=6.4$ dB calculated with equation (3.9). Table 3.5 also presents the results of the total ASE noise power generated in two polarizations by the post, in-line, and pre-amplifiers. The total ASE noise power along a link is calculated by summing the ASE noise power generated by each in-line amplifier need in link e_i calculated with equation (3.8), the noise power of the pre-amplifiers calculated with equation (3.6) and the ASE noise power generated by the post-amplifiers calculated with equation (3.7).

From Table 3.5, the longest link, e_1 , is the one that needs more in-line amplifiers to compensate for the fiber losses, and consequently, leads to the higher total ASE noise power. The link that requires amplifiers with the highest gain is e_{14} with $G_{pre}=24.8$ dB. The shortest link of this network topology e_9 is also the one that introduces the lower ASE noise power. The total OSNR

Link e	Number of in-line amplifiers $N_{in,i}$	Gain [dB] G_{pre}	Noise Figure [dB] $F_{n,pre}$	ASE noise power [μW] $2p_{ASE}$
$e_1 = [1, 2]$	9	23.8	5.2	34.06
$e_2 = [1, 3]$	6	22.2	5.6	18.22
$e_3 = [1, 4]$	3	22.6	5.5	18.22
$e_4 = [1, 7]$	6	22.9	5.4	20.52
$e_5 = [2, 3]$	3	22.3	5.6	10.96
$e_6 = [2, 5]$	3	20.1	6	7.666
$e_7 = [2, 8]$	3	21.4	5.7	9.578
$e_8 = [3, 4]$	5	24	5.2	21.53
$e_9 = [3, 5]$	1	21.4	5.7	5.297
$e_{10} = [3, 6]$	3	19.9	6	7.441
$e_{11} = [4, 7]$	2	23.4	5.3	10.28
$e_{13} = [4, 10]$	5	21.9	5.6	14.89
$e_{14} = [5, 6]$	1	23.8	5.3	7.613
$e_{15} = [5, 8]$	2	22.2	5.6	8.382
$e_{17} = [6, 7]$	5	24.8	5.1	24.57
$e_{21} = [7, 10]$	2	20.9	5.8	6.876

Table 3.5. Number of in-line amplifiers needed in link e_i , gain of each pre and in-line amplifier and corresponding noise figure for each optical link, and total ASE noise power of the links belonging to the candidate paths used in the four demands in COST 239 network.

for each candidate path is calculated using equations (3.10) and (3.11) and the corresponding results are presented in Table 3.6.

P_{dp}	OSNR $_{tot,m}$ [dB]	P_{dp}	OSNR $_{tot,m}$	P_{dp}	OSNR $_{tot,m}$	P_{dp}	OSNR $_{tot,m}$	P_{dp}	OSNR $_{tot,m}$
P_{11}	14.7	P_{12}	15.4	P_{13}	15.1	P_{14}	13.6	P_{15}	13.8
P_{21}	17.4	P_{22}	14.8	P_{23}	13.5	P_{24}	13.3	P_{25}	12.8
P_{31}	19.4	P_{32}	15.1	P_{33}	14	P_{34}	13.7	P_{35}	12.2
P_{41}	16.3	P_{42}	14.2	P_{43}	14.8	P_{44}	13.8	P_{45}	14.3

Table 3.6. OSNRs for the candidate paths for the four demands considered in COST 239 network.

From the results of the total OSNR in the candidate paths presented in Table 3.6, the path with the lowest OSNR is the longest and the one that passes through the higher number of amplifiers, P_{35} . As expected, paths that use longer links lead also to lower OSNRs. For example, in candidate path P_{23} that uses link e_1 and passes through sixteen amplifiers, the OSNR is lower than in path P_{15} that crosses twenty amplifiers, but has shorter links, leading to lower ASE noise power accumulation. The path with the highest OSNR is the direct path that uses the shortest link, P_{31} . Analyzing the OSNR results in Table 3.6, the candidate path that is chosen to serve each demand is the path with the best OSNR, i.e. the highest OSNR, as highlighted in Table 3.7.

Demand d	Path P_{dp}	OSNR $_{tot,m}$ [dB]
$d = 1$	$P_{12} = \{2, 5\}$	15.4
$d = 2$	$P_{21} = \{2\}$	17.4
$d = 3$	$P_{31} = \{3\}$	19.4
$d = 4$	$P_{41} = \{2, 9\}$	16.3

Table 3.7. Optical paths with highest OSNR for the four demands considered in COST 239 network.

If the EDFA considered had a lower maximum gain of 23 dB instead of 25 dB as considered in Table 3.3, the longer links would require more spans with shorter length. In particular, for a maximum gain of 23 dB links e_1 , e_8 , e_{11} and e_{17} need one more span than when the EDFA maximum gain is 25 dB, which results on spans 8.7 km shorter in e_1 and 23.4 km in e_{11} . This leads to a lower ASE noise power accumulation in those links that would result in higher OSNR. For example, in P_{11} that only uses e_1 , the OSNR with only ASE noise is 16 dB, 1.3 dB higher than the result shown in Table 3.6. The results in the other paths are presented in Table B.1 of Appendix B.

3.4. Nonlinear interference and stimulated Raman scattering

In this section, the impact of the NLI power on the calculation of the OSNR is assessed. In this case, equation (3.11) is rewritten as [17]:

$$osnr_k = \frac{p_m}{2p_{ASE,k} + p_{NLI}} \quad \text{where } k = pre, i, \text{ or } pos, i, \text{ or } in, i, j. \quad (3.12)$$

where the NLI power, p_{NLI} , is calculated by:

$$p_{NLI} = \eta_{GN} \cdot p_m^3 \quad (3.13)$$

where η_{GN} is the NLI coefficient after N_{spans} spans depending on the central frequency of the channel m , which is referred in this section as channel of interest (COI) [17]. To calculate the NLI coefficient, we use the theory described in [17] that relies on the cross-phase modulation (XPM) assumption. Hence, the NLI coefficient after N_{spans} at the center channel frequency f_m is calculated with:

$$\eta_{GN}(f_m) \approx \sum_{j=1}^{N_{spans}} \left[\frac{p_{m,j}}{p_m} \right]^2 \times [\eta_{SPM,j}(f_m) N_{spans}^\varepsilon + \eta_{XPM,j}(f_m)] \quad (3.14)$$

where the coherence factor ε is $\varepsilon=0$, for incoherent accumulation of NLI along multiple fiber spans, or $\varepsilon \neq 0$, if coherent accumulation is considered. In the latter case, the coherence factor must be calculated using closed-form formulas or numerically, for each optical path considered [18]. The launch power of the COI m in the j span is represented by $p_{m,j}$. The coefficient $\eta_{XPM,j}$ is the closed-form approximation of the XPM contribution in span j and $\eta_{SPM,j}$ is the closed-form approximation of the self-phase modulation (SPM) contribution [17], given, respectively by:

$$\eta_{XPM}(f_m) \approx \frac{32}{27} \sum_{k=1, k \neq m}^{N_{ch}} \left(\frac{p_k}{p_m} \right)^2 \frac{\gamma^2}{B_k \phi_{m,k} \bar{\alpha} (2\alpha + \bar{\alpha})} \left[\frac{T_k - \alpha^2}{\alpha} \arctan \left(\frac{\phi_{m,k} B_m}{\alpha} \right) + \frac{A^2 - T_k}{A} \arctan \left(\frac{\phi_{m,k} B_m}{A} \right) \right] \quad (3.15)$$

$$\eta_{SPM}(f_m) \approx \frac{4}{9} \frac{\gamma^2}{B_m^2 \phi_m \bar{\alpha} (2\alpha + \bar{\alpha})} \left[\frac{T_m - \alpha^2}{\alpha} \arcsin \left(\frac{\phi_m B_m^2}{\pi \alpha} \right) + \frac{A^2 - T_m}{A} \arcsin \left(\frac{\phi_m B_m^2}{\pi A} \right) \right] \quad (3.16)$$

with $\phi_m = \frac{3}{2} \pi^2 (\beta_2 + 2\pi \beta_3 f_m)$, $T_m = (\alpha + \bar{\alpha} - P_{tot} C_r f_m)^2$, $A = \alpha + \bar{\alpha}$, $\alpha = \bar{\alpha}$, $\phi_{m,k} = 2\pi^2 (f_k - f_m) [\beta_2 + \pi \beta_3 (f_k + f_m)]$, and $T_k = (\alpha + \bar{\alpha} - P_{tot} C_r f_k)^2$. The COI channel bandwidth is represented by B_m , B_k is the bandwidth of k -th interfering channel, and P_{tot} is the total

transmitted optical power at the input of the fiber link. The Raman gain slope is represented by C_r and the nonlinear coefficient γ is calculated with,

$$\gamma = \frac{2\pi\bar{n}_2}{A_{eff}\lambda_0} \quad (3.17)$$

with nonlinear refractive index represented by \bar{n}_2 , A_{eff} is the fiber effective area and λ_0 is the reference wavelength. In equations (3.15) and (3.16), the attenuation coefficient should be substituted in linear units [Np/m], using,

$$\alpha[\text{Np/m}] = \frac{\alpha[\text{Np/m}]}{4.343} \times 10^{-3} \quad (3.18)$$

The group velocity dispersion parameter β_2 and third order dispersion parameter β_3 are calculated, respectively, with

$$\beta_2 = -\frac{D_{\lambda_0}\lambda_0^2}{2\pi c_{light}} \quad (3.19)$$

$$\beta_3 = \frac{\lambda_0^2}{(2\pi c_{light})^2} \times (\lambda_0^2 S_0 + 2\lambda_0 D_{\lambda_0}) \quad (3.20)$$

where D_{λ_0} is the fiber dispersion parameter at the reference wavelength, λ_0 , S_0 the dispersion slope at the same wavelength and c_{light} is the speed of light. Notice that in equation (3.12), although only the NLI power is present in the OSNR formula, the SRS effect (power transfer from lower to higher channel wavelengths) is included in equations (3.14)-(3.16). The formulation developed in [17] is valid for optical bandwidths up to 15 THz, much larger than the C+L bandwidth.

To validate the Matlab implementation of the NLI formulation, Figure 6 of [17] has been obtained (see Figure 3.4). This figure represents the NLI coefficient as a function of the channel frequency without SRS ($C_r=0$) and with SRS ($C_r=0.028$ 1/W/km/THz), considering both coherent ($\varepsilon \neq 0$) and incoherent ($\varepsilon=0$) scenarios. The parameters used to obtain Figure 3.4 are in Table 3.8.

Parameters	Values
Channel Spacing Δ_{ch}	40 GHz
Total number of channels N_{ch}	251
Channel launch power p_m	0 dBm
Reference wavelength λ_0	1550 nm
Symbol Rate $R_{s,l}$	40 Gbaud
Dispersion D_{λ_0}	17 ps/nm/km
Dispersion slope S_0	67 fs/nm ² /km
Fiber effective area A_{eff}	80 μm^2
NL coefficient	1.2 1/W/km
Fiber attenuation coefficient α	0.2 dB/km
Number of spans $N_{spans,i}$	6

Table 3.8. Parameters used to obtain Figure 3.4.

From Figure 3.4 without SRS, the NLI coefficient increases with the channel frequency increase due to the third order dispersion β_3 , since the lower the frequency the higher is the dispersion, leading to lower NLI penalties [17]. With SRS, due to the power transfer, the power of the channels with lower frequency is enhanced, and as a result those channels experience

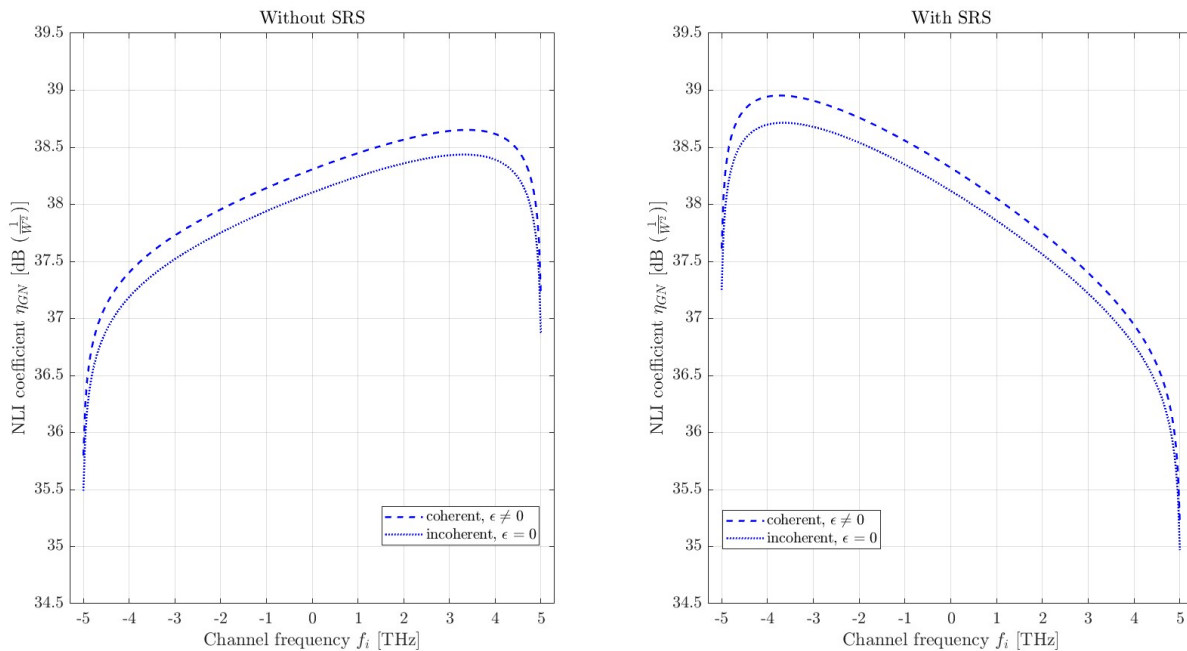


Figure 3.4. NLI coefficient as a function of the channel frequency without SRS and with SRS, considering both coherent and incoherent scenarios with the parameters of Table 3.8.

a higher non-linearity. With and without SRS, the estimated NLI coefficient is higher for the coherent scenario than for the incoherent one. The average gap between the coherent and incoherent accumulations without SRS is 0.1 dB and with SRS is 0.2 dB [17]. Using an incoherent accumulation simplifies the formalism, since the NLI noise can be calculated at the end of each link separately, and adds only a slight loss of accuracy. As the results shown in Figure 3.4 are very similar to the ones presented in Figure 6 of [17], the NLI formulation implementation can be considered validated.

Considering the example of the $\text{OSNR}_{tot,m}$ calculations in the C-band presented in Section 3.3, for the COST 239, the impact of NLI is going to be included next in that example. The parameters used to calculate the OSNR with NLI are presented in Tables 3.3 and 3.9.

Parameters	Values
Dispersion D_{λ_0}	17 ps/nm/km
Dispersion slope S_0	67 fs/nm ² /km
Reference wavelength λ_0	1550 nm
Raman gain slope C_r	0.028 1/W/km/THz
Nonlinear refractive index \bar{n}_2	2.6×10^{-20} m ² /W
Fiber effective area A_{eff}	80 μm^2
Coherent factor ε	0
Fiber attenuation coefficient α	5.756×10^{-5} Np/m
Group velocity β_2	-2.168×10^{-26} s ² /m
Third order dispersion parameter β_3	1.447×10^{-40} s ³ /m
Total transmitted optical power P_{tot}	87 mW

Table 3.9. WDM system parameters used to calculate the OSNR with NLI and SRS for the four demands considered in COST 239 network.

The COI channel considered to calculate the NLI power is the central channel, $m=44$, so the frequency of this channel (in lowpass equivalent form) is $f_m=0$. The WDM channel

frequencies range from $f_k = [-2.2; 2.2]$ THz. With the formulation proposed in [17], the length of each span does not influence the calculations of the XPM and SPM contributions, so for the COI m , $\eta_{XPM,j} = 442.84$ dB obtained with equation (3.15) and $\eta_{SPM,j} = 112.61$ dB reached using equation (3.16). The coherence factor considered for this example is zero, so incoherent accumulation of NLI is considered along the spans. Therefore, the NLI power can be calculated at the end of each optical link, independently of the optical path. Table 3.10 shows the links used by the 20 candidate paths, the number of spans in each link and the NLI power at each link end.

Link e	Number of spans N_{spans}	NLI coefficient $[10^3/W^2] \eta_{GN}$	NLI noise power $[\mu W] p_{NLI}$
$e_1 = [1, 2]$	10	5.515	5.515
$e_2 = [1, 3]$	7	3.860	3.860
$e_3 = [1, 4]$	4	2.206	2.206
$e_4 = [1, 7]$	7	3.860	3.860
$e_5 = [2, 3]$	4	2.206	2.206
$e_6 = [2, 5]$	4	2.206	2.206
$e_7 = [2, 8]$	4	2.206	2.206
$e_8 = [3, 4]$	6	3.309	3.309
$e_9 = [3, 5]$	2	1.103	1.103
$e_{10} = [3, 6]$	4	2.206	2.206
$e_{11} = [4, 7]$	3	1.655	1.655
$e_{13} = [4, 10]$	6	3.309	3.309
$e_{14} = [5, 6]$	2	1.103	1.103
$e_{15} = [5, 8]$	3	1.655	1.655
$e_{17} = [6, 7]$	6	3.309	3.309
$e_{21} = [7, 10]$	3	1.655	1.655

Table 3.10. Number of spans needed in each link, NLI coefficient and noise power at the end of each link used by the candidate path for the four demands considered in the COST 239 network.

By analyzing Table 3.10, the link with the higher NLI noise power is e_1 , since this link is also the one with the higher number of spans. The links e_9 and e_{14} with a smaller number of spans are the links with the lowest NLI noise power. For links with different distances but with the same number of spans, ($e_3=361$ km and $e_6=321$ km), the NLI noise powers and coefficients predicted by the formulation (3.14)-(3.16) are the same. With the results of Table 3.10, the OSNR considering only the NLI noise is calculated for each candidate path and the results are presented in Table 3.11.

P_{dp}	OSNR $_{tot,m}$ [dB]	P_{dp}	OSNR $_{tot,m}$	P_{dp}	OSNR $_{tot,m}$	P_{dp}	OSNR $_{tot,m}$	P_{dp}	OSNR $_{tot,m}$
P_{11}	22.6	P_{12}	22.2	P_{13}	21.5	P_{14}	21.1	P_{15}	20.5
P_{21}	24.1	P_{22}	22.6	P_{23}	21.1	P_{24}	20.5	P_{25}	20.5
P_{31}	26.6	P_{32}	22.6	P_{33}	21.5	P_{34}	20.5	P_{35}	19.6
P_{41}	23	P_{42}	21.8	P_{43}	21.5	P_{44}	21.1	P_{45}	20.8

Table 3.11. OSNR considering only the NLI noise for the candidate paths of the four demands considered in COST 239 network.

Comparing the results obtained in Table 3.11, considering only the NLI power effect on the OSNR, with the OSNR obtained only with ASE noise presented in Table 3.6, it can be concluded that the ASE noise power degrades the paths performance much more significantly, for a channel

input power of 0 dBm. The OSNR calculated only with NLI noise is about 7 dB higher than the OSNR obtained with only ASE noise. The greatest difference between OSNRs is in P_{11} , where the OSNR obtained only with NLI is 7.9 dB higher, and the smaller difference is 6.4 dB in P_{13} . As shown in Appendix B, for the optimal channel power, 1.46 dBm, calculated in the longest path P_{35} , the difference between the two OSNRs (only with ASE noise and only with NLI) would be about 2.8 dB (Tables 3.6 and 3.11 comparing with Tables B.2 and B.3), where the highest decrease is observed in path P_{11} and the lowest decrease in path P_{45} . For this channel power, the PLI that would degrade more the signal quality is still the ASE noise. However, when comparing the total OSNRs obtained with the channel powers 0 dBm and 1.46 dBm, the OSNRs obtained only with considering the NLI decreases more with the latter, around 2.9 dB (compare with Table 3.11), while the OSNR obtained with only ASE noise decreases around 1.5 dB (comparing with Table 3.6).

The OSNRs with both NLI and ASE calculated with equation (3.12) with the parameters described in Tables 3.3 and 3.9 are presented in Table 3.12, where the ASE noise dominates the performance degradation, for a channel power of 0 dBm.

P_{dp}	OSNR _{tot,m} [dB]	P_{dp}	OSNR _{tot,m}	P_{dp}	OSNR _{tot,m}	P_{dp}	OSNR _{tot,m}	P_{dp}	OSNR _{tot,m}
P_{11}	14	P_{12}	14.5	P_{13}	14.1	P_{14}	12.9	P_{15}	13
P_{21}	16.6	P_{22}	14.1	P_{23}	12.8	P_{24}	12.5	P_{25}	12.1
P_{31}	18.6	P_{32}	14.4	P_{33}	13.3	P_{34}	12.9	P_{35}	11.5
P_{41}	15.5	P_{42}	13.5	P_{43}	13.9	P_{44}	13.1	P_{45}	13.5

Table 3.12. Total OSNR with ASE and NLI noises for the candidate paths for the four demands considered in COST 239 network.

From the results of the total OSNR of each candidate path obtained in Table 3.12, the path chosen to serve one demand is the path with the best OSNR, as shown in Table 3.13.

Demand d	Path P_{dp}	OSNR _{tot,m} [dB]
$d = 1$	$P_{12} = \{2, 5\}$	14.5
$d = 2$	$P_{21} = \{2\}$	16.6
$d = 3$	$P_{31} = \{3\}$	18.6
$d = 4$	$P_{41} = \{2, 9\}$	15.5

Table 3.13. Optical paths with highest OSNR for the four demands considered in COST 239 network.

The paths obtained with the highest OSNR considering the OSNR with only the ASE noise power effect, as in Table 3.6, and with the ASE and NLI noises powers, as shown in Table 3.12, using the Gaussian noise model, are the same. However, the OSNR decreases with the NLI effect inclusion, with a maximum OSNR decrease of 0.9 dB in candidate path P_{13} and the lowest of 0.65 dB in P_{11} . Anyhow, as concluded from Table 3.11, for a channel power of 0 dBm, the PLI that mostly degrades the signal quality is the ASE noise.

Notice that the NLI closed-formulas derived in [17] are independent of the modulation format used. So, a modulation format correction for the estimation of the NLI in a more accurate way is presented in the following and its results are analyzed for several QAM modulations. The previous NLI formulation presented in equations (3.14)-(3.16) assumes that the transmitted signal has a Gaussian modulation, which means that the signal statistically behaves as stationary Gaussian noise at the transmitter, which makes it independent of the modulation format [19]. With the modulation correction, the NLI coefficient changes from equation (3.14) to [19]:

$$\eta_{N_{spans}}(f_m) = \eta_{GN}(f_m) + \eta_{corr}(f_m) \quad (3.21)$$

where η_{corr} is the correction added to the NLI coefficient due to the modulation format. This correction is calculated with [19]:

$$\begin{aligned} \eta_{corr, N_{spans}}(f_m) \approx & \frac{80}{81} \Phi \sum_{k=0, k \neq m}^{N_{ch}} \left(\frac{P_k}{P_m} \right)^2 \frac{\gamma^2}{B_k} \left\{ \frac{1}{\phi_{m,k} \bar{\alpha} (2\alpha + \bar{\alpha})} \times \left[\frac{T_k - \alpha^2}{\alpha} \arctan \left(\frac{\phi_{m,k} B_m}{\alpha} \right) \right. \right. \\ & \left. \left. + \frac{A^2 - T_k}{A} \arctan \left(\frac{\phi_{m,k} B_m}{A} \right) + \frac{2\pi \tilde{n} T_k}{|\phi| B_k^2 \alpha^2 A^2} \left[(2|\Delta f| - B_k) \log \left(\frac{2|\Delta f| - B_k}{2|\Delta f| + B_k} \right) + 2B_k \right] \right\} \end{aligned} \quad (3.22)$$

with $\Delta f = f_k - f_i$, $\phi = -4\pi^2 [\beta_2 + \pi\beta_3(f_i + f_k)] L_{span}$ and $\tilde{n} = 0$ if $n=1$; otherwise $\tilde{n} = n$. The excess kurtosis represented by Φ , depends on the modulation format as shown in Table 3.14 and ϕ is the phase mismatch term, accounting for coherent NLI accumulation depending on the length of the span L_{span} [19].

Modulation format M	Excess kurtosis Φ
QPSK	-1
16-QAM	-0.6800
64-QAM	-0.6190
256-QAM	-0.6050
∞ -QAM	-0.6000
Gaussian modulation	0

Table 3.14. Modulation formats and corresponding excess kurtosis.

In order to ensure that our Matlab implementation of equation (3.22) is well implemented, we have obtained in Figures 3.5 and 3.6, the results of Figures 2 and 3 of [19]. These figures represent the NLI coefficient as a function of the number of spans with SRS and without SRS, considering several modulation formats and also the Gaussian modulation, for channel frequencies of $f=-4$ THz (Figure 3.5) and $f=0$ THz (Figure 3.6). The parameters used are presented in Table 3.8, with coherent accumulation ($\epsilon \neq 0$) for both channel frequencies. The coherent accumulation was calculated with the formula available in the Matlab script, given in [20].

In both Figures 3.5 and 3.6, the Gaussian modulation leads to the highest NLI coefficient, hence overestimating the NLI, and the QPSK modulation exhibits the lowest NLI coefficient, meaning that it is the less susceptible to the fiber nonlinearity. As the number of spans grows, the difference between the obtained NLI coefficients is reduced. In Figure 3.6 with SRS, a NLI coefficient difference of around 5 dB between the Gaussian and QPSK modulations is observed after one span, while, for ten spans, the difference is only around 2 dB. The 64-QAM and 16-QAM in both scenarios with and without SRS have a difference of around 0.4 dB when only one span is considered and around 0.1 dB for ten spans. Comparing these two modulations with QPSK, the difference between them for one span is around 2.4 dB and for ten spans is less than 1 dB. In Figure 3.6, there is no observable difference between the results obtained with and without SRS, for all four modulations because when $f_k=0$ THz, the third order dispersion parameter β_3 does not affect the calculations of the the NLI parameter. For $f=-4$ THz, there is a 1 dB difference of the NLI coefficient estimated after 10 spans with and without SRS. The

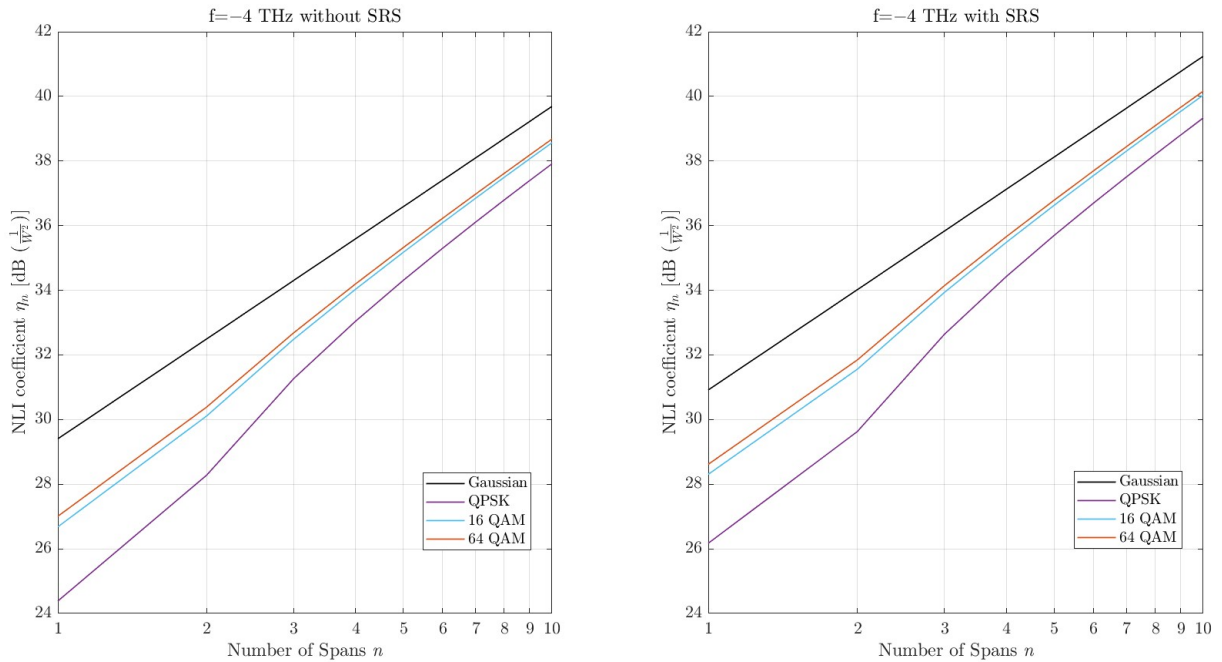


Figure 3.5. NLI coefficient as a function of the number of spans without SRS and with SRS, considering $f=-4$ THz and several modulation formats.

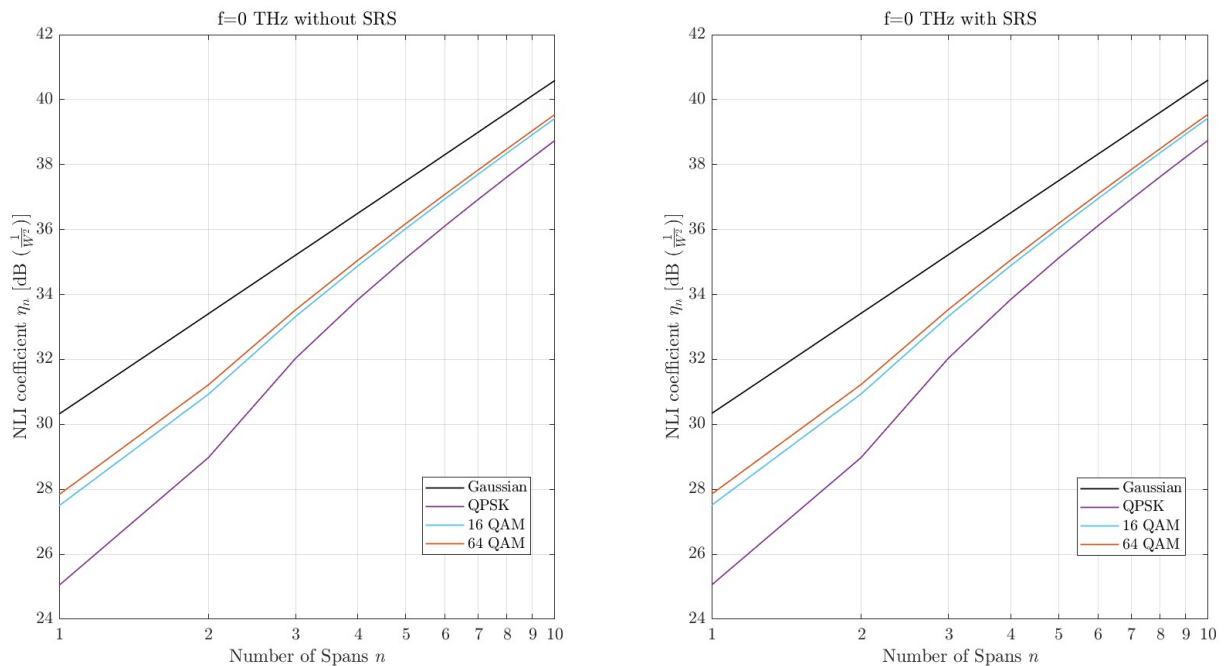


Figure 3.6. NLI coefficient as a function of the number of spans without SRS and with SRS, considering $f=0$ THz and several modulation formats.

results obtained in Figure 3.5 and 3.6 are in a very good agreement with the results presented in Figures 2 and 3 of [19], validating the modulation format correction implementation.

Next, we return to the example of the $\text{OSNR}_{tot,m}$ calculation and improve it by adding the modulation correction just presented, considering the QPSK modulation. In this case, the NLI coefficient with the modulation format given by equation (3.21), is obtained from the η_{GN} results presented in Table 3.10, and the modulation format correction η_{corr} obtained using equation (3.22) for each link corresponding to the candidate paths. The modulation format

correction coefficient is shown in Table 3.15 for all the links considered in the example. Table 3.15 also shows the NLI power calculated with equation (3.13) but using η_{corr} , and the length of each span.

Link e	Span length [km] L_{span}	Correction factor [$10^3/W^2$] η_{corr}	NLI noise power [μW] p_{NLI}
$e_1 = [1, 2]$	95.3	3.856	3.856
$e_2 = [1, 3]$	88.86	2.523	2.523
$e_3 = [1, 4]$	90.25	1.294	1.294
$e_4 = [1, 7]$	91.57	2.552	2.552
$e_5 = [2, 3]$	89	1.286	1.286
$e_6 = [2, 5]$	80.25	1.226	1.226
$e_7 = [2, 8]$	85.75	1.265	1.265
$e_8 = [3, 4]$	96	2.173	2.173
$e_9 = [3, 5]$	85.50	0.449	0.449
$e_{10} = [3, 6]$	79.5	1.220	1.220
$e_{11} = [4, 7]$	93.67	0.894	0.894
$e_{12} = [4, 8]$	97.44	3.459	3.459
$e_{13} = [4, 10]$	87.50	2.098	2.098
$e_{14} = [5, 6]$	95	0.478	0.478
$e_{15} = [5, 8]$	88.67	0.871	0.871
$e_{17} = [6, 7]$	99	2.196	2.196
$e_{21} = [7, 10]$	83.67	0.847	0.847

Table 3.15. Link spans lengths, correction factor and NLI noise power.

As with the modulation format correction, the span length affects the calculation of the NLI coefficient, the estimated NLI noise power is no longer the same for links with an equal number of spans, and becomes lower for links with shorter spans. For example, links e_{11} and e_{21} both have three spans but link e_{11} has spans 10 km longer than e_{21} and consequently the correction factor and NLI noise power are higher on e_{11} . By comparing Tables 3.10 and 3.15, it can be seen that the NLI power is overestimated with the Gaussian modulation. This overestimation is observed in every links, e.g. in link e_1 the NLI power is $1.66 \mu W$ lower when using the QPSK modulation. With the results from Tables 3.5 and 3.15, the total OSNR for each candidate path for the modulation QPSK is represented in Table 3.16.

P_{dp}	OSNR _{tot,m} [dB]	P_{dp}	OSNR _{tot,m}	P_{dp}	OSNR _{tot,m}	P_{dp}	OSNR _{tot,m}	P_{dp}	OSNR _{tot,m}
P_{11}	14.2	P_{12}	14.8	P_{13}	14.5	P_{14}	13.1	P_{15}	13.3
P_{21}	16.8	P_{22}	14.4	P_{23}	13	P_{24}	12.8	P_{25}	12.4
P_{31}	18.9	P_{32}	14.7	P_{33}	13.5	P_{34}	13.2	P_{35}	11.7
P_{41}	15.8	P_{42}	13.7	P_{43}	14.3	P_{44}	13.3	P_{45}	13.8

Table 3.16. Total OSNR for the candidate paths for the four demands considered in COST 239 network for the QPSK modulation.

For each modulation format, a minimum OSNR is required (ROSNR) to ensure a minimal system margin [14]. Table 3.17 shows the theoretical ROSNR for M -QAM signals (which is equivalent to the OSNR for polarization-division multiplexing (PDM) systems) calculated with equation (3.23) [18], and the practical ROSNR for the different modulations considered in this work, QPSK, 16-QAM, and 64-QAM for a bit error rate (BER) of 10^{-3} , taken from [21].

$$BER = \frac{2}{\log_2(M)} \cdot \left(1 - \frac{1}{\sqrt{M}}\right) \cdot \operatorname{erfc} \left(\sqrt{\frac{3 \cdot snr}{2(M-1)}} \right) \quad (3.23)$$

where $\text{erfc}(\cdot)$ is the complementary error function.

Modulation format M	Theoretical ROSNR [dB]	Practical ROSNR [dB]
QPSK	9.8	12
16-QAM	16.5	18.6
64-QAM	22.6	24.6

Table 3.17. Modulation formats with corresponding theoretical ROSNRs and practical ROSNRs for $\text{BER}=10^{-3}$.

From Table 3.17, it can be observed that the theoretical ROSNR and the practical ROSNR have a maximum difference of around 2 dB. So, the OSNR calculated in Table 3.16 must be above the minimum OSNR of 12 dB as in Table 3.17, for the QPSK, to guarantee the optical path quality. Analyzing the results obtained for the four demands, all candidate paths, except path P_{35} , satisfy the minimum OSNR. Hence, the path chosen for each demand is the one with the best OSNR as represented in Table 3.18.

Demand d	Path P_{dp}	OSNR [dB]
$d = 1$	$P_{12} = \{2, 5\}$	14.8
$d = 2$	$P_{21} = \{2\}$	16.8
$d = 3$	$P_{31} = \{3\}$	18.9
$d = 4$	$P_{41} = \{2, 9\}$	15.8

Table 3.18. Optical paths with best OSNR for the four demands considered in COST 239 network for QPSK modulation.

To see if higher modulations can be used in the considered links of the COST 239 network, in order to increase link capacity, the OSNRs of the candidate paths have been also obtained with the 16-QAM (Tables 3.19 and 3.20) modulation format.

P_{dp}	OSNR _{tot,m}	P_{dp}	OSNR _{tot,m}	P_{dp}	OSNR _{tot,m}	P_{dp}	OSNR _{tot,m}	P_{dp}	OSNR _{tot,m}
P_{11}	14.2	P_{12}	14.7	P_{13}	14.4	P_{14}	13	P_{15}	13.2
P_{21}	16.7	P_{22}	14.3	P_{23}	12.9	P_{24}	12.7	P_{25}	12.3
P_{31}	18.8	P_{32}	14.5	P_{33}	13.4	P_{34}	13.	P_{35}	11.6
P_{41}	15.7	P_{42}	13.7	P_{43}	14.2	P_{44}	13.2	P_{45}	13.7

Table 3.19. Total OSNR for the candidate paths for the four demands considered in COST 239 network for 16-QAM modulation.

For the 16-QAM, the minimum OSNR is 18.6 dB as in Table 3.17. From Table 3.19, only demand $d=3$ has a candidate path that guarantees the OSNR threshold, P_{31} , with an OSNR that reaches the optical receiver of $\text{OSNR}_{tot,m}=18.8$ dB. For the 64-QAM, the OSNR minimum is not accomplished for any of the candidate paths, and the corresponding results are not shown. Table 3.20 represents the chosen path with the highest OSNR and highest modulation format (higher capacity).

Comparing the results reached considering the QAM format and the Gaussian noise model, the best path is the same in both cases.

3.5. Other physical layer impairments

Other physical layer impairments that can degrade the multiband network performance are the crosstalk, optical filtering and system aging [5]. These impairments can be accounted in the safety margin (SM_m) defined as [22], [23].

Demand d	Path P_{dp}	OSNR [dB]	Modulation
$d = 1$	$P_{12} = \{2, 5\}$	14.8	QPSK
$d = 2$	$P_{21} = \{2\}$	16.8	QPSK
$d = 3$	$P_{31} = \{3\}$	18.8	16-QAM
$d = 4$	$P_{41} = \{2, 9\}$	15.8	QPSK

Table 3.20. Optical paths with best OSNR for the four demands considered in COST 239 network with the respective modulation format.

$$SM_m = 0.05 \times (N_a + N_v) + P_{filt} + P_{xtalk} \quad (3.24)$$

where N_v is the number of cascaded ROADMs in the optical path and N_a is the number of optical amplifiers in the path, P_{filt} is the filtering penalty and P_{xtalk} is the crosstalk penalty. The crosstalk impact is usually very small and is dependent on the channel spacing, so P_{xtalk} is set to be between 0 and 0.5 dB [22]. In this work, it is assumed $P_{xtalk}=0.5$ dB. The filtering penalty depends on the number of cascaded WSSs and the modulation format used. Considering ROADMs with a route and select architecture, two WSSs are traversed in the transit nodes and with a colorless add/drop structure, one WSS is traversed in the source and destination nodes [22]. Hence, the number of cascaded WSSs (C_{WSS}) along an optical path can be calculated by [22]:

$$C_{WSS} = 2 \times N_v - 2 \quad (3.25)$$

The feasibility of the path can be assessed with its residual margin (RM). The residual margin determines the full potential of the system, and the possibility of adding new amplified spans to the optical path without surpassing the margin limit [23], and is calculated with [22]:

$$RM = OSNR_{tot,m} - ROSNR - SM_m \quad (3.26)$$

where $ROSNR$ is the minimal OSNR corresponding to a specific modulation format, as shown in Table 3.17.

Continuing with the example of the previous sections, we are now going to calculate the safety margins and verify the residual margin for the paths selected for each demand in Table 3.20. The filtering penalty considered in this work was calculated based on the results presented in [5], [22]. For the paths selected, in Table 3.20, the maximum number of cascaded nodes is three, and $C_{WSS}=4$. Hence, the filtering penalty in the four paths is practically null [5], [22]. With the results of the path OSNRs in Table 3.20, knowing the modulation format used and consequently the minimum $ROSNR$ (Table 3.17), and the safety margin calculated from equation (3.24), the residual margin can be calculated with equation (3.26). Table 3.21 shows the number of cascaded nodes in each path, the number of amplifiers and the corresponding safety margin and residual margin.

Demand d	Path P_{dp}	Number of Nodes N_v	Number of amplifiers N_a	Safety margin SM_m [dB]	Residual margin RM [dB]
$d = 1$	$P_{12} = \{2, 5\}$	3	11	1.20	1.61
$d = 2$	$P_{21} = \{2\}$	2	7	0.95	3.88
$d = 3$	$P_{31} = \{3\}$	2	4	0.80	-0.58
$d = 4$	$P_{41} = \{2, 9\}$	3	9	1.10	2.67

Table 3.21. Number of nodes and amplifiers, safety margin and residual margin of the optical paths for the four demands considered in the COST 239 network.

Analyzing Table 3.21, the paths with more cascaded ROADMs and amplifiers have a slightly higher safety margin than the paths that use the direct link. From this table, it can also be observed that demands 1, 2 and 4 satisfy a null residual margin, and so the QPSK modulation format can be used. For demand 3, the residual margin is not fulfilled and a lower modulation than 16-QAM needs to be considered.

The previous results have been obtained considering a hard-decision forward error-correction (HD-FEC) with a BER of 10^{-3} . Next, we will assume a soft-decision (SD)-FEC with a BER of 4×10^{-2} . A better FEC allows for the minimum ROSNR to decrease [18]. Table 3.22 shows the theoretical ROSNR calculated for $\text{BER} = 4 \times 10^{-2}$ using equation (3.23). The difference between the practical ROSNR and the theoretical ROSNR is of 2.2 dB, the same considered with HD-FEC, in Table 3.17.

Modulation format M	Theoretical ROSNR [dB]	Practical ROSNR [dB]
QPSK	4.9	7.1
16-QAM	11.1	13.3
64-QAM	16.7	18.9

Table 3.22. Modulation formats with corresponding theoretical ROSNRs and practical ROSNRs for $\text{BER} = 4 \times 10^{-2}$.

From Table 3.22, it can be observed that the ROSNR has decreased more than 4.9 dB for all three modulation formats. So, the ROSNR can be fulfilled for the selected paths in Table 3.20 with a higher modulation, 16-QAM. Since the paths considered are the same, their safety margin is maintained (see Table 3.21), with the new ROSNR, the residual margin is improved, as shown in Table 3.23.

Demand d	Path P_{dp}	OSNR [dB]	Modulation Format M	Residual margin RM [dB]
$d = 1$	$P_{12} = \{2, 5\}$	14.8	16-QAM	0.22
$d = 2$	$P_{21} = \{2\}$	16.8	16-QAM	2.49
$d = 3$	$P_{31} = \{3\}$	18.8	16-QAM	4.72
$d = 4$	$P_{41} = \{2, 9\}$	15.8	16-QAM	1.67

Table 3.23. Optical paths with best OSNR for the four demands considered in COST 239 network with the respective modulation format for $\text{BER} = 4 \times 10^{-2}$.

With the results from Table 3.23, it can be observed that for a higher $\text{BER} = 4 \times 10^{-2}$, the residual margin is fulfilled for all the optical paths, being above 1.5 dB for the three shorter paths (P_{21} , P_{31} and P_{41}), and a higher capacity/lower symbol rate can be used in demands 1, 2 and 4 (i.e a 16-QAM modulation format can be used instead of a QPSK format).

3.6. Conclusion

In this chapter, we studied the performance degradation induced by the PLIs along several optical paths in the COST 239 network considering a C+L multiband solution, for both fixed and flexible grids.

The first PLI studied was the ASE noise caused by the amplifiers along an optical path. This impairment is more relevant for longer paths, where the number of amplifiers is higher and in links with longer spans, as expected. These conclusions can be taken by observing the candidate path P_{11} , which uses the longer link in the COST 239 network, and, therefore has a higher number of amplifiers and the accumulated ASE noise power is $34.06 \mu\text{W}$.

The second PLI studied was the NLI noise caused by the Kerr effect and the SRS due to the power transfer from lower to higher wavelengths. For this PLI, the performance has been assessed considering a Gaussian model with and without a modulation format correction. We have concluded that the ASE noise degrades more significantly the system performance than the NLI noise. In particular, a 7.2 dB OSNR difference was found in path P_{31} of the COST 239 network using Gaussian model without the modulation correction factor. We have also observed that when using an unoptimized channel launch power, the paths performance is more degraded, being the NLI the PLI most affected. When signal power is optimal, 1.46 dBm, the difference between the OSNR with only ASE noise and with only NLI in path P_{31} becomes only 2.8 dB.

When the influence of the modulation formats QPSK, 16-QAM and 64-QAM are included in the Gaussian model, it was concluded that without the modulation format correction (Gaussian modulation), the NLI predictions are worst-case. In particular, for the QPSK and path P_{31} , there is a 0.3 dB difference in the total OSNR between the two models (with and without the modulation correction factor). We have also studied the influence of the FEC code on the ROSNR and have concluded that stronger FECs (higher line BERs) allow an improved system capacity. In particular, with a BER of 4×10^{-2} (SD-FEC), path P_{11} can use a 16-QAM modulation format, whereas with a lower BER of 10^{-3} (HD-FEC), the QPSK modulation format must be used.

The impact of crosstalk, filtering and components aging was also studied in this chapter. We have concluded that, although their influence is generally low, in some cases, the residual margin is not fulfilled when these impairments are added to the performance analysis, as it has been demonstrated for path P_{31} with a BER= 10^{-3} .

C+L Multiband Network Design Considering Physical Layer Impairments

4.1. Introduction

Planning optical networks in an efficient and cost less way is, nowadays, a crucial function for every service provider [1]. This chapter focus on two main goals regarding the design of optical networks. The first goal, presented in Section 4.2, is to analyze and compare the traditional heuristic planning tools used to solve the RWA problem in static networks working on a fixed grid with an ILP formulation, in terms of the number of wavelengths used and the computation time in real networks. The second goal of this chapter, presented in Section 4.3, is to develop a simulator for planning C+L multiband networks having in mind the PLIs impact to solve the RMSA problem. In Section 4.4 an analysis of the performance of several real networks, considering a C+L flexible grid multiband scenario, in terms of the number of frequency slots used as a function of the BER is also performed. Section 4.5 resumes the chapter with the main results and conclusions.

4.2. RWA problem with ILP and heuristic solutions

In this section, we are going to study the RWA problem in static optical networks operating on a fixed grid C-band, considering the traditional heuristic algorithms and also an ILP formulation. The networks considered are the COST 239 [16], NSFNET [24], UBN [25] and CONUS 30 [6], and the respective physical topologies are presented in Appendix C.1. The static traffic matrix for these networks is obtained assuming a full mesh logical topology, which means that there is a demand between every pair of nodes with one transport unit (e.g. OTU1). Table 4.1 presents some physical (number of nodes, number of links, average node degree [26] and the longest and shortest link in the topology) and logical (number of demand requests) parameters of the real network topologies considered.

Network	#Demands	#Nodes	#Links	Average node degree	Longest link [km]	Shortest link [km]
COST 239	55	11	26	4.73	953	171
NSFNET	91	14	21	3	2828	246
UBN	276	24	43	3.58	2600	250
CONUS 30	435	30	36	2.40	1463	69

Table 4.1. Physical and logical features for the network topologies considered.

As can be observed in Table 4.1, the network with more nodes is the CONUS 30, and therefore, this is the network with more demands (possible logical connections in a full mesh topology). The shortest link is also in the CONUS 30 network with only 69 km. The NSFNET network has the longest link of the networks considered with 2828 km. The COST 239 network has the highest average node degree, meaning that, in this network the nodes are more

interconnected, and the lowest average node degree is in the CONUS 30 network (lower node interconnection).

The RWA problem in a static optical network, with the aim of minimizing the number of wavelengths, can be solved with the traditional heuristic tools by first finding the paths for carrying the demands and then assigning the wavelengths for each demand. The path finding, in particular finding the shortest path in distance, is done with the well-known Dijkstra algorithm [10] (the Matlab function `shortestpath` is used). After that, the paths must be ordered so that the wavelengths can be assigned. Three ordering strategies are used: shortest path first (SPF), longest path first (LPF) and random path (RP) [8]. The results presented for the random path strategy result from the average of ten simulations. After the shortest paths for the requested demands have been found, the wavelengths are going to be assigned with the heuristic algorithms First-Fit (FF) and Most Used (MU) for the three ordering strategies. The Matlab scripts used to implement these algorithms are presented in Appendix C.2. The minimum number of wavelengths required in the four networks studied for the different ordering strategies is presented in Table 4.2.

Network	Ordering Strategy	First-Fit	Most Used
COST 239	Shortest path first	8	8
	Longest path first	8	8
	Random path	8.1	8.1
NSFNET	Shortest path first	24	24
	Longest path first	24	24
	Random path	23.3	23.3
UBN	Shortest path first	70	70
	Longest path first	64	64
	Random path	64.9	64.6
CONUS 30	Shortest path first	134	133
	Longest path first	123	123
	Random path	123.3	123.1

Table 4.2. Total number of wavelengths obtained for the different network topologies with the WA heuristic algorithms, FF and MU, for different ordering strategies.

From the results in Table 4.2, it can be observed that for the different topologies, the number of wavelengths computed by the FF and MU algorithms is the same, except for the CONUS 30 network. In this topology, with the shortest path first, the MU gives one less wavelength than the FF. The results obtained with the different strategies for the smaller topologies, COST 239 and NSFNET, are the same. In the NSFNET network, the RP average results are slightly better than the ones obtained with SPF and LPF. However, for the topologies with more nodes, CONUS 30 and UBN, the results achieved with the LPF and RP predict a smaller number of wavelengths than the one predicted with the SPF. These results mean that the random path strategy gives, in the majority of the cases, a very good solution, indicating that the ordering strategy does not have a significant impact on this calculation. The computation time to obtain each one of the solutions presented in Table 4.2 took less than 1 second, with a PC with CPU of 1.8 GHz and 12 GB of RAM. These heuristics tools used to solve the RWA problem have already been used by several other authors and it can be concluded that our results of Table 4.2 are in complete agreement with [27], for example.

Now we are going to consider an ILP formulation to solve the RWA for the same networks. The strategy implemented for solving the RWA problem is based on a single-step, which means

that the routing and wavelength assigning tasks are done at the same time, as opposed to the two-step strategy used previously in this section, where the routing task is performed first and the wavelength assignment is performed after, that led to the results presented in Table 4.2. Another difference between these two strategies is that in the two-step heuristic strategy, only one path is computed for each demand, whereas in the single-step ILP strategy, a set of candidate paths for delivering the request is computed. In the next analysis, we consider four cases; a single path is computed, which is the same scenario analyzed in the heuristic approach; and two, three, and four candidate paths are computed. The candidate paths are computed with the Yen's k shortest path algorithm [28]. After this path computation, the ILP formulation presented in Section 2.2.4, equation (2.36), is used, but the objective function \mathbf{F} is different, since now the number of times color c is used in link e_i must be minimized instead of the capacity cost. The new ILP formulation can be written as,

$$\begin{aligned}
& \mathbf{minimize:} \quad \mathbf{F} = \sum_e z_{ce} \\
\mathbf{subject\ to:} \quad & \sum_p \theta_{dps} \sum_c x_{dpc} \geq h_{ds} \quad d = 1, \dots, D \quad s = 0 \\
& \sum_d \sum_p \delta_{edp} x_{dpc} = z_{ce} \quad c = 1, \dots, C \quad e = 1, \dots, E \\
& y_e \leq z_{ce} \quad c = 1, \dots, C \quad e = 1, \dots, E.
\end{aligned} \tag{4.1}$$

The ILP formulation for solving this RWA problem, is implemented in Matlab with function `intlinprog` (Appendix C.3). The solution for this RWA problem, based on the ILP formulation is presented in Table 4.3, which shows the number of wavelengths needed when there is only one, two, three, and four candidate paths available for each demand considering various real network topologies.

Network	Number of candidate paths	ILP	Time [s]
COST 239	One candidate path	8	1.157
	Two candidate paths	5	1.392
	Three candidate paths	5	1.596
	Four candidate paths	4	1.387
NSFNET	One candidate path	24	17.424
	Two candidate paths	15	23.158
	Three candidate paths	13	12.189
	Four candidate paths	13	16.511
UBN	One candidate path	64	787
	Two candidate paths	47	2283
	Three candidate paths	37	1356
	Four candidate paths	35	9648

Table 4.3. Total number of wavelengths used in the different network topologies obtained with the ILP formulation, given in equation (4.1), as well as the respective computation time.

By comparing the results shown in Tables 4.2 and 4.3 with only one candidate path, the number of wavelengths obtained with the ILP formulation is the same than the best one obtained with the heuristic solution (the results obtained with the LPF). But when there is more than one candidate path for each demand, the ILP algorithm gives a smaller number of wavelengths, since it has several paths that can be chosen, instead of just one. As can be observed in Table 4.3, for the UBN network, for one candidate path, 64 wavelengths are required, which is the same value shown in Table 4.2 (heuristic approach with LPF strategy), whereas for two,

three, and four candidate paths, respectively, 47, 37, and 35 wavelengths are needed. If further candidate paths are added to the RWA problem, the number of wavelengths reduces further until a minimum value is reached, which corresponds to the optimum number of wavelengths. This minimum value was computed for the four networks studied: for the NSFNET, the minimum number is obtained with three candidate paths, and is 13 wavelengths, whereas for the COST 239 and UBN, the minimum number of wavelengths is respectively, 4 and 35 and is obtained with four candidate paths. Another conclusion that can be drawn from Table 4.3 is related with the computation time. As can be observed, as the number of candidate paths increases, the computation time becomes higher when the number of candidate paths increases from one to two, but for the NSFNET and UBN networks, when the number of paths reaches three, the computation time decreases in comparison with the two paths scenario, and then increases again with four candidate paths. We were not able to obtain the results for the CONUS 30 network - the Matlab script stopped because it exceeded its allocated memory and temporary disk space after 5 days running.

Next, a comparison between the performance of the ILP and heuristic formulations just presented is performed in the COST 239 network. So, based on the heuristic solution presented in Table 4.2, and the optimal solution obtained with ILP formulation while having four candidate paths, as shown in Table 4.3, we are going to compare the number of wavelengths in each network link (i.e. capacity). The link capacities (number of wavelengths used) obtained for the COST 239 network are presented in Figure 4.1, assuming a full mesh logical topology. As can be observed in Figure 4.1, the link capacity is distributed more evenly with the ILP solution that uses four candidate paths (the optimal number of wavelengths) for each demand. For example, in the heuristic solution, based on the Dijkstra and FF algorithms, the links $e=[5,6]$ and $e=[6,7]$ are clearly more overloaded than the rest of the links in the network, whereas, with the ILP solution, the capacity in these links reduces 50%, leading to a more evenly distributed capacity in the links of the network. In particular, in the heuristic solution link $e=[5,6]$ is used in the paths for the following eight demands, $d=[2-6]$, $d=[2-7]$, $d=[2-9]$, $d=[2-10]$, $d=[5-6]$, $d=[5-7]$, $d=[5-9]$, and $d=[5-10]$, whereas in the ILP formulation only the paths for the following four demands $d=[2-6]$, $d=[5-6]$, $d=[5-7]$, and $d=[5-10]$ used that link. The path lists used in both the heuristic and ILP solutions are presented in Appendix C.4.

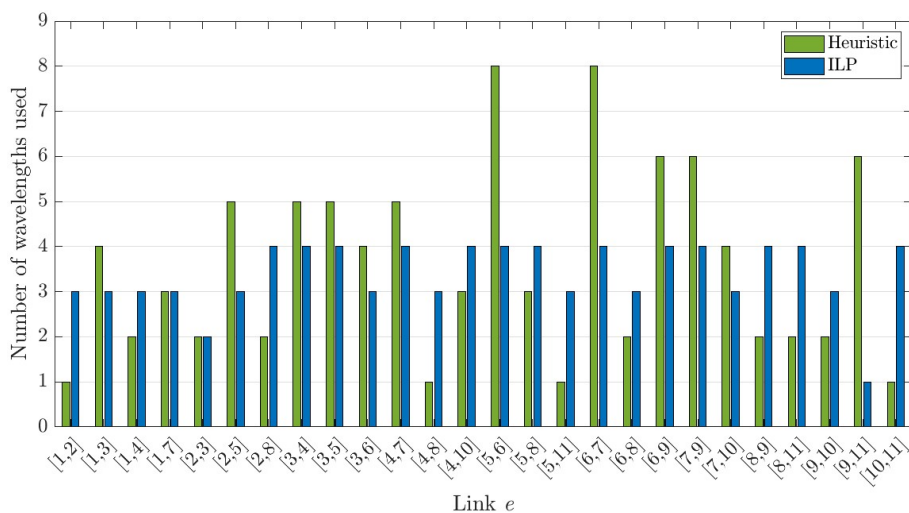


Figure 4.1. Link capacity obtained with heuristic solution and ILP with four candidate paths per demand for COST 239 network.

4.3. Multiband optical network simulator

In this section, we present the simulator developed in Matlab to solve the routing, modulation format and spectrum assignment (RMSA) problem in a flexible grid C+L multiband optical network aware of the PLIs [1], [22].

The flowchart of the developed simulator is shown in Figure 4.2, and it has three main steps: network topology definition, routing and modulation format assignment and, lastly, spectrum assignment. The simulator inputs are the network topology, traffic matrix, the number of candidate paths, the available bands and the total number of FSs per band. In all networks analyzed, a full-mesh logical topology is considered and, hence, the total number of demands corresponds to the total number of possible logical paths. The first step is to compute the list of the k -th candidate paths for each demand. The candidate paths are computed with an algorithm based on the Yen's k -shortest path algorithm [28]. After computing the k_{paths} candidate paths for every demand, the OSNR of each candidate path is then calculated using equations (3.10) and (3.12), considering the ASE noise along the path (equation (3.11)) and the NLI (equation (3.21)). The ASE noise and NLI noise contributions for each link must be computed for the three modulation formats considered (QPSK, 16-QAM and 64-QAM).

Some simplifications are assumed in these calculations: 1) the NLI noise at the end of a link is calculated considering that all FSs are being used in the C+L band (worst case scenario); 2) the coherent factor is assumed zero, which means that the NLI noise is calculated at the end of each link independently of the NLI noises calculated for the other links of a given path; 3) the channel launch power is optimized for the longest candidate path in the network [13] (worst case scenario), so the optimal power obtained for each modulation format is used in all channels across the network that use that specific modulation format; and 4) the NLI noise and corresponding OSNR are calculated for the center channel, since there is no knowledge of how the spectrum will be assigned. As shown in Figure 3.4, with this last assumption, the NLI coefficient is underestimated in the WDM signal lower frequencies, overestimated for the higher frequencies, and the OSNR becomes equal for all optical channels in a particular link. Some other simulators have been developed that do not use these simplifications, such as [1] and [22]. With these simplifications, the OSNR is calculated for each path, from the highest modulation format to the lowest, and it is checked if the ROSNR is achieved for that particular modulation format. If none of the modulation formats meets the ROSNR, then, the corresponding candidate path is not used. Moreover, if no candidate paths for the demand satisfy the ROSNR, that demand is blocked, as can be seen in the flowchart of Figure 4.2. After calculating the OSNR for all demands and candidate paths and assigning the modulation format, the paths are sorted based on the OSNR in descending order, for each demand.

The path list just built is then used by the spectrum assignment algorithm to assign the FSs using the First-Fit algorithm, starting with the candidate path with the highest OSNR, and trying different candidate paths when this one does not work. Since we are considering a flexible grid scenario, the FSs assigned to each demand must be contiguous, and must be the same in every link of a specific optical path [1]. The number of FSs allocated for each demand depends on the symbol rate, which depends on the modulation format used in the candidate path [1]. Therefore, depending on the modulation format used in the path, the FF algorithm tries to assign a certain number of FSs. If it cannot assign those FSs in the whole C+L band, then another candidate path from the list is chosen. If the FSs can not be assigned in any of the candidate paths corresponding to a specific demand, then that demand is blocked.

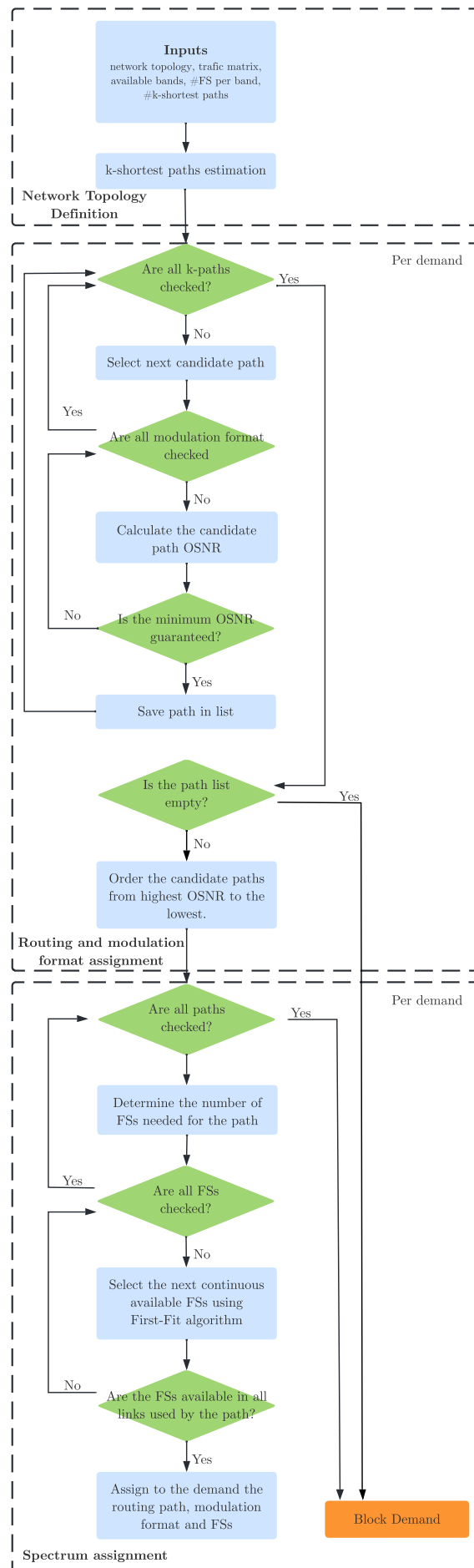


Figure 4.2. Flowchart of the Matlab simulator used to solve the RMSA problem in a flexible grid C+L multiband network aware of the PLIs.

4.4. Results and discussion

In this section, we use the simulator presented in Section 4.3 with the parameters shown in Tables 4.4 and 4.5 to study the RMSA problem in real network scenarios (COST 239, NSFNET, UBN and CONUS 30 networks). Our goal is to assign the optical path, FSs and modulation format to every demand of the network, assuming a full mesh logical topology with 100 Gbps demands and considering a BER= 4×10^{-2} (SD-FEC). In the following analysis, we have assumed that a QPSK signal needs 4 FSs to transmit a 100 Gbps signal, a 16-QAM signal needs 3 FSs and a 64-QAM signal 2 FSs. Hence, each modulation format has one FS that is used as a guard-band between channels.

Table 4.4 shows the system and network parameters considered, and Table 4.5 shows the transmitted signal features that depend on the chosen modulation format, in particular the average launch signal power per channel and the channel spacing. The average launch signal power is calculated for the longest path in the COST 239 network, $P=\{1,3,6,7,4\}$ (source node 1, destination node 4 and transit nodes 3, 6 and 7) with 1815 km, which is one of the candidate paths for demand $d=[1-4]$.

Parameters	Values
Number of candidate paths k_{paths}	5
Total number of FSs	862
Frequency of the central channel ν_0	189.90 THz
Line bit rate $R_{b,l}$	128 Gbps
Information bit rate $R_{b,i}$	100 Gbps
Amplifier maximum gain G_{max}	25 dB
Fiber attenuation coefficient α	0.25 dB/km
Fiber effective area A_{eff}	80 μm^2
Dispersion D_{λ_0}	17 ps/nm/km
Dispersion slope S_0	67 fs/nm ² /km
Reference wavelength λ_0	1550 nm
Raman gain slope C_r	0.028 1/W/km/THz
Nonlinear refractive index \bar{n}_2	2.6×10^{-20} m ² /W
Coherent factor ε	0
Group velocity β_2	-2.168×10^{-26} s ² /m
Third order dispersion parameter β_3	1.447×10^{-40} s ³ /m

Table 4.4. System parameters used to solve the RMSA problem.

Parameters	64-QAM	16-QAM	QPSK
Channel Spacing Δ_{ch}	25 GHz	37.5 GHz	50 GHz
Number of FSs	432	289	217
Symbol rate $R_{s,l}$	10.67 Gbaud	16 Gbaud	32 Gbaud
Average launch signal power per channel P_m	-2.39 dBm	-1.59 dBm	-0.69 dBm
Total transmitted optical power P_{tot}	23.97 dBm	23.01 dBm	22.68 dBm

Table 4.5. System parameters used to calculate the OSNR of each path.

We start our study by solving the RMSA problem for the COST 239 network, assuming a BER= 4×10^{-2} and the parameters given in Tables 4.4 and 4.5. The NLI and ASE noises powers calculated at the end of each link in the COST 239 network are presented in Appendix C.6, and the ROSNRs for each one of the modulation formats with this BER are shown in Table 3.22.

The solution of the RMSA problem is described in Table 4.6 and Figure 4.3. Table 4.6 shows the path assigned to each demand, and the corresponding OSNR, modulation format, and FSs allocated. In Figure 4.3, it is represented the FSs used in each network link, alongside with their

corresponding central frequency. In this figure, the FSs used by a path on a particular link are depicted with the same color.

		Link <i>e</i>																								
FS [THz]	[1,2]	[1,3]	[1,4]	[1,7]	[2,3]	[2,5]	[2,8]	[3,4]	[3,5]	[3,6]	[4,7]	[4,8]	[4,10]	[5,6]	[5,8]	[5,11]	[6,7]	[6,8]	[6,9]	[7,9]	[7,10]	[8,9]	[8,11]	[9,10]	[9,11]	[10,11]
195.9		1	1	1	1	1	1	1	1	1	1	1	1	1	1			1	1	1	1		1		1	1
195.8875		2	2	2	2	2	2	2	2	2	2	2	2	2	2			2	2	2	2		2		2	2
195.875		3	3	3	3	3		3	3	3			3	3	3				3				3			3
195.8625		4	4		4	4			4	4			4	4	4				4				4			4
195.85		5	5		5	5							5	5					5	5			5			5
195.8375		6			6	6		6						6					6	6			6			6
195.825		7			7	7		7	7					7					7	7						
195.8125		8			8	8		8	8			8		8					8	8						
195.8		9			9	9		9	9			9	9	9	9				9	9						
195.7875		10			10	10		10	10		10	10	10	10	10				10	10						
195.775		11			11	11		11	11			11	11	11	11		11		11	11		11				11
195.7625		12			12	12		12	12			12	12	12	12		12		12	12		12				12
195.75		13			13	13		13	13			13	13	13	13		13		13	13		13				
195.7375		14			14	14		14	14			14	14	14	14				14	14		14				
195.725		15			15	15		15	15			15	15	15	15				15	15		15				
195.7125		16			16	16		16	16		16	16	16	16	16				16	16		16				16
195.7		17			17	17		17	17		17	17	17	17	17				17	17		17				17
195.6875		18			18	18		18	18		18	18	18	18	18				18	18		18				18
195.675		19			19	19		19	19			19	19	19	19				19	19	19	19				19
195.6625		20			20	20		20	20			20	20	20	20				20	20	20	20				20
195.65		21			21	21		21	21			21	21	21	21				21	21	21	21				21
195.6375					22	22		22	22			22	22	22	22				22	22		22				22
195.625					23	23		23	23			23	23	23	23				23	23		23				23
195.6125					24	24		24	24			24	24	24	24				24	24		24				24
195.6									25										25	25		25				25
195.5875									26										26	26		26				26
195.575									27										27	27		27				27
195.5625														28					28	28		28				
195.55														29					29	29		29				
195.5375														30					30	30		30				
195.525														31					31							
195.5125														32					32							
195.5														33					33	33	33					
195.4875														34					34	34	34					
195.475														35					35	35	35					
195.4625														36					36							36
195.45														37					37							37
195.4375														38					38							38
195.425																			39	39						
195.4125																			40	40						
195.4																			41	41						
195.3875																			42	42		42				
195.375																			43	43		43				
195.3625																			44	44		44				
195.35																			45	45		45				
195.3375																			46	46		46				
195.325																			47	47		47				
195.3125																			48	48		48				48
195.3																			49	49		49				49
195.2875																			50	50		50				50

Figure 4.3. FSs allocated in the different links for the different demands in the COST 239 network for $BER=4 \times 10^{-2}$.

Demand d	Path	OSNR [dB]	Modulation format M	Frequency slots
[1 – 2]	{1,3,2}	16	16-QAM	1,2,3
[1 – 3]	{1,3}	18	16-QAM	4,5,6
[1 – 4]	{1,4}	20.5	64-QAM	1,2
[1 – 5]	{1,3,5}	17	16-QAM	7,8,9
[1 – 6]	{1,3,6}	16.5	16-QAM	10,11,12
[1 – 7]	{1,7}	17.6	16-QAM	1,2,3
[1 – 8]	{1,3,5,8}	15.7	16-QAM	13,14,15
[1 – 9]	{1,3,6,9}	15.5	16-QAM	16,17,18
[1 – 10]	{1,4,10}	16.5	16-QAM	3,4,5
[1 – 11]	{1,3,6,9,11}	14.6	16-QAM	19,20,21
[2 – 3]	{2,3}	20.7	64-QAM	4,5
[2 – 4]	{2,3,4}	15.7	16-QAM	6,7,8
[2 – 5]	{2,5}	21.8	64-QAM	1,2
[2 – 6]	{2,5,6}	19.2	64-QAM	3,4
[2 – 7]	{2,5,6,9,7}	14.9	16-QAM	5,6,7
[2 – 8]	{2,8}	21.1	64-QAM	1,2
[2 – 9]	{2,5,6,9}	17.3	16-QAM	8,9,10
[2 – 10]	{2,5,6,7,10}	14.1	16-QAM	11,12,13
[2 – 11]	{2,5,6,9,11}	15.9	16-QAM	22,23,24
[3 – 4]	{3,4}	17.5	16-QAM	1,2,3
[3 – 5]	{3,5}	24	64-QAM	1,2
[3 – 6]	{3,6}	21.9	64-QAM	1,2
[3 – 7]	{3,6,9,7}	15.9	16-QAM	13,14,15
[3 – 8]	{3,5,8}	19.8	64-QAM	3,4
[3 – 9]	{3,6,9}	19.2	64-QAM	3,4
[3 – 10]	{3,4,10}	15.1	16-QAM	9,10,11
[3 – 11]	{3,6,9,11}	17.2	16-QAM	25,26,27
[4 – 5]	{4,3,5}	16.6	16-QAM	16,17,18
[4 – 6]	{4,3,6}	16.1	16-QAM	22,23,24
[4 – 7]	{4,7}	21.2	64-QAM	1,2
[4 – 8]	{4,8}	15.6	16-QAM	1,2,3
[4 – 9]	{4,7,9}	16.7	16-QAM	8,9,10
[4 – 10]	{4,10}	19.2	64-QAM	1,2
[4 – 11]	{4,7,9,11}	15.5	16-QAM	16,17,18
[5 – 6]	{5,6}	22.8	64-QAM	1,2
[5 – 7]	{5,6,9,7}	16	16-QAM	28,29,30
[5 – 8]	{5,8}	21.9	64-QAM	1,2
[5 – 9]	{5,6,9}	19.7	64-QAM	31,32
[5 – 10]	{5,6,9,7,10}	15.1	16-QAM	33,34,35
[5 – 11]	{5,6,9,11}	17.3	16-QAM	36,37,38
[6 – 7]	{6,9,7}	17.2	16-QAM	39,40,41
[6 – 8]	{6,8}	20.6	64-QAM	1,2
[6 – 9]	{6,9}	22.6	64-QAM	1,2
[6 – 10]	{6,9,7,10}	16	16-QAM	42,43,44
[6 – 11]	{6,9,11}	19.3	64-QAM	11,12
[7 – 8]	{7,9,6,8}	15.4	16-QAM	45,46,47
[7 – 9]	{7,9}	19.1	64-QAM	1,2
[7 – 10]	{7,10}	22.6	64-QAM	1,2
[7 – 11]	{7,9,11}	17	16-QAM	48,49,50
[8 – 9]	{8,6,9}	18	16-QAM	48,49,50
[8 – 10]	{8,11,10}	14.8	16-QAM	1,2,3
[8 – 11]	{8,11}	17.6	16-QAM	4,5,6
[9 – 10]	{9,7,10}	17.2	16-QAM	19,20,21
[9 – 11]	{9,11}	22.2	64-QAM	1,2
[10 – 11]	{10,11}	18	16-QAM	4,5,6

Table 4.6. RMSA solution for the COST 239 optical network with $BER=4 \times 10^{-2}$.

By analyzing the results shown in Table 4.6 and Figure 4.3, it is observed that none of the demands are blocked, and that the lowest modulation format used is the 16-QAM, which is also the most used (in a total of 55 paths, 35 paths use the 16-QAM, which corresponds to 63.6%). The 64-QAM has been attributed a few times for the paths with shorter links (higher OSNR) and usually occupying the first FSs in the C-band. The QPSK modulation format has not been necessary, because the minimum ROSNR was satisfied by the higher modulation formats. In particular, the lowest OSNR achieved in all paths is 14.1 dB, for demand $d=[2-10]$, which is 0.8 dB above the ROSNR for the 16-QAM. This path distance is 1356 km, the second longest path used. The longest path with a demand assigned has a 1452 km distance corresponding to $d=[1-11]$. Notice that the longest path of 1815 km has not been attributed, since the direct link has been assigned to demand $d=[1-4]$. The demand with the highest OSNR, of 24 dB, is demand $d=[3-5]$. This demand uses the direct path with the shortest link (171 km) in the network. From Figure 4.3, it can be observed that links $e=[1,2]$, $e=[5,11]$, $e=[8,9]$, and $e=[9,10]$ are not used, since these links are some of the longest links in the network, and lead to an enhanced performance degradation due to PLIs in the network. The most used link is $e=[6,9]$ and it is used by 18 paths for a total of 50 FSs assigned, which is the maximum number of FSs used in this solution. In this link 76.4% of the FSs allocated are assigned to paths with the 16-QAM modulation format, whereas 14.6% correspond to paths with 64-QAM format. The reasons for such usage are its short distance (251 km) and the fact that this link is located in the center of the network. The RMSA solution presented in Table 4.6 and Figure 4.3 for the COST 239 network considering a $BER=4\times 10^{-2}$ allocates only 5.8% of the 862 FSs available, using only 50 FSs in the C-band, without requiring a multiband solution, due to the low demand volume.

For the solution presented in Table 4.6 and Figure 4.3, the impact caused by the crosstalk, filtering, and system aging is not taken into account. To assess the solution of the RMSA problem with these PLIs, the residual margin has been calculated with equation (3.26). From these calculations it results that in eight paths a positive residual margin was not achieved, and consequently, these paths must use a lower modulation format. The paths that do not fulfill the residual margin correspond to the demands: $d=[1-11]$, $d=[2-6]$, $d=[2-10]$, $d=[3-9]$, $d=[4-10]$, $d=[5-9]$, $d=[6-11]$, and $d=[7-9]$. For demands $d=[1-11]$ and $d=[2-10]$, the new assigned modulation format is the QPSK, with four FSs allocated. For the other six demands, the new modulation format is 16-QAM, occupying three FSs. Since, now, these paths require more FSs, the total number of FSs allocated in this RMSA solution is 55, which corresponds to 6.4% of the FSs in the C+L multiband spectrum.

Next, we are going to solve the same RMSA problem using the COST239 network, but considering a $BER=10^{-3}$, typically used for HD-FEC. The ROSNRs for this BER are shown in Table 3.17. The parameters used for this study are the same presented in Tables 4.4 and 4.5. Table 4.7 and Figure 4.4 presents the solution for this RMSA problem.

From Table 4.7 and Figure 4.4, it is observed that with this BER, the OSNRs at the end of each path are lower than with $BER=4\times 10^{-2}$ (Table 4.6). Due to the reduced OSNRs and higher ROSNR, the 64-QAM format is no longer a possible solution and the QPSK becomes the most used modulation format in the network, used in 63.6% of the paths. Therefore, the highest and lowest OSNRs are obtained for the same demands as in the scenario with $BER=4\times 10^{-2}$, but using lower modulation formats, due to the lower OSNRs. The highest OSNR achieved in this solution is 23.6 dB in demand $d=[3-5]$. The lowest OSNR of 12.4 dB is achieved for demand $d=$

Demand d	Path	OSNR [dB]	Modulation format M	Frequency slots
[1 – 2]	{1,3,2}	14.4	QPSK	1,2,3,4
[1 – 3]	{1,3}	16.4	QPSK	5,6,7,8
[1 – 4]	{1,4}	20.1	16-QAM	1,2,3
[1 – 5]	{1,3,5}	15.3	QPSK	9,10,11,12
[1 – 6]	{1,3,6}	14.9	QPSK	13,14,15,16
[1 – 7]	{1,7}	15.9	QPSK	1,2,3,4
[1 – 8]	{1,3,5,8}	14.0	QPSK	17,18,19,20
[1 – 9]	{1,3,6,9}	13.9	QPSK	21,22,23,24
[1 – 10]	{1,4,10}	14.8	QPSK	4,5,6,7
[1 – 11]	{1,3,6,9,11}	12.9	QPSK	25,26,27,28
[2 – 3]	{2,3}	20.3	16-QAM	5,6,7
[2 – 4]	{2,3,4}	14.0	QPSK	8,9,10,11
[2 – 5]	{2,5}	21.6	16-QAM	1,2,3
[2 – 6]	{2,5,6}	18.9	16-QAM	4,5,6
[2 – 7]	{2,5,6,9,7}	13.3	QPSK	7,8,9,10
[2 – 8]	{2,8}	20.8	16-QAM	1,2,3
[2 – 9]	{2,5,6,9}	15.6	QPSK	11,12,13,14
[2 – 10]	{2,5,6,7,10}	12.4	QPSK	15,16,17,18
[2 – 11]	{2,5,6,9,11}	14.3	QPSK	29,30,31,32
[3 – 4]	{3,4}	15.8	QPSK	1,2,3,4
[3 – 5]	{3,5}	23.6	16-QAM	1,2,3
[3 – 6]	{3,6}	21.7	16-QAM	1,2,3
[3 – 7]	{3,6,9,7}	14.3	QPSK	17,18,19,20
[3 – 8]	{3,5,8}	19.5	16-QAM	4,5,6
[3 – 9]	{3,6,9}	19.0	16-QAM	4,5,6
[3 – 10]	{3,4,10}	13.4	QPSK	12,13,14,15
[3 – 11]	{3,6,9,11}	15.6	QPSK	33,34,35,36
[4 – 5]	{4,3,5}	14.8	QPSK	21,22,23,24
[4 – 6]	{4,3,6}	14.4	QPSK	29,30,31,32
[4 – 7]	{4,7}	20.8	16-QAM	1,2,3
[4 – 8]	{4,8}	13.8	QPSK	1,2,3,4
[4 – 9]	{4,7,9}	15.0	QPSK	11,12,13,14
[4 – 10]	{4,10}	18.9	16-QAM	1,2,3
[4 – 11]	{4,7,9,11}	13.8	QPSK	21,22,23,24
[5 – 6]	{5,6}	22.2	16-QAM	1,2,3
[5 – 7]	{5,6,9,7}	14.3	QPSK	37,38,39,40
[5 – 8]	{5,8}	21.6	16-QAM	1,2,3
[5 – 9]	{5,6,9}	19.2	16-QAM	41,42,43
[5 – 10]	{5,6,9,7,10}	13.4	QPSK	44,45,46,47
[5 – 11]	{5,6,9,11}	15.6	QPSK	48,49,50,51
[6 – 7]	{6,9,7}	15.5	QPSK	52,53,54,55
[6 – 8]	{6,8}	20.1	16-QAM	1,2,3
[6 – 9]	{6,9}	22.3	16-QAM	1,2,3
[6 – 10]	{6,9,7,10}	14.4	QPSK	56,57,58,59
[6 – 11]	{6,9,11}	19.0	16-QAM	60,61,62
[7 – 8]	{7,9,6,8}	13.7	QPSK	63,64,65,66
[7 – 9]	{7,9}	18.8	16-QAM	1,2,3
[7 – 10]	{7,10}	22.3	16-QAM	1,2,3
[7 – 11]	{7,9,11}	15.4	QPSK	67,68,69,70
[8 – 9]	{8,6,9}	16.3	QPSK	67,68,69,70
[8 – 10]	{8,11,10}	13.1	QPSK	1,2,3,4
[8 – 11]	{8,11}	15.9	QPSK	5,6,7,8
[9 – 10]	{9,7,10}	15.5	QPSK	25,26,27,28
[9 – 11]	{9,11}	21.8	16-QAM	1,2,3
[10 – 11]	{10,11}	16.3	QPSK	5,6,7,8

Table 4.7. RMSA solution for the COST 239 optical network with BER=10⁻³.

FS [THz]	Link e																									
	[1,2]	[1,3]	[1,4]	[1,7]	[2,3]	[2,5]	[2,8]	[3,4]	[3,5]	[3,6]	[4,7]	[4,8]	[4,10]	[5,6]	[5,8]	[5,11]	[6,7]	[6,8]	[6,9]	[7,9]	[7,10]	[8,9]	[8,11]	[9,10]	[9,11]	[10,11]
195.9		1	1	1	1	1	1	1	1	1	1	1	1	1	1			1	1	1	1		1		1	1
195.8875		2	2	2	2	2	2	2	2	2	2	2	2	2	2			2	2	2	2		2		2	2
195.875		3	3	3	3	3	3	3	3	3	3	3	3	3	3			3	3	3	3		3		3	3
195.8625		4	4	4	4	4		4	4	4		4	4		4				4				4			4
195.85		5	5		5	5			5	5			5		5				5				5			5
195.8375		6	6		6	6			6	6			6		6				6				6			6
195.825		7	7		7	7							7	7					7	7			7			7
195.8125		8			8	8		8					8						8	8			8			8
195.8		9			9	9		9					9						9	9						
195.7875		10			10	10		10					10						10	10						
195.775		11			11	11						11							11	11						
195.7625		12			12	12		12				12	12						12	12						
195.75		13			13	13		13	13			13	13						13	13						
195.7375		14			14	14		14	14			14	14						14	14						
195.725		15			15	15		15	15			15	15				15					15				
195.7125		16			16	16		16	16			16	16						16	16						
195.7		17			17	17		17	17			17	17				17	17	17	17						
195.6875		18			18	18		18	18			18	18				18	18	18	18						
195.675		19			19	19		19	19			19	19						19	19						
195.6625		20			20	20		20	20			20	20						20	20						
195.65		21			21	21	21	21	21			21	21						21	21						21
195.6375		22			22	22		22	22			22	22						22	22						22
195.625		23			23	23		23	23			23	23						23	23						23
195.6125		24			24	24		24	24			24	24						24	24						24
195.6		25			25	25		25	25			25	25						25	25	25					25
195.5875		26			26	26		26	26			26	26						26	26	26					26
195.575		27			27	27		27	27			27	27						27	27	27					27
195.5625		28			28	28		28	28			28	28						28	28	28					28
195.55					29	29		29	29			29	29						29	29						29
195.5375					30	30		30	30			30	30						30	30						30
195.525					31	31		31	31			31	31						31	31						31
195.5125					32	32		32	32			32	32						32	32						32
195.5								33	33			33	33						33	33						33
195.4875								34	34			34	34						34	34						34
195.475								35	35			35	35						35	35						35
195.4625								36	36			36	36						36	36						36
195.45												37	37						37	37						
195.4375												38	38						38	38						
195.425												39	39						39	39						
195.4125												40	40						40	40						
195.4												41	41						41	41						
195.3875												42	42						42	42						
195.375												43	43						43	43						
195.3625												44	44						44	44	44					
195.35												45	45						45	45	45					
195.3375												46	46						46	46	46					
195.325												47	47						47	47	47					
195.3125												48	48						48	48						48
195.3												49	49						49	49						49
195.2875												50	50						50	50						50
195.275												51	51						51	51						51
195.2625																			52	52						
195.25																			53	53						
195.2375																			54	54						
195.225																			55	55						
195.2125																			56	56	56					
195.2																			57	57	57					
195.1875																			58	58	58					
195.175																			59	59	59					
195.1625																			60	60						60
195.15																			61	61						61
195.1375																			62	62						62
195.125																			63	63	63					
195.1125																			64	64	64					
195.1																			65	65	65					
195.0875																			66	66	66					
195.075																			67	67	67					67
195.0625																			68	68	68					68
195.05																			69	69	69					69
195.0375																			70	70	70					70

Figure 4.4. FSs allocated in the different links for the different demands in the COST 239 network for BER=10⁻³.

[2-10], showing a 1.7 dB OSNR reduction in comparison to the $\text{BER}=4 \times 10^{-2}$ case, that imposes the use of the QPSK, instead of the 16-QAM in this path. The paths list used in the two solutions are the same, so the four links $e=[1,2]$, $e=[5,11]$, $e=[8,9]$, and $e=[9,10]$ remain unused in the solution with $\text{BER}=10^{-3}$, as shown in Figure 4.4. With this BER, the ROSNRs are higher (Table 3.17), and, hence, the modulation formats used require more FSs. In particular, this solution allocates 70 FSs, twenty more than in the results shown in Figure 4.3, allocating 8.12% of the total FSs available. From Figure 4.4, it can be observed that the most used link is again $e=[6,9]$, with 68 FSs allocated, corresponding to 7.9% of the total FSs available in the C+L multiband solution.

Then, we have also solved the RMSA problem for other network topologies, NSFNET, UBN and CONUS 30, which have more nodes, and consequently, more demands than the COST 239 network. The detailed solutions for these RMSA problems, are presented in Appendix C.7. Table 4.8 indicates the number of FSs allocated in the different networks for the $\text{BERs}=4 \times 10^{-2}$, 10^{-2} , and 10^{-3} , the blocked demands, the demands served, and also shows the demands that achieved the highest and lowest OSNRs, as well as the longest path served.

Network	BER	#Blocked demands	#Demands served	#FSs allocated	Demand with the highest OSNR	Demand with the lowest OSNR	Demand with the longest path p used
COST 239	4×10^{-2}	0 0%	55 100%	50 5.8%	[3-5]→24.0 dB 64-QAM	[2-10]→14.1 dB 16-QAM	[1-11]→1452 km
	1×10^{-2}	0 0%	55 100%	62 7.2%	[3-5]→24.0 dB 64-QAM	[2-10]→12.4 dB QPSK	[1-11]→1452 km
	1×10^{-3}	0 0%	55 100%	70 8.1%	[3-5]→23.6 dB 16-QAM	[2-10]→12.4 dB QPSK	[1-11]→1452 km
NSFNET	4×10^{-2}	2 2.2%	89 97.8%	114 13.2%	[10-11]→22.8 dB 64-QAM	[10-11]→7.2 dB QPSK	[10-11]→4467 km
	1×10^{-2}	32 35.2%	57 64.8%	71 8.2%	[10-14]→22.8 dB 64-QAM	[6-13]→9.6 dB QPSK	[6-14]→2885 km
	1×10^{-3}	62 68.1%	29 31.9%	28 3.2%	[10-14]→22.6 dB 16-QAM	[6-8]→12.3 dB QPSK	[8-13]→1545 km
UBN	4×10^{-2}	66 23.9%	210 76.1%	133 15.4%	[3-4]→22.6 dB 64-QAM	[2-14]→7.1 dB QPSK	[2-14], [5-17], [5-18]→4150 km
	1×10^{-2}	168 60.9%	108 39.1%	44 5.1%	[3-4]→22.6 dB 64-QAM	[16-24]→9.5 dB QPSK	[2-9], [16-24]→2300 km
	1×10^{-3}	232 84.1%	44 15.9%	16 1.9%	[3-4]→22.5 dB 16-QAM	[11-15], [15-20]→12.0 dB QPSK	[11-15], [15-20]→1300 km
CONUS 30	4×10^{-2}	91 20.9%	344 79.1%	350 40.6%	[24-25]→27.9 dB 64-QAM	[13-28]→7.6 dB QPSK	[14-15]→4850 km
	1×10^{-2}	249 57.2%	186 42.8%	156 18.1%	[24-25]→27.9 dB 64-QAM	[1-26]→9.5 dB QPSK	[8-13]→2835 km
	1×10^{-3}	350 80.5%	85 19.5%	73 8.5%	[24-25]→27.9 dB 64-QAM	[6-26]→12.0 dB QPSK	[1-16]→1602 km

Table 4.8. RMSA solution for the real network topologies COST 239, NSFNET, UBN, and CONUS 30, for three different BERs - Part 1.

In Table 4.8, the highest OSNR is always obtained for the same demand in the networks considered, independently of the BER, whereas that the lowest OSNR is reached for different demands for the various BERs considered. The highest OSNR is obtained in all four networks in the direct path that uses the shortest link in the network. On the other hand, the lowest OSNR is obtained in one of the longest paths in the network, that has not been blocked due to not fulfilling the ROSNR. In the three larger networks, the path reach is similar for all BERs, the maximum distance with $\text{BER}=4 \times 10^{-2}$ is around 4000 km, for a $\text{BER}=10^{-2}$ is about 2500 km, and around 1500 km for $\text{BER}=10^{-3}$. From Table 4.8, it can also be observed that for the

three larger networks, the number of blocked demands increases with the decrease of the BER considered, and the total number of FSs used decreases with the increase of the BER.

Having in mind the number of blocked demands and FSs used presented in Table 4.8, the percentage of blocked demands as a function of the BER, for the four network topologies considered in this section (solid lines), as well as the percentage of allocated FSs as a function of the BER (dashed lines) are shown in Figure 4.5.

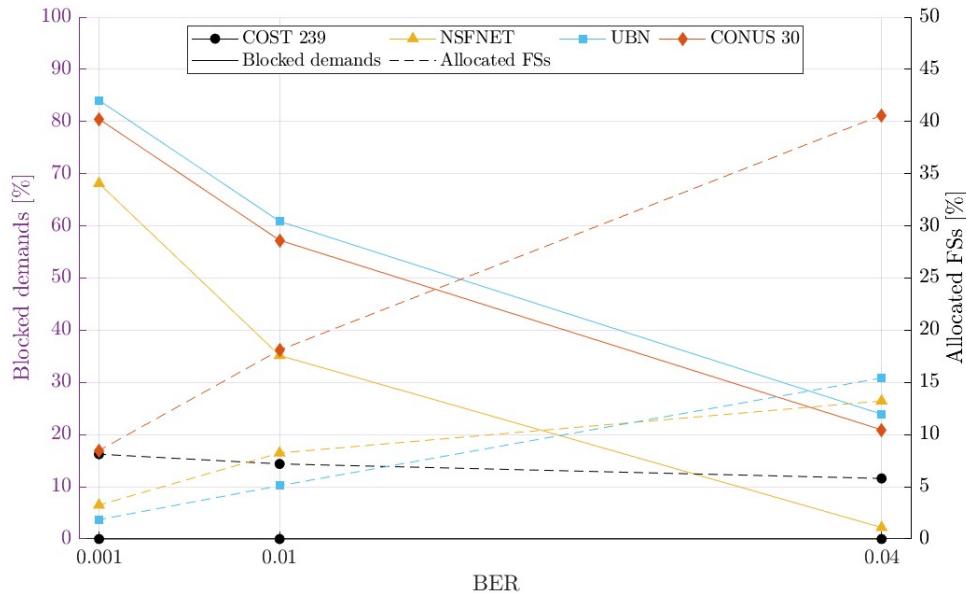


Figure 4.5. Blocked demands percentage and allocated FSs percentage for three BERs, 4×10^{-2} , 10^{-2} , and 10^{-3} .

From Figure 4.5, it can be observed that the UBN and CONUS 30 networks have more than 50% of the demands blocked when the BER is 10^{-2} or lower, and that when $\text{BER}=10^{-3}$, the NSFNET network blocks 68.1% of the demands and the UBN and CONUS 30 reach an undesirable 80% blocking, due to their larger size and higher ROSNR. The number of blocked demands increases since the OSNRs of the candidate paths do not guarantee the ROSNR for lower BERs. For all three BERs, the network with the highest percentage of blocked demands is the UBN optical network. In the COST 239 network, all demands were satisfied.

Figure 4.5 also shows the FSs used percentage (dashed lines) for the BERs analyzed in this section. As observed in Figure 4.5, the COST 239 network uses more FSs as the BER decreases, because lower BERs require the utilization of a lower modulation format (see Table 4.9), which consequently requires more FSs. The opposite happens for the other three networks, since the number of blocked demands increases for lower BERs. As observed in Figure 4.5, none of the networks use more than 40% of the multiband spectrum. Thus, the reason for blocking the demands is the insufficient OSNR, and not the unavailability of FSs. The maximum number of FSs allocated is 350 in the CONUS 30 network, which corresponds to a 40.6% total spectrum allocation, leaving more than half of the multiband spectrum available, being this network, the only network that assigns FSs in the L-band spectrum using only 5 FSs in this band.

In Table 4.9, we present the unused links, the link with most paths assigned and the link with the most FSs allocated in the network, as well as the usage percentage of the three modulation formats for the different BERs considering $R_{b,i}=100$ Gbps, as in Table 4.8.

Network	BER	Link e with the most paths assigned	Link e with the most #FSs allocated	Unused link e	#Paths using 64-QAM format	#Paths using 16-QAM format	#Paths using QPSK format
COST 239	4×10^{-2}	[6,9]=18 paths 32.7%	[6,9]=50 FSs 5.8%	[1,2], [5,11] [8,9], [9,10]	20 paths 36.4%	35 paths 63.6%	0 paths 0%
	1×10^{-2}	[6,9]=18 paths 32.7%	[6,9]=62 FSs 7.2%	[1,2], [5,11] [8,9], [9,10]	10 paths 10.9%	32 paths 58.2%	17 paths 30.9%
	1×10^{-3}	[6,9]=18 paths 32.7%	[6,9]=68 FSs 7.9%	[1,2], [5,11] [8,9], [9,10]	0 paths 0%	20 paths 36.4%	35 paths 63.6%
NSFNET	4×10^{-2}	[8,9]=30 paths 33.0%	[8,9]=113 FSs 13.1%	-	4 paths 4.4%	28 paths 30.8%	57 paths 62.6%
	1×10^{-2}	[8,9]=18 paths 19.8%	[8,9]=71 FSs 8.2%	[1,8]	1 paths 1.1%	12 paths 13.2%	46 paths 50.5%
	1×10^{-3}	[8,9], [9,10], [10,14]=6 paths 6.6%	[8,9]= 15 FSs 1.7%	[1,8], [1,11], [2,5], [6,12], [11,12], [12,14]	0 paths 0%	4 paths 4.4%	25 paths 27.5%
UBN	4×10^{-2}	[12,16]=33 paths 12.0%	[12,16]=131 FSs 15.2%	[3,5], [3,7], [15,19]	2 paths 0.7%	46 paths 16.6%	162 paths 58.7%
	1×10^{-2}	[3,4], [4,7], [21,22]=10 paths 3.6%	[4,7], [21,22]=39 FSs 4.5%	[3,5], [3,7], [15,19]	1 path 0.4%	9 paths 3.3%	98 paths 35.5%
	1×10^{-3}	[3,4], [21,22]=4 paths 1.4%	[3,4], [21,22]= 15 FSs 1.7%	[3,5], [3,7], [6,11], [9,11], [15,19]	0 paths 0%	2 paths 0.7%	42 paths 15.2%
CONUS 30	4×10^{-2}	[5,30]= 75 paths 17.2%	[5,30]= 289 FSs 33.5%	-	19 paths 4.4%	73 paths 16.8%	252 paths 57.9%
	1×10^{-2}	[2,30]=35 paths 8.0%	[16,30]=132 FSs 15.3%	-	7 paths 1.6%	35 paths 8.0%	144 paths 33.1%
	1×10^{-3}	[2,30]=19 paths 4.4%	[2,30]=71 FSs 8.23%	[2,19], [21,27], [22,27]	2 paths 0.5%	17 paths 3.9%	66 paths 15.2%

Table 4.9. RMSA solution for the real network topologies COST 239, NSFNET, UBN, and CONUS 30, for three different BERs - Part 2.

From Table 4.9, it can be observed that, in general, the number of paths utilized in the most used link is higher for higher BERs, since the other paths with lower OSNRs tend to be blocked (i.e. the ROSNR is not achieved) when the BER is lower. The link with the most paths assigned, in general, is also the one with the most FSs allocated, however, in some cases it is not. For example, in the CONUS 30 network, for BER= 10^{-2} , there are 35 paths assigned to link $e=[2,30]$, but this link has allocated 130 FSs, and the maximum number of FSs allocated in this solution is 132 for link $e=[16,30]$. In all the solutions obtained, the maximum number of FSs assigned to a link is 289 (CONUS 30 network), which represents 33.5% of the spectrum available on that link. Generally, the number of unused links increases for lower BERs, since the unused links are some of the longest in the network, thus originating a higher OSNR degradation, and ultimately not satisfying the ROSNR for those BERs. In Table 4.9, it can be also observed that in the larger networks (NSFNET, UBN, and CONUS 30), the QPSK is the most preponderant modulation format for the three BERs, and as the BER decreases, less paths use higher modulation formats. Only in the CONUS 30 network, the 64-QAM format is assigned when the BER= 10^{-3} , and the two paths assigned with this format use direct links that do not need in-line amplification. On the other hand, the COST 239 network is the only one that does not use the QPSK format when BER= 4×10^{-2} .

The number of FSs required for each modulation format increases for information bit rates higher than 100 Gbps, since more bandwidth is required to transmit the signal. With a 200 Gbps information bit rate and assuming a symbol rate of 64 Gbaud, for the QPSK, 7 FSs are required to accommodate the signal, 4 FSs for the 16-QAM with 32 Gbaud and 3 FSs for the 64-QAM with 21.3 Gbaud. As previously, a guard band FS is considered to avoid channel interference. With this information bit rate, we have also solved the RMSA problem for the CONUS 30 network with BER= 4×10^{-2} , and in this case, 53 more demands are blocked of a total of 144 demands, than in the solution presented in Table 4.8, due to the unaccomplishment

of the ROSNR. Moreover, 513 FSs are required, which corresponds to 59.5% of the 862 FSs available. Hence, this solution uses 18.9% more spectrum than with $R_{b,i}=100$ Gbps, requiring 168 FSs in the L-band (32.2% of the available).

4.5. Conclusion

In this chapter, we developed and studied planning tools to solve the RWA and RMSA problems in optical multiband networks using fixed and flexible grids. First, we compared heuristic and ILP solutions of the RWA problem in real network topologies considering a static optical network scenario using the C+L multiband with a fixed grid. We have concluded that the number of available candidate paths influences the optimum number of wavelengths required. In particular, our one-step ILP solution reaches the optimum value of the number of wavelengths with a maximum of 4 candidate paths, whereas the two-step heuristic approach that only uses one candidate path does not reach the optimum number of wavelengths. However, the computation time of the heuristics approach is always faster (less than 1s) than the one obtained with the ILP approach, that can be more than 2 hours, and can not achieve the optimal solution, for networks with a high number of nodes, as the CONUS 30 network due to computational constraints.

To study the RMSA problem in a flexible grid C+L multiband network, we developed a simulator in Matlab and applied it to four network topologies (COST 239, NSFNET, UBN, and CONUS 30), considering three different BERs and a 100 Gbps information bit rate. In the COST 239 network, we observed that using low BERs leads to the utilization of lower modulation formats, which require the assignment of more FSs, e.g. for $BER=4 \times 10^{-2}$, 50 FSs are allocated, while for $BER=10^{-3}$, 70 FSs are required. However, in larger networks, the decrease of the BER increases the number of blocked demands, and, consequently, the number of FSs allocated becomes lower. Since the paths are longer, the PLIs introduce more degradation to the paths OSNR, and the ROSNR is not satisfied for that specific BER. The maximum percentage of FSs assigned in the C+L multiband is 40.6% in the CONUS 30 network, which is the only network that assigns FSs in the L-band. It can be concluded, that in the four networks studied, the demand volume can grow since there are a lot of unused FSs. For higher information bit rates, (more than 100 Gbps) more FSs are required, even though the percentage of blocked demands becomes higher. Regarding the attributed modulation formats, only in the COST 239 network, for $BER=4 \times 10^{-2}$, the QPSK format is not used. However, this is the most used format in the networks with more nodes and longer links.

Conclusions and Future Work

In this chapter, we present this dissertation final conclusions and some suggestions for future work are proposed.

5.1. Final conclusions

In this dissertation, we studied heuristic and ILP formulations to solve the network planning problem in static C+L multiband networks with fixed and flexible grids aware of PLIs. The goal in static network planning problems is to minimize the optical spectrum used to satisfy all traffic demands.

In Chapter 2, we reviewed the most common ILP formulations and the heuristic algorithms used to solve the network planning problems. In particular, we have started by reviewing two ILP formulations for routing, the Link-Path and the Node-Link formulations. The Node-Link formulation requires less pre-processing, since it always considers all possible paths guaranteeing the optimal solution. However, this formulation can be very time consuming for networks with a large number of nodes, since a lot of possible paths need to be checked. For this reason, we choose to use the Link-Path formulation in the remaining studies, since it considers only a predefined number of paths and typically the best paths are easily computed, ensuring also the optimum solution for the problem. Based on this formulation, we reviewed two restoration design problems. In both problems, the disjoint backup paths are selected before the failure happens. Also, based on the Link-Path formulation, we have reviewed an ILP formulation to solve the RWA problem in WDM optical networks in a single step, meaning that the routing and wavelength assignment problems are solved at the same time. Besides, the ILP formulations reviewed, this chapter also briefly reviews some of the most common heuristic algorithms used for routing, like the Fixed-Path and the Alternative-Path, and for spectrum assignment such as, First-Fit, Most Used and Random algorithms. Chapter 2 ends with a briefly planning study where both an heuristic and ILP formulations are used to find the capacity of each link in the network. It has been concluded that for the studied network scenario, the ILP solution presents a more evenly distributed link capacity.

Chapter 3 is focused on the PLIs study that degrade the path OSNR in a C+L multiband network. The PLIs considered are the ASE noise power induced by the path optical amplification and the NLI noise due to the Kerr effect calculated with closed-form formulas based on the Gaussian noise model with and without a modulation format correction and in the presence of the SRS effect. For the examples studied, among these PLIs, the ASE noise degrades the path OSNR more 7 dB than the NLI, when the channel launch power is not optimized. With optimized channel launch power, the difference between the OSNRs is 2 dB. The modulation format correction allows for a better estimation of the OSNR at the end of the paths, because the NLI coefficient is not as overestimated, especially for the QPSK format. To guarantee the feasibility of the path with the modulation format selected, the residual margin is also calculated. The residual margin of a particular path takes in consideration the ROSNR, the calculated

OSNR, and a system margin that includes the impact of crosstalk, filtering, and the system components aging. When the residual margin is not fulfilled, a lower modulation format has to be considered for that particular path. So, in this chapter, we have also assessed the residual margin for various paths in the COST239 network. We have concluded that higher BERs (due to stronger FECs) have lower ROSNRs and allow to utilize higher modulation formats in the path.

Chapter 4 had two main goals. The first one was to compare, assuming a static network scenario and a fixed grid, the performance of a two step RWA heuristic formulation with a single step RWA ILP formulation (presented in Chapter 2, Section 2.2.4) in several network topologies (COST 239, NSFNET, UBN and CONUS 30). It has been concluded that the ILP formulation gives always the optimum number of wavelengths, as long the number of candidate paths considered is enough. The number of wavelengths obtained with the heuristic solution, which only uses one candidate path, never reaches the optimum value. However, the computation time is always less than a second with this solution, whereas with the ILP solution, the computation time can achieve more than 2 hours. The second goal of Chapter 4 was to develop a simulator in Matlab for studying the RMSA problem in C+L multiband networks, considering several real topologies. By analyzing the RMSA problem solutions, with 100 Gbps channels, we have observed that the allocation of FSs with different BERs leads to different behaviors in smaller networks with shorter links and a lower number of nodes and, in larger networks, with longer links and more nodes. In smaller networks (COST 239), the decrease of the BER increases the number of FSs allocated, since these solutions may use lower modulation formats. In contrast, in larger networks (UBN, CONUS 30), lower BERs led to less FSs allocated, due to higher blocking of demands. In these solutions only the CONUS 30 network assigned some FSs in the L-band, in the highest BER studied. With higher information bit rates, 200 Gbps, more spectrum is assigned, since more FSs are required to transmit the signal, especially for the QPSK format case, even though more demands are blocked due to the higher path OSNR degradation in networks with longer paths, i.e. lower OSNR. It is concluded that, in the larger networks, the most used modulation format is always the QPSK format. We also concluded, that the link that is used by most paths is not always the one with more FSs assigned.

5.2. Future work

Some suggestions for future work are the following:

- Improve the developed simulator in order to solve the simplifications used in this work. In particular, consider the real network utilization, instead of assuming that all FSs are being used when the NLI is calculated. Also, consider the NLI calculation in the corresponding FSs and not on the center channel [1], [22].
- Improve the simulator to operate in networks with dynamic traffic demands [13].
- Improve the simulator in order to deal with other bands, such as the S-band [29].
- Extend the ILP formulation used in Chapter 4, Section 2, to solve the RMSA problem aware of PLIs in a multiband network with flexible grid and compare its performance with the ones obtained in this work considering heuristic tools.
- Use a more rigorous approach than the one used in Chapter 3, for assessing the filtering and crosstalk penalties introduced by the ROADMs nodes.

References

- [1] M. Mehrabi, H. Beyranvand, and M. Emadi, “Multi-band elastic optical networks: Inter-channel stimulated Raman scattering-aware routing, modulation level and spectrum assignment,” *Journal of Lightwave Technology*, vol. 39, pp. 3360–3370, 2021.
- [2] N. Sheikh, E. Paz, J. Pinto, and A. Beghelli, “Multi-band provisioning in dynamic elastic optical networks: A comparative study of a heuristic and a deep reinforcement learning approach,” *25th International Conference on Optical Network Design and Modelling, ONDM 2021*, 2021.
- [3] A. Ferrari, A. Napoli, J. Fischer, N. Costa, A. D’Amico, J. Pedro, W. Forysiak, E. Pincemin, A. Lord, A. Stavdas, J. Gimenez, G. Roelkens, N. Calabretta, S. Abrate, B. Sommerkorn-Krombholz, and V. Curri, “Assessment on the achievable throughput of multi-band ITU-T G.652.D fiber transmission systems,” *Journal of Lightwave Technology*, vol. 38, pp. 4279–4291, 2020.
- [4] N. Sambo, A. Ferrari, A. Napoli, N. Costa, J. Pedro, B. Sommerkorn-Krombholz, P. Castoldi, and V. Curri, “Provisioning in multi-band optical networks,” *Journal of Lightwave Technology*, vol. 38, pp. 2598–2605, 2020.
- [5] A. Morea, J. Renaudier, T. Zami, A. Ghazisaeidi, and O. Bertran-Pardo, “Throughput comparison between 50-GHz and 37.5-GHz grid transparent networks,” *Journal of Optical Communications and Networking*, vol. 7, no. 2, pp. A293–A300, 2015.
- [6] J. Simmons, *Optical Network Design and Planning*. Optical Networks, Springer International Publishing, 2 ed., 2014.
- [7] M. Pioro and D. Medhi, *Routing, Flow, and Capacity Design in Communication and Computer Networks*. Elsevier Science, 2004.
- [8] D. Chadha, *Optical WDM Networks: From Static to Elastic Networks*. IEEE Press, Wiley, 2019.
- [9] P. Saengudomlert, “Optical networks handout 8.” University Lecture, 2019.
- [10] B. Chatterjee, N. Sarma, P. Sahu, and E. Oki, *Routing and Wavelength Assignment for WDM-based Optical Networks: Quality-of-Service and Fault Resilience*. Lecture Notes in Electrical Engineering, Springer International Publishing, 2016.
- [11] L. Cancela, “Slides from the course in optical networks. In *Telecommunications and Computer Engineering MSc*.” Iscte-Instituto Universitário de Lisboa, 2020.
- [12] I.-T. R. G. Telecommunication Standardization Sector of ITU, G.694.1, “Spectral grids for WDM applications: DWDM frequency grid,” 2020.
- [13] D. Uzumidis, E. Kosmatos, C. Matrakidis, A. Stavdas, and A. Lord, “Strategies for upgrading an operator’s backbone network beyond the c-band: Towards multi-band optical networks,” *IEEE Photonics Journal*, vol. 13, no. 2, pp. 1–18, 2021.
- [14] J. Pedro, “Designing transparent flexible-grid optical networks for maximum spectral efficiency,” *Journal of Optical Communications and Networking*, vol. 9, pp. C35–C44, 2017.
- [15] J. Rebola and A. Cartaxo, “Slides from the course in advanced fiber optic communications systems. In *Telecommunications and Computer Engineering MSc*.” Iscte-Instituto universitário de Lisboa, 2020.
- [16] M. Niksirat, S. Hashemi, and M. Ghatee, “Branch-and-price algorithm for fuzzy integer programming problems with block angular structure,” *Fuzzy Sets and Systems*, vol. 296, pp. 70–96, 2016.
- [17] D. Semrau, R. Killey, and P. Bayvel, “A closed-form approximation of the Gaussian noise model in the presence of inter-channel stimulated Raman scattering,” *Journal of Lightwave Technology*, vol. 37, pp. 1924–1936, 2019.
- [18] X. Zhou and C. Xie, *Enabling Technologies for High Spectral-efficiency Coherent Optical Communication Networks*. Wiley Series in Microwave and Optical Engineering, Wiley, 2016.

- [19] D. Semrau, E. Sillekens, R. Killey, and P. Bayvel, "A modulation format correction formula for the Gaussian noise model in the presence of inter-channel stimulated Raman scattering," *Journal of Lightwave Technology*, vol. 37, pp. 5122–5131, 2019.
- [20] D. Semrau, E. Sillekens, R. Killey, and P. Bayvel, "ISRS GN model implementation." <https://github.com/dsemrau/ISRSGNmodel#readme>, 2019.
- [21] A. Mitra, D. Semrau, N. Gahlawat, A. Srivastava, P. Bayvel, and A. Lord, "Effect of reduced link margins on C + L band elastic optical networks," *Journal of Optical Communications and Networking*, vol. 11, pp. C86–C93, 10 2019.
- [22] J. Pedro, "Designing transparent flexible-grid optical networks for maximum spectral efficiency," *Journal of Optical Communications and Networking*, vol. 9, no. 4, pp. C35–C44, 2017.
- [23] R. Hui and M. O'Sullivan, *Fiber Optic Measurement Techniques*. Elsevier Science, 2009.
- [24] T. LaQuey, *The User's Directory of Computer Networks*. Digital Press, 1990.
- [25] E. Biernacka, J. Domżał, and T. Wójcik, "Investigation of dynamic routing and spectrum allocation methods in elastic optical networks," *International Journal of Electronics and Telecommunications*, vol. 63, 2017.
- [26] X. Zhang, X. Lin, Z. Zheng, and Q. Yang, "Research on relation between average degree and convergence performance of distributed synchronization algorithm in WSNs," in *2017 12th International Conference on Computer Science and Education (ICCSE)*, pp. 392–396, 2017.
- [27] I. Duarte, "Exploring graph coloring heuristics for optical networks planning," Master's thesis, Iscte-Instituto Universitário de Lisboa, October 2020.
- [28] E. Amir, "K-shortest paths in a graph represented by a sparse matrix (Yen's algorithm)." <https://www.mathworks.com/matlabcentral/fileexchange/35397-k-shortest-paths-in-a-graph-represented-by-a-sparse-matrix-yen-s-algorithm>, 2012.
- [29] B. Correia, R. Sadeghi, E. Virgillito, A. Napoli, N. Costa, J. Pedro, and V. Curri, "Power control strategies and network performance assessment for C+L+S multiband optical transport," *Journal of Optical Communications and Networking*, vol. 13, no. 7, pp. 147–157, 2021.

Appendices

APPENDIX A

Matlab scripts used in Chapter 2

A.1. Example 1

This appendix shows the solution for the problem presented in subsection 2.2.1, equation (2.8), using software Matlab. The code used is:

```
F=[0; 0; 0; 0; 0; 2; 1; 1; 3; 1];

c=[0 0 0 1 0 -1 0 0 0 0;
   1 0 0 0 1 0 -1 0 0 0;
   0 0 1 0 1 0 0 -1 0 0;
   1 0 1 0 0 0 0 0 -1 0;
   0 1 0 0 0 0 0 0 0 -1];
Capacity= [0; 0; 0; 0; 0];

d=[1 0 0 0 0 0 0 0 0 0;
   0 1 1 0 0 0 0 0 0 0;
   0 0 0 1 1 0 0 0 0 0];
Demand=[15; 20; 10];

lb=zeros(11,1);
[X O]=linprog(F, c, Capacity, d, Demand, lb)
```

The matrix \mathbf{F} represents the objective function for the problem. In addition to the cost per link capacity, was added to the matrix the flow of each candidate path. The flow is zero for all the candidate paths since it is an unknown variable.

The matrix \mathbf{c} represents the link loads of the capacity inequalities (2.3). To this matrix was added the link capacity of each inequality ($y_e=-1$).

Capacity represents the right side of the same inequality (2.3) used to demonstrate matrix \mathbf{c} . The capacity is zero for all inequalities since it is a variable for the problem.

Matrix \mathbf{d} shows equations (2.1a), (2.1b), and (2.1c) to each was added the link capacities, which are zero. It is necessary since all matrices have to be the same size as the objective function (\mathbf{F}).

Demand is the right side of equations (2.1a), (2.1b), and (2.1c).

The matrix **aux** represents the low boundaries for the function `linprog`, this means that the flow or capacity can only be as low as zero.

So the optimal solution obtained using Matlab function `linprog` is $\mathbf{F}^{opt}=100$. The flows of each candidate path and the link capacity of each connection are illustrated in the Table A.1.

Flow x_e	Link Capacity y_e
$x_{11} = 15$	$y_1 = 0$
$x_{21} = 20$	$y_2 = 25$
$x_{22} = 0$	$y_3 = 10$
$x_{31} = 0$	$y_4 = 15$
$x_{32} = 10$	$y_5 = 20$

Table A.1. Matlab results for Example 2

A.2. Example 3

This appendix will demonstrate the solution obtained using software Matlab, for the problem presented in subsection 2.2.1, equation (2.11). This problem varies from the one shown in appendix A by adding one other candidate path for demand $d=1$. With that, the only variance in the code is the addition of that path to the tables, as shown in the code below:

```
F=[0; 0; 0; 0; 0; 0; 2; 1; 1; 3; 1];

c=[0 1 0 0 1 0 -1 0 0 0 0;
   1 0 0 0 0 1 0 -1 0 0 0;
   0 0 0 1 0 1 0 0 -1 0 0;
   1 0 0 1 0 0 0 0 0 -1 0;
   0 1 1 0 0 0 0 0 0 0 -1];
Capacity= [0; 0; 0; 0; 0];

d=[1 1 0 0 0 0 0 0 0 0 0;
   0 0 1 1 0 0 0 0 0 0 0;
   0 0 0 0 1 1 0 0 0 0 0];
Demand=[15; 20; 10];

lb=zeros(11,1);

[X O]=linprog(F, c, Capacity, d, Demand, lb)
```

This solution was the same as the one got in subsection 2.2.1 $\mathbf{F}^{opt}=85$, and the distribution of flow of each path and the link capacity is represented in Table A.2:

Flow x_e	Link Capacity y_e
$x_{11} = 0$	$y_1 = 15$
$x_{12} = 15$	$y_2 = 10$
$x_{21} = 20$	$y_3 = 10$
$x_{22} = 0$	$y_4 = 0$
$x_{31} = 0$	$y_5 = 35$
$x_{32} = 10$	

Table A.2. Matlab results for Example 3

A.3. Example 4

This appendix demonstrates the solution for the capacitated problem presented in subsection 2.2.1, equation (2.14). To solve this problem was software Matlab, the code used is:

```
F=[4; 3; 1; 4; 2; 2];

c=[0 1 0 0 1 0 ;
   1 0 0 0 0 1 ;
   0 0 0 1 0 1 ;
   1 0 0 1 0 0 ;
   0 1 1 0 0 0 ];
```

Appendix A Matlab scripts used in Chapter 2

```
Capacity=[10; 15; 5; 15; 30];

d=[1 1 0 0 0 0 ;
   0 0 1 1 0 0 ;
   0 0 0 0 1 1 ];
Demand=[15; 20; 10];

lb=zeros(7,1);

[X O]=linprog(F, c, Capacity, d, Demand, lb)
```

The solution obtained using function `linprog` is $\mathbf{F}^{opt}=100$ and the flow is:

Flow x_e
$x_{11} = 10$
$x_{12} = 5$
$x_{21} = 20$
$x_{22} = 0$
$x_{31} = 5$
$x_{32} = 5$

Table A.3. Matlab results for Example 4

A.4. Example 7

```
%ORIGEM
o= [1 1 3 3 3 2 2 4 4 4];
%DESTINO
d= [3 4 1 4 2 3 4 2 1 3];
%DISTANCIA
c= [1 3 1 1 2 2 1 1 3 1];
%GRAFO
grafo= digraph(o,d,c);
%INTERFACE GRAFO
figure
p=plot(grafo, 'Edglabel', grafo.Edges.Weight);
nos=4;
links=length(o)/2;
origem=[2 2 3 1 1]; %node source
destino=[3 4 4 4 3];
trafego_rede =[0 15 20 0;
               15 0 10 0;
               20 10 0 0;
               0 0 0 0];
[matriz_rede_caminhos]=caminhos_protecao(nos, grafo, trafego_rede);
cost=[2 1 1 3 1];
numero_caminho=size(matriz_rede_caminhos,1)*2;
numero_demand=size(matriz_rede_caminhos,1);
Caminhos={};
aux_c=0;
aux_p=0;
for i=1:numero_caminho
    if(floor(i/2)==i/2)
        aux_p=aux_p+1;
        Caminhos{i,1}=cell2mat(matriz_rede_caminhos(aux_p,3));
        Caminhos{i,2}=i;
    else
        aux_c=aux_c+1;
        Caminhos{i,1}=cell2mat(matriz_rede_caminhos(aux_c,1));
        Caminhos{i,2}=i;
    end
end
for l=1:numel(origem)
```

Appendix A *Matlab scripts used in Chapter 2*

```

matrix_aux{1,1}=origem(1);
matrix_aux{1,2}=destino(1);
matrix_aux{1,3}=1;
end
count=numero_caminho+links;
F=zeros(count,1);
for i=1:count
    if(i>numero_caminho)
        F(i,1)=cost(i-numero_caminho);
    end
end
D=[];
W=triu(trafego_rede,1);
m=0;
for i=1:nos
    for y=1:nos
        if(W(i,y)~=0)
            m=m+1;
            D(m,1)=W(i,y);
            d_aux{m,1}=i;
            d_aux{m,2}=y;
            d_aux{m,3}=m;
        end
    end
end
C=zeros(numel(origem),1);
d=zeros(numel(D),numel(F));
for z=1:size(Caminhos,1)
    caminho=cell2mat(Caminhos(z,1));
    p=size(caminho,2);
    for i=1:size(d_aux,1)
        if(cell2mat(d_aux(i,1))==caminho(1) &&
            cell2mat(d_aux(i,2))==caminho(p))
            x=cell2mat(d_aux(i,3))
            y=cell2mat(Caminhos(z,2));
            d(x,y)=1;
        end
    end
end
resultados=zeros(links+1,links);
aux_Caminhos_escolhidos=[];
for t=0:size(C,1)
    c=zeros(numel(C),numel(F));
    for z=1:size(Caminhos,1)
        caminho=cell2mat(Caminhos(z,1));
        for j=1:(numel(caminho)-1)
            for i=1:size(matrix_aux,1)
                if(cell2mat(matrix_aux(i,1))==caminho(j) &&
                    cell2mat(matrix_aux(i,2))==caminho(j+1))
                    x=cell2mat(matrix_aux(i,3));
                    y=cell2mat(Caminhos(z,2));
                    c(x,y)=1;
                elseif(cell2mat(matrix_aux(i,2))==caminho(j) &&
                    cell2mat(matrix_aux(i,1))==caminho(j+1))
                    x=cell2mat(matrix_aux(i,3));
                    y=cell2mat(Caminhos(z,2));
                    c(x,y)=1;
                end
            end
        end
    end
end
count=numero_caminho;
for j=1:size(C,1)
    if(j~=t)
        count=count+1;
    end
end

```


Appendix A *Matlab scripts used in Chapter 2*

```
        c(j, count)=-1;
    else
        count=count+1;
    end
end
lb=zeros(count,1);
ub=inf(count,1);
for i=1:size(F)
    int(i)=i;
end
[X, O, G, K]=intlinprog(F,int, c, C, d, D, lb, ub)
for y=numero_caminho+1:height(X)
    resultados(t+1,y-numero_caminho)=X(y);
end
Caminhos_escolhidos=[];
c_ =0;
for y=1:numero_caminho
    disp(y)
    if(X(y)~=0)
        disp(Caminhos(y,1))
        c_ =c_ +1;
        aux_Caminhos_escolhidos(c_, t+1)=y;
    end
end
end
aux_resultados=[];
for i=1:size(aux_Caminhos_escolhidos,1)
    int=aux_Caminhos_escolhidos(i,1);
    caminho=cell2mat(Caminhos(int,1));
    Caminhos_escolhidos{i,1}=caminho
end
R=zeros(links,1);
for i=1:size(resultados,2)
    aux_resultados=resultados(:,i);
    for j=1:size(aux_resultados,1)
        aux_R=(R(i));
        aux_R=[aux_R, (aux_resultados(j))];
        R(i)=(max(aux_R));
    end
end
end
F=sum(R);
```

A.5. Examples 8 and 9

```
%ORIGEM
o= [1 1 3 3 3 2 2 4 4 4];
%DESTINO
d= [3 4 1 4 2 3 4 2 1 3];
%DISTANCIA
c= [1 3 1 1 2 2 1 1 3 1];
%GRAFO
grafo= digraph(o,d,c);
%INTERFACE GRAFO
figure
p=plot(grafo, 'Edglabel', grafo.Edges.Weight);
nos=4;
links=length(o)/2;
origem=[2 2 3 1 1];
destino=[3 4 4 4 3];
trafego_rede =[0 15 20 0;
               15 0 10 0;
               20 10 0 0;
               0 0 0 0];
[matriz_rede_caminhos]=caminhos_protecao(nos, grafo, trafego_rede);
numero_caminho=size(matriz_rede_caminhos,1)*2;
```

Appendix A *Matlab scripts used in Chapter 2*

```

numero_demand=size (matriz_rede_caminhos ,1);
Caminhos={};
for i=1:numero_demand
    Caminhos{i,1}=cell2mat (matriz_rede_caminhos (i ,1));
    Caminhos{i,2}=cell2mat (matriz_rede_caminhos (i ,3));
    Caminhos{i,3}=i;
end
for l=1:numel(origem)
    matrix_aux{1,1}=origem (1);
    matrix_aux{1,2}=destino (1);
    matrix_aux{1,3}=1;
end
count=numero_caminho+links;
F=zeros (count ,1);
for i=1:count
    if (i>numero_caminho)
        F(i,1)=1;
    end
end
D=[];
W=triu (trafego_rede ,1);
m=0;
for i=1:nos
    for y=1:nos
        if (W(i , y)~=0)
            m=m+1;
            D(m,1)=W(i ,y);
            d_aux {m,1}=i;
            d_aux {m,2}=y;
            d_aux {m,3}=m;
        end
    end
end
C=zeros (numel (origem) ,1);
c=zeros (numel (C) ,numel (F));
R_link = 5; %failed link
for i=1:links
    if (R_link==i)
        Random_link(i,1)=0;
    else
        Random_link(i,1)=-1;
    end
end
for z=1:size (Caminhos ,1)
    caminho=cell2mat (Caminhos(z ,1));
    caminho_protecao=cell2mat (Caminhos(z ,2));
    for j=1:(numel (caminho)-1)
        for i=1:size (matrix_aux ,1)
            if (cell2mat (matrix_aux (i,1))==caminho (j) &&
                cell2mat (matrix_aux (i,2))==caminho (j+1))
                aux_vetor {j,1}=cell2mat (matrix_aux (i ,3));
            elseif (cell2mat (matrix_aux (i,2))==caminho (j) &&
                cell2mat (matrix_aux (i,1))==caminho (j+1))
                aux_vetor {j,1}=cell2mat (matrix_aux (i ,3));
            end
        end
        if (ismember (cell2mat (aux_vetor) , R_link)==0)
            aux_caminhos {z,1}=cell2mat (Caminhos(z ,1));
            aux_caminhos {z,2}=cell2mat (Caminhos(z ,3));
        else
            aux_caminhos {z,1}=cell2mat (Caminhos(z ,2));
            aux_caminhos {z,2}=cell2mat (Caminhos(z ,3));
        end
    end
end
end

```

Appendix A *Matlab scripts used in Chapter 2*

```

for z=1:size(aux_caminhos,1)
    caminho=cell2mat(aux_caminhos(z,1));
    for j=1:(numel(caminho)-1)
        for i=1:size(matrix_aux,1)
            if(cell2mat(matrix_aux(i,3))~=R_link)
                if(cell2mat(matrix_aux(i,1))==caminho(j) &&
                    cell2mat(matrix_aux(i,2))==caminho(j+1))
                    x=cell2mat(matrix_aux(i,3));
                    y=cell2mat(aux_caminhos(z,2));
                    c(x,y)=1;
                elseif(cell2mat(matrix_aux(i,2))==caminho(j) &&
                    cell2mat(matrix_aux(i,1))==caminho(j+1))
                    x=cell2mat(matrix_aux(i,3));
                    y=cell2mat(aux_caminhos(z,2));
                    c(x,y)=1;
                end
            end
        end
    end
    for m=1:size(c,1)
        c(m,numero_caminho+m)=Random_link(m,1);
    end
end
d=zeros(numel(D),numel(F));
for z=1:size(aux_caminhos,1)
    caminho=cell2mat(aux_caminhos(z,1));
    p=size(caminho,2);
    for i=1:size(d_aux,1)
        if(cell2mat(d_aux(i,1))==caminho(1) && cell2mat(d_aux(i,2))==caminho(p))
            x=cell2mat(d_aux(i,3));
            y=cell2mat(aux_caminhos(z,2));
            d(x,y)=1;
        end
    end
end
lb=zeros(count,1);
ub=inf(count,1);
for i=1:size(F)
    int(i)=i;
end
[X, O, G, K]=intlinprog(F,int,c,C,d,D,lb,ub)
aux_resultados=[];
for i=1:numero_caminho
    aux_resultados{i,1}=X(i);
    aux_resultados{i,2}=i;
end
for z=1:size(aux_caminhos,1)
    caminho=cell2mat(aux_caminhos(z,1));
    for j=1:(numel(caminho)-1)
        for i=1:size(matrix_aux,1)
            if(cell2mat(matrix_aux(i,3))~=R_link)
                if(cell2mat(matrix_aux(i,1))==caminho(j) &&
                    cell2mat(matrix_aux(i,2))==caminho(j+1))
                    x=cell2mat(matrix_aux(i,3));
                    y=cell2mat(aux_caminhos(z,2));
                    for t=1:size(aux_caminhos,1)
                        if(cell2mat(aux_resultados(t,2))==y)
                            resultados(x,y)=cell2mat(aux_resultados(t,1));
                        end
                    end
                elseif(cell2mat(matrix_aux(i,2))==caminho(j) &&
                    cell2mat(matrix_aux(i,1))==caminho(j+1))
                    x=cell2mat(matrix_aux(i,3));
                    y=cell2mat(aux_caminhos(z,2));
                    for t=1:size(aux_caminhos,1)

```

Appendix A Matlab scripts used in Chapter 2

```

                if (cell2mat(aux_resultados(t,2))==y)
                    resultados(x,y)=cell2mat(aux_resultados(t,1));
                end
            end
        end
    end
end
end
end
end
end
end
R=zeros(numel(C),3);
for i=1:size(resultados,1)
    R(i,1)=cell2mat(matrix_aux(i,1));
    R(i,2)=cell2mat(matrix_aux(i,2));
    for j=1:size(resultados,2)
        aux_count=R(i,3);
        count=resultados(i,j);
        R(i,3)=aux_count+count;
    end
end
end

```

A.6. Example 10

```

%ORIGEM
o= [1 1 2 2 3 3 3 4 4 4];
%DESTINO
d= [3 4 3 4 1 2 4 1 2 3];
%DISTANCIA
c= [1 3 2 1 1 2 1 3 1 1];
%GRAFO
grafo= digraph(o,d,c);
%INTERFACE GRAFO
figure
p_principal=plot(grafo, 'Edglabel', grafo.Edges.Weight);
nos=4; %total number of nodes
origem=[1 1 2 2 3]; % source node
destino=[3 4 3 4 4]; % destination node
links=5; % total number of links
Cores=2;
trafego= [0 1 1 0; % network traffic
          1 0 1 0;
          1 1 0 0;
          0 0 0 0];
numero_caminho=6; %total number of paths
numero_demands=3; %total number of demands
[matriz_rede_caminhos]=caminhos_protecao(nos,grafo,trafego); % disjoint paths
Caminhos={};
aux_c=0;
aux_p=0;
for i=1:numero_caminho % path list
    if (floor(i/2)==i/2)
        aux_p=aux_p+1;
        Caminhos{i,1}=cell2mat(matriz_rede_caminhos(aux_p,3));
        Caminhos{i,2}=i;
    else
        aux_c=aux_c+1;
        Caminhos{i,1}=cell2mat(matriz_rede_caminhos(aux_c,1));
        Caminhos{i,2}=i;
    end
end
end
for l=1:numel(origem) % links with source and destination node numbered
    matrix_aux{l,1}=origem(l);
    matrix_aux{l,2}=destino(l);
    matrix_aux{l,3}=1;
end
end
count=(numero_caminho*Cores)+(links*Cores)+links; %total number of variables used corresponding to flow

```

Appendix A Matlab scripts used in Chapter 2

```

%per demand per color , links per color and links
F=zeros(count,1);
for i=1:count % Objective Function
    if(i>count - links)
        F(i,1)=1;
    end
end
D=zeros((numero_demands+links*Cores),1); % right side of the demand equation
W=triu(trafego,1);
m=0;
for i=1:nos
    for y=1:nos
        if(W(i, y)~=0)
            m=m+1;
            d_aux{m,1}=i;
            d_aux{m,2}=y;
            d_aux{m,3}=m;
        end
    end
end
for i=1:numero_demands
    D(i,1)=1;
end
Z=zeros(numel(origem)*Cores,1);
d=zeros(numel(D),numel(F));
for t=1:Cores
    for z=1:size(Caminhos,1)
        caminho=cell2mat(Caminhos(z,1));
        p=size(caminho,2);
        for i=1:size(d_aux,1)
            if (cell2mat(d_aux(i,1))==caminho(1) &&
                cell2mat(d_aux(i,2))==caminho(p))
                x=cell2mat(d_aux(i,3));
                y=cell2mat(Caminhos(z,2))+(numero_caminho*(t-1));
                d(x, y)=1;
            end
        end
    end
end
count_aux=numero_caminho*Cores+1;
for z=numero_demands+1:size(d,1)
    d(z, count_aux)=-1;
    count_aux=count_aux+1;
end
g=(size(F,1) - links)+1;
for z=numero_demands+1:(size(d,1))
    if g<(size(F,1))+1
        d(z, g)=1;
        g=g+1;
    else
        g=(size(F,1) - links)+1;
        d(z, g)=1;
        g=g+1;
    end
end
c=zeros(numel(Z),numel(F));
for r=1:Cores
    for z=1:size(Caminhos,1)
        caminho=cell2mat(Caminhos(z,1));
        for j=1:(numel(caminho)-1)
            for i=1:size(matrix_aux,1)
                if (cell2mat(matrix_aux(i,1))==caminho(j) &&
                    cell2mat(matrix_aux(i,2))==caminho(j+1))
                    x=cell2mat(matrix_aux(i,3))+(links*(r-1));
                    y=cell2mat(Caminhos(z,2))+(numero_caminho*(r-1));
                end
            end
        end
    end
end

```

Appendix A Matlab scripts used in Chapter 2

```

        c(x, y)=1;
    elseif (cell2mat(matrix_aux(i,2))==caminho(j) &&
cell2mat(matrix_aux(i,1))==caminho(j+1))
        x=cell2mat(matrix_aux(i,3))+(links*(r-1));
        y=cell2mat(Caminhos(z,2))+(numero_caminho*(r-1));
        c(x, y)=1;
    end
end
end
end
k=numero_caminho*Cores+1;
for j=1:size(c,1)
    if k<size(c,2)-links+1
        c(j,k)=-1;
        k=k+1;
    end
end
lb=zeros(count,1);
for i=1:size(F,1)
    if i>(numero_caminho*Cores) && i<=(size(F,1)-links)
        ub(i,1)=1;
    else
        ub(i,1)=inf;
    end
end
int=1:size(F,1);
[X O G K]=intlinprog(F,int,-d,-D,c,Z,lb,ub)
Caminhos_usados=[];
t=0;
for color=1:Cores
    for x=1:numero_caminho
        if (X(x+(color-1)*numero_caminho)~=0)
            t=t+1;
            Caminhos_usados{t,1}=cell2mat(Caminhos(x,1));
            Caminhos_usados{t,2}=color;
        end
    end
end
end
end

```

A.7. Examples 11 and 12

```

%% Anel Trabalho
%ORIGEM
o= [1 2 3 4 5 6 1 6 5 4 3 2 2 6 3 5];
%DESTINO
d= [2 3 4 5 6 1 6 5 4 3 2 1 6 2 5 3];
%DISTANCIA
c= [500 500 500 800 500 800 800 500 800 500 500 500 300 300 300 300];
%GRAFO
grafo= digraph(o,d,c);
%INTERFACE GRAFO
figure
p_principal=plot(grafo, 'Edglabel', grafo.Edges.Weight);
nos=6;
origem=[1 2 3 4 5 6 2 3];
destino=[2 3 4 5 6 1 6 5];
distancia=[500 500 500 800 500 800 300 300];
links=8;
Cores=5;
tot_o=[1 1 1 1 1 2 2 2 2 3 3 3 4 4 5];
tot_d=[2 3 4 5 6 3 4 5 6 4 5 6 5 6 6];
tot_l= [0 1 0 0 0 1;
        1 0 1 0 0 1;
        0 1 0 1 1 0;

```

Appendix A *Matlab scripts used in Chapter 2*

```

    0 0 1 0 1 0;
    0 0 1 1 0 1;
    1 1 0 0 1 0];
[trafego_rede]=trafego(nos);
N=2;
for m=1:numel(tot_o)
    [DIST_T, PATH_T] = graphkshortestpaths(tot_l, tot_o(m), tot_d(m), N);
    n=3;
    for i=1:N
        j=i-2;
        matriz_caminhos{m,i}=cell2mat(PATH_T(i));%candidate path list per demand
        matriz_caminhos_dist{m,i}=(DIST_T(i));
    end
end
numero_caminho=size(matriz_caminhos,1)*N;
numero_demands=length(tot_d);
Caminhos={};
aux_c=0;
aux_p=0;
for i=1:numero_caminho
    if(floor(i/2)==i/2)
        aux_p=aux_p+1;
        Caminhos{i,1}=cell2mat(matriz_caminhos(aux_p,2));
        Caminhos{i,2}=i;

    else
        aux_c=aux_c+1;
        Caminhos{i,1}=cell2mat(matriz_caminhos(aux_c,1));
        Caminhos{i,2}=i;
    end
end
for l=1:numel(origem)
    matrix_aux{1,1}=origem(l);
    matrix_aux{1,2}=destino(l);
    matrix_aux{1,3}=1;
end
count=(numero_caminho*Cores)+(links*Cores)+size(matrix_aux,1);
F=zeros(count,1);
for i=1:count
    if(i>count-links)
        F(i,1)=1;
    end
end
D=zeros((numero_demands+links*Cores),1);
W=triu(Trafego,1);
m=0;
for i=1:nos
    for y=1:nos
        if(W(i,y)~=0)
            m=m+1;
            D(m,1)=1;
            d_aux{m,1}=i;
            d_aux{m,2}=y;
            d_aux{m,3}=m;
        end
    end
end
Z=zeros(numel(origem)*Cores,1);
d=zeros(numel(D),numel(F));
for t=1:Cores
    for z=1:size(Caminhos,1)
        caminho=cell2mat(Caminhos(z,1));
        p=size(caminho,2);
        for i=1:size(d_aux,1)
            if(cell2mat(d_aux(i,1))==caminho(1) && cell2mat(d_aux(i,2))==caminho(p))

```

Appendix A Matlab scripts used in Chapter 2

```

        x=cell2mat(d_aux(i,3));
        y=cell2mat(Caminhos(z,2))+(numero_caminho*(t-1));
        d(x,y)=1;
    end
end
end
count_aux=numero_caminho*Cores+1;
for z=numero_demands+1:size(d,1)
    d(z,count_aux)=-1;
    count_aux=count_aux+1;
end
g=(size(F,1)-links)+1;
for z=numero_demands+1:(size(d,1))
    if g<(size(F,1))+1
        d(z,g)=1;
        g=g+1;
    else
        g=(size(F,1)-links)+1;
        d(z,g)=1;
        g=g+1;
    end
end
c=zeros(numel(Z),numel(F));
for r=1:Cores
    for z=1:size(Caminhos,1)
        caminho=cell2mat(Caminhos(z,1));
        for j=1:(numel(caminho)-1)
            for i=1:size(matrix_aux,1)
                if (cell2mat(matrix_aux(i,1))==caminho(j) &&
                    cell2mat(matrix_aux(i,2))==caminho(j+1))
                    x=cell2mat(matrix_aux(i,3))+(links*(r-1));
                    y=cell2mat(Caminhos(z,2))+(numero_caminho*(r-1));
                    c(x,y)=1;
                elseif (cell2mat(matrix_aux(i,2))==caminho(j) &&
                    cell2mat(matrix_aux(i,1))==caminho(j+1))
                    x=cell2mat(matrix_aux(i,3))+(links*(r-1));
                    y=cell2mat(Caminhos(z,2))+(numero_caminho*(r-1));
                    c(x,y)=1;
                end
            end
        end
    end
end
k=numero_caminho*Cores+1;
for j=1:size(c,1)
    if k<size(c,2)-links+1
        c(j,k)=-1;
        k=k+1;
    end
end
lb=zeros(count,1);
for i=1:size(F,1)
    if i>(numero_caminho*Cores) && i<=(size(F,1)-links)
        ub(i,1)=1;
    else
        ub(i,1)=inf;
    end
end
int=1:1:size(F,1);
[X, O, G, K]=intlinprog(F,int,-d,-D,c,Z,lb,ub)
Caminhos_usados=[];
t=0;
for color=1:Cores
    for x=1:numero_caminho

```


Appendix A Matlab scripts used in Chapter 2

```

if (X(x+(color -1)*numero_caminho)~=0)
    t=t+1;
    Caminhos_usados{t,1}=cell2mat(Caminhos(x,1));
    Caminhos_usados{t,2}=color;
end
end
end

```

A.8. Example 13

The equivalent parameter used in the Alternative ILP Formulation and RWA formulation are shown in Table A.4.

Variable	RWA ILP formulation	Alternative RWA formulation
Total number of nodes	V	\mathcal{N}
Specific node	v	n
Total number of links	E	\mathcal{L}
Specific link	e	l
Total number of demands	D	\mathcal{S}
Specific demand	d	s
Total number of colors	C	\mathcal{W}
Specific color	c	w
Number of times the color is used	z_{ce}	F_l
Demand volume	h_{ds}	t^s
Link capacity	y_e	–
Total number of candidate paths per demand	P_d	\mathcal{P}^s
Specific path	p	p
Specific candidate path for demand	P_{dp}	p^s
Flow	x_{dpc}	f_w^p
Link-path relation	δ_{edp}	F_l

Table A.4. Comparison between RWA ILP formulation parameters and alternative RWA formulation parameters.

```

%ORIGEM
o= [1 2 3 4 5 1 5 4 3 2 1 2 4 4];
%DESTINO
d= [2 3 4 5 1 5 4 3 2 1 4 4 1 2];
%DISTANCIA
c= [1 1 1 1 1 1 1 1 1 1 1 1 1 1];
%GRAFO
grafo= digraph(o,d,c);
%INTERFACE GRAFO
figure
p_principal=plot(grafo, 'Edgelabel', grafo.Edges.Weight);
nos=5;
origem=[1 2 3 4 5 1 5 4 3 2 1 2 4 4];
destino=[2 3 4 5 1 5 4 3 2 1 4 4 1 2];
distancia=[1 1 1 1 1 1 1 1 1 1 1 1 1 1];
links=14;
Cores=2;
tot_o=[1 2 3 3 4 4 5 5];
tot_d=[3 4 1 5 2 5 3 4];
tot_l= [0 0 1 0 0;
        0 0 0 1 0;
        1 0 0 0 1;
        0 1 0 0 1;
        0 0 1 1 0];
[trafego_rede]=trafego(nos);
matriz_caminhos{1,1}=[1,2,3];

```

Appendix A *Matlab scripts used in Chapter 2*

```

matriz_caminhos{1,2}=1;
matriz_caminhos{2,1}=[1,4,3];
matriz_caminhos{2,2}=2;
matriz_caminhos{3,1}=[2,4];
matriz_caminhos{3,2}=3;
matriz_caminhos{4,1}=[2,1,4];
matriz_caminhos{4,2}=4;
matriz_caminhos{5,1}=[3,2,1];
matriz_caminhos{5,2}=5;
matriz_caminhos{6,1}=[3,4,1];
matriz_caminhos{6,2}=6;
matriz_caminhos{7,1}=[3,4,5];
matriz_caminhos{7,2}=7;
matriz_caminhos{8,1}=[3,2,1,5];
matriz_caminhos{8,2}=8;
matriz_caminhos{9,1}=[4,2];
matriz_caminhos{9,2}=9;
matriz_caminhos{10,1}=[4,3,2];
matriz_caminhos{10,2}=10;
matriz_caminhos{11,1}=[4,5];
matriz_caminhos{11,2}=11;
matriz_caminhos{12,1}=[4,1,5];
matriz_caminhos{12,2}=12;
matriz_caminhos{13,1}=[5,4,3];
matriz_caminhos{13,2}=13;
matriz_caminhos{14,1}=[5,1,2,3];
matriz_caminhos{14,2}=14;
matriz_caminhos{15,1}=[5,4];
matriz_caminhos{15,2}=15;
matriz_caminhos{16,1}=[5,1,4];
matriz_caminhos{16,2}=16;
numero_caminho=size(matriz_caminhos,1);
numero_demands=length(tot_o);
Caminhos={};
aux_c=0;
aux_p=0;
for i=1:size(matriz_caminhos,1)
    Caminhos{i,1}=cell2mat(matriz_caminhos(i,1));
    Caminhos{i,2}=i;
end
for l=1:numel(origem)
    matrix_aux{1,1}=origem(l);
    matrix_aux{1,2}=destino(l);
    matrix_aux{1,3}=1;
end
count=(numero_caminho*Cores)+(links*Cores)+size(matrix_aux,1);
F=zeros(count,1);
for i=1:count
    %if(i>count-links) %minimizar capacidade
    if(i>numero_caminho && i<=count-links) %minimizar cores
        F(i,1)=1;
    end
end
aux_D=links*Cores+numero_demands
D=zeros((aux_D),1);
for i=1:numero_demands
    D(i,1)=1;
end
W=tot_l;
m=0;
for i=1:nos
    for y=1:nos
        if(W(i,y)~=0)
            m=m+1;
            d_aux{m,1}=i;
        end
    end
end

```

Appendix A *Matlab scripts used in Chapter 2*

```

        d_aux{m,2}=y;
        d_aux{m,3}=m;
    end
end
end
Z=zeros(links*Cores,1);
d=zeros(numel(D),numel(F));
for t=1:Cores
    for z=1:size(Caminhos,1)
        caminho=cell2mat(Caminhos(z,1));
        p=size(caminho,2);
        for i=1:size(d_aux,1)
            if (cell2mat(d_aux(i,1))==caminho(1) && cell2mat(d_aux(i,2))==caminho(p))
                x=cell2mat(d_aux(i,3));
                y=cell2mat(Caminhos(z,2)+(numero_caminho*(t-1)));
                d(x,y)=1;
            end
        end
    end
end
count_aux=numero_caminho*Cores+1;
for z=numero_demands+1:size(d,1)
    d(z,count_aux)=-1;
    count_aux=count_aux+1;
end
g=(size(F,1)-links)+1;
for z=numero_demands+1:(size(d,1))
    if g<(size(F,1))+1
        d(z,g)=1;
        g=g+1;
    else
        g=(size(F,1)-links)+1;
        d(z,g)=1;
        g=g+1;
    end
end
end
c=zeros(numel(Z),numel(F));
for r=1:Cores
    for z=1:size(Caminhos,1)
        caminho=cell2mat(Caminhos(z,1));
        for j=1:(numel(caminho)-1)
            for i=1:size(matrix_aux,1)
                if (cell2mat(matrix_aux(i,1))==caminho(j) &&
                    cell2mat(matrix_aux(i,2))==caminho(j+1))
                    x=cell2mat(matrix_aux(i,3)+(links*(r-1)));
                    y=cell2mat(Caminhos(z,2)+(numero_caminho*(r-1)));
                    c(x,y)=1;
                end
            end
        end
    end
end
end
k=numero_caminho*Cores+1;
for j=1:size(c,1)
    if k<size(c,2)-links+1
        c(j,k)=-1;
        k=k+1;
    end
end
end
lb=zeros(count,1);
for i=1:size(F,1)
    if i>(numero_caminho*Cores) && i<=(size(F,1)-links)
        ub(i,1)=1;
    else
        ub(i,1)=inf;
    end
end

```

Appendix A Matlab scripts used in Chapter 2

```

end
end
int=1:size(F,1);
[X, O, G, K]=intlinprog(F,int, -d, -D, c, Z, lb, ub )
toc
Caminhos_usados=[];
t=0;
for color=1:Cores
    for x=1:numero_caminho
        if (X(x+(color-1)*numero_caminho)~=0)
            t=t+1;
            Caminhos_usados{t,1}=cell2mat(Caminhos(x,1));
            Caminhos_usados{t,2}=color;
        end
    end
end
end

```

A.9. ILP formulations applied in the portuguese backbone networked

```

M={ [1,3,2];[1,2,3];[1,3,5,4];[1,2,3,5];[1,2,4,6];[1,2,4,6,8,7];[1,2,4,6,8];[1,3,5,4,9];
[1,2,4,9,10];[1,2,4,9,10,11];[1,11,12]; [2,1,3];[2,3,5,4];[2,4,5];[2,4,6];[2,4,6,8,7];
[2,4,6,8];[2,3,5,4,9];[2,1,11,10];[2,4,9,10,11];[2,1,11,12]; [3,2,4];[3,2,4,5];[3,2,4,6];
[3,2,4,6,7];[3,2,4,6,8];[3,2,4,9];[3,2,4,9,10];[3,2,1,11];[3,2,1,12]; [4,2,3,5];[4,5,6];
[4,5,6,7];[4,5,6,8];[4,6,8,9];[4,2,1,11,10];[4,5,3,1,11];[4,5,3,1,12]; [5,4,6];[5,4,6,7];
[5,4,6,8];[5,6,4,9];[5,6,4,9,10];[5,3,2,1,11];[5,3,2,1,12]; [6,8,7];[6,7,8];[6,5,4,9];
[6,5,4,9,10];[6,5,3,2,1,11];[6,5,3,2,1,12]; [7,6,8];[7,8,6,4,9];[7,8,6,4,9,10];
[7,6,5,3,2,1,11];[7,6,5,3,2,1,12]; [8,6,7,4,9];[8,7,6,4,9,10];[8,6,5,3,2,1,11];
[8,6,5,3,2,1,12]; [9,4,2,1,11,10];[9,4,5,3,1,11];[9,4,5,3,1,12]; [10,9,4,2,1,11];
[10,9,4,2,1,12] [11,1,12]};
%% Topologia
Origem=[1 1 2 2 3 5 5 4 6 7 6 4 8 9 10 1 11 12 2 3 3 4 5 4 6 6 7 8 8 9 9 10 11 11 12 1];
Destino=[2 3 3 4 5 4 6 6 7 8 8 9 9 10 11 11 12 1 1 1 2 2 3 5 5 4 6 7 6 4 8 9 10 1 11 12];
Distancia=[76 142 70 136 113 58 67 116 70 47 53 84 424 386 278 298 1010 1050 76 142 70 136
113 58 67 116 70 47 53 84 424 386 278 298 1010 1050];
grafo= digraph(Origem, Destino, Distancia);
p=plot(grafo, 'EdgeLabel', grafo.Edges.Weight);
Nos=12;
max_fibra=87;
d.caminho= [0 76 142 0 0 0 0 0 0 298 1050;
76 0 70 136 0 0 0 0 0 0 0 0;
142 70 0 0 113 0 0 0 0 0 0 0;
0 136 0 0 58 116 0 0 84 0 0 0;
0 0 113 58 0 67 0 0 0 0 0 0;
0 0 0 116 67 0 70 53 0 0 0 0;
0 0 0 0 70 0 47 0 0 0 0 0;
0 0 0 0 53 47 0 424 0 0 0 0;
0 0 0 84 0 0 0 424 0 386 0 0;
0 0 0 0 0 0 0 0 386 0 1010 0;
298 0 0 0 0 0 0 0 0 278 0 1010;
1050 0 0 0 0 0 0 0 0 1010 0];
Trafego=[0 104 137 104 207 3322 21 104 91 104 203 75;
104 0 21 104 21 21 104 21 75 21 21 21;
137 21 0 104 21 21 125 21 21 63 42 21;
104 104 104 0 89 21 53 21 21 21 21 21;
207 21 21 89 0 42 63 21 83 21 42 87;
3322 21 21 21 42 0 83 42 42 21 21 21;
21 104 125 53 63 83 0 116 53 42 145 42;
104 21 21 21 21 42 116 0 21 21 21 21;
91 75 21 21 83 42 53 21 0 42 21 21;
104 21 63 21 21 21 42 21 42 0 68 42;
203 21 42 21 42 21 145 21 21 68 0 21;
75 21 21 21 87 21 42 21 21 42 21 0];
[caminhos]=caminhos_R(Nos, grafo);
%%existem 18 links
Orig=[1 1 2 2 3 5 5 4 6 7 6 4 8 9 10 1 11 1];

```

Appendix A *Matlab scripts used in Chapter 2*

```

Dest=[2 3 3 4 5 4 6 6 7 8 8 9 9 10 11 11 12 12];
Dist=[76; 142; 70; 136; 113; 58; 67; 116; 70; 47; 53; 84; 424; 386; 278; 298; 1010; 1050];
O=[1 1 1 1 1 1 1 1 1 1 1 2 2 2 2 2 2 2 2 2 3 3 3 3 3 3 3 3 4 4 4 4 4 4 4 4 5 5 5 5 5 5
5 6 6 6 6 6 6 7 7 7 7 7 8 8 8 8 9 9 9 9 10 10 11];
D=[2 3 4 5 6 7 8 9 10 11 12 3 4 5 6 7 8 9 10 11 12 4 5 6 7 8 9 10 11 12 5 6 7 8 9 10 11 12
6 7 8 9 10 11 12 7 8 9 10 11 12 8 9 10 11 12 9 10 11 12 10 11 12 11 12 12];
x=numel(caminhos);
p=x/2;
aux=zeros(p,1);
for m=1:numel(O)
    [ DIST_T, PATH_T ] = graphkshortestpaths(d.caminho, O(m), D(m), 2);
    matriz_caminhos{m,1}=cell2mat(PATH_T(1));
    matriz_caminhos{m,2}=DIST_T(1);
    matriz_caminhos{m,3}=cell2mat(M(m));
    matriz_caminhos{m,4}=DIST_T(2);
end
for l=1:numel(Orig)
    matrix_aux{1,1}=Orig(l);
    matrix_aux{1,2}=Dest(l);
    matrix_aux{1,3}=1;
end
count=numel(aux)+1;
F=zeros(count,1);
for i=1:count
    if(i>numel(aux))
        F(i,1)=1;
    end
end
aux_caminhos=[];
for i=1:size(aux)
    if bitget(i,1)
        c=i/2+0.5;
        aux_caminhos{i,1}=cell2mat(matriz_caminhos(c,1));
        aux_caminhos{i,2}=i;
    else
        c=i/2;
        aux_caminhos{i,1}=cell2mat(matriz_caminhos(c,3));
        aux_caminhos{i,2}=i;
    end
end
D=[];
W=triu(Trafego,1);
m=0;
for i=1:Nos
    for y=1:Nos
        if(W(i,y)~=0)
            m=m+1;
            D(m,1)=W(i,y);
            d_aux{m,1}=i;
            d_aux{m,2}=y;
            d_aux{m,3}=m;
        end
    end
end
C=zeros(numel(Orig),1);
c=zeros(numel(C),numel(F));
for z=1:size(aux_caminhos,1)
    caminho=cell2mat(aux_caminhos(z,1));
    for j=1:(numel(caminho)-1)
        for i=1:size(matrix_aux,1)
            if (cell2mat(matrix_aux(i,1))==caminho(j) &&
cell2mat(matrix_aux(i,2))==caminho(j+1))
                x=cell2mat(matrix_aux(i,3));
                y=cell2mat(aux_caminhos(z,2));
                c(x,y)=1;
            end
        end
    end
end

```

Appendix A *Matlab scripts used in Chapter 2*

```

        elseif (cell2mat (matrix_aux (i,2))==caminho(j) &&
cell2mat (matrix_aux (i,1))==caminho(j+1))
            x=cell2mat (matrix_aux (i,3));
            y=cell2mat (aux_caminhos (z,2));
            c(x, y)=1;
        end
    end
end
for m=1:size (c,1)
    c(m, numel (aux)+1)=-1;
end
end
d=zeros (numel(D), numel(F));
for z=1:size (aux_caminhos,1)
    caminho=cell2mat (aux_caminhos (z,1));
    p=size (caminho,2);
    for i=1:size (d_aux,1)
        if (cell2mat (d_aux (i,1))==caminho(1) &&
cell2mat (d_aux (i,2))==caminho(p))
            x=cell2mat (d_aux (i,3));
            y=cell2mat (aux_caminhos (z,2));
            d(x, y)=1;
        end
    end
end
end
lb=zeros (count,1);
ub=inf (count,1);
for i=1:size (F)
    int (i)=i;
end
[X, O, G, K]=intlinprog (F,int, c, C, d, D, lb, ub)
aux_resultados=[];
for i=1:size (aux,1)
    aux_resultados {i,1}=X(i);
    aux_resultados {i,2}=i;
end
for z=1:size (aux_caminhos,1)
    caminho=cell2mat (aux_caminhos (z,1));
    for j=1:(numel (caminho)-1)
        for i=1:size (matrix_aux,1)
            if (cell2mat (matrix_aux (i,1))==caminho(j)
&& cell2mat (matrix_aux (i,2))==caminho(j+1))
                x=cell2mat (matrix_aux (i,3));
                y=cell2mat (aux_caminhos (z,2));
                for t=1:size (aux_caminhos,1)
                    if (cell2mat (aux_resultados (t,2))==y)
                        resultados (x, y)=cell2mat (aux_resultados (t,1));
                    end
                end
            elseif (cell2mat (matrix_aux (i,2))==caminho(j)
&& cell2mat (matrix_aux (i,1))==caminho(j+1))
                x=cell2mat (matrix_aux (i,3));
                y=cell2mat (aux_caminhos (z,2));
                for t=1:size (aux_caminhos,1)
                    if (cell2mat (aux_resultados (t,2))==y)
                        resultados (x, y)=cell2mat (aux_resultados (t,1));
                    end
                end
            end
        end
    end
end
end
end
R=zeros (numel(C),3);
for i=1:size (resultados,1)
    R(i,1)=cell2mat (matrix_aux (i,1));

```

Appendix A *Matlab scripts used in Chapter 2*

```
R(i,2)=cell2mat(matrix_aux(i,2));
for j=1:size(resultados,2)
    aux_count=R(i,3);
    count=resultados(i,j);
    R(i,3)=aux_count+count;
end
end
```


APPENDIX B

OSNR path calculation details in Chapter 3

In this appendix, some additional results concerning the paths example used throughout Chapter 3 are presented.

Firstly, the total OSNRs calculated only with the ASE noise for each one of the candidate paths are presented in Table B.1, for an amplifier maximum gain of 23 dB. In Tables B.2 and B.3, for the optical channel power of 1.46 dBm obtained for the longest candidate path in the COST 239 network, P_{35} , the total OSNRs are shown, respectively calculated considering only the ASE noise (Table B.2) and considering only the NLI (Table B.3).

P_{dp}	OSNR _{tot,m} [dB]	P_{dp}	OSNR _{tot,m}	P_{dp}	OSNR _{tot,m}	P_{dp}	OSNR _{tot,m}	P_{dp}	OSNR _{tot,m}
P_{11}	16	P_{12}	15.4	P_{13}	15.1	P_{14}	14.4	P_{15}	13.8
P_{21}	17.4	P_{22}	16	P_{23}	14.4	P_{24}	14.2	P_{25}	14
P_{31}	19.4	P_{32}	15.9	P_{33}	15	P_{34}	13.7	P_{35}	13.4
P_{41}	16.3	P_{42}	15.2	P_{43}	15.4	P_{44}	14.8	P_{45}	14.3

Table B.1. Total OSNR with ASE noise for the candidate paths for demands 1 to 4 with $G_{max}=23$ dB for network COST 239.

P_{dp}	OSNR _{tot,m} [dB]	P_{dp}	OSNR _{tot,m}	P_{dp}	OSNR _{tot,m}	P_{dp}	OSNR _{tot,m}	P_{dp}	OSNR _{tot,m}
P_{11}	16.1	P_{12}	16.8	P_{13}	16.5	P_{14}	15	P_{15}	15.3
P_{21}	18.9	P_{22}	16.3	P_{23}	14.9	P_{24}	14.7	P_{25}	14.3
P_{31}	20.8	P_{32}	16.6	P_{33}	15.5	P_{34}	15.2	P_{35}	13.6
P_{41}	17.7	P_{42}	15.6	P_{43}	16.2	P_{44}	15.3	P_{45}	15.8

Table B.2. Total OSNR with ASE noise for the candidate paths for demands 1 to 4 with $P_m=1.46$ dBm for network COST 239.

P_{dp}	OSNR _{tot,m} [dB]	P_{dp}	OSNR _{tot,m}	P_{dp}	OSNR _{tot,m}	P_{dp}	OSNR _{tot,m}	P_{dp}	OSNR _{tot,m}
P_{11}	19.7	P_{12}	19.2	P_{13}	18.5	P_{14}	18.2	P_{15}	17.6
P_{21}	21.2	P_{22}	19.7	P_{23}	18.2	P_{24}	17.6	P_{25}	17.6
P_{31}	23.6	P_{32}	19.7	P_{33}	18.5	P_{34}	17.6	P_{35}	16.6
P_{41}	20.1	P_{42}	18.9	P_{43}	18.5	P_{44}	18.2	P_{45}	17.9

Table B.3. Total OSNR with NLI noise for the candidate paths for demands 1 to 4 with $P_m=1.46$ dBm for network COST 239.

Complementary material used in Chapter 4

C.1. Real network topologies

The real network topologies that are presented are used in Chapter 4 to solve the RWA problem. In the four network topologies the nodes are numbered sequentially with no particular order.

Figure C1 shows the physical topology of the network COST 239 [16]. The physical topology has eleven nodes and twenty-six links. The longest connection has 953 km between nodes one and two, the shortest link is between nodes three and five with 171 km. The average node degree is 4.73.

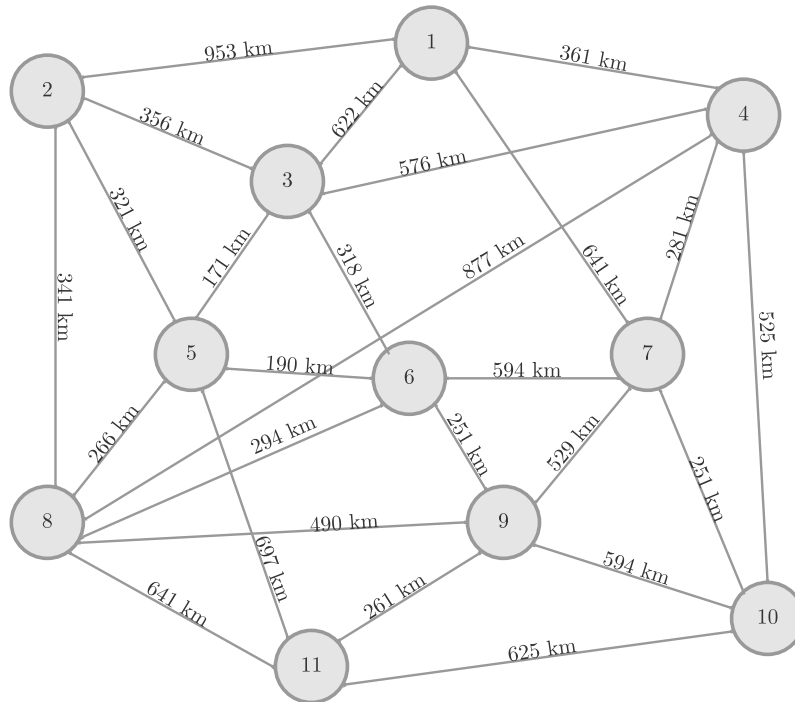


Figure C1. Optical network COST 239 physical topology.

Figure C2 shows the physical topology of the network NSFNET [24]. The physical topology has fourteen nodes and twenty-one links. The longest connection has 2828 km between nodes one and eight, the shortest link is between nodes ten and fourteen with 246 km. The average node degree is 3.

Figure C3 shows the physical topology of the network UBN [25]. The physical topology has twenty-four nodes and forty-three links. The longest connection has 2600 km between nodes fifteen and nineteen, the shortest link is between nodes three and four with 250 km. The average node degree is 3.58.

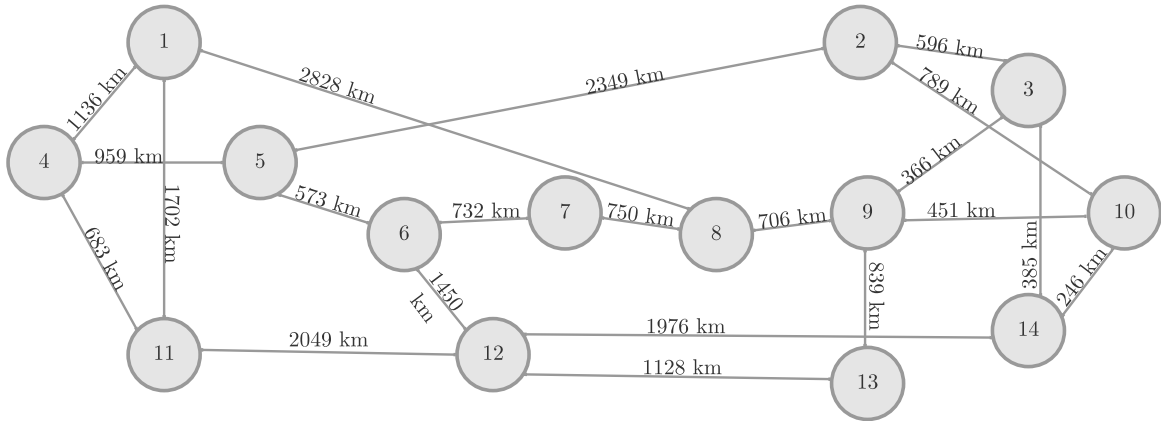


Figure C2. Optical network NSFNET physical topology.

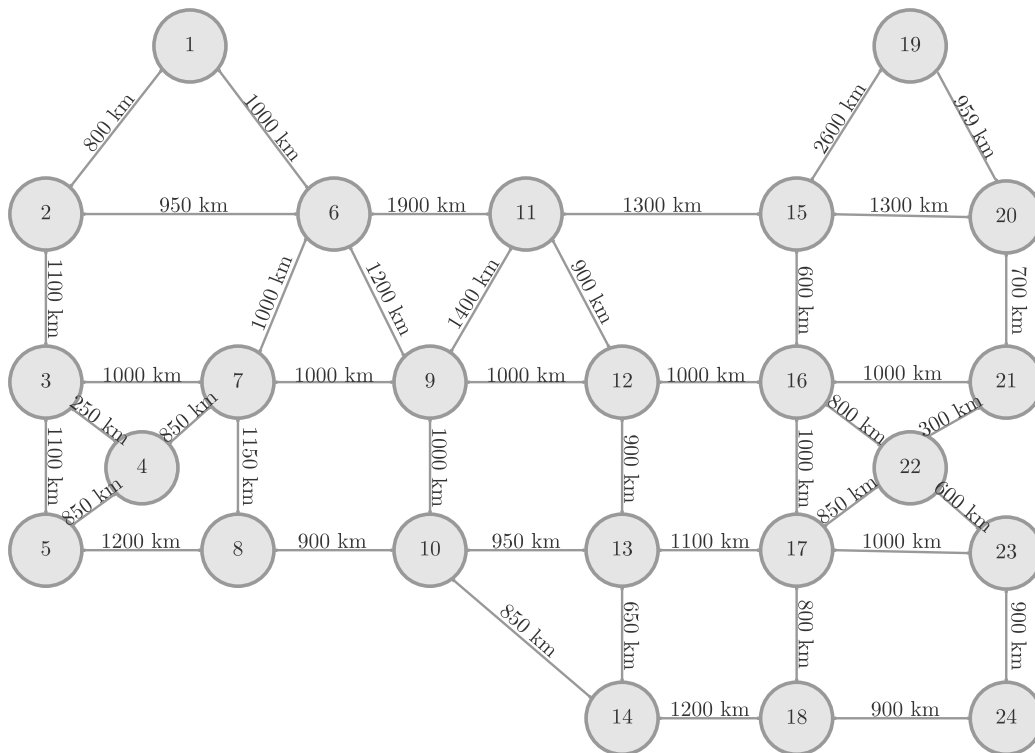


Figure C3. Optical network UBN physical topology.

Figure C4 shows the physical topology of the network CONUS 30 [6]. The physical topology has thirty nodes and thirty-six links. The longest connection has 1463 km between nodes twenty-two and twenty-seven, the shortest link is between nodes twenty-four and twenty-five with 69 km. The average node degree is 2.40.

C.2. First Fit and Most Used algorithms

First Fit algorithm

Appendix C Complementary material used in Chapter 4

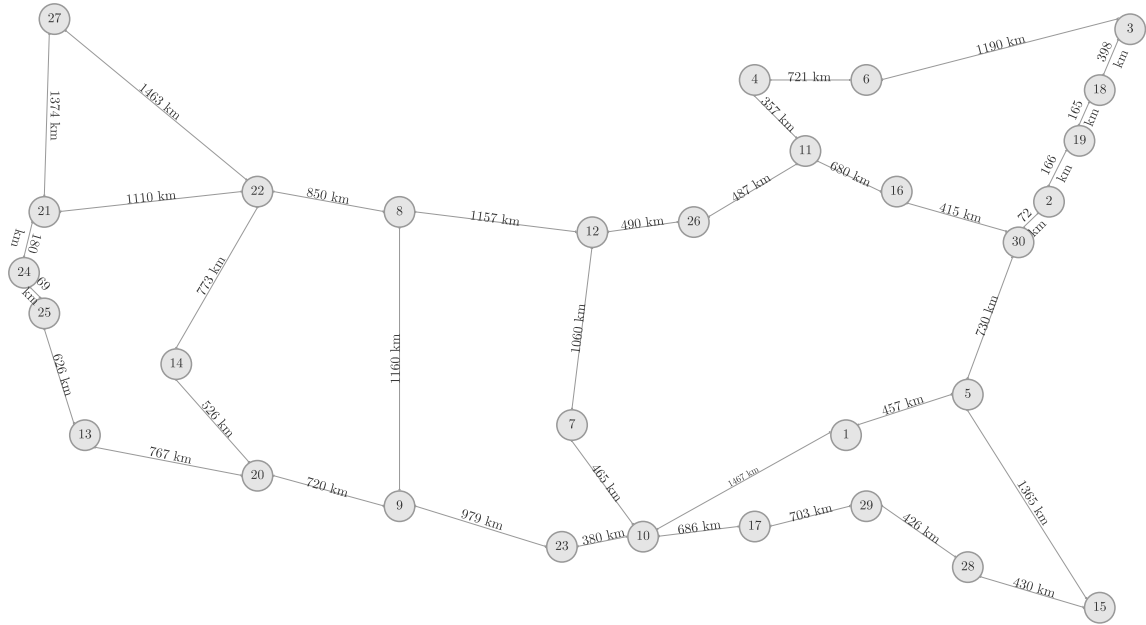


Figure C4. Optical network CONUS 30 physical topology.

```

function [comp_onda]=First_Fit(origem, destino, trafego_rede, caminhos, max_fibra)
matrix_aux={};
comp_onda=cell(height(caminhos),3);
for l=1:numel(origem) %links source and destination numbered
    matrix_aux{1,1}=origem(l);
    matrix_aux{1,2}=destino(l);
    matrix_aux{1,3}=1;
end
count=0;
while true %wavelengths available
    if count<max_fibra
        count=count+1;
        Wavelengths(count,1)=count;
    else
        break;
    end
end
for i=1:size(max_fibra,1) %wavelengths available per links
    for x=2:(size(matrix_aux,1)+1)
        Wavelengths(i,x)=0;
    end
end
for l=1:size(caminhos,1) %path and traffic
    p=cell2mat(caminhos(l,1));
    trafego_aux=trafego_rede(p(1), p(numel(p)));
    comp_onda(l,1)=caminhos(l,1);
    for i=1:trafego_aux
        comp_onda{1,2}=i;
    end
end
for i=1:size(comp_onda,1)
    p=cell2mat(comp_onda(i,1));
    aux_caminho={};
    for j=1:numel(p)-1
        for x=1:size(matrix_aux,1) %%list with links used in the path numbered
            if (cell2mat(matrix_aux(x,1))==p(j) && cell2mat(matrix_aux(x,2))==p(j+1))
                m=height(aux_caminho);
                m=m+1;
            end
        end
    end
end

```

Appendix C Complementary material used in Chapter 4

```

        aux_caminho{m,1}=matrix_aux{x,1};
        aux_caminho{m,2}=matrix_aux{x,2};
        aux_caminho{m,3}=matrix_aux{x,3}+1; %numbered link corresponds to Wavelengths
    elseif (cell2mat(matrix_aux(x,2))==p(j) && cell2mat(matrix_aux(x,1))==p(j+1))
        m=height(aux_caminho);
        m=m+1;
        aux_caminho{m,1}=matrix_aux{x,1};
        aux_caminho{m,2}=matrix_aux{x,2};
        aux_caminho{m,3}=matrix_aux{x,3}+1;
    end
end
end
total_links_used_path=size(aux_caminho,1);
flag=1;
blocked_path=0;
link={};
t=0;
for y=1:cell2mat(comp_onda(i,2)) %Traffic
    for w=1:size(aux_caminho,1)
        link{1,w}=(aux_caminho{w,3});
    end
    link_1=link{1,1};
    while true
        t=t+1;
        if Wavelengths(t,link_1)==0 %verifies if the wavelengths is not being
            aux_count=t; %used in the 1st link
            FS_selected={};
            FS_selected{1,1}=aux_count;
            flag=0;
        else
            flag=1;
        end
        if total_links_used_path~=1
            for w=2:total_links_used_path %verifies the wavelength in the other links
                link_dif_1=link{1,w};
                for kj=1:length(FS_selected)
                    fs_using=FS_selected{1,kj};
                    if Wavelengths(fs_using,link_dif_1)==1
                        flag=1;
                        break;
                    end
                end
            end
        end
        if flag==0
            break;
        end
        if t==max_fibra
            blocked_path=1;
            break;
        end
    end
end
for w=1:total_links_used_path %saves the paths wavelength
    x=link{1,w};
    if blocked_path~=1
        for u=1:size(FS_selected,2)
            r=FS_selected{1,u};
            Wavelengths(r,x)=1;
            comp_onda{i,2+y}=Wavelengths(r,1);
        end
    else
        comp_onda{i,4}='blocked';
    end
end
end
end
end

```

Appendix C Complementary material used in Chapter 4

end

Most Used algorithm

```
function [comp_onda]=Most-Used(origem, destino, trafego_rede, caminhos, max_fibra)
matrix_aux={};
comp_onda=cell(height(caminhos),3);
for l=1:numel(origem) %links source and destination numbered
    matrix_aux{1,1}=origem(l);
    matrix_aux{1,2}=destino(l);
    matrix_aux{1,3}=1;
end
links=size(matrix_aux,1);%number of links
count=0;
while true %wavelengths available
    if count<max_fibra
        count=count+1;
        Wavelengths(count,1)=count;
    else
        break;
    end
end
for i=1:size(max_fibra,1)%wavelengths available per links
    for x=2:(links+2)
        Wavelengths(i,x)=0;
    end
end
for l=1:size(caminhos,1) %path and traffic
    p=cell2mat(caminhos(l,1));
    trafego_aux=trafego_rede(p(1), p(numel(p)));
    comp_onda(l,1)=caminhos(l,1);
    for i=1:trafego_aux
        comp_onda{1,2}=i;
    end
end
for i=1:size(comp_onda,1)
    p=cell2mat(comp_onda(i,1));
    aux_caminho={};
    for j=1:numel(p)-1
        for x=1:size(matrix_aux,1) %list with links used in the path numbered
            if (cell2mat(matrix_aux(x,1))==p(j) && cell2mat(matrix_aux(x,2))==p(j+1))
                m=height(aux_caminho);
                m=m+1;
                aux_caminho{m,1}=matrix_aux{x,1};
                aux_caminho{m,2}=matrix_aux{x,2};
                aux_caminho{m,3}=matrix_aux{x,3}+1; %numbered link corresponds to Wavelengths
            elseif (cell2mat(matrix_aux(x,2))==p(j) && cell2mat(matrix_aux(x,1))==p(j+1))
                m=height(aux_caminho);
                m=m+1;
                aux_caminho{m,1}=matrix_aux{x,1};
                aux_caminho{m,2}=matrix_aux{x,2};
                aux_caminho{m,3}=matrix_aux{x,3}+1;
            end
        end
    end
    total_links_used_path=size(aux_caminho,1);
    flag=1;
    blocked_path=0;
    link={};
    t=0;
    for y=1:cell2mat(comp_onda(i,2)) %Traffic
        for w=1:size(aux_caminho,1) list of links
            link{1,w}=(aux_caminho{w,3});
        end
        link_1=link{1,1};
        while true
```

Appendix C Complementary material used in Chapter 4

```

t=t+1;
if Wavelengths(t,link_1)==0 %verifies if the wavelengths is not being
    aux_count=t; %used in the 1st link
    FS_selected={};
    FS_selected{1,1}=aux_count;
    flag=0;
else
    flag=1;
end
if total_links_used_path~=1
    for w=2:total_links_used_path %verifies the wavelength in the other links
        link_dif_1=link{1,w};
        for kj=1:length(FS_selected)
            fs_using=FS_selected{1,kj};
            if Wavelengths(fs_using,link_dif_1)==1
                flag=1;
                break;
            end
        end
    end
end
if flag==0
    break;
end
if t==max_fibra
    blocked_path=1;
    break;
end
end
for w=1:total_links_used_path %saves the paths wavelength
    x=link{1,w};
    if blocked_path~=1
        for u=1:size(FS_selected,2)
            r=FS_selected{1,u};
            Wavelengths(r,x)=1;
            comp_onda{i,2+y}=Wavelengths(r,1);
        end
    else
        comp_onda{i,1}='blocked';
    end
end
end
e=size(Wavelengths,2);
for r=1:size(Wavelengths,1) %organizes the wavelengths from the most used to the least
    Sum_aux=sum(Wavelengths(r,2:(links+1)),2);
    Wavelengths(r,e)=Sum_aux;
end
Wavelengths=sortrows(Wavelengths,-(links+2));
end

```

C.3. ILP solution for RWA

```

function [Caminhos_usados, R, resultados, Tempo]=
ILP_RWA(Cores, N, nos, links, tot_o, tot_d, tot_l, origem, destino)
tic
[trafego_rede]=trafego(nos);
for m=1:numel(tot_o)
    [DIST_T, PATH_T] = graphshortestpaths(tot_l, tot_o(m), tot_d(m), N);
    matriz_caminhos{m,1}= tot_o(m);
    matriz_caminhos{m,2}=tot_d(m);
    matriz_caminhos_dist{m,1}= tot_o(m);
    matriz_caminhos_dist{m,2}=tot_d(m);
    for i=3:(N+2)
        j=i-2;
        matriz_caminhos{m,i}=cell2mat(PATH_T(j));
    end
end

```


Appendix C *Complementary material used in Chapter 4*

```

        matriz_caminhos_dist{m,i}=(DIST-T(j));
    end
end
numero_caminho=size(matriz_caminhos,1)*N;
numero_demands=length(tot_o);
Caminhos={};
aux_c=0;
for i=1:size(matriz_caminhos,1)
    for j=3:N+2
        aux_c=aux_c+1;
        Caminhos{aux_c,1}=cell2mat(matriz_caminhos(i,j));
        Caminhos{aux_c,2}=aux_c;
        %Caminhos{aux_c,3}=cell2mat(matriz_caminhos_dist(i,j));
    end
end
for l=1:numel(origem)
    matrix_aux{1,1}=origem(l);
    matrix_aux{1,2}=destino(l);
    matrix_aux{1,3}=1;
end
N_variables=(numero_caminho*Cores)+(links*Cores)+links;
F=zeros(N_variables,1);
for i=1:N_variables
    %if(i>N_variables-links) %minimizar capacidade
    if(i>numero_caminho*Cores && i<=N_variables-links) %minimizar cores
        F(i,1)=1;
    end
end
aux_D=links*Cores+numero_demands
D=zeros((aux_D),1);
for i=1:numero_demands
    D(i,1)=1;
end
W=triu(trafego_rede,1);
m=0;
for i=1:nos
    for y=1:nos
        if(W(i,y)~=0)
            m=m+1;
            d_aux{m,1}=i;
            d_aux{m,2}=y;
            d_aux{m,3}=m;
        end
    end
end
Z=zeros(links*Cores,1);
d=zeros(numel(D),numel(F));
for t=1:Cores
    for z=1:size(Caminhos,1)
        caminho=cell2mat(Caminhos(z,1));
        p=size(caminho,2);
        for i=1:size(d_aux,1)
            if(cell2mat(d_aux(i,1))==caminho(1) && cell2mat(d_aux(i,2))==caminho(p))
                x=cell2mat(d_aux(i,3));
                y=cell2mat(Caminhos(z,2))+ (numero_caminho*(t-1));
                d(x,y)=1;
            end
        end
    end
end
count_aux=numero_caminho*Cores+1;
for z=numero_demands+1:size(d,1)
    d(z,count_aux)=-1;
    count_aux=count_aux+1;
end
end

```

Appendix C *Complementary material used in Chapter 4*

```

g=(size(F,1)-links)+1;
for z=numero_demands+1:(size(d,1))
    if g<(size(F,1))+1
        d(z,g)=1;
        g=g+1;
    else
        g=(size(F,1)-links)+1;
        d(z,g)=1;
        g=g+1;
    end
end
c=zeros(numel(Z),numel(F));
for r=1:Cores
    for z=1:size(Caminhos,1)
        caminho=cell2mat(Caminhos(z,1));
        for j=1:(numel(caminho)-1)
            for i=1:size(matrix_aux,1)
                if (cell2mat(matrix_aux(i,1))==caminho(j) &&
                    cell2mat(matrix_aux(i,2))==caminho(j+1))
                    x=cell2mat(matrix_aux(i,3))+(links*(r-1));
                    y=cell2mat(Caminhos(z,2))+(numero_caminho*(r-1));
                    c(x,y)=1;
                elseif (cell2mat(matrix_aux(i,2))==caminho(j) &&
                    cell2mat(matrix_aux(i,1))==caminho(j+1))
                    x=cell2mat(matrix_aux(i,3))+(links*(r-1));
                    y=cell2mat(Caminhos(z,2))+(numero_caminho*(r-1));
                    c(x,y)=1;
                end
            end
        end
    end
end
k=numero_caminho*Cores+1;
for j=1:size(c,1)
    if k<size(c,2)-links+1
        c(j,k)=-1;
        k=k+1;
    end
end
lb=zeros(N_variables,1);
for i=1:size(F,1)
    if i>(numero_caminho*Cores) && i<=(size(F,1)-links)
        ub(i,1)=1;
    else
        ub(i,1)=inf;
    end
end
int=1:1:size(F,1);
options = optimoptions(@intlinprog,'Maxtime',inf);
[X, O, G, K]=intlinprog(F,int,-d,-D,c,Z,lb,ub,options)
Tempo=toc;
Caminhos_usados=[];
t=0;
for color=1:Cores
    for x=1:numero_caminho
        if (X(x+(color-1)*numero_caminho)~=0)
            t=t+1;
            Caminhos_usados{t,1}=cell2mat(Caminhos(x,1));
            Caminhos_usados{t,2}=color;
            Caminhos_usados{t,3}=t;
        end
    end
end
for z=1:size(Caminhos_usados,1)
    caminho=cell2mat(Caminhos_usados(z,1));

```

Appendix C Complementary material used in Chapter 4

```
for j=1:(numel(caminho)-1)
    for i=1:size(matrix_aux,1)
        if (cell2mat(matrix_aux(i,1))==caminho(j) &&
            cell2mat(matrix_aux(i,2))==caminho(j+1))
            x=cell2mat(matrix_aux(i,3));
            y=cell2mat(Caminhos_usados(z,3));
            for t=1:size(Caminhos_usados,1)
                if (cell2mat(Caminhos_usados(t,3))==y)
                    resultados(x, y)=1;
                end
            end
        elseif (cell2mat(matrix_aux(i,2))==caminho(j) &&
            cell2mat(matrix_aux(i,1))==caminho(j+1))
            x=cell2mat(matrix_aux(i,3));
            y=cell2mat(Caminhos_usados(z,3));
            for t=1:size(Caminhos_usados,1)
                if (cell2mat(Caminhos_usados(t,3))==y)
                    resultados(x, y)=1;
                end
            end
        end
    end
end
end
end
end
R=zeros(links,3);
for i=1:size(resultados,1) %gives the link capacity
    R(i,1)=cell2mat(matrix_aux(i,1));
    R(i,2)=cell2mat(matrix_aux(i,2));
    for j=1:size(resultados,2)
        aux_count=(R(i,3));
        count=resultados(i,j);
        R(i,3)=aux_count+count;
    end
end
end
```

C.4. Paths used to solve the RWA problem

In this appendix section, the paths used to obtain Figure 4.1 are presented. In Table C.1 the shortest path in distance of each demand used in the heuristic solution are represented. The path list used in the ILP solution consisted of 4 candidate paths, in Table C.1 the path picked by the ILP formalism, as well as, the number of the candidate path in the list are shown. The different paths chosen are signaled in blue.

C.5. Multiband optical network simulator

OSNR calculation

```
function [comp_onda, Freq_slots, OSNR_TOT, Time, bloqueados]=
OSNR_FS(BER, origens, destinos, distancia, O, D, d, N, Amp_ganho, nos_rede)

%% start clock
tic
%% Constantes
h_planck=6.62607015e-34;
c_luz=299792458;
%% values
alfa_fibra_dB=0.25;
alfa_fibra_linear=(alfa_fibra_dB/4.343)*10^-3;
area_efetiva_fibra=80*10^-6*10^-6;
indice_refracao_nlinear=2.56688e-20;
D_fibra=17 *1e-12/1e-9/1e3; % ps/(mm*km)
S_fibra=0.067 *1e-12/1e-9/1e3/1e-9; % ps/(mm^2*km)
Comp_onda_ref_fibra=1550e-9;
FS=12.5e9;
```

Appendix C Complementary material used in Chapter 4

Demand d	Paths Heuristic	Paths ILP	# of the candidate path	Demand d	Paths Heuristic	Paths ILP	# of the candidate path
[1 – 2]	{1,2}	{1,2}	1	[4 – 6]	{4,7,6}	{4,7,6}	1
[1 – 3]	{1,3}	{1,3}	1	[4 – 7]	{4,7}	{4,7}	1
[1 – 4]	{1,4}	{1,4}	1	[4 – 8]	{4,8}	{4,8}	1
[1 – 5]	{1,3,5}	{1,2,5}	4	[4 – 9]	{4,7,9}	{4,7,9}	1
[1 – 6]	{1,3,6}	{1,3,6}	1	[4 – 10]	{4,10}	{4,10}	1
[1 – 7]	{1,7}	{1,7}	1	[4 – 11]	{4,7,9,11}	{4,10,11}	2
[1 – 8]	{1,3,5,8}	{1,4,8}	3	[5 – 6]	{5,6}	{5,6}	1
[1 – 9]	{1,7,9}	{1,7,9}	1	[5 – 7]	{5,6,7}	{5,6,7}	1
[1 – 10]	{1,4,10}	{1,7,10}	2	[5 – 8]	{5,8}	{5,8}	1
[1 – 11]	{1,7,9,11}	{1,3,5,11}	4	[5 – 9]	{5,6,9}	{5,8,9}	3
[2 – 3]	{2,3}	{2,3}	1	[5 – 10]	{5,6,7,10}	{5,6,9,10}	2
[2 – 4]	{2,3,4}	{2,1,4}	4	[5 – 11]	{5,11}	{5,11}	1
[2 – 5]	{2,5}	{2,5}	1	[6 – 7]	{6,7}	{6,7}	1
[2 – 6]	{2,5,6}	{2,5,6}	1	[6 – 8]	{6,8}	{6,8}	1
[2 – 7]	{2,5,6,7}	{2,8,6,7}	3	[6 – 9]	{6,9}	{6,9}	1
[2 – 8]	{2,8}	{2,8}	1	[6 – 10]	{6,7,10}	{6,9,10}	2
[2 – 9]	{2,5,6,9}	{2,8,9}	2	[6 – 11]	{6,9,11}	{6,8,11}	3
[2 – 10]	{2,5,6,7,10}	{2,3,4,10}	4	[7 – 8]	{7,6,8}	{7,9,8}	2
[2 – 11]	{2,8,11}	{2,8,11}	1	[7 – 9]	{7,9}	{7,9}	1
[3 – 4]	{3,4}	{3,4}	1	[7 – 10]	{7,10}	{7,10}	1
[3 – 5]	{3,5}	{3,5}	1	[7 – 11]	{7,9,11}	{7,10,11}	2
[3 – 6]	{3,6}	{3,6}	1	[8 – 9]	{8,9}	{8,9}	1
[3 – 7]	{3,4,7}	{3,4,7}	1	[8 – 10]	{8,9,10}	{8,11,10}	4
[3 – 8]	{3,5,8}	{3,5,8}	1	[8 – 11]	{8,11}	{8,11}	1
[3 – 9]	{3,6,9}	{3,6,9}	1	[9 – 10]	{9,10}	{9,10}	1
[3 – 10]	{3,4,10}	{3,4,10}	1	[9 – 11]	{9,11}	{9,11}	1
[3 – 11]	{3,6,9,11}	{3,5,11}	2	[10 – 11]	{10,11}	{10,11}	1
[4 – 5]	{4,3,5}	{4,8,5}	4				

Table C.1. Path list used to obtain Figure 4.1

```

Prx.dBm=0;
prx.linear=10^-3*10^(Prx.dBm/10);
%% Modulation values
if BER==1e-3
    Modulacao{1,2}=24.8;
    Modulacao{2,2}=18.6;
    Modulacao{3,2}=12;
    pFEC=0.07;
elseif BER==4e-2
    Modulacao{1,2}=18.9;
    Modulacao{2,2}=13.3;
    Modulacao{3,2}=7.1;
    pFEC=0.28;
elseif BER==1e-2
    Modulacao{1,2}=21.9;
    Modulacao{2,2}=16.1;
    Modulacao{3,2}=9.5;
    pFEC=0.28;
end
Modulacao_QPSK=4;
Rb.l.QPSK=128;  %[Gb/s]
Rs.l.QPSK=Rb.l.QPSK/(2*log2( Modulacao_QPSK ));  %[Gbaud]
Rb.i.QPSK=Rb.l.QPSK/(1+pFEC);
PHLQPSK=-1;
Modulacao_QAM=16;
Rb.l.QAM=128;
Rs.l.QAM=Rb.l.QAM/(2*log2( Modulacao_QAM ));

```

Appendix C Complementary material used in Chapter 4

```

Rb_i_QAM=Rb_l_QAM/(1+pFEC);
PHL_QAM=-0.68;
Modulacao_QAM_64=64;
Rb_l_QAM_64=128;
Rs_l_QAM_64=Rb_l_QAM_64/(2*log2(Modulacao_QAM_64));
Rb_i_QAM_64=Rb_l_QAM_64/(1+pFEC);
PHL_QAM_64=-0.619;
Modulacao{1,1}=PHL_QAM_64;
Modulacao{2,1}=PHL_QAM;
Modulacao{3,1}=PHL_QPSK;
Modulacao{1,3}='64QAM';
Modulacao{2,3}='16QAM';
Modulacao{3,3}='QPSK';
Modulacao{1,4}=25e9;
Modulacao{2,4}=37.5e9;
Modulacao{3,4}=50e9;
Modulacao{1,8}=Rs_l_QAM_64;
Modulacao{2,8}=Rs_l_QAM;
Modulacao{3,8}=Rs_l_QPSK;
%% full mesh traffic
[trafego_rede]=trafego(nos_rede);
%% Candidate paths
for m=1:numel(O)
    [DIST_T, PATH_T] = graphkshortestpaths(d, O(m), D(m), N);
    matriz_caminhos{m,1}= O(m);
    matriz_caminhos{m,2}=D(m);
    matriz_caminhos_dist{m,1}= O(m);
    matriz_caminhos_dist{m,2}=D(m);
    n=3;
    for i=3:(N+2)
        j=i-2;
        matriz_caminhos{m,i}=cell2mat(PATH_T(j));%candidate path list per demand
        matriz_caminhos_dist{m,i}=(DIST_T(j));
    end
end
Caminhos={}; % candidate paths list with distance
aux_c=0;
for i=1:size(matriz_caminhos,1)
    for j=3:N+2
        aux_c=aux_c+1;
        Caminhos{aux_c,1}=cell2mat(matriz_caminhos(i,j));
        Caminhos{aux_c,2}=cell2mat(matriz_caminhos_dist(i,j));
    end
end
%% Frequency and wavelengths
for z=1:size(Modulacao,1)
    delta_VC=Modulacao{z,4};
    freq=195.9e12;
    gap=190.95e12;
    count=0;
    new_count=0;
    while true
        if freq>191.6e12
            count=count+1;
            aux=((count-1)*delta_VC);
            aux_Freq=195.9e12-aux;
            freq=aux_Freq;
            Matriz_freq_comp(count,1)=aux_Freq;
            aux_Comp_onda=c_luz/aux_Freq;
            Matriz_freq_comp(count,2)=aux_Comp_onda;
        elseif freq>184.5e12
            new_count=new_count+1;
            count=count+1;
            aux_Freq=gap-((new_count-1)*delta_VC);
            freq=aux_Freq;

```

Appendix C *Complementary material used in Chapter 4*

```

        Matriz_freq_comp(count,1)=aux_Freq;
        aux_Comp_onda=c_luz/aux_Freq;
        Matriz_freq_comp(count,2)=aux_Comp_onda;
    else
        break;
    end
end
Canais=count;
Canal_central=round(Canais/2);
Modulacao{z,5}=Matriz_freq_comp(Canal_central,1);
Modulacao{z,6}=Canais;
Modulacao{z,7}=Canal_central;
end
count=0;
new_count=0;
freq=195.9e12;
gap=190.95e12;
while true
    if freq>191.6e12 %184.5e12
        count=count+1;
        aux_Freq=195.9e12-((count-1)*FS);
        freq=aux_Freq;
        Frequency_Slots(count,1)=count;
        aux_Comp_onda=c_luz/aux_Freq;
        Frequency_Slots(count,2)=aux_Freq;
        Frequency_Slots(count,3)=0;
    else
        break;
    end
end
while true
    if freq>184.5e12
        new_count=new_count+1;
        count=count+1;
        aux_Freq=gap-((new_count-1)*FS);
        freq=aux_Freq;
        Frequency_Slots(count,1)=count;
        aux_Comp_onda=c_luz/aux_Freq;
        Frequency_Slots(count,2)=aux_Freq;
        Frequency_Slots(count,3)=0;
    else
        break;
    end
end
Canais_FS=count;
Canal_FS_central=round(Canais_FS/2);
%% Links distance and source and destination nodes numbered
for i=1:length(origens)
    Distancia(i,1)=origens(1,i);
    Distancia(i,2)=destinos(1,i);
    Distancia(i,3)=distancia(1,i);
    Distancia(i,4)=i;
end
%% N spans per link
for i=1:size(Distancia)
    Ganho_aux=Distancia(i,3)*alfa_fibra_dB;
    if(Ganho_aux>Amp_ganho)
        amps_aux=ceil(Ganho_aux/Amp_ganho);
        Ganho_aux=Ganho_aux/amps_aux;
    else
        amps_aux=1;
    end
    %Amplifier gain and number of in-line and pre-amplifiers in the link
    Ganho_ligacao_pre_dB(i,1)=Distancia(i,1);
    Ganho_ligacao_pre_dB(i,2)=Distancia(i,2);

```

Appendix C Complementary material used in Chapter 4

```

    Ganho_ligacao_pre_dB(i,3)=Ganho_aux;
    Ganho_ligacao_pre_dB(i,4)=amps_aux;
    %%span length
    Distancia_amp(i,1)=Distancia(i,1);
    Distancia_amp(i,2)=Distancia(i,2);
    Distancia_amp(i,3)=Distancia(i,3)*10^3/amps_aux;
    Distancia_amp(i,4)=Distancia(i,4);
end
for i=1:size(Ganho_ligacao_pre_dB)
    Ganho_aux=10^(Ganho_ligacao_pre_dB(i,3)/10);
    ganho_ligacao_pre_linear(i,1)=Distancia(i,1);
    ganho_ligacao_pre_linear(i,2)=Distancia(i,2);
    ganho_ligacao_pre_linear(i,3)=Ganho_aux;
    ganho_ligacao_pre_linear(i,4)=Ganho_ligacao_pre_dB(i,4);
end
%% post - amplifier gain
Ganho_pos_dB=18; %dB
ganho_pos_linear=10^(Ganho_pos_dB/10);
%% pASE values
for i=1:size(Ganho_ligacao_pre_dB,1)
    Fn_pre_dB(i,1)=Distancia(i,1);
    Fn_pre_dB(i,2)=Distancia(i,2);
    Fn_pre_dB(i,3)=-0.2*Ganho_ligacao_pre_dB(i,3)+10;
    fn_pre_linear(i,1)=Distancia(i,1);
    fn_pre_linear(i,2)=Distancia(i,2);
    fn_pre_linear(i,3)=10^(Fn_pre_dB(i,3)/10);
end
Fn_pos_dB=-0.2*Ganho_pos_dB+10;
fn_pos_linear=10^(Fn_pos_dB/10);
%% pASE pre
for i=1:size(ganho_ligacao_pre_linear)
    aux_ASE=(ganho_ligacao_pre_linear(i,4));
    p_ASE_pre(i,1)=Distancia(i,1);
    p_ASE_pre(i,2)=Distancia(i,2);
    p_ASE_pre(i,3)=Distancia(i,4);
    for t=1:size(Modulacao)
        B0=cell2mat(Modulacao(t,8));
        v0=cell2mat(Modulacao(t,5));
        aux_p_ASE_preK=(fn_pre_linear(i,3))*(ganho_ligacao_pre_linear(i,3)-1)*h_planck*v0*
            (B0*10^9);
        p_ASE_pre(i,3+t)=aux_p_ASE_preK*aux_ASE;
    end
end
%% pASE pos
for t=1:size(Modulacao)
    B0=cell2mat(Modulacao(t,8));
    v0_pos=cell2mat(Modulacao(t,5));
    p_ASE_pos(t,1)=(fn_pos_linear)*(ganho_pos_linear-1)*h_planck*v0_pos*(B0*10^9);
end
%% pASE
for i=1:size(p_ASE_pre,1)
    for t=1:size(Modulacao)
        p_ASE(i,1)=Distancia(i,1);
        p_ASE(i,2)=Distancia(i,2);
        p_ASE(i,3)=Distancia(i,4);
        p_ASE(i,3+t)=p_ASE_pos(t,1)+p_ASE_pre(i,3+t);
    end
end
%% NLI Values
for w=1:size(Distancia_amp,1)
    p_NLI(w,1)=(Distancia_amp(w,1));
    p_NLI(w,2)=(Distancia_amp(w,2));
    eta_NLI(w,1)=(Distancia_amp(w,1));
    eta_NLI(w,2)=(Distancia_amp(w,2));
    p_NLI_corr(w,1)=(Distancia_amp(w,1));

```

Appendix C Complementary material used in Chapter 4

```

p_NLI_corr(w,2)=(Distancia_amp(w,2));
eta_NLI_corr(w,1)=(Distancia_amp(w,1));
eta_NLI_corr(w,2)=(Distancia_amp(w,2));
end
for r=1:size(Modulacao,1)
NLI=[];eta=[];NLI_corr=[];eta_corr=[];
for h=1:size(Distancia_amp,1)
delta_canal=Modulacao{r,4};
canal=Modulacao{r,6};
canal_central=Modulacao{r,7};
Dados.n=Ganho_ligacao_pre_dB(h,4);
Dados.Bch= delta_canal * ones(canal, Dados.n);
Dados.fi = -canal*delta_canal/2+0.5*delta_canal+(0:(canal-1))*delta_canal;
Dados.fi = repmat(Dados.fi, 1, Dados.n);
Dados.D=D_fibra * ones(1, Dados.n);
Dados.S=S_fibra * ones(1, Dados.n);
Dados.RefLambda=Comp_onda_ref_fibra;
Dados.Att=alfa_fibra_linear * ones(canal, Dados.n); %%
Dados.Att_bar = Dados.Att;
Dados.Cr= 0.028 /1e3/1e12 * ones(canal, Dados.n);
Coeficiente_nlinearidade=(2*pi*indice_refracao_nlinear)/
(area_efetiva_fibra*Comp_onda_ref_fibra);
Dados.Gamma=Coeficiente_nlinearidade * ones(1, Dados.n);
Dados.Length=Distancia_amp(h,3);
Dados.coherent = 0;
Dados.Pch= prx_linear * ones(canal, Dados.n);
Dados.PHI=cell2mat(Modulacao(r,1));
[NLI(:,h),eta(:,h)] = ISRSGNmodel( Dados );
end
%% NLI coefficient
for w=1:size(Distancia_amp,1)
p_NLI(w,r+2)=NLI( canal_central,w);
eta_NLI(w,r+2)=eta( canal_central,w);
end
end
%% prx for the longest path
Caminhos_aux=sortrows(Caminhos,-2);
p=cell2mat(Caminhos_aux(1,1));
aux_caminho={};
for y=1:numel(p)-1
for x=1:length(p_ASE)
if ((p_ASE(x,1))==p(y) && (p_ASE(x,2))==p(y+1))
m=height(aux_caminho);
m=m+1;
aux_caminho{m,1}=p_ASE(x,1);
aux_caminho{m,2}=p_ASE(x,2);
aux_caminho{m,3}=p_ASE(x,3);
aux_caminho{m,4}=p_ASE(x,4);
aux_caminho{m,5}=p_ASE(x,5);
aux_caminho{m,6}=p_ASE(x,6);
elseif ((p_ASE(x,2))==p(y) && (p_ASE(x,1))==p(y+1))
m=height(aux_caminho);
m=m+1;
aux_caminho{m,1}=p_ASE(x,1);
aux_caminho{m,2}=p_ASE(x,2);
aux_caminho{m,3}=p_ASE(x,3);
aux_caminho{m,4}=p_ASE(x,4);
aux_caminho{m,5}=p_ASE(x,5);
aux_caminho{m,6}=p_ASE(x,6);
end
end
end
aux_p_NLI=0;
aux_p_ASE=0;
for i=1:size(Modulacao)

```


Appendix C Complementary material used in Chapter 4

```

for t=1:height(aux_caminho)
    c=aux_caminho{t,3};
    aux_ASE=cell2mat(aux_caminho(t,3+i));
    aux_p_ASE=aux_p_ASE+aux_ASE;
    aux_NLI=(eta_NLI(c,2+i));
    aux_p_NLI=aux_p_NLI+aux_NLI;
end
pm(i,1)=(aux_p_ASE/(2*aux_p_NLI))^(1/3);
pm_dBm(i,1)=10*log10(pm(i,1)/10^-3);
end
%% NLI for each link for the 3 modulations
for r=1:size(Modulacao,1)
    NLI=[]; eta=[]; NLI_corr=[]; eta_corr=[];
    for h=1:size(Distancia_amp,1)
        delta_canal=Modulacao{r,4};
        canal=Modulacao{r,6};
        canal_central=Modulacao{r,7};
        Dados.n=Ganho_ligacao_pre_dB(h,4);
        Dados.Bch= delta_canal * ones(canal, Dados.n);
        Dados.fi = -canal*delta_canal/2+0.5*delta_canal+(0:(canal-1))*delta_canal;
        Dados.fi = repmat(Dados.fi, 1, Dados.n);
        Dados.D=D_fibra * ones(1, Dados.n);
        Dados.S=S_fibra * ones(1, Dados.n);
        Dados.RefLambda=Comp_onda_ref_fibra;
        Dados.Att=alfa_fibra_linear * ones(canal, Dados.n); %
        Dados.Att_bar = Dados.Att;
        Dados.Cr= 0.028 /1e3/1e12 * ones(canal, Dados.n); %valor ??
        Coeficiente_nlinearidade=(2*pi*indice_refracao_nlinear)/
        (area_efetiva_fibra*Comp_onda_ref_fibra);
        Dados.Gamma=Coeficiente_nlinearidade * ones(1, Dados.n);
        Dados.Length=Distancia_amp(h,3);
        Dados.coherent = 0;
        Dados.Pch= pm(r,1) * ones(canal, Dados.n);
        Dados.PHI=cell2mat(Modulacao(r,1));

        [NLI(:,h),eta(:,h),eta_corr(:,h),NLI_corr(:,h)] = ISRSNGmodel( Dados );
    end
end
%% NLI
for w=1:size(Distancia_amp,1)
    p_NLI_corr(w,r+2)=NLI_corr(canal_central,w);
    eta_NLI_corr(w,r+2)=eta_corr(canal_central,w);
end
end
%% OSNR
for i=1:size(matriz_caminhos)
    aux_matriz_caminhos=matriz_caminhos(i,:);
    aux_matriz_caminhos=aux_matriz_caminhos.';
    osnr(i,1)=aux_matriz_caminhos(1);
    osnr(i,2)=aux_matriz_caminhos(2);
    OSNR(i,1)=aux_matriz_caminhos(1);
    OSNR(i,2)=aux_matriz_caminhos(2);
    count=3;
    for j=3:length(aux_matriz_caminhos)
        aux_p_ASE=0;
        p=cell2mat(aux_matriz_caminhos(j,1));
        aux_caminho={};
        for y=1:numel(p)-1
            for x=1:length(p_ASE)
                if ((p_ASE(x,1))==p(y) && (p_ASE(x,2))==p(y+1))
                    m=height(aux_caminho);
                    m=m+1;
                    aux_caminho{m,1}=p_ASE(x,1);
                    aux_caminho{m,2}=p_ASE(x,2);
                    aux_caminho{m,3}=p_ASE(x,3);
                    aux_caminho{m,4}=p_ASE(x,4);
                end
            end
        end
    end
end

```


Appendix C Complementary material used in Chapter 4

```

count=0;
aux_OSNR=OSNR(i,:);
aux_OSNR=aux_OSNR.';
aux_OSNR_TOT={};
null='null';
for c=3:4:size(aux_OSNR)
    is_null=cell2mat(aux_OSNR(c+2,1));
    if strcmp(null,is_null)==1
        break;
    else
        count=count+1;
        aux_OSNR_TOT(count,1)=aux_OSNR(c,1);
        aux_OSNR_TOT(count,2)=aux_OSNR(c+1,1);
        aux_OSNR_TOT(count,3)=aux_OSNR(c+2,1);
        aux_OSNR_TOT(count,4)=aux_OSNR(c+3,1);
    end
end
if isempty(aux_OSNR_TOT)==0
    osnr_tot_count=osnr_tot_count+1;
    OSNR_TOT(osnr_tot_count,1)=OSNR(i,1);
    OSNR_TOT(osnr_tot_count,2)=OSNR(i,2);
    aux_OSNR_TOT=sortrows(aux_OSNR_TOT,-3);
    new_count=2;
    for c=1:size(aux_OSNR_TOT,1)
        for t=1:size(aux_OSNR_TOT,2)
            new_count=new_count+1;
            OSNR_TOT(osnr_tot_count,new_count)=aux_OSNR_TOT(c,t);
        end
    end
else
    osnr_tot_count=osnr_tot_count+1;
    OSNR_TOT(osnr_tot_count,1)=OSNR(i,1);
    OSNR_TOT(osnr_tot_count,2)=OSNR(i,2);
    OSNR_TOT{osnr_tot_count,3}='Blocked';
end
end
end
%% First Fit
[comp_onda,Freq_slots,bloqueados]=first_fit_FS(origens,destinos,trafego_rede,OSNR_TOT,FS);
%% End clock
Time=toc;

```

First Fit algorithm for the flexible grid

```

function [comp_onda_escolhido,Freq_slots,bloqueados]=
first_fit_FS(origem,destino,trafego_rede,caminhos,FS)
%% Constants
c_luz=299792458;
%% Number of FS needed per modulation
FS_Mod{1,1}='64QAM';
FS_Mod{2,1}='16QAM';
FS_Mod{3,1}='QPSK';
FS_Mod{1,2}=2;
FS_Mod{2,2}=3;
FS_Mod{3,2}=4;
%%Links numbered
for l=1: numel(origem)
    matrix_aux{1,1}=origem(l);
    matrix_aux{1,2}=destino(l);
    matrix_aux{1,3}=1;
end
%% FS for the C+L band
count=0;
new_count=0;
freq=195.9e12;
gap=190.95e12;
while true

```

Appendix C Complementary material used in Chapter 4

```

    if freq > 191.6e12
        count=count+1;
        aux_Freq=195.9e12 - ((count-1)*FS);
        freq=aux_Freq;
        Freq_slots(count,1)=count;
        aux_Comp_onda=c_luz/aux_Freq;
        Freq_slots(count,2)=aux_Freq;
        Freq_slots(count,3)=0;
    else
        break;
    end
end
while true
    if freq > 184.5e12
        new_count=new_count+1;
        count=count+1;
        aux_Freq=gap - ((new_count-1)*FS);
        freq=aux_Freq;
        Freq_slots(count,1)=count;
        aux_Comp_onda=c_luz/aux_Freq;
        Freq_slots(count,2)=aux_Freq;
        Freq_slots(count,3)=0;
    else
        break;
    end
end
for i=1:size(Freq_slots,1)
    for x=3:(size(matrix_aux,1)+2)
        Freq_slots(i,x)=0;
    end
end
max_fibra=size(Freq_slots,1);
%%matrix with candidate paths
for l=1:size(caminhos,1)
    count=0;
    for c=3:4:size(caminhos,2)
        bloqueado='Blocked';
        if isempty(cell2mat(caminhos(l,c)))==1
            break;
        elseif strcmp(bloqueado,cell2mat(caminhos(l,c)))==1
            comp_onda_escolhido{1,1}=caminhos{1,1};
            comp_onda_escolhido{1,2}=caminhos{1,2};
            comp_onda_escolhido{1,3}=bloqueado;
            bloqueados=bloqueados+1;
            break;
        else
            count=count+1;
            p=cell2mat(caminhos(l,3)); %caminho
            trafego_aux=trafego_rede(p(1), p(numel(p)));
            comp_onda(l,count)=caminhos(l,c);
            count=count+1;
            for i=1:trafego_aux
                comp_onda{1,count}=i;
            end
            count=count+1;
            mod_selected=cell2mat(caminhos(l,c+3));
            for t=1:size(FS_Mod,1)
                mod=cell2mat(FS_Mod(t,1));
                if strcmp(mod,mod_selected)==1
                    comp_onda{1,count}=cell2mat(FS_Mod(t,2));
                end
            end
        end
    end
end
end
end
end

```

Appendix C Complementary material used in Chapter 4

```

for i=1:size(comp_onda,1)
    aux_n_caminhos=comp_onda(i,:);
    aux_n_caminhos=aux_n_caminhos.';
    aux_size=0;
    for t=1:size(aux_n_caminhos,1)
        if isempty(cell2mat(aux_n_caminhos(t,1)))==0
            aux_size =aux_size+1;
        end
    end
    numero_caminhos(i,1)=aux_size/3;
end
for i=1:size(comp_onda,1) %percorre a matriz com os caminhos
    for z=1:numero_caminhos(i,1)
        aux_caminho={};
        p=cell2mat(comp_onda(i,1+(z-1)*3));
        m=0;
        for j=1:numel(p)-1
            for x=1:size(matrix_aux,1) %percorre a lista com as origens e destino
                if (cell2mat(matrix_aux(x,1))==p(j) && cell2mat(matrix_aux(x,2))==p(j+1))
                    m=m+1;
                    aux_caminho{m,1}=matrix_aux{x,1};
                    aux_caminho{m,2}=matrix_aux{x,2};
                    aux_caminho{m,3}=matrix_aux{x,3}+2;
                    aux_caminho{m,4}=comp_onda{i,3+(z-1)*3};
                elseif (cell2mat(matrix_aux(x,2))==p(j) && cell2mat(matrix_aux(x,1))==p(j+1))
                    m=m+1;
                    aux_caminho{m,1}=matrix_aux{x,1};
                    aux_caminho{m,2}=matrix_aux{x,2};
                    aux_caminho{m,3}=matrix_aux{x,3}+2;
                    aux_caminho{m,4}=comp_onda{i,3+(z-1)*3};
                end
            end
        end
        FS_needed=aux_caminho{1,4};
        total_links_used_path=size(aux_caminho,1);
        flag=1;
        done=0;
        blocked_path=0;
        link={};
        t=0;
        for y=1:cell2mat(comp_onda(i,2)) %vai buscar o valor do trafego
            for w=1:size(aux_caminho,1)
                link{1,w}=(aux_caminho{w,3});
            end
            link_1=link{1,1};
            while true
                t=t+1;
                if Freq_slots(t,link_1)==0
                    aux_count=t;
                    FS_selected={};
                    FS_selected{1,1}=aux_count;
                    flag=1;
                    for y=1:FS_needed-1
                        check=y+aux_count;
                        link_picked=link{1,1};
                        if Freq_slots(check,link_picked)==0
                            FS_selected{1,y+1}=aux_count+y;
                            flag=0;
                        else
                            flag=1;
                            break;
                        end
                    end
                end
            end
        else
            flag=1;
        end
    end
end

```

Appendix C Complementary material used in Chapter 4

```

end
if total_links_used_path~=1
    for w=2:total_links_used_path
        link_dif_1=link{1,w};
        for kj=1:length(FS_selected)
            fs_using=FS_selected{1,kj};
            if Freq_slots(fs_using,link_dif_1)==1
                flag=1;
                break;
            end
        end
    end
end
if flag==0
    break;
end
if t>max_fibra-FS_needed
    blocked_path=1;
    break;
end
end
for w=1:total_links_used_path
    x=link{1,w};
    if blocked_path~=1
        for u=1:size(FS_selected,2)
            r=FS_selected{1,u};
            Freq_slots(r,x)=1;
            comp_onda_escolhido{i,1}=comp_onda{i,1};
            comp_onda_escolhido{i,2}=comp_onda{i,2};
            comp_onda_escolhido{i,3}=comp_onda{i,3};
            comp_onda_escolhido{i,3+u}=Freq_slots(r,1);
            done=1;
        end
    else
        comp_onda_escolhido{i,1}='blocked';
    end
end
end
if done==1
    break;
end
end
end

```

C.6. ASE and NLI noise power in the COST 239 network

In Table C.2, we present the ASE and NLI noises estimated at the end of each link of the COST 239 network for the three modulation formats.

From Table C.2, we can observed that the NLI noise power decreases with lower modulation formats, and the opposite happens for the ASE noise power, where the highest modulation format studied, induces the least noise. It can also be analyzed that the difference between modulation formats is higher in the ASE noise power, i.e. for link $e=[1,2]$ the difference between the QPSK and 64-QAM format for NLI noise power is of $1.05 \mu\text{W}$ and in the ASE noise power is of $22.26 \mu\text{W}$.

C.7. RMSA solution

In this appendix, we present the detailed results of the RMSA solution for the COST 239 optical network with $\text{BER}=10^{-2}$, as well as the results for the NSFNET, UBN, and CONUS

Appendix C *Complementary material used in Chapter 4*

Link e	NLI noise power p_{NLI} [μW]			ASE noise power $2p_{ASE}$ [μW]		
	64-QAM	16-QAM	QPSK	64-QAM	16-QAM	QPSK
[1,2]	3.810	2.940	2.760	11.130	16.690	33.390
[1,3]	2.550	1.970	1.800	5.950	8.930	17.860
[1,4]	1.360	1.050	0.920	3.770	5.660	11.310
[1,7]	2.570	1.980	1.820	6.700	10.060	20.110
[2,3]	1.360	1.040	0.910	3.580	5.370	10.740
[2,5]	1.320	1.010	0.860	2.500	3.760	7.510
[2,8]	1.350	1.030	0.890	3.130	4.690	9.390
[3,4]	2.200	1.690	1.550	7.040	10.550	21.110
[3,5]	0.560	0.420	0.310	1.730	2.600	5.190
[3,6]	1.320	1.010	0.860	2.430	3.650	7.290
[4,7]	0.970	0.750	0.630	3.360	5.040	10.070
[4,8]	3.420	2.640	2.480	11.060	16.590	33.190
[4,10]	2.150	1.650	1.490	4.860	7.290	14.590
[5,6]	0.570	0.440	0.330	2.490	3.730	7.460
[5,8]	0.960	0.740	0.610	2.740	4.110	8.220
[5,11]	2.620	2.020	1.880	9.550	14.320	28.640
[6,7]	2.210	1.700	1.570	8.030	12.040	24.090
[6,8]	0.990	0.760	0.640	4.020	6.030	12.070
[6,9]	0.940	0.720	0.590	2.250	3.370	6.740
[7,9]	2.150	1.660	1.500	5.000	7.510	15.010
[7,10]	0.940	0.720	0.590	2.250	3.370	6.740
[8,9]	1.800	1.390	1.260	6.460	9.690	19.390
[8,11]	2.570	1.980	1.820	6.700	10.060	20.110
[9,10]	2.210	1.700	1.570	8.030	12.040	24.090
[9,11]	0.950	0.730	0.610	2.560	3.840	7.690
[10,11]	2.560	1.970	1.800	6.070	9.100	18.200

Table C.2. NLI and ASE noise powers at the end of each link in the COST 239 optical network for the modulation formats 64-QAM, 16-QAM and QPSK.

30 networks for the $BER=4 \times 10^{-2}$, $BER=10^{-2}$, and $BER=10^{-3}$ with the respective blocked demands. It is also shown the theoretical and practical ROSNR for $BER=10^{-2}$.

Modulation format M	Theoretical ROSNR [dB]	Practical ROSNR [dB]
QPSK	7.3	9.5
16-QAM	13.9	16.1
64-QAM	19.7	21.9

Table C.3. Modulation formats with corresponding theoretical ROSNRs and practical ROSNRs for $BER=10^{-3}$.

Appendix C Complementary material used in Chapter 4

Demand d	Path	OSNR [dB]	Modulation format M	Frequency slots	Demand d	Path	OSNR [dB]	Modulation format M	Frequency slots
[1-2]	{1,3,2}	14.4	QPSK	1,2,3,4	[4-6]	{4,3,6}	16.1	16-QAM	26,27,28
[1-3]	{1,3}	18.0	16-QAM	5,6,7	[4-7]	{4,7}	20.8	16-QAM	1,2,3
[1-4]	{1,4}	20.1	16-QAM	1,2,3	[4-8]	{4,8}	13.8	QPSK	1,2,3,4
[1-5]	{1,3,5}	17.0	16-QAM	8,9,10	[4-9]	{4,7,9}	16.7	16-QAM	4,5,6
[1-6]	{1,3,6}	16.5	16-QAM	11,12,13	[4-10]	{4,10}	18.9	16-QAM	1,2,3
[1-7]	{1,7}	17.6	16-QAM	1,2,3	[4-11]	{4,7,9,11}	13.8	QPSK	18,19,20,21
[1-8]	{1,3,5,8}	14.0	QPSK	14,15,16,17	[5-6]	{5,6}	22.8	64-QAM	1,2
[1-9]	{1,3,6,9}	13.9	QPSK	18,19,20,21	[5-7]	{5,6,9,7}	14.3	QPSK	33,34,35,36
[1-10]	{1,4,10}	16.5	16-QAM	4,5,6	[5-8]	{5,8}	21.9	64-QAM	1,2
[1-11]	{1,3,6,9,11}	12.9	QPSK	22,23,24,25	[5-9]	{5,6,9}	19.2	16-QAM	37,38,39
[2-3]	{2,3}	20.3	16-QAM	5,6,7	[5-10]	{5,6,9,7,10}	13.4	QPSK	40,41,42,43
[2-4]	{2,3,4}	14.0	QPSK	8,9,10,11	[5-11]	{5,6,9,11}	17.3	16-QAM	44,45,46
[2-5]	{2,5}	21.6	16-QAM	1,2,3	[6-7]	{6,9,7}	17.2	16-QAM	1,2,3
[2-6]	{2,5,6}	18.9	16-QAM	4,5,6	[6-8]	{6,8}	20.1	16-QAM	1,2,3
[2-7]	{2,5,6,9,7}	13.3	QPSK	7,8,9,10	[6-9]	{6,9}	22.6	64-QAM	47,48
[2-8]	{2,8}	20.8	16-QAM	1,2,3	[6-10]	{6,9,7,10}	14.4	QPSK	49,50,51,52
[2-9]	{2,5,6,9}	17.5	16-QAM	11,12,13	[6-11]	{6,9,11}	19.0	16-QAM	53,54,55
[2-10]	{2,5,6,7,10}	12.4	QPSK	14,15,16,17	[7-8]	{7,9,6,8}	13.7	QPSK	56,57,58,59
[2-11]	{2,5,6,9,11}	14.3	QPSK	26,27,28,29	[7-9]	{7,9}	18.8	16-QAM	11,12,13
[3-4]	{3,4}	17.5	16-QAM	1,2,3	[7-10]	{7,10}	22.6	64-QAM	1,2
[3-5]	{3,5}	24.0	64-QAM	1,2	[7-11]	{7,9,11}	17.0	16-QAM	37,38,39
[3-6]	{3,6}	21.7	16-QAM	1,2,3	[8-9]	{8,6,9}	18.0	16-QAM	60,61,62
[3-7]	{3,6,9,7}	14.7	QPSK	14,15,16,17	[8-10]	{8,11,10}	13.1	QPSK	1,2,3,4
[3-8]	{3,5,8}	19.5	16-QAM	3,4,5	[8-11]	{8,11}	17.6	16-QAM	5,6,7
[3-9]	{3,6,9}	19.0	16-QAM	4,5,6	[9-10]	{9,7,10}	17.2	16-QAM	22,23,24
[3-10]	{3,4,10}	13.4	QPSK	12,13,14,15	[9-11]	{9,11}	22.2	64-QAM	1,2
[3-11]	{3,6,9,11}	17.2	16-QAM	30,31,32	[10-11]	{10,11}	18.0	16-QAM	5,6,7
[4-5]	{4,3,5}	16.6	16-QAM	18,19,20					

Table C.4. RMSA solution for the COST 239 optical network with BER= 10^{-2} .

Appendix C Complementary material used in Chapter 4

Demand d	Path	OSNR [dB]	Modulation format M	Frequency slots	Demand d	Path	OSNR [dB]	Modulation format M	Frequency slots
[1-3]	{1,8,9,3}	7.8	QPSK	1,2,3,4	[5-7]	{5,6,7}	14.4	16-QAM	16,17,18
[1-4]	{1,4}	14.9	16-QAM	1,2,3	[5-8]	{5,6,7,8}	10.8	QPSK	19,20,21,22
[1-5]	{1,4,5}	10.5	QPSK	4,5,6,7	[5-9]	{5,6,7,8,9}	9.7	QPSK	60,61,62,63
[1-6]	{1,4,5,6}	9.4	QPSK	8,9,10,11	[5-10]	{5,6,7,8,9,10}	9.0	QPSK	64,65,66,67
[1-7]	{1,4,5,6,7}	8.5	QPSK	12,13,14,15	[5-11]	{5,4,11}	11.4	QPSK	36,37,38,39
[1-8]	{1,8}	8.9	QPSK	5,6,7,8	[5-12]	{5,6,12}	10.5	QPSK	4,5,6,7
[1-9]	{1,8,9}	8.2	QPSK	9,10,11,12	[5-13]	{5,6,12,13}	8.7	QPSK	40,41,42,43
[1-10]	{1,8,9,10}	7.7	QPSK	13,14,15,16	[5-14]	{5,6,7,8,9,10,14}	8.8	QPSK	68,69,70,71
[1-11]	{1,11}	11.5	QPSK	1,2,3,4	[6-7]	{6,7}	17.2	16-QAM	1,2,3
[1-12]	{1,11,12}	7.9	QPSK	5,6,7,8	[6-8]	{6,7,8}	14.0	16-QAM	9,10,11
[1-13]	{1,8,9,13}	7.3	QPSK	17,18,19,20	[6-9]	{6,7,8,9}	10.8	QPSK	72,73,74,75
[1-14]	{1,8,9,10,14}	7.5	QPSK	21,22,23,24	[6-10]	{6,7,8,9,10}	10.0	QPSK	76,77,78,79
[2-3]	{2,3}	17.1	16-QAM	1,2,3	[6-11]	{6,5,4,11}	10.1	QPSK	44,45,46,47
[2-4]	{2,5,4}	8.3	QPSK	16,17,18,19	[6-12]	{6,12}	13.6	16-QAM	1,2,3
[2-5]	{2,5}	9.7	QPSK	1,2,3,4	[6-13]	{6,12,13}	9.6	QPSK	8,9,10,11
[2-6]	{2,3,9,8,7,6}	9.0	QPSK	5,6,7,8	[6-14]	{6,7,8,9,10,14}	9.7	QPSK	80,81,82,83
[2-7]	{2,3,9,8,7}	10.1	QPSK	25,26,27,28	[7-8]	{7,8}	16.8	16-QAM	1,2,3
[2-8]	{2,3,9,8}	13.3	16-QAM	29,30,31	[7-9]	{7,8,9}	14.2	16-QAM	84,85,86
[2-9]	{2,3,9}	15.3	16-QAM	9,10,11	[7-10]	{7,8,9,10}	11.4	QPSK	87,88,89,90
[2-10]	{2,10}	16.0	16-QAM	1,2,3	[7-11]	{7,6,5,4,11}	9.0	QPSK	84,85,86,87
[2-11]	{2,5,4,11}	7.4	QPSK	20,21,22,23	[7-12]	{7,6,12}	10.4	QPSK	23,24,25,26
[2-12]	{2,3,9,13,12}	9.1	QPSK	12,13,14,15	[7-13]	{7,8,9,13}	10.5	QPSK	91,92,93,94
[2-13]	{2,3,9,13}	11.1	QPSK	21,22,23,24	[7-14]	{7,8,9,10,14}	11.0	QPSK	95,96,97,98
[2-14]	{2,10,14}	15.1	16-QAM	4,5,6	[8-9]	{8,9}	17.7	16-QAM	99,100,101
[3-4]	{3,9,8,7,6,5,4}	7.8	QPSK	32,33,34,35	[8-10]	{8,9,10}	15.4	16-QAM	102,103,104
[3-5]	{3,9,8,7,6,5}	9.1	QPSK	36,37,38,39	[8-11]	{8,7,6,5,4,11}	8.1	QPSK	99,100,101,102
[3-6]	{3,9,8,7,6}	10.1	QPSK	40,41,42,43	[8-12]	{8,9,13,12}	9.8	QPSK	105,106,107,108
[3-7]	{3,9,8,7}	11.6	QPSK	44,45,46,47	[8-13]	{8,9,13}	14.0	16-QAM	109,110,111
[3-8]	{3,9,8}	15.7	16-QAM	48,49,50	[8-14]	{8,9,10,14}	14.7	16-QAM	112,113,114
[3-9]	{3,9}	20.4	64-QAM	16,17	[9-10]	{9,10}	19.6	64-QAM	1,2
[3-10]	{3,14,10}	17.7	16-QAM	1,2,3	[9-11]	{9,13,12,11}	7.6	QPSK	1,2,3,4
[3-11]	{3,9,13,12,11}	7.3	QPSK	51,52,53,54	[9-12]	{9,13,12}	11.0	QPSK	25,26,27,28
[3-12]	{3,9,13,12}	10.3	QPSK	55,56,57,58	[9-13]	{9,13}	16.4	16-QAM	5,6,7
[3-13]	{3,9,13}	14.8	16-QAM	59,60,61	[9-14]	{9,10,14}	17.7	16-QAM	7,8,9
[3-14]	{3,14}	19.7	64-QAM	4,5	[10-11]	{10,9,13,12,11}	7.2	QPSK	29,30,31,32
[4-5]	{4,5}	15.5	16-QAM	1,2,3	[10-12]	{10,9,13,12}	10.2	QPSK	33,34,35,36
[4-6]	{4,5,6}	13.5	16-QAM	24,25,26	[10-13]	{10,9,13}	14.6	16-QAM	37,38,39
[4-7]	{4,5,6,7}	10.2	QPSK	27,28,29,30	[10-14]	{10,14}	22.8	64-QAM	10,11
[4-8]	{4,5,6,7,8}	9.0	QPSK	48,49,50,51	[11-12]	{11,12}	10.3	QPSK	20,21,22,23
[4-9]	{4,5,6,7,8,9}	8.2	QPSK	52,53,54,55	[11-13]	{11,12,13}	8.6	QPSK	44,45,46,47
[4-10]	{4,5,6,7,8,9,10}	7.8	QPSK	56,57,58,59	[11-14]	{11,12,14}	7.3	QPSK	24,25,26,27
[4-11]	{4,11}	16.7	16-QAM	1,2,3	[12-13]	{12,13}	15.0	16-QAM	5,6,7
[4-12]	{4,11,12}	9.1	QPSK	9,10,11,12	[12-14]	{12,14}	10.3	QPSK	1,2,3,4
[4-13]	{4,11,12,13}	7.7	QPSK	16,17,18,19	[13-14]	{13,9,10,14}	14.0	16-QAM	40,41,42
[5-6]	{5,6}	17.7	16-QAM	1,2,3					

Table C.5. RMSA solution for the NSFNET optical network with $BER=4 \times 10^{-2}$.

Blocked Demands	[1-2], [1-4].
-----------------	---------------

Table C.6. Blocked demands in the RMSA solution for the NSFNET optical network with $BER=4 \times 10^{-2}$.

Appendix C Complementary material used in Chapter 4

Demand d	Path	OSNR [dB]	Modulation Format M	Frequency slots	Demand d	Path	OSNR [dB]	Modulation Format M	Frequency slots
[1-4]	{1,4}	13,3	QPSK	1,2,3,4	[6-8]	{6,7,8}	12,3	QPSK	8,9,10,11
[1-5]	{1,4,5}	10,5	QPSK	5,6,7,8	[6-9]	{6,7,8,9}	10,7979	QPSK	36,37,38,39
[1-11]	{1,11}	11,5	QPSK	1,2,3,4	[6-10]	{6,7,8,9,10}	10,0	QPSK	40,41,42,43
[2-3]	{2,3}	17,1	16-QAM	1,2,3	[6-11]	{6,5,4,11}	10,1	QPSK	21,22,23,24
[2-5]	{2,5}	9,7	QPSK	1,2,3,4	[6-12]	{6,12}	11,9	QPSK	1,2,3,4
[2-7]	{2,3,9,8,7}	10,1	QPSK	4,5,6,7	[6-13]	{6,12,13}	9,6	QPSK	5,6,7,8
[2-8]	{2,3,9,8}	11,7	QPSK	8,9,10,11	[6-14]	{6,7,8,9,10,14}	9,7	QPSK	44,45,46,47
[2-9]	{2,3,9}	13,6	QPSK	12,13,14,15	[7-8]	{7,8}	16,8	16-QAM	1,7,8
[2-10]	{2,10}	14,3	QPSK	1,2,3,4	[7-9]	{7,8,9}	12,6	QPSK	12,13,14,15
[2-13]	{2,3,9,13}	11,1	QPSK	16,17,18,19	[7-10]	{7,8,9,10}	11,4	QPSK	16,17,18,19
[2-14]	{2,10,14}	13,5	QPSK	5,6,7,8	[7-12]	{7,6,12}	10,4	QPSK	24,25,26,27
[3-6]	{3,9,8,7,6}	10,1	QPSK	20,21,22,23	[7-13]	{7,8,9,13}	10,5	QPSK	48,49,50,51
[3-7]	{3,9,8,7}	11,6	QPSK	24,25,26,27	[7-14]	{7,8,9,10,14}	11,0	QPSK	52,53,54,55
[3-8]	{3,9,8}	14,1	QPSK	28,29,30,31	[8-9]	{8,9}	17,7	16-QAM	1,8,9
[3-9]	{3,9}	20,1	16-QAM	1,3,9	[8-10]	{8,9,10}	13,8	QPSK	56,57,58,59
[3-10]	{3,14,10}	17,7	16-QAM	1,3,10	[8-12]	{8,9,13,12}	9,8	QPSK	60,61,62,63
[3-12]	{3,9,13,12}	10,3	QPSK	32,33,34,35	[8-13]	{8,9,13}	12,4	QPSK	64,65,66,67
[3-13]	{3,9,13}	13,2	QPSK	36,37,38,39	[8-14]	{8,9,10,14}	13,1	QPSK	68,69,70,71
[3-14]	{3,14}	19,3	16-QAM	4,3,14	[9-10]	{9,10}	19,3	16-QAM	1,9,10
[4-5]	{4,5}	13,8	QPSK	1,2,3,4	[9-12]	{9,13,12}	11,0	QPSK	1,2,3,4
[4-6]	{4,5,6}	11,8	QPSK	9,10,11,12	[9-13]	{9,13}	16,4	16-QAM	5,9,13
[4-7]	{4,5,6,7}	10,2	QPSK	13,14,15,16	[9-14]	{9,10,14}	17,7	16-QAM	9,9,14
[4-11]	{4,11}	16,8	16-QAM	1,4,11	[10-12]	{10,9,13,12}	10,2	QPSK	12,13,14,15
[5-6]	{5,6}	17,7	16-QAM	1,5,6	[10-13]	{10,9,13}	13,0	QPSK	20,21,22,23
[5-7]	{5,6,7}	12,8	QPSK	4,5,6,7	[10-14]	{10,14}	22,8	64-QAM	12,10,14
[5-8]	{5,6,7,8}	10,8	QPSK	28,29,30,31	[11-12]	{11,12}	10,3	QPSK	1,2,3,4
[5-9]	{5,6,7,8,9}	9,7	QPSK	32,33,34,35	[12-13]	{12,13}	13,4	QPSK	16,17,18,19
[5-11]	{5,4,11}	11,4	QPSK	17,18,19,20	[12-14]	{12,14}	10,3	QPSK	1,2,3,4
[5-12]	{5,6,12}	10,5	QPSK	17,18,19,20	[13-14]	{13,9,10,14}	12,3	QPSK	24,25,26,27
[6-7]	{6,7}	17,2	16-QAM	1,6,7					

Table C.7. RMSA solution for the NSFNET optical network with BER= 10^{-2} .

Blocked Demands	[1-2], [1-3], [1-6], [1-7], [1-8], [1-9], [1-10], [1-12], [1-13], [1-14], [2-4], [2-6], [2-11], [2-12], [3-4], [3-5], [3-11], [4-8], [4-9], [4-10], [4-12], [4-13], [4-14], [5-10], [5-13], [5-14], [7-11], [8-11], [9-11], [10-11], [11-13], [11-14].
-----------------	--

Table C.8. Blocked demands in the RMSA solution for the NSFNET optical network with BER= 10^{-2} .

Demand d	Path	OSNR [dB]	Modulation format M	Frequency slots	Demand d	Path	OSNR [dB]	Modulation format M	Frequency slots
[1-4]	{1,4}	13.3	QPSK	1,2,3,4	[6-8]	{6,7,8}	12.3	QPSK	9,10,11,12
[2-3]	{2,3}	15.4	QPSK	1,2,3,4	[7-8]	{7,8}	15.1	QPSK	1,2,3,4
[2-9]	{2,3,9}	13.6	QPSK	5,6,7,8	[7-9]	{7,8,9}	12.6	QPSK	5,6,7,8
[2-10]	{2,10}	14.3	QPSK	1,2,3,4	[8-9]	{8,9}	16.1	QPSK	9,10,11,12
[2-14]	{2,10,14}	13.4	QPSK	5,6,7,8	[8-10]	{8,9,10}	13.8	QPSK	13,14,15,16
[3-8]	{3,9,8}	14.1	QPSK	1,2,3,4	[8-13]	{8,9,13}	12.3	QPSK	17,18,19,20
[3-9]	{3,9}	20.1	16-QAM	9,10,11	[8-14]	{8,9,10,14}	13.1	QPSK	21,22,23,24
[3-10]	{3,14,10}	16.0	QPSK	1,2,3,4	[9-10]	{9,10}	19.3	16-QAM	1,2,3
[3-13]	{3,9,13}	13.2	QPSK	12,13,14,15	[9-13]	{9,13}	14.7	QPSK	1,2,3,4
[3-14]	{3,14}	19.3	16-QAM	5,6,7	[9-14]	{9,10,14}	16.1	QPSK	9,10,11,12
[4-5]	{4,5}	13.8	QPSK	1,2,3,4	[10-13]	{10,9,13}	13.0	QPSK	5,6,7,8
[4-11]	{4,11}	15.0	QPSK	1,2,3,4	[10-14]	{10,14}	22.6	16-QAM	13,14,15
[5-6]	{5,6}	16.0	QPSK	1,2,3,4	[12-13]	{12,13}	13.4	QPSK	1,2,3,4
[5-7]	{5,6,7}	12.8	QPSK	5,6,7,8	[13-14]	{13,9,10,14}	12.3	QPSK	25,26,27,28
[6-7]	{6,7}	15.5	QPSK	1,2,3,4					

Table C.9. RMSA solution for the NSFNET optical network with BER= 10^{-3} .

Appendix C *Complementary material used in Chapter 4*

Blocked Demands	[1-2], [1-3], [1-5], [1-6], [1-7], [1-8], [1-9], [1-10], [1-11], [1-12], [1-13], [1-14], [2-4], [2-5], [2-6], [2-7], [2-8], [2-11], [2-12], [2-13], [3-4], [3-5], [3-6], [3-7], [3-11], [3-12], [4-6], [4-7], [4-8], [4-9], [4-10], [4-12], [4-13], [4-14], [5-8], [5-9], [5-10], [5-11], [5-12], [5-13], [5-14], [6-9], [6-10], [6-11], [6-12], [6-13], [6-14], [7-10], [7-11], [7-12], [7-13], [7-14], [8-11], [8-12], [9-11], [9-12], [10-11], [10-12], [11-12], [11-13], [11-14], [12-14].
-----------------	--

Table C.10. Blocked demands in the RMSA solution for the NSFNET optical network with $\text{BER}=10^{-3}$.

Appendix C Complementary material used in Chapter 4

Demand d	Path	OSNR [dB]	Modulation format M	Frequency slots	Demand d	Path	OSNR [dB]	Modulation format M	Frequency slots
[1-2]	{1,2}	15.8	16-QAM	1,2,3	[9-22]	{9,12,16,22}	8.7	QPSK	70,71,72,73
[1-3]	{1,2,3}	11.1	QPSK	4,5,6,7	[9-23]	{9,12,16,22,23}	7.8	QPSK	78,79,80,81
[1-4]	{1,2,3,4}	10.7	QPSK	8,9,10,11	[9-24]	{9,10,14,18,24}	7.3	QPSK	70,71,72,73
[1-5]	{1,2,3,4,5}	9.2	QPSK	12,13,14,15	[10-11]	{10,9,11}	9.4	QPSK	24,25,26,27
[1-6]	{1,6}	14.9	16-QAM	1,2,3	[10-12]	{10,13,12}	10.8	QPSK	16,17,18,19
[1-7]	{1,6,7}	10.2	QPSK	4,5,6,7	[10-13]	{10,13}	15.7	16-QAM	1,2,3
[1-8]	{1,6,7,8}	8.4	QPSK	8,9,10,11	[10-14]	{10,14}	16.2	16-QAM	1,2,3
[1-9]	{1,6,9}	9.7	QPSK	12,13,14,15	[10-15]	{10,13,12,16,15}	8.0	QPSK	24,25,26,27
[1-10]	{1,6,9,10}	8.1	QPSK	16,17,18,19	[10-16]	{10,13,12,16}	8.8	QPSK	40,41,42,43
[1-11]	{1,6,11}	8.6	QPSK	20,21,22,23	[10-17]	{10,13,17}	10.4	QPSK	28,29,30,31
[1-12]	{1,6,9,12}	8.1	QPSK	24,25,26,27	[10-18]	{10,14,18}	10.3	QPSK	4,5,6,7
[1-14]	{1,6,9,10,14}	7.2	QPSK	28,29,30,31	[10-20]	{10,13,17,22,21,20}	7.5	QPSK	62,63,64,65
[2-3]	{2,3}	15.7	16-QAM	1,2,3	[10-21]	{10,13,17,22,21}	8.5	QPSK	66,67,68,69
[2-4]	{2,3,4}	14.9	16-QAM	16,17,18	[10-22]	{10,13,17,22}	9.0	QPSK	74,75,76,77
[2-5]	{2,3,4,5}	10.9	QPSK	19,20,21,22	[10-23]	{10,13,17,23}	8.5	QPSK	82,83,84,85
[2-6]	{2,6}	14.5	16-QAM	1,2,3	[10-24]	{10,14,18,24}	8.7	QPSK	8,9,10,11
[2-7]	{2,3,4,7}	10.9	QPSK	23,24,25,26	[11-12]	{11,12}	15.3	16-QAM	1,2,3
[2-8]	{2,3,4,7,8}	8.8	QPSK	27,28,29,30	[11-13]	{11,12,13}	10.6	QPSK	4,5,6,7
[2-9]	{2,6,9}	9.6	QPSK	4,5,6,7	[11-14]	{11,12,13,14}	9.5	QPSK	8,9,10,11
[2-10]	{2,6,9,10}	8.0	QPSK	8,9,10,11	[11-15]	{11,15}	13.8	16-QAM	1,2,3
[2-11]	{2,6,11}	8.4	QPSK	12,13,14,15	[11-16]	{11,12,16}	10.4	QPSK	12,13,14,15
[2-12]	{2,6,9,12}	8.0	QPSK	20,21,22,23	[11-17]	{11,12,13,17}	8.5	QPSK	44,45,46,47
[2-14]	{2,6,9,10,14}	7.1	QPSK	32,33,34,35	[11-18]	{11,12,13,14,18}	7.7	QPSK	20,21,22,23
[3-4]	{3,4}	22.6	64-QAM	1,2	[11-19]	{11,15,20,19}	7.8	QPSK	9,10,11,12
[3-5]	{3,4,5}	15.3	16-QAM	3,4,5	[11-20]	{11,15,20}	9.0	QPSK	13,14,15,16
[3-6]	{3,4,7,6}	10.4	QPSK	31,32,33,34	[11-21]	{11,12,16,21}	8.5	QPSK	52,53,54,55
[3-7]	{3,4,7}	15.3	16-QAM	35,36,37	[11-22]	{11,12,16,22}	8.8	QPSK	74,75,76,77
[3-8]	{3,4,7,8}	10.4	QPSK	38,39,40,41	[11-23]	{11,12,16,22,23}	8.0	QPSK	82,83,84,85
[3-9]	{3,4,7,9}	10.4	QPSK	42,43,44,45	[12-13]	{12,13}	15.3	16-QAM	1,2,3
[3-10]	{3,4,7,8,10}	8.7	QPSK	46,47,48,49	[12-14]	{12,13,14}	13.3	16-QAM	12,13,14
[3-11]	{3,4,7,9,11}	8.0	QPSK	50,51,52,53	[12-15]	{12,16,15}	11.1	QPSK	20,21,22,23
[3-12]	{3,4,7,9,12}	8.6	QPSK	54,55,56,57	[12-16]	{12,16}	14.9	16-QAM	1,2,3
[3-13]	{3,4,7,9,10,13}	7.5	QPSK	58,59,60,61	[12-17]	{12,13,17}	10.2	QPSK	48,49,50,51
[3-14]	{3,4,7,8,10,14}	7.7	QPSK	62,63,64,65	[12-18]	{12,13,14,18}	9.0	QPSK	28,29,30,31
[3-16]	{3,4,7,9,12,16}	7.3	QPSK	66,67,68,69	[12-19]	{12,16,21,20,19}	7.7	QPSK	94,95,96,97
[4-5]	{4,5}	16.2	16-QAM	6,7,8	[12-20]	{12,16,21,20}	8.8	QPSK	98,99,100,101
[4-6]	{4,7,6}	10.8	QPSK	12,13,14,15	[12-21]	{12,16,21}	10.2	QPSK	102,103,104,105
[4-7]	{4,7}	16.2	16-QAM	1,2,3	[12-22]	{12,16,22}	10.6	QPSK	106,107,108,109
[4-8]	{4,7,8}	10.8	QPSK	4,5,6,7	[12-23]	{12,16,22,23}	9.3	QPSK	110,111,112,113
[4-9]	{4,7,9}	10.8	QPSK	8,9,10,11	[12-24]	{12,16,22,23,24}	8.0	QPSK	114,115,116,117
[4-10]	{4,7,8,10}	9.0	QPSK	16,17,18,19	[13-14]	{13,14}	17.6	16-QAM	1,2,3
[4-11]	{4,7,9,11}	8.2	QPSK	70,71,72,73	[13-15]	{13,12,16,15}	9.2	QPSK	118,119,120,121
[4-12]	{4,7,9,12}	8.8	QPSK	74,75,76,77	[13-16]	{13,12,16}	10.4	QPSK	122,123,124,125
[4-13]	{4,7,8,10,13}	7.8	QPSK	78,79,80,81	[13-17]	{13,17}	14.5	16-QAM	1,2,3
[4-14]	{4,7,8,10,14}	7.9	QPSK	82,83,84,85	[13-18]	{13,14,18}	10.8	QPSK	15,16,17,18
[4-16]	{4,7,9,12,16}	7.5	QPSK	86,87,88,89	[13-19]	{13,17,22,21,20,19}	7.5	QPSK	4,5,6,7
[5-6]	{5,4,7,6}	9.3	QPSK	90,91,92,93	[13-20]	{13,17,22,21,20}	8.6	QPSK	8,9,10,11
[5-7]	{5,4,7}	11.6	QPSK	94,95,96,97	[13-21]	{13,17,22,21}	9.9	QPSK	16,17,18,19
[5-8]	{5,8}	14.1	16-QAM	1,2,3	[13-22]	{13,17,22}	10.6	QPSK	24,25,26,27
[5-9]	{5,4,7,9}	9.3	QPSK	98,99,100,101	[13-23]	{13,17,23}	9.9	QPSK	32,33,34,35
[5-10]	{5,8,10}	9.9	QPSK	4,5,6,7	[13-24]	{13,14,18,24}	9.0	QPSK	32,33,34,35
[5-11]	{5,4,7,9,11}	7.3	QPSK	102,103,104,105	[14-15]	{14,13,12,16,15}	8.3	QPSK	126,127,128,129
[5-12]	{5,4,7,9,12}	7.8	QPSK	106,107,108,109	[14-16]	{14,13,12,16}	9.3	QPSK	130,131,132,133
[5-13]	{5,8,10,13}	8.5	QPSK	8,9,10,11	[14-17]	{14,13,17}	11.1	QPSK	36,37,38,39
[5-14]	{5,8,10,14}	8.7	QPSK	12,13,14,15	[14-18]	{14,18}	14.1	16-QAM	1,2,3
[5-17]	{5,8,10,13,17}	7.1	QPSK	20,21,22,23	[14-20]	{14,13,17,22,21,20}	7.9	QPSK	40,41,42,43
[5-18]	{5,8,10,14,18}	7.1	QPSK	24,25,26,27	[14-21]	{14,13,17,22,21}	8.9	QPSK	58,59,60,61
[6-7]	{6,7}	14.9	16-QAM	1,2,3	[14-22]	{14,13,17,22}	9.5	QPSK	70,71,72,73
[6-8]	{6,7,8}	10.1	QPSK	20,21,22,23	[14-23]	{14,13,17,23}	9.0	QPSK	78,79,80,81
[6-9]	{6,9}	14.1	16-QAM	1,2,3	[14-24]	{14,18,24}	9.9	QPSK	36,37,38,39
[6-10]	{6,9,10}	9.7	QPSK	36,37,38,39	[15-16]	{15,16}	17.1	16-QAM	1,2,3
[6-11]	{6,11}	10.4	QPSK	1,2,3,4	[15-17]	{15,16,17}	11.1	QPSK	8,9,10,11
[6-12]	{6,9,12}	9.7	QPSK	40,41,42,43	[15-18]	{15,16,17,18}	9.3	QPSK	12,13,14,15
[6-13]	{6,9,10,13}	8.4	QPSK	44,45,46,47	[15-19]	{15,20,19}	9.9	QPSK	17,18,19,20
[6-14]	{6,9,10,14}	8.5	QPSK	48,49,50,51	[15-20]	{15,20}	13.8	16-QAM	1,2,3
[6-15]	{6,11,15}	8.1	QPSK	5,6,7,8	[15-21]	{15,16,21}	11.1	QPSK	28,29,30,31
[6-16]	{6,9,12,16}	8.1	QPSK	58,59,60,61	[15-22]	{15,16,22}	13.4	16-QAM	32,33,34
[6-22]	{6,9,12,16,22}	7.1	QPSK	62,63,64,65	[15-23]	{15,16,22,23}	10.1	QPSK	40,41,42,43
[7-8]	{7,8}	14.8	16-QAM	1,2,3	[15-24]	{15,16,22,23,24}	8.5	QPSK	44,45,46,47
[7-9]	{7,9}	14.9	16-QAM	1,2,3	[16-17]	{16,17}	14.9	16-QAM	1,2,3
[7-10]	{7,8,10}	10.4	QPSK	31,32,33,34	[16-18]	{16,17,18}	10.6	QPSK	4,5,6,7
[7-11]	{7,9,11}	9.4	QPSK	4,5,6,7	[16-19]	{16,21,20,19}	9.1	QPSK	13,14,15,16
[7-12]	{7,9,12}	10.2	QPSK	12,13,14,15	[16-20]	{16,21,20}	10.8	QPSK	17,18,19,20
[7-13]	{7,8,10,13}	8.8	QPSK	50,51,52,53	[16-21]	{16,21}	14.9	16-QAM	1,2,3
[7-14]	{7,8,10,14}	9.0	QPSK	42,43,44,45	[16-22]	{16,22}	15.8	16-QAM	1,2,3

Appendix C Complementary material used in Chapter 4

[7-15]	{7,9,12,16,15}	7.6	QPSK	16,17,18,19	[16-23]	{16,22,23}	13.4	16-QAM	4,5,6
[7-16]	{7,9,12,16}	8.4	QPSK	28,29,30,31	[16-24]	{16,22,23,24}	9.5	QPSK	7,8,9,10
[7-17]	{7,8,10,13,17}	7.3	QPSK	54,55,56,57	[17-18]	{17,18}	15.8	16-QAM	1,2,3
[7-18]	{7,8,10,14,18}	7.3	QPSK	58,59,60,61	[17-19]	{17,22,21,20,19}	9.1	QPSK	28,29,30,31
[7-21]	{7,9,12,16,21}	7.1	QPSK	32,33,34,35	[17-20]	{17,22,21,20}	10.8	QPSK	32,33,34,35
[7-22]	{7,9,12,16,22}	7.4	QPSK	36,37,38,39	[17-21]	{17,22,21}	14.7	16-QAM	1,2,3
[8-9]	{8,10,9}	10.4	QPSK	66,67,68,69	[17-22]	{17,22}	16.2	16-QAM	12,13,14
[8-10]	{8,10}	15.3	16-QAM	1,2,3	[17-23]	{17,23}	14.9	16-QAM	1,2,3
[8-11]	{8,10,9,11}	8.0	QPSK	74,75,76,77	[17-24]	{17,18,24}	10.8	QPSK	16,17,18,19
[8-12]	{8,10,13,12}	9.0	QPSK	35,36,37,38	[18-19]	{18,17,22,21,20,19}	7.9	QPSK	36,37,38,39
[8-13]	{8,10,13}	10.8	QPSK	70,71,72,73	[18-20]	{18,17,22,21,20}	9.1	QPSK	48,49,50,51
[8-14]	{8,10,14}	11.1	QPSK	86,87,88,89	[18-21]	{18,17,22,21}	10.5	QPSK	20,21,22,23
[8-16]	{8,10,13,12,16}	7.6	QPSK	90,91,92,93	[18-22]	{18,17,22}	11.3	QPSK	44,45,46,47
[8-17]	{8,10,13,17}	8.7	QPSK	94,95,96,97	[18-23]	{18,17,23}	10.6	QPSK	8,9,10,11
[8-18]	{8,10,14,18}	8.7	QPSK	98,99,100,101	[18-24]	{18,24}	15.3	16-QAM	1,2,3
[8-21]	{8,10,13,17,22,21}	7.3	QPSK	102,103,104,105	[19-20]	{19,20}	15.6	16-QAM	1,2,3
[8-22]	{8,10,13,17,22}	7.7	QPSK	106,107,108,109	[19-21]	{19,20,21}	11.3	QPSK	21,22,23,24
[8-23]	{8,10,13,17,23}	7.4	QPSK	110,111,112,113	[19-22]	{19,20,21,22}	10.5	QPSK	52,53,54,55
[8-24]	{8,10,14,18,24}	7.5	QPSK	114,115,116,117	[19-23]	{19,20,21,22,23}	9.2	QPSK	70,71,72,73
[9-10]	{9,10}	14.9	16-QAM	1,2,3	[19-24]	{19,20,21,22,23,24}	7.9	QPSK	74,75,76,77
[9-11]	{9,11}	13.4	16-QAM	1,2,3	[20-21]	{20,21}	16.4	16-QAM	1,2,3
[9-12]	{9,12}	14.9	16-QAM	1,2,3	[20-22]	{20,21,22}	14.8	16-QAM	25,26,27
[9-13]	{9,10,13}	10.6	QPSK	4,5,6,7	[20-23]	{20,21,22,23}	11.1	QPSK	86,87,88,89
[9-14]	{9,10,14}	10.8	QPSK	20,21,22,23	[20-24]	{20,21,22,23,24}	9.1	QPSK	90,91,92,93
[9-15]	{9,12,16,15}	9.0	QPSK	4,5,6,7	[21-22]	{21,22}	20.5	64-QAM	12,13
[9-16]	{9,12,16}	10.2	QPSK	8,9,10,11	[21-23]	{21,22,23}	15.3	16-QAM	94,95,96
[9-17]	{9,10,13,17}	8.5	QPSK	12,13,14,15	[21-24]	{21,22,23,24}	10.6	QPSK	97,98,99,100
[9-18]	{9,10,14,18}	8.5	QPSK	52,53,54,55	[22-23]	{22,23}	17.1	16-QAM	1,2,3
[9-20]	{9,12,16,21,20}	7.5	QPSK	44,45,46,47	[22-24]	{22,23,24}	11.4	QPSK	11,12,13,14
[9-21]	{9,12,16,21}	8.4	QPSK	48,49,50,51	[23-24]	{23,24}	15.3	16-QAM	1,2,3

Table C.11. RMSA solution for the UBN optical network with $BER=4\times 10^{-2}$.

Blocked Demands	[1-13], [1-15], [1-16], [1-17], [1-18], [1-19], [1-20], [1-21], [1-22], [1-23], [1-24], [2-13], [2-15], [2-16], [2-17], [2-18], [2-19], [2-20], [2-21], [2-22], [2-23], [2-24], [3-15], [3-17], [3-18], [3-19], [3-20], [3-21], [3-22], [3-23], [3-24], [4-15], [4-17], [4-18], [4-19], [4-20], [4-21], [4-22], [4-23], [4-24], [5-15], [5-16], [5-19], [5-20], [5-21], [5-22], [5-23], [5-24], [6-17], [6-18], [6-19], [6-20], [6-21], [6-23], [6-24], [7-19], [7-20], [7-23], [7-24], [8-15], [8-19], [8-20], [9-19], [10-19], [11-24], [14-19].
-----------------	--

Table C.12. Blocked demands in the RMSA solution for the UBN optical network with $BER=4\times 10^{-2}$.

Appendix C Complementary material used in Chapter 4

Demand d	Path	OSNR [dB]	Modulation format M	Frequency slots	Demand d	Path	OSNR [dB]	Modulation format M	Frequency slots
[1-2]	{1,2}	14.1	QPSK	1,2,3,4	[11-16]	{11,12,16}	10.4	QPSK	13,14,15,16
[1-3]	{1,2,3}	11.1	QPSK	5,6,7,8	[12-13]	{12,13}	13.6	QPSK	9,10,11,12
[1-4]	{1,2,3,4}	10.7	QPSK	9,10,11,12	[12-14]	{12,13,14}	11.6	QPSK	13,14,15,16
[1-6]	{1,6}	13.2	QPSK	1,2,3,4	[12-15]	{12,16,15}	11.1	QPSK	1,2,3,4
[1-7]	{1,6,7}	10.2	QPSK	5,6,7,8	[12-16]	{12,16}	13.2	QPSK	5,6,7,8
[1-9]	{1,6,9}	9.7	QPSK	9,10,11,12	[12-17]	{12,13,17}	10.2	QPSK	21,22,23,24
[2-3]	{2,3}	14.1	QPSK	1,2,3,4	[12-21]	{12,16,21}	10.2	QPSK	17,18,19,20
[2-4]	{2,3,4}	13.3	QPSK	13,14,15,16	[12-22]	{12,16,22}	10.6	QPSK	21,22,23,24
[2-5]	{2,3,4,5}	10.9	QPSK	17,18,19,20	[13-14]	{13,14}	17.6	16-QAM	1,2,3
[2-6]	{2,6}	12.8	QPSK	1,2,3,4	[13-16]	{13,12,16}	10.4	QPSK	25,26,27,28
[2-7]	{2,3,4,7}	10.9	QPSK	21,22,23,24	[13-17]	{13,17}	12.8	QPSK	1,2,3,4
[2-9]	{2,6,9}	9.6	QPSK	5,6,7,8	[13-18]	{13,14,18}	10.8	QPSK	8,9,10,11
[3-4]	{3,4}	22.6	64-QAM	1,2	[13-21]	{13,17,22,21}	9.9	QPSK	5,6,7,8
[3-5]	{3,4,5}	13.7	QPSK	3,4,5,6	[13-22]	{13,17,22}	10.6	QPSK	9,10,11,12
[3-6]	{3,4,7,6}	10.4	QPSK	25,26,27,28	[13-23]	{13,17,23}	9.9	QPSK	13,14,15,16
[3-7]	{3,4,7}	13.7	QPSK	29,30,31,32	[14-17]	{14,13,17}	11.1	QPSK	25,26,27,28
[3-8]	{3,4,7,8}	10.4	QPSK	33,34,35,36	[14-18]	{14,18}	12.4	QPSK	12,13,14,15
[3-9]	{3,4,7,9}	10.4	QPSK	37,38,39,40	[14-24]	{14,18,24}	9.9	QPSK	16,17,18,19
[4-5]	{4,5}	16.2	16-QAM	7,8,9	[15-16]	{15,16}	17.1	16-QAM	5,6,7
[4-6]	{4,7,6}	10.8	QPSK	1,2,3,4	[15-17]	{15,16,17}	11.1	QPSK	8,9,10,11
[4-7]	{4,7}	16.2	16-QAM	5,6,7	[15-19]	{15,20,19}	9.9	QPSK	1,2,3,4
[4-8]	{4,7,8}	10.8	QPSK	8,9,10,11	[15-20]	{15,20}	12.0	QPSK	5,6,7,8
[4-9]	{4,7,9}	10.8	QPSK	12,13,14,15	[15-21]	{15,16,21}	11.1	QPSK	12,13,14,15
[5-7]	{5,4,7}	11.6	QPSK	41,42,43,44	[15-22]	{15,16,22}	11.7	QPSK	16,17,18,19
[5-8]	{5,8}	12.4	QPSK	1,2,3,4	[15-23]	{15,16,22,23}	10.1	QPSK	25,26,27,28
[5-10]	{5,8,10}	9.9	QPSK	5,6,7,8	[16-17]	{16,17}	13.2	QPSK	1,2,3,4
[6-7]	{6,7}	13.2	QPSK	9,10,11,12	[16-18]	{16,17,18}	10.6	QPSK	12,13,14,15
[6-8]	{6,7,8}	10.1	QPSK	13,14,15,16	[16-20]	{16,21,20}	10.8	QPSK	1,2,3,4
[6-9]	{6,9}	12.4	QPSK	1,2,3,4	[16-21]	{16,21}	13.2	QPSK	5,6,7,8
[6-10]	{6,9,10}	9.7	QPSK	13,14,15,16	[16-22]	{16,22}	14.1	QPSK	1,2,3,4
[6-11]	{6,11}	10.4	QPSK	1,2,3,4	[16-23]	{16,22,23}	11.7	QPSK	5,6,7,8
[6-12]	{6,9,12}	9.7	QPSK	17,18,19,20	[16-24]	{16,22,23,24}	9.5	QPSK	9,10,11,12
[7-8]	{7,8}	13.1	QPSK	1,2,3,4	[17-18]	{17,18}	14.1	QPSK	1,2,3,4
[7-9]	{7,9}	13.2	QPSK	1,2,3,4	[17-20]	{17,22,21,20}	10.8	QPSK	13,14,15,16
[7-10]	{7,8,10}	10.4	QPSK	17,18,19,20	[17-21]	{17,22,21}	13.0	QPSK	1,2,3,4
[7-12]	{7,9,12}	10.2	QPSK	5,6,7,8	[17-22]	{17,22}	16.2	16-QAM	17,18,19
[8-9]	{8,10,9}	10.4	QPSK	1,2,3,4	[17-23]	{17,23}	13.2	QPSK	1,2,3,4
[8-10]	{8,10}	13.6	QPSK	9,10,11,12	[17-24]	{17,18,24}	10.8	QPSK	5,6,7,8
[8-13]	{8,10,13}	10.8	QPSK	13,14,15,16	[18-21]	{18,17,22,21}	10.5	QPSK	20,21,22,23
[8-14]	{8,10,14}	11.1	QPSK	21,22,23,24	[18-22]	{18,17,22}	11.3	QPSK	24,25,26,27
[9-10]	{9,10}	13.2	QPSK	5,6,7,8	[18-23]	{18,17,23}	10.6	QPSK	28,29,30,31
[9-11]	{9,11}	11.7	QPSK	1,2,3,4	[18-24]	{18,24}	13.6	QPSK	1,2,3,4
[9-12]	{9,12}	13.2	QPSK	1,2,3,4	[19-20]	{19,20}	13.9	QPSK	5,6,7,8
[9-13]	{9,10,13}	10.6	QPSK	9,10,11,12	[19-21]	{19,20,21}	11.3	QPSK	9,10,11,12
[9-14]	{9,10,14}	10.8	QPSK	17,18,19,20	[19-22]	{19,20,21,22}	10.5	QPSK	24,25,26,27
[9-16]	{9,12,16}	10.2	QPSK	9,10,11,12	[20-21]	{20,21}	16.4	16-QAM	5,6,7
[10-12]	{10,13,12}	10.8	QPSK	1,2,3,4	[20-22]	{20,21,22}	13.1	QPSK	28,29,30,31
[10-13]	{10,13}	14.1	QPSK	5,6,7,8	[20-23]	{20,21,22,23}	11.1	QPSK	32,33,34,35
[10-14]	{10,14}	16.2	16-QAM	1,2,3	[21-22]	{21,22}	20.0	16-QAM	9,10,11
[10-17]	{10,13,17}	10.4	QPSK	17,18,19,20	[21-23]	{21,22,23}	13.5	QPSK	36,37,38,39
[10-18]	{10,14,18}	10.3	QPSK	4,5,6,7	[21-24]	{21,22,23,24}	10.6	QPSK	40,41,42,43
[11-12]	{11,12}	13.6	QPSK	1,2,3,4	[22-23]	{22,23}	17.1	16-QAM	1,2,3
[11-13]	{11,12,13}	10.6	QPSK	5,6,7,8	[22-24]	{22,23,24}	11.4	QPSK	13,14,15,16
[11-15]	{11,15}	12.0	QPSK	1,2,3,4	[23-24]	{23,24}	13.6	QPSK	1,2,3,4

Table C.13. RMSA solution for the UBN optical network with BER=10⁻².

Appendix C Complementary material used in Chapter 4

Blocked Demands	[1-5], [1-8], [1-10], [1-11], [1-12], [1-13], [1-14], [1-15], [1-16], [1-17], [1-18], [1-19], [1-20], [1-21], [1-22], [1-23], [1-24], [2-8], [2-10], [2-11], [2-12], [2-13], [2-14], [2-15], [2-16], [2-17], [2-18], [2-19], [2-20], [2-21], [2-22], [2-23], [2-24], [3-10], [3-11], [3-12], [3-13], [3-14], [3-15], [3-16], [3-17], [3-18], [3-19], [3-20], [3-21], [3-22], [3-23], [3-24], [4-10], [4-11], [4-12], [4-13], [4-14], [4-15], [4-16], [4-17], [4-18], [4-19], [4-20], [4-21], [4-22], [4-23], [4-24], [5-6], [5-9], [5-11], [5-12], [5-13], [5-14], [5-15], [5-16], [5-17], [5-18], [5-19], [5-20], [5-21], [5-22], [5-23], [5-24], [6-13], [6-14], [6-15], [6-16], [6-17], [6-18], [6-19], [6-20], [6-21], [6-22], [6-23], [6-24], [7-11], [7-13], [7-14], [7-15], [7-16], [7-17], [7-18], [7-19], [7-20], [7-21], [7-22], [7-23], [7-24], [8-11], [8-12], [8-15], [8-16], [8-17], [8-18], [8-19], [8-20], [8-21], [8-22], [8-23], [8-24], [9-15], [9-17], [9-18], [9-19], [9-20], [9-21], [9-22], [9-23], [9-24], [10-11], [10-15], [10-16], [10-19], [10-20], [10-21], [10-22], [10-23], [10-24], [11-14], [11-17], [11-18], [11-19], [11-20], [11-21], [11-22], [11-23], [11-24], [12-18], [12-19], [12-20], [12-23], [12-24], [13-15], [13-19], [13-20], [13-24], [14-15], [14-16], [14-19], [14-20], [14-21], [14-22], [14-23], [15-18], [15-24], [16-19], [17-19], [18-19], [18-20], [19-23], [19-24], [20-24].
-----------------	---

Table C.14. Blocked demands in the RMSA solution for the UBN optical network with BER=10⁻².

Demand d	Path	OSNR [dB]	Modulation format M	Frequency slots	Demand d	Path	OSNR [dB]	Modulation format M	Frequency slots
[1-2]	{1,2}	14.1	QPSK	1,2,3,4	[12-13]	{12,13}	13.6	QPSK	1,2,3,4
[1-6]	{1,6}	13.2	QPSK	1,2,3,4	[12-16]	{12,16}	13.2	QPSK	1,2,3,4
[2-3]	{2,3}	14.1	QPSK	1,2,3,4	[13-14]	{13,14}	15.9	QPSK	1,2,3,4
[2-4]	{2,3,4}	13.3	QPSK	5,6,7,8	[13-17]	{13,17}	12.8	QPSK	1,2,3,4
[2-6]	{2,6}	12.8	QPSK	1,2,3,4	[14-18]	{14,18}	12.4	QPSK	1,2,3,4
[3-4]	{3,4}	22.5	16-QAM	1,2,3	[15-16]	{15,16}	15.3	QPSK	1,2,3,4
[3-5]	{3,4,5}	13.7	QPSK	9,10,11,12	[15-20]	{15,20}	12.0	QPSK	1,2,3,4
[3-7]	{3,4,7}	13.7	QPSK	13,14,15,16	[16-17]	{16,17}	13.2	QPSK	1,2,3,4
[4-5]	{4,5}	14.6	QPSK	1,2,3,4	[16-21]	{16,21}	13.2	QPSK	1,2,3,4
[4-7]	{4,7}	14.6	QPSK	1,2,3,4	[16-22]	{16,22}	14.1	QPSK	1,2,3,4
[5-8]	{5,8}	12.4	QPSK	1,2,3,4	[17-18]	{17,18}	14.1	QPSK	1,2,3,4
[6-7]	{6,7}	13.2	QPSK	1,2,3,4	[17-21]	{17,22,21}	13.0	QPSK	1,2,3,4
[6-9]	{6,9}	12.4	QPSK	1,2,3,4	[17-22]	{17,22}	14.6	QPSK	5,6,7,8
[7-8]	{7,8}	13.1	QPSK	1,2,3,4	[17-23]	{17,23}	13.2	QPSK	1,2,3,4
[7-9]	{7,9}	13.2	QPSK	1,2,3,4	[18-24]	{18,24}	13.6	QPSK	1,2,3,4
[8-10]	{8,10}	13.6	QPSK	1,2,3,4	[19-20]	{19,20}	13.9	QPSK	1,2,3,4
[9-10]	{9,10}	13.2	QPSK	1,2,3,4	[20-21]	{20,21}	14.7	QPSK	1,2,3,4
[9-12]	{9,12}	13.2	QPSK	1,2,3,4	[20-22]	{20,21,22}	13.1	QPSK	5,6,7,8
[10-13]	{10,13}	14.1	QPSK	1,2,3,4	[21-22]	{21,22}	20.0	16-QAM	9,10,11
[10-14]	{10,14}	14.6	QPSK	1,2,3,4	[21-23]	{21,22,23}	13.5	QPSK	12,13,14,15
[11-12]	{11,12}	13.6	QPSK	1,2,3,4	[22-23]	{22,23}	15.3	QPSK	1,2,3,4
[11-15]	{11,15}	12.0	QPSK	1,2,3,4	[23-24]	{23,24}	13.6	QPSK	1,2,3,4

Table C.15. RMSA solution for the UBN optical network with BER=10⁻³.

Blocked Demands	[1-3], [1-4], [1-5], [1-7], [1-8], [1-9], [1-10], [1-11], [1-12], [1-13], [1-14], [1-15], [1-16], [1-17], [1-18], [1-19], [1-20], [1-21], [1-22], [1-23], [1-24], [2-5], [2-7], [2-8], [2-9], [2-10], [2-11], [2-12], [2-13], [2-14], [2-15], [2-16], [2-17], [2-18], [2-19], [2-20], [2-21], [2-22], [2-23], [2-24], [3-6], [3-8], [3-9], [3-10], [3-11], [3-12], [3-13], [3-14], [3-15], [3-16], [3-17], [3-18], [3-19], [3-20], [3-21], [3-22], [3-23], [3-24], [4-6], [4-8], [4-9], [4-10], [4-11], [4-12], [4-13], [4-14], [4-15], [4-16], [4-17], [4-18], [4-19], [4-20], [4-21], [4-22], [4-23], [4-24], [5-6], [5-7], [5-9], [5-10], [5-11], [5-12], [5-13], [5-14], [5-15], [5-16], [5-17], [5-18], [5-19], [5-20], [5-21], [5-22], [5-23], [5-24], [6-8], [6-10], [6-11], [6-12], [6-13], [6-14], [6-15], [6-16], [6-17], [6-18], [6-19], [6-20], [6-21], [6-22], [6-23], [6-24], [7-10], [7-11], [7-12], [7-13], [7-14], [7-15], [7-16], [7-17], [7-18], [7-19], [7-20], [7-21], [7-22], [7-23], [7-24], [8-9], [8-11], [8-12], [8-13], [8-14], [8-15], [8-16], [8-17], [8-18], [8-19], [8-20], [8-21], [8-22], [8-23], [8-24], [9-11], [9-13], [9-14], [9-15], [9-16], [9-17], [9-18], [9-19], [9-20], [9-21], [9-22], [9-23], [9-24], [10-11], [10-12], [10-15], [10-16], [10-17], [10-18], [10-19], [10-20], [10-21], [10-22], [10-23], [10-24], [11-13], [11-14], [11-16], [11-17], [11-18], [11-19], [11-20], [11-21], [11-22], [11-23], [11-24], [12-14], [12-15], [12-17], [12-18], [12-19], [12-20], [12-21], [12-22], [12-23], [12-24], [13-15], [13-16], [13-18], [13-19], [13-20], [13-21], [13-22], [13-23], [13-24], [14-15], [14-16], [14-17], [14-19], [14-20], [14-21], [14-22], [14-23], [14-24], [15-17], [15-18], [15-19], [15-21], [15-22], [15-23], [15-24], [16-18], [16-19], [16-20], [16-23], [16-24], [17-19], [17-20], [17-24], [18-19], [18-20], [18-21], [18-22], [18-23], [19-21], [19-22], [19-23], [19-24], [20-23], [20-24], [21-24], [22-24].
-----------------	---

Table C.16. Blocked demands in the RMSA solution for the UBN optical network with BER=10⁻³.

Appendix C Complementary material used in Chapter 4

Demand d	Path	OSNR [dB]	Modulation Format M	Frequency slots	Demand d	Path	OSNR [dB]	Modulation Format M	Frequency slots
1-2	{1,5,30,2}	14.8	16-QAM	1,2,3	{9,20}	{9,20}	17.4	16-QAM	13,14,15
1-3	{1,5,30,2,19,18,3}	11.0	QPSK	4,5,6,7	{9,21}	{9,20,13,25,24,21}	10.3	QPSK	28,29,30,31
1-4	{1,5,30,16,11,4}	9.9	QPSK	8,9,10,11	{9,22}	{9,20,14,22}	11.0	QPSK	16,17,18,19
1-5	{1,5}	19.4	64-QAM	12,13	{9,23}	{9,23}	15.2	16-QAM	13,14,15
1-6	{1,5,30,16,11,4,6}	8.9	QPSK	14,15,16,17	{9,24}	{9,20,13,25,24}	10.7	QPSK	36,37,38,39
1-7	{1,10,7}	10.6	QPSK	1,2,3,4	{9,25}	{9,20,13,25}	10.8	QPSK	40,41,42,43
1-8	{1,10,23,9,8}	7.4	QPSK	5,6,7,8	{9,26}	{9,8,12,26}	9.0	QPSK	85,86,87,88
1-9	{1,10,23,9}	8.9	QPSK	9,10,11,12	{9,27}	{9,20,13,25,24,21,27}	8.4	QPSK	54,55,56,57
1-10	{1,10}	13.4	16-QAM	13,14,15	{9,28}	{9,23,10,17,29,28}	8.8	QPSK	135,136,137,138
1-11	{1,5,30,16,11}	10.5	QPSK	18,19,20,21	{9,29}	{9,23,10,17,29}	9.3	QPSK	139,140,141,142
1-12	{1,10,7,12}	8.8	QPSK	16,17,18,19	{9,30}	{9,23,10,1,5,30}	7.6	QPSK	155,156,157,158
1-13	{1,10,23,9,20,13}	7.2	QPSK	20,21,22,23	{10,11}	{10,7,12,26,11}	9.5	QPSK	147,148,149,150
1-14	{1,10,23,9,20,14}	7.6	QPSK	24,25,26,27	{10,12}	{10,7,12}	13.5	16-QAM	37,38,39
1-15	{1,5,15}	11.0	QPSK	22,23,24,25	{10,13}	{10,23,9,20,13}	9.1	QPSK	147,148,149,150
1-16	{1,5,30,16}	13.9	16-QAM	26,27,28	{10,14}	{10,23,9,20,14}	9.7	QPSK	151,152,153,154
1-17	{1,10,17}	10.0	QPSK	28,29,30,31	{10,15}	{10,17,29,28,15}	10.7	QPSK	16,17,18,19
1-18	{1,5,30,2,19,18}	13.9	16-QAM	29,30,31	{10,16}	{10,1,5,30,16}	9.0	QPSK	227,228,229,230
1-19	{1,5,30,2,19}	14.3	16-QAM	32,33,34	{10,17}	{10,17}	16.7	16-QAM	1,2,3
1-20	{1,10,23,9,20}	8.1	QPSK	32,33,34,35	{10,18}	{10,1,5,30,2,19,18}	9.0	QPSK	231,232,233,234
1-23	{1,10,23}	10.8	QPSK	36,37,38,39	{10,19}	{10,1,5,30,2,19}	9.2	QPSK	235,236,237,238
1-26	{1,5,30,16,11,26}	9.5	QPSK	35,36,37,38	{10,20}	{10,23,9,20}	10.5	QPSK	159,160,161,162
1-28	{1,5,15,28}	10.3	QPSK	39,40,41,42	{10,21}	{10,23,9,20,13,25,24,21}	8.1	QPSK	163,164,165,166
1-29	{1,5,15,28,29}	9.7	QPSK	43,44,45,46	{10,22}	{10,23,9,20,14,22}	8.5	QPSK	167,168,169,170
1-30	{1,5,30}	15.0	16-QAM	47,48,49	{10,23}	{10,23}	19.9	64-QAM	28,29
1-24	{2,19,18,3}	16.8	16-QAM	1,2,3	{10,24}	{10,23,9,20,13,25,24}	8.3	QPSK	171,172,173,174
2-4	{2,30,16,11,4}	13.9	16-QAM	22,23,24	{10,25}	{10,23,9,20,13,25}	8.4	QPSK	175,176,177,178
2-5	{2,30,5}	16.8	16-QAM	39,40,41	{10,26}	{10,7,12,26}	10.5	QPSK	151,152,153,154
2-6	{2,30,16,11,4,6}	10.6	QPSK	42,43,44,45	{10,28}	{10,17,29,28}	11.5	QPSK	37,38,39,40
2-7	{2,30,5,1,10,7}	8.7	QPSK	50,51,52,53	{10,29}	{10,17,29}	14.1	16-QAM	10,11,12
2-8	{2,30,16,11,26,12,8}	8.4	QPSK	46,47,48,49	{10,30}	{10,1,5,30}	9.5	QPSK	104,105,106,107
2-9	{2,30,5,1,10,23,9}	7.5	QPSK	54,55,56,57	{11,12}	{11,26,12}	15.1	16-QAM	5,6,7
2-10	{2,30,5,1,10}	9.4	QPSK	58,59,60,61	{11,14}	{11,26,12,8,22,14}	7.8	QPSK	155,156,157,158
2-11	{2,30,16,11}	15.0	16-QAM	62,63,64	{11,15}	{11,16,30,5,15}	8.7	QPSK	239,240,241,242
2-12	{2,30,16,11,26,12}	10.3	QPSK	65,66,67,68	{11,16}	{11,16}	16.8	16-QAM	1,2,3
2-15	{2,30,5,15}	10.3	QPSK	69,70,71,72	{11,17}	{11,26,12,7,10,17}	8.4	QPSK	159,160,161,162
2-16	{2,30,16}	19.7	64-QAM	12,13	{11,18}	{11,16,30,2,19,18}	14.0	16-QAM	243,244,245
2-17	{2,30,5,15,28,29,17}	8.4	QPSK	73,74,75,76	{11,19}	{11,16,30,2,19}	14.5	16-QAM	246,247,248
2-18	{2,19,18}	21.4	64-QAM	8,9	{11,20}	{11,26,12,8,9,20}	7.6	QPSK	186,187,188,189
2-19	{2,19}	24.4	64-QAM	10,11	{11,21}	{11,26,12,8,22,21}	7.5	QPSK	163,164,165,166
2-22	{2,30,16,11,26,12,8,22}	7.5	QPSK	77,78,79,80	{11,22}	{11,26,12,8,22}	8.8	QPSK	167,168,169,170
2-23	{2,30,5,1,10,23}	8.8	QPSK	81,82,83,84	{11,23}	{11,26,12,7,10,23}	8.9	QPSK	190,191,192,193
2-26	{2,30,16,11,26}	11.6	QPSK	85,86,87,88	{11,24}	{11,26,12,8,22,21,24}	7.4	QPSK	178,179,180,181
2-28	{2,30,5,15,28}	9.7	QPSK	89,90,91,92	{11,25}	{11,26,12,8,22,21,24,25}	7.3	QPSK	199,200,201,202
2-29	{2,30,5,15,28,29}	9.2	QPSK	93,94,95,96	{11,26}	{11,26}	18.2	16-QAM	22,23,24
2-30	{2,30}	27.7	64-QAM	8,9	{11,28}	{11,16,30,5,15,28}	8.3	QPSK	249,250,251,252
3-4	{3,6,4}	10.8	QPSK	1,2,3,4	{11,29}	{11,16,30,5,15,28,29}	7.9	QPSK	253,254,255,256
3-5	{3,18,19,2,30,5}	13.8	16-QAM	97,98,99	{11,30}	{11,16,30}	15.2	16-QAM	4,5,6
3-6	{3,6}	14.2	16-QAM	5,6,7	{12,13}	{12,8,22,21,24,25,13}	7.9	QPSK	54,55,56,57
3-7	{3,18,19,2,30,5,1,10,7}	7.8	QPSK	100,101,102,103	{12,14}	{12,8,22,14}	9.2	QPSK	37,38,39,40
3-8	{3,18,19,2,30,16,11,26,12,8}	7.6	QPSK	104,105,106,107	{12,15}	{12,7,10,17,29,28,15}	8.2	QPSK	66,67,68,69
3-10	{3,18,19,2,30,5,1,10}	8.3	QPSK	108,109,110,111	{12,16}	{12,26,11,16}	11.1	QPSK	227,228,229,230
3-11	{3,18,19,2,30,16,11}	11.1	QPSK	112,113,114,115	{12,17}	{12,7,10,17}	10.1	QPSK	74,75,76,77
3-12	{3,18,19,2,30,16,11,26,12}	9.1	QPSK	116,117,118,119	{12,18}	{12,26,11,16,30,2,19,18}	9.8	QPSK	257,258,259,260
3-15	{3,18,19,2,30,5,15}	9.1	QPSK	120,121,122,123	{12,19}	{12,26,11,16,30,2,19}	10.1	QPSK	261,262,263,264
3-16	{3,18,19,2,30,16}	15.0	16-QAM	124,125,126	{12,20}	{12,8,9,20}	8.9	QPSK	65,66,67,68
3-17	{3,18,19,2,30,5,15,28,29,17}	7.5	QPSK	127,128,129,130	{12,21}	{12,8,22,21}	8.9	QPSK	41,42,43,44
3-18	{3,18}	19.2	64-QAM	8,9	{12,22}	{12,8,22}	10.6	QPSK	89,90,91,92
3-19	{3,18,19}	17.7	16-QAM	10,11,12	{12,23}	{12,7,10,23}	10.8	QPSK	179,180,181,182
3-23	{3,18,19,2,30,5,1,10,23}	7.9	QPSK	131,132,133,134	{12,24}	{12,8,22,21,24}	8.6	QPSK	93,94,95,96
3-26	{3,18,19,2,30,16,11,26}	10.0	QPSK	135,136,137,138	{12,25}	{12,8,22,21,24,25}	8.5	QPSK	112,113,114,115
3-28	{3,18,19,2,30,5,15,28}	8.6	QPSK	139,140,141,142	{12,26}	{12,26}	18.1	16-QAM	22,23,24
3-29	{3,18,19,2,30,5,15,28,29}	8.2	QPSK	143,144,145,146	{12,27}	{12,8,22,27}	8.1	QPSK	116,117,118,119
3-30	{3,18,19,2,30}	16.4	16-QAM	14,15,16	{12,28}	{12,7,10,17,29,28}	8.7	QPSK	78,79,80,81
4-5	{4,11,16,30,5}	10.7	QPSK	147,148,149,150	{12,29}	{12,7,10,17,29}	9.1	QPSK	82,83,84,85
4-6	{4,6}	17.4	16-QAM	5,6,7	{12,30}	{12,26,11,16,30}	10.5	QPSK	231,232,233,234
4-7	{4,11,26,12,7}	9.8	QPSK	1,2,3,4	{13,14}	{13,20,14}	14.5	16-QAM	7,8,9
4-8	{4,11,26,12,8}	9.6	QPSK	18,19,20,21	{13,17}	{13,20,9,23,10,17}	8.1	QPSK	194,195,196,197
4-9	{4,11,26,12,8,9}	7.9	QPSK	25,26,27,28	{13,20}	{13,20}	16.4	16-QAM	4,5,6
4-10	{4,11,26,12,7,10}	9.0	QPSK	29,30,31,32	{13,21}	{13,25,24,21}	16.5	16-QAM	5,6,7
4-11	{4,11}	20.7	64-QAM	5,6	{13,22}	{13,25,24,21,22}	11.2	QPSK	24,25,26,27
4-12	{4,11,26,12}	14.0	16-QAM	39,40,41	{13,23}	{13,20,9,23}	9.8	QPSK	78,79,80,81
4-14	{4,11,26,12,8,22,14}	7.4	QPSK	50,51,52,53	{13,24}	{13,25,24}	17.6	16-QAM	8,9,10
4-15	{4,11,16,30,5,15}	8.3	QPSK	151,152,153,154	{13,25}	{13,25}	18.0	16-QAM	11,12,13
4-16	{4,11,16}	15.2	16-QAM	54,55,56	{13,26}	{13,25,24,21,22,8,12,26}	7.3	QPSK	132,133,134,135
4-17	{4,11,26,12,7,10,17}	8.0	QPSK	57,58,59,60	{13,27}	{13,25,24,21,27}	10.2	QPSK	32,33,34,35
4-18	{4,11,16,30,2,19,18}	11.5	QPSK	155,156,157,158	{13,28}	{13,20,9,23,10,17,29,28}	7.2	QPSK	198,199,200,201
4-19	{4,11,16,30,2,19}	13.5	16-QAM	159,160,161	{13,29}	{13,20,9,23,10,17,29}	7.5	QPSK	202,203,204,205
4-20	{4,11,26,12,8,9,20}	7.3	QPSK	61,62,63,64	{14,15}	{14,20,9,23,10,17,29,28,15}	7.2	QPSK	206,207,208,209
4-21	{4,11,26,12,8,22,21}	7.2	QPSK	69,70,71,72	{14,17}	{14,20,9,23,10,17}	8.6	QPSK	210,211,212,213
4-22	{4,11,26,12,8,22}	8.4	QPSK	73,74,75,76	{14,20}	{14,20}	19.1	64-QAM	1,2
4-23	{4,11,26,12,7,10,23}	8.5	QPSK	89,90,91,92	{14,21}	{14,20,13,25,24,21}	11.1	QPSK	28,29,30,31
4-26	{4,11,26}	16.1	16-QAM	81,82,83	{14,22}	{14,22}	16.3	16-QAM	1,2,3
4-28	{4,11,16,30,5,15,28}	7.9	QPSK	162,163,164,165	{14,23}	{14,20,9,23}	10.5	QPSK	89,90,91,92
4-29	{4,11,16,30,5,15,28,29}	7.6	QPSK	166,167,168,169	{14,24}	{14,20,13,25,24}	11.1	QPSK	48,49,50,51
4-30	{4,11,16,30}	14.1	16-QAM	93,94,95	{14,25}	{14,22,21,24,25}	11.3	QPSK	58,59,60,61

Appendix C Complementary material used in Chapter 4

5-6	{5,30,16,11,4,6}	9.5	QPSK	170,171,172,173	14-26	{14,22,8,12,26}	8.4	QPSK	194,195,196,197
5-7	{5,1,10,7}	9.8	QPSK	62,63,64,65	14-27	{14,22,27}	9.9	QPSK	9,10,11,12
5-8	{5,30,16,11,26,12,8}	7.7	QPSK	174,175,176,177	14-28	{14,20,9,23,10,17,29,28}	7.5	QPSK	214,215,216,217
5-9	{5,1,10,23,9}	8.3	QPSK	66,67,68,69	14-29	{14,20,9,23,10,17,29}	7.9	QPSK	227,228,229,230
5-10	{5,1,10}	10.7	QPSK	70,71,72,73	15-16	{15,5,30,16}	9.9	QPSK	265,266,267,268
5-11	{5,30,16,11}	11.4	QPSK	178,179,180,181	15-17	{15,28,29,17}	14.3	16-QAM	1,2,3
5-12	{5,30,16,11,26,12}	9.3	QPSK	182,183,184,185	15-18	{15,5,30,2,19,18}	9.8	QPSK	269,270,271,272
5-14	{5,1,10,23,9,20,14}	7.2	QPSK	74,75,76,77	15-19	{15,5,30,2,19}	10.1	QPSK	273,274,275,276
5-15	{5,15}	13.8	16-QAM	1,2,3	15-20	{15,28,29,17,10,23,9,20}	7.6	QPSK	231,232,233,234
5-16	{5,30,16}	15.5	16-QAM	186,187,188	15-23	{15,28,29,17,10,23}	9.9	QPSK	183,184,185,186
5-17	{5,15,28,29,17}	9.4	QPSK	4,5,6,7	15-26	{15,5,30,16,11,26}	8.1	QPSK	277,278,279,280
5-18	{5,30,2,19,18}	15.4	16-QAM	189,190,191	15-28	{15,28}	20.1	64-QAM	24,25
5-19	{5,30,2,19}	16.0	16-QAM	192,193,194	15-29	{15,28,29}	17.0	16-QAM	28,29,30
5-20	{5,1,10,23,9,20}	7.6	QPSK	85,86,87,88	15-30	{15,5,30}	10.5	QPSK	62,63,64,65
5-23	{5,1,10,23}	9.9	QPSK	93,94,95,96	16-17	{16,30,5,15,28,29,17}	8.1	QPSK	281,282,283,284
5-26	{5,30,16,11,26}	10.3	QPSK	195,196,197,198	16-18	{16,30,2,19,18}	17.3	16-QAM	285,286,287
5-28	{5,15,28}	11.2	QPSK	8,9,10,11	16-19	{16,30,2,19}	18.3	16-QAM	288,289,290
5-29	{5,15,28,29}	10.4	QPSK	12,13,14,15	16-22	{16,11,26,12,8,22}	7.9	QPSK	235,236,237,238
5-30	{5,30}	17.2	16-QAM	22,23,24	16-23	{16,30,5,1,10,23}	8.5	QPSK	291,292,293,294
6-7	{6,4,11,26,12,7}	8.8	QPSK	96,97,98,99	16-26	{16,11,26}	14.4	16-QAM	265,266,267
6-8	{6,4,11,26,12,8}	8.6	QPSK	100,101,102,103	16-28	{16,30,5,15,28}	9.3	QPSK	295,296,297,298
6-9	{6,4,11,26,12,8,9}	7.3	QPSK	108,109,110,111	16-29	{16,30,5,15,28,29}	8.8	QPSK	299,300,301,302
6-10	{6,4,11,26,12,7,10}	8.2	QPSK	112,113,114,115	16-30	{16,30}	20.5	64-QAM	1,2
6-11	{6,4,11}	15.6	16-QAM	33,34,35	17-18	{17,29,28,15,5,30,2,19,18}	8.1	QPSK	303,304,305,306
6-12	{6,4,11,26,12}	10.7	QPSK	120,121,122,123	17-19	{17,29,28,15,5,30,2,19}	8.2	QPSK	307,308,309,310
6-15	{6,4,11,16,30,5,15}	7.6	QPSK	199,200,201,202	17-20	{17,10,23,9,20}	9.2	QPSK	235,236,237,238
6-16	{6,4,11,16}	11.5	QPSK	124,125,126,127	17-21	{17,10,23,9,20,13,25,24,21}	7.3	QPSK	239,240,241,242
6-17	{6,4,11,26,12,7,10,17}	7.4	QPSK	128,129,130,131	17-22	{17,10,23,9,20,14,22}	7.6	QPSK	243,244,245,246
6-18	{6,3,18}	11.1	QPSK	17,18,19,20	17-23	{17,10,23}	14.8	16-QAM	101,102,103
6-19	{6,3,18,19}	10.8	QPSK	21,22,23,24	17-24	{17,10,23,9,20,13,25,24}	7.5	QPSK	247,248,249,250
6-22	{6,4,11,26,12,8,22}	7.6	QPSK	139,140,141,142	17-25	{17,10,23,9,20,13,25}	7.5	QPSK	251,252,253,254
6-23	{6,4,11,26,12,7,10,23}	7.7	QPSK	143,144,145,146	17-26	{17,10,7,12,26}	9.2	QPSK	265,266,267,268
6-26	{6,4,11,26}	13.7	16-QAM	132,133,134	17-28	{17,29,28}	15.7	16-QAM	47,48,49
6-30	{6,4,11,16,30}	10.8	QPSK	189,190,191,192	17-29	{17,29}	17.7	16-QAM	13,14,15
7-8	{7,12,8}	10.1	QPSK	5,6,7,8	17-30	{17,29,28,15,5,30}	8.5	QPSK	116,117,118,119
7-9	{7,10,23,9}	10.9	QPSK	40,41,42,43	18-19	{18,19}	24.4	64-QAM	17,18
7-10	{7,10}	19.2	64-QAM	5,6	18-22	{18,19,2,30,16,11,26,12,8,22}	7.2	QPSK	311,312,313,314
7-11	{7,12,26,11}	10.3	QPSK	9,10,11,12	18-23	{18,19,2,30,5,1,10,23}	8.4	QPSK	315,316,317,318
7-12	{7,12}	15.0	16-QAM	13,14,15	18-26	{18,19,2,30,16,11,26}	10.9	QPSK	319,320,321,322
7-13	{7,10,23,9,20,13}	8.5	QPSK	44,45,46,47	18-28	{18,19,2,30,5,15,28}	9.3	QPSK	323,324,325,326
7-14	{7,10,23,9,20,14}	9.0	QPSK	70,71,72,73	18-29	{18,19,2,30,5,15,28,29}	8.8	QPSK	327,328,329,330
7-15	{7,10,17,29,28,15}	9.8	QPSK	20,21,22,23	18-30	{18,19,2,30}	20.5	64-QAM	19,2
7-16	{7,12,26,11,16}	9.1	QPSK	203,204,205,206	19-22	{19,2,30,16,11,26,12,8,22}	7.3	QPSK	331,332,333,334
7-17	{7,10,17}	14.6	16-QAM	7,8,9	19-23	{19,2,30,5,1,10,23}	8.6	QPSK	335,336,337,338
7-18	{7,10,1,5,30,2,19,18}	8.4	QPSK	203,204,205,206	19-26	{19,2,30,16,11,26}	11.3	QPSK	339,340,341,342
7-19	{7,10,1,5,30,2,19}	8.5	QPSK	207,208,209,210	19-28	{19,2,30,5,15,28}	9.5	QPSK	343,344,345,346
7-20	{7,10,23,9,20}	9.7	QPSK	104,105,106,107	19-29	{19,2,30,5,15,28,29}	9.0	QPSK	347,348,349,350
7-21	{7,10,23,9,20,13,25,24,21}	7.6	QPSK	108,109,110,111	19-30	{19,2,30}	22.7	64-QAM	17,18
7-22	{7,12,8,22}	8.8	QPSK	33,34,35,36	20-21	{20,13,25,24,21}	13.5	16-QAM	62,63,64
7-23	{7,10,23}	16.2	16-QAM	13,14,15	20-22	{20,14,22}	14.4	16-QAM	13,14,15
7-24	{7,10,23,9,20,13,25,24}	7.8	QPSK	116,117,118,119	20-23	{20,9,23}	11.4	QPSK	93,94,95,96
7-25	{7,10,23,9,20,13,25}	7.9	QPSK	120,121,122,123	20-24	{20,13,25,24}	14.0	16-QAM	14,15,16
7-26	{7,12,26}	11.6	QPSK	42,43,44,45	20-25	{20,13,25}	14.2	16-QAM	17,18,19
7-28	{7,10,17,29,28}	10.5	QPSK	24,25,26,27	20-26	{20,9,8,12,26}	8.2	QPSK	269,270,271,272
7-29	{7,10,17,29}	11.2	QPSK	33,34,35,36	20-27	{20,13,25,24,21,27}	9.2	QPSK	20,21,22,23
7-30	{7,10,1,5,30}	8.8	QPSK	135,136,137,138	20-28	{20,9,23,10,17,29,28}	8.0	QPSK	257,258,259,260
8-9	{8,9}	14.6	16-QAM	1,2,3	20-29	{20,9,23,10,17,29}	8.4	QPSK	261,262,263,264
8-10	{8,9,23,10}	9.4	QPSK	16,17,18,19	21-22	{21,22}	15.3	16-QAM	5,6,7
8-11	{8,12,26,11}	10.1	QPSK	13,14,15,16	21-23	{21,24,25,13,20,9,23}	8.6	QPSK	128,129,130,131
8-12	{8,12}	14.6	16-QAM	1,2,3	21-24	{21,24}	23.5	64-QAM	8,9
8-13	{8,22,21,24,25,13}	9.5	QPSK	1,2,3,4	21-25	{21,24,25}	22.2	64-QAM	11,12
8-14	{8,22,14}	11.5	QPSK	5,6,7,8	21-26	{21,22,8,12,26}	8.1	QPSK	239,240,241,242
8-16	{8,12,26,11,16}	8.9	QPSK	207,208,209,210	21-27	{21,27}	13.7	16-QAM	1,2,3
8-17	{8,9,23,10,17}	8.4	QPSK	48,49,50,51	22-23	{22,14,20,9,23}	9.0	QPSK	143,144,145,146
8-18	{8,12,26,11,16,30,2,19,18}	8.1	QPSK	211,212,213,214	22-24	{22,21,24}	14.6	16-QAM	13,14,15
8-19	{8,12,26,11,16,30,2,19}	8.3	QPSK	215,216,217,218	22-25	{22,21,24,25}	14.4	16-QAM	45,46,47
8-20	{8,9,20}	11.1	QPSK	9,10,11,12	22-26	{22,8,12,26}	9.6	QPSK	243,244,245,246
8-21	{8,22,21}	11.0	QPSK	9,10,11,12	22-27	{22,27}	13.5	16-QAM	1,2,3
8-22	{8,22}	16.2	16-QAM	13,14,15	22-30	{22,8,12,26,11,16,30}	7.5	QPSK	273,274,275,276
8-23	{8,9,23}	10.1	QPSK	36,37,38,39	23-24	{23,9,20,13,25,24}	8.8	QPSK	179,180,181,182
8-24	{8,22,21,24}	10.6	QPSK	16,17,18,19	23-25	{23,9,20,13,25}	8.9	QPSK	190,191,192,193
8-25	{8,22,21,24,25}	10.5	QPSK	20,21,22,23	23-26	{23,10,7,12,26}	9.8	QPSK	277,278,279,280
8-26	{8,12,26}	11.3	QPSK	81,82,83,84	23-28	{23,10,17,29,28}	10.6	QPSK	269,270,271,272
8-27	{8,22,27}	9.9	QPSK	24,25,26,27	23-29	{23,10,17,29}	11.4	QPSK	273,274,275,276
8-28	{8,9,23,10,17,29,28}	7.4	QPSK	97,98,99,100	23-30	{23,10,1,5,30}	8.9	QPSK	285,286,287,288
8-29	{8,9,23,10,17,29}	7.7	QPSK	112,113,114,115	24-25	{24,25}	27.9	64-QAM	17,18
8-30	{8,12,26,11,16,30}	8.5	QPSK	219,220,221,222	24-26	{24,21,22,8,12,26}	7.9	QPSK	247,248,249,250
9-10	{9,23,10}	13.8	16-QAM	1,2,3	24-27	{24,21,27}	11.5	QPSK	36,37,38,39
9-11	{9,8,12,26,11}	8.3	QPSK	124,125,126,127	25-26	{25,24,21,22,8,12,26}	7.9	QPSK	251,252,253,254

Appendix C Complementary material used in Chapter 4

[9-12]	{9,8,12}	9.9	QPSK	29,30,31,32	[25-27]	{25,24,21,27}	11.3	QPSK	40,41,42,43
[9-13]	{9,20,13}	13.9	16-QAM	1,2,3	[26-27]	{26,12,8,22,27}	7.5	QPSK	281,282,283,284
[9-14]	{9,20,14}	15.1	16-QAM	4,5,6	[26-28]	{26,12,7,10,17,29,28}	8.0	QPSK	285,286,287,288
[9-15]	{9,23,10,17,29,28,15}	8.3	QPSK	61,62,63,64	[26-29]	{26,12,7,10,17,29}	8.4	QPSK	289,290,291,292
[9-16]	{9,8,12,26,11,16}	7.5	QPSK	223,224,225,226	[26-30]	{26,11,16,30}	13.5	16-QAM	269,270,271
[9-17]	{9,23,10,17}	10.3	QPSK	124,125,126,127	[28-29]	{28,29}	20.2	64-QAM	8,9
[9-18]	{9,23,10,1,5,30,2,19,18}	7.2	QPSK	219,220,221,222	[28-30]	{28,15,5,30}	9.8	QPSK	77,78,79,80
[9-19]	{9,23,10,1,5,30,2,19}	7.4	QPSK	223,224,225,226	[29-30]	{29,28,15,5,30}	9.3	QPSK	85,86,87,88

Table C.17. RMSA solution for the CONUS 30 optical network with $BER=4 \times 10^{-2}$.

Blocked Demands	[1-21], [1-22], [1-24], [1-25], [1-27], [2-13], [2-14], [2-20], [2-21], [2-24], [2-25], [2-27], [3-9], [3-13], [3-14], [3-20], [3-21], [3-22], [3-24], [3-25], [3-27], [4-13], [4-24], [4-25], [4-27], [5-13], [5-21], [5-22], [5-24], [5-25], [5-27], [6-13], [6-14], [6-20], [6-21], [6-24], [6-25], [6-27], [6-28], [6-29], [7-27], [8-15], [10-27], [11-13], [11-27], [13-15], [13-16], [13-18], [13-19], [13-30], [14-16], [14-18], [14-19], [14-30], [15-21], [15-22], [15-24], [15-25], [15-27], [16-20], [16-21], [16-24], [16-25], [16-27], [17-27], [18-20], [18-21], [18-24], [18-25], [18-27], [19-20], [19-21], [19-24], [19-25], [19-27], [20-30], [21-28], [21-29], [21-30], [22-28], [22-29], [23-27], [24-28], [24-29], [24-30], [25-28], [25-29], [25-30], [27-28], [27-29], [27-30]
-----------------	--

Table C.18. Blocked demands in the RMSA solution for the CONUS 30 optical network with $BER=4 \times 10^{-2}$.

Appendix C Complementary material used in Chapter 4

Demand d	Path	OSNR [dB]	Modulation Format M	Frequency slots	Demand d	Path	OSNR [dB]	Modulation Format M	Frequency slots
1-2	{1,5,30,2}	13.2	QPSK	1,2,3,4	8-27	{8,22,27}	9.9	QPSK	24,25,26,27
1-3	{1,5,30,2,19,18,3}	11.0	QPSK	5,6,7,8	9-10	{9,23,10}	12.1	QPSK	1,2,3,4
1-4	{1,5,30,16,11,4}	9.9	QPSK	9,10,11,12	9-12	{9,8,12}	9.9	QPSK	13,14,15,16
1-5	{1,5}	19.1	16-QAM	13,14,15	9-13	{9,20,13}	12.2	QPSK	1,2,3,4
1-7	{1,10,7}	10.6	QPSK	1,2,3,4	9-14	{9,20,14}	13.5	QPSK	9,10,11,12
1-10	{1,10}	11.7	QPSK	5,6,7,8	9-17	{9,23,10,17}	10.3	QPSK	36,37,38,39
1-11	{1,5,30,16,11}	10.5	QPSK	16,17,18,19	9-20	{9,20}	17.4	16-QAM	13,14,15
1-15	{1,5,15}	11.0	QPSK	20,21,22,23	9-21	{9,20,13,25,24,21}	10.3	QPSK	25,26,27,28
1-16	{1,5,30,16}	12.3	QPSK	24,25,26,27	9-22	{9,20,14,22}	11.0	QPSK	16,17,18,19
1-17	{1,10,17}	10.0	QPSK	9,10,11,12	9-23	{9,23}	13.4	QPSK	13,14,15,16
1-18	{1,5,30,2,19,18}	12.3	QPSK	28,29,30,31	9-24	{9,20,13,25,24}	10.7	QPSK	29,30,31,32
1-19	{1,5,30,2,19}	12.7	QPSK	32,33,34,35	9-25	{9,20,13,25}	10.8	QPSK	33,34,35,36
1-23	{1,10,23}	10.8	QPSK	13,14,15,16	10-11	{10,7,12,26,11}	9.5	QPSK	40,41,42,43
1-26	{1,5,30,16,11,26}	9.5	QPSK	36,37,38,39	10-12	{10,7,12}	11.8	QPSK	36,37,38,39
1-28	{1,5,15,28}	10.3	QPSK	40,41,42,43	10-14	{10,23,9,20,14}	9.7	QPSK	40,41,42,43
1-29	{1,5,15,28,29}	9.7	QPSK	44,45,46,47	10-15	{10,17,29,28,15}	10.7	QPSK	1,2,3,4
1-30	{1,5,30}	13.4	QPSK	48,49,50,51	10-17	{10,17}	16.7	16-QAM	5,6,7
1-24	{2,19,18,3}	16.8	16-QAM	1,2,3	10-20	{10,23,9,20}	10.5	QPSK	44,45,46,47
2-4	{2,30,16,11,4}	12.2	QPSK	20,21,22,23	10-23	{10,23}	19.5	16-QAM	9,10,11
2-5	{2,30,5}	16.8	16-QAM	13,14,15	10-26	{10,7,12,26}	10.5	QPSK	56,57,58,59
2-6	{2,30,16,11,4,6}	10.6	QPSK	40,41,42,43	10-28	{10,17,29,28}	11.5	QPSK	21,22,23,24
2-11	{2,30,16,11}	13.3	QPSK	44,45,46,47	10-29	{10,17,29}	12.5	QPSK	40,41,42,43
2-12	{2,30,16,11,26,12}	10.3	QPSK	48,49,50,51	11-12	{11,26,12}	13.4	QPSK	9,10,11,12
2-15	{2,30,5,15}	10.3	QPSK	52,53,54,55	11-16	{11,16}	16.8	16-QAM	1,2,3
2-16	{2,30,16}	19.6	16-QAM	56,57,58	11-18	{11,16,30,2,19,18}	12.4	QPSK	115,116,117,118
2-18	{2,19,18}	21.1	16-QAM	9,10,11	11-19	{11,16,30,2,19}	12.8	QPSK	119,120,121,122
2-19	{2,19}	24.4	64-QAM	12,13	11-26	{11,26}	18.2	16-QAM	13,14,15
2-26	{2,30,16,11,26}	11.6	QPSK	59,60,61,62	11-30	{11,16,30}	13.6	QPSK	4,5,6,7
2-28	{2,30,5,15,28}	9.7	QPSK	63,64,65,66	12-16	{12,26,11,16}	11.1	QPSK	75,76,77,78
2-30	{2,30}	27.7	64-QAM	9,1	12-17	{12,7,10,17}	10.1	QPSK	44,45,46,47
3-4	{3,6,4}	10.8	QPSK	1,2,3,4	12-18	{12,26,11,16,30,2,19,18}	9.8	QPSK	123,124,125,126
3-5	{3,18,19,2,30,5}	12.1	QPSK	67,68,69,70	12-19	{12,26,11,16,30,2,19}	10.1	QPSK	127,128,129,130
3-6	{3,6}	12.4	QPSK	5,6,7,8	12-22	{12,8,22}	10.6	QPSK	39,40,41,42
3-11	{3,18,19,2,30,16,11}	11.1	QPSK	71,72,73,74	12-23	{12,7,10,23}	10.8	QPSK	48,49,50,51
3-16	{3,18,19,2,30,16}	13.3	QPSK	75,76,77,78	12-26	{12,26}	18.1	16-QAM	13,14,15
3-18	{3,18}	18.8	16-QAM	9,10,11	12-30	{12,26,11,16,30}	10.5	QPSK	103,104,105,106
3-19	{3,18,19}	17.7	16-QAM	12,13,14	13-14	{13,20,14}	12.9	QPSK	5,6,7,8
3-26	{3,18,19,2,30,16,11,26}	10.0	QPSK	79,80,81,82	13-20	{13,20}	16.4	16-QAM	9,10,11
3-30	{3,18,19,2,30}	16.4	16-QAM	16,17,18	13-21	{13,25,24,21}	16.5	16-QAM	5,6,7
4-5	{4,11,16,30,5}	10.7	QPSK	83,84,85,86	13-22	{13,25,24,21,22}	11.2	QPSK	37,38,39,40
4-6	{4,6}	17.4	16-QAM	5,6,7	13-23	{13,20,9,23}	9.8	QPSK	48,49,50,51
4-7	{4,11,26,12,7}	9.8	QPSK	1,2,3,4	13-24	{13,25,24}	17.6	16-QAM	8,9,10
4-8	{4,11,26,12,8}	9.6	QPSK	5,6,7,8	13-25	{13,25}	18.0	16-QAM	11,12,13
4-11	{4,11}	20.4	16-QAM	13,14,15	13-27	{13,25,24,21,27}	10.2	QPSK	41,42,43,44
4-12	{4,11,26,12}	12.3	QPSK	16,17,18,19	14-20	{14,20}	19.0	16-QAM	1,2,3
4-16	{4,11,16}	13.5	QPSK	24,25,26,27	14-21	{14,20,13,25,24,21}	11.1	QPSK	24,25,26,27
4-18	{4,11,16,30,2,19,18}	11.5	QPSK	87,88,89,90	14-22	{14,22}	16.3	16-QAM	1,2,3
4-19	{4,11,16,30,2,19}	11.8	QPSK	91,92,93,94	14-23	{14,20,9,23}	10.5	QPSK	52,53,54,55
4-26	{4,11,26}	16.1	16-QAM	28,29,30	14-24	{14,20,13,25,24}	11.1	QPSK	56,57,58,59
4-30	{4,11,16,30}	12.4	QPSK	31,32,33,34	14-25	{14,22,21,24,25}	11.3	QPSK	20,21,22,23
5-7	{5,1,10,7}	9.8	QPSK	52,53,54,55	14-27	{14,22,27}	9.9	QPSK	9,10,11,12
5-10	{5,1,10}	10.7	QPSK	56,57,58,59	15-16	{15,5,30,16}	9.9	QPSK	131,132,133,134
5-11	{5,30,16,11}	11.4	QPSK	95,96,97,98	15-17	{15,28,29,17}	12.8	QPSK	17,18,19,20
5-15	{5,15}	12.1	QPSK	1,2,3,4	15-18	{15,5,30,2,19,18}	9.8	QPSK	135,136,137,138
5-16	{5,30,16}	13.9	QPSK	99,100,101,102	15-19	{15,5,30,2,19}	10.1	QPSK	139,140,141,142
5-18	{5,30,2,19,18}	13.8	QPSK	103,104,105,106	15-23	{15,28,29,17,10,23}	9.9	QPSK	52,53,54,55
5-19	{5,30,2,19}	14.4	QPSK	107,108,109,110	15-28	{15,28}	20.0	16-QAM	21,22,23
5-23	{5,1,10,23}	9.9	QPSK	60,61,62,63	15-29	{15,28,29}	17.0	16-QAM	25,26,27
5-26	{5,30,16,11,26}	10.3	QPSK	111,112,113,114	15-30	{15,5,30}	10.5	QPSK	56,57,58,59
5-28	{5,15,28}	11.2	QPSK	5,6,7,8	16-18	{16,30,2,19,18}	17.3	16-QAM	143,144,145
5-29	{5,15,28,29}	10.4	QPSK	9,10,11,12	16-19	{16,30,2,19}	18.3	16-QAM	146,147,148
5-30	{5,30}	17.2	16-QAM	20,21,22	1-26	{16,11,26}	12.7	QPSK	99,100,101,102
6-11	{6,4,11}	14.0	QPSK	35,36,37,38	16-30	{16,30}	20.4	16-QAM	1,2,3
6-12	{6,4,11,26,12}	10.7	QPSK	44,45,46,47	17-23	{17,10,23}	13.1	QPSK	56,57,58,59
6-16	{6,4,11,16}	11.5	QPSK	52,53,54,55	17-28	{17,29,28}	14.2	QPSK	5,6,7,8
6-18	{6,3,18}	11.1	QPSK	19,20,21,22	17-29	{17,29}	17.7	16-QAM	9,10,11
6-19	{6,3,18,19}	10.8	QPSK	23,24,25,26	18-19	{18,19}	24.4	64-QAM	19,2
6-26	{6,4,11,26}	12.0	QPSK	63,64,65,66	18-26	{18,19,2,30,16,11,26}	10.9	QPSK	149,150,151,152
6-30	{6,4,11,16,30}	10.8	QPSK	67,68,69,70	18-30	{18,19,2,30}	20.2	16-QAM	36,37,38
7-8	{7,12,8}	10.1	QPSK	9,10,11,12	19-26	{19,2,30,16,11,26}	11.3	QPSK	153,154,155,156
7-9	{7,10,23,9}	10.9	QPSK	5,6,7,8	19-30	{19,2,30}	22.7	64-QAM	24,25
7-10	{7,10}	18.9	16-QAM	9,10,11	20-21	{20,13,25,24,21}	11.8	QPSK	52,53,54,55
7-11	{7,12,26,11}	10.3	QPSK	20,21,22,23	20-22	{20,14,22}	12.8	QPSK	28,29,30,31
7-12	{7,12}	13.3	QPSK	5,6,7,8	20-23	{20,9,23}	11.4	QPSK	56,57,58,59
7-15	{7,10,17,29,28,15}	9.8	QPSK	13,14,15,16	20-24	{20,13,25,24}	12.3	QPSK	14,15,16,17
7-17	{7,10,17}	12.9	QPSK	17,18,19,20	20-25	{20,13,25}	12.5	QPSK	60,61,62,63
7-20	{7,10,23,9,20}	9.7	QPSK	21,22,23,24	21-22	{21,22}	13.6	QPSK	5,6,7,8
7-23	{7,10,23}	16.2	16-QAM	25,26,27	21-24	{21,24}	23.5	64-QAM	8,9
7-26	{7,12,26}	11.6	QPSK	24,25,26,27	21-25	{21,24,25}	22.2	64-QAM	11,12
7-28	{7,10,17,29,28}	10.5	QPSK	28,29,30,31	21-27	{21,27}	11.9	QPSK	1,2,3,4

Appendix C Complementary material used in Chapter 4

[7-29]	{7,10,17,29}	11.2	QPSK	32,33,34,35	[22-24]	{22,21,24}	13.0	QPSK	29,30,31,32
[8-9]	{8,9}	12.9	QPSK	1,2,3,4	[22-25]	{22,21,24,25}	12.7	QPSK	33,34,35,36
[8-11]	{8,12,26,11}	10.1	QPSK	31,32,33,34	[22-26]	{22,8,12,26}	9.6	QPSK	52,53,54,55
[8-12]	{8,12}	12.9	QPSK	1,2,3,4	[22-27]	{22,27}	11.8	QPSK	1,2,3,4
[8-13]	{8,22,21,24,25,13}	9.5	QPSK	1,2,3,4	[23-26]	{23,10,7,12,26}	9.8	QPSK	64,65,66,67
[8-14]	{8,22,14}	11.5	QPSK	5,6,7,8	[23-28]	{23,10,17,29,28}	10.6	QPSK	68,69,70,71
[8-20]	{8,9,20}	11.1	QPSK	5,6,7,8	[23-29]	{23,10,17,29}	11.4	QPSK	72,73,74,75
[8-21]	{8,22,21}	11.0	QPSK	9,10,11,12	[24-25]	{24,25}	27.9	64-QAM	18,19
[8-22]	{8,22}	16.2	16-QAM	13,14,15	[24-27]	{24,21,27}	11.5	QPSK	45,46,47,48
[8-23]	{8,9,23}	10.1	QPSK	9,10,11,12	[25-27]	{25,24,21,27}	11.3	QPSK	60,61,62,63
[8-24]	{8,22,21,24}	10.6	QPSK	16,17,18,19	[26-30]	{26,11,16,30}	11.8	QPSK	107,108,109,110
[8-25]	{8,22,21,24,25}	10.5	QPSK	20,21,22,23	[28-29]	{28,29}	20.1	16-QAM	32,33,34
[8-26]	{8,12,26}	11.3	QPSK	35,36,37,38	[28-30]	{28,15,5,30}	9.8	QPSK	71,72,73,74

Table C.19. RMSA solution for the CONUS 30 optical network with BER=10⁻².

Blocked Demands	[1-6], [1-8], [1-9], [1-12], [1-13], [1-14], [1-20], [1-21], [1-22], [1-24], [1-25], [1-27], [2-7], [2-8], [2-9], [2-10], [2-13], [2-14], [2-17], [2-20], [2-21], [2-22], [2-23], [2-24], [2-25], [2-27], [2-29], [3-7], [3-8], [3-9], [3-10], [3-12], [3-13], [3-14], [3-15], [3-17], [3-20], [3-21], [3-22], [3-23], [3-24], [3-25], [3-27], [3-28], [3-29], [4-9], [4-10], [4-13], [4-14], [4-15], [4-17], [4-20], [4-21], [4-22], [4-23], [4-24], [4-25], [4-27], [4-28], [4-29], [5-6], [5-8], [5-9], [5-12], [5-13], [5-14], [5-17], [5-20], [5-21], [5-22], [5-24], [5-25], [5-27], [6-7], [6-8], [6-9], [6-10], [6-13], [6-14], [6-15], [6-17], [6-20], [6-21], [6-22], [6-23], [6-24], [6-25], [6-27], [6-28], [6-29], [7-13], [7-14], [7-16], [7-18], [7-19], [7-21], [7-22], [7-24], [7-25], [7-27], [7-30], [8-10], [8-15], [8-16], [8-17], [8-18], [8-19], [8-28], [8-29], [8-30], [9-11], [9-15], [9-16], [9-18], [9-19], [9-26], [9-27], [9-28], [9-29], [9-30], [10-13], [10-16], [10-18], [10-19], [10-21], [10-22], [10-24], [10-25], [10-27], [10-30], [11-13], [11-14], [11-15], [11-17], [11-20], [11-21], [11-22], [11-23], [11-24], [11-25], [11-27], [11-28], [11-29], [12-13], [12-14], [12-15], [12-20], [12-21], [12-24], [12-25], [12-27], [12-28], [12-29], [13-15], [13-16], [13-17], [13-18], [13-19], [13-26], [13-28], [13-29], [13-30], [14-15], [14-16], [14-17], [14-18], [14-19], [14-26], [14-28], [14-29], [14-30], [15-20], [15-21], [15-22], [15-24], [15-25], [15-26], [15-27], [16-17], [16-20], [16-21], [16-22], [16-23], [16-24], [16-25], [16-27], [16-28], [16-29], [17-18], [17-19], [17-20], [17-21], [17-22], [17-24], [17-25], [17-26], [17-27], [17-30], [18-20], [18-21], [18-22], [18-23], [18-24], [18-25], [18-27], [18-28], [18-29], [19-20], [19-21], [19-22], [19-23], [19-24], [19-25], [19-27], [19-28], [19-29], [20-26], [20-27], [20-28], [20-29], [20-30], [21-23], [21-26], [21-28], [21-29], [21-30], [22-23], [22-28], [22-29], [22-30], [23-24], [23-25], [23-27], [23-30], [24-26], [24-28], [24-29], [24-30], [25-26], [25-28], [25-29], [25-30], [26-27], [26-28], [26-29], [27-28], [27-29], [27-30], [29-30].
-----------------	--

Table C.20. Blocked demands in the RMSA solution for the CONUS 30 optical network with BER=10⁻².

Appendix C Complementary material used in Chapter 4

Demand d	Path	OSNR [dB]	Modulation Format M	Frequency slots	Demand d	Path	OSNR [dB]	Modulation Format M	Frequency slots
[1-2]	{1,5,30,2}	13.2	QPSK	1,2,3,4	[9-20]	{9,20}	15.8	QPSK	9,10,11,12
[1-5]	{1,5}	19.1	16-QAM	5,6,7	[9-23]	{9,23}	13.4	QPSK	5,6,7,8
[1-16]	{1,5,30,16}	12.3	QPSK	8,9,10,11	[10-17]	{10,17}	14.9	QPSK	8,9,10,11
[1-18]	{1,5,30,2,19,18}	12.3	QPSK	12,13,14,15	[10-23]	{10,23}	19.5	16-QAM	5,6,7
[1-19]	{1,5,30,2,19}	12.7	QPSK	16,17,18,19	[10-29]	{10,17,29}	12.5	QPSK	12,13,14,15
[1-30]	{1,5,30}	13.4	QPSK	20,21,22,23	[11-12]	{11,26,12}	13.4	QPSK	8,9,10,11
[1-24]	{2,19,18,3}	15.1	QPSK	1,2,3,4	[11-16]	{11,16}	15.1	QPSK	1,2,3,4
[2-4]	{2,30,16,11,4}	12.2	QPSK	20,21,22,23	[11-18]	{11,16,30,2,19,18}	12.4	QPSK	52,53,54,55
[2-5]	{2,30,5}	15.2	QPSK	24,25,26,27	[11-19]	{11,16,30,2,19}	12.8	QPSK	56,57,58,59
[2-11]	{2,30,16,11}	13.3	QPSK	28,29,30,31	[11-26]	{11,26}	16.4	QPSK	16,17,18,19
[2-16]	{2,30,16}	19.6	16-QAM	5,6,7	[11-30]	{11,16,30}	13.6	QPSK	12,13,14,15
[2-18]	{2,19,18}	21.1	16-QAM	5,6,7	[12-26]	{12,26}	16.3	QPSK	12,13,14,15
[2-19]	{2,19}	24.1	16-QAM	8,9,10	[13-14]	{13,20,14}	12.9	QPSK	9,10,11,12
[2-30]	{2,30}	27.7	64-QAM	8,9	[13-20]	{13,20}	14.7	QPSK	5,6,7,8
[3-5]	{3,18,19,2,30,5}	13.3	QPSK	32,33,34,35	[13-21]	{13,25,24,21}	14.9	QPSK	1,2,3,4
[3-6]	{3,6}	12.1	QPSK	1,2,3,4	[13-24]	{13,25,24}	16.0	QPSK	5,6,7,8
[3-16]	{3,18,19,2,30,16}	12.4	QPSK	36,37,38,39	[13-25]	{13,25}	16.4	QPSK	9,10,11,12
[3-18]	{3,18}	18.8	16-QAM	5,6,7	[14-20]	{14,20}	19.0	16-QAM	1,2,3
[3-19]	{3,18,19}	15.9	QPSK	8,9,10,11	[14-22]	{14,22}	14.6	QPSK	1,2,3,4
[3-30]	{3,18,19,2,30}	14.7	QPSK	40,41,42,43	[15-17]	{15,28,29,17}	12.8	QPSK	1,2,3,4
[4-6]	{4,6}	15.8	QPSK	1,2,3,4	[15-28]	{15,28}	20.0	16-QAM	5,6,7
[4-11]	{4,11}	20.4	16-QAM	1,2,3	[15-29]	{15,28,29}	15.5	QPSK	8,9,10,11
[4-12]	{4,11,26,12}	12.3	QPSK	4,5,6,7	[16-18]	{16,30,2,19,18}	15.7	QPSK	60,61,62,63
[4-16]	{4,11,16}	13.5	QPSK	8,9,10,11	[16-19]	{16,30,2,19}	16.7	QPSK	64,65,66,67
[4-26]	{4,11,26}	14.4	QPSK	12,13,14,15	[16-26]	{16,11,26}	12.7	QPSK	24,25,26,27
[4-30]	{4,11,16,30}	12.4	QPSK	16,17,18,19	[16-30]	{16,30}	20.4	16-QAM	1,2,3
[5-15]	{5,15}	12.1	QPSK	1,2,3,4	[17-23]	{17,10,23}	13.1	QPSK	16,17,18,19
[5-16]	{5,30,16}	13.9	QPSK	40,41,42,43	[17-28]	{17,29,28}	14.2	QPSK	16,17,18,19
[5-18]	{5,30,2,19,18}	13.8	QPSK	44,45,46,47	[17-29]	{17,29}	16.1	QPSK	5,6,7,8
[5-19]	{5,30,2,19}	14.4	QPSK	48,49,50,51	[18-19]	{18,19}	24.1	16-QAM	16,17,18
[5-30]	{5,30}	15.6	QPSK	28,29,30,31	[18-30]	{18,19,2,30}	20.2	16-QAM	68,69,70
[6-11]	{6,4,11}	14.0	QPSK	24,25,26,27	[19-30]	{19,2,30}	22.4	16-QAM	71,72,73
[6-26]	{6,4,11,26}	12.0	QPSK	28,29,30,31	[20-22]	{20,14,22}	12.8	QPSK	13,14,15,16
[7-10]	{7,10}	18.9	16-QAM	1,2,3	[20-24]	{20,13,25,24}	12.3	QPSK	13,14,15,16
[7-12]	{7,12}	13.3	QPSK	1,2,3,4	[20-25]	{20,13,25}	12.5	QPSK	17,18,19,20
[7-17]	{7,10,17}	12.9	QPSK	4,5,6,7	[21-22]	{21,22}	13.6	QPSK	1,2,3,4
[7-23]	{7,10,23}	14.5	QPSK	8,9,10,11	[21-24]	{21,24}	23.1	16-QAM	5,6,7
[8-9]	{8,9}	12.9	QPSK	1,2,3,4	[21-25]	{21,24,25}	21.8	16-QAM	9,10,11
[8-12]	{8,12}	12.9	QPSK	1,2,3,4	[22-24]	{22,21,24}	13.0	QPSK	12,13,14,15
[8-22]	{8,22}	14.5	QPSK	1,2,3,4	[22-25]	{22,21,24,25}	12.7	QPSK	17,18,19,20
[9-10]	{9,23,10}	12.1	QPSK	1,2,3,4	[24-25]	{24,25}	27.9	64-QAM	21,22
[9-13]	{9,20,13}	12.2	QPSK	1,2,3,4	[28-29]	{28,29}	20.1	16-QAM	5,6,7
[9-14]	{9,20,14}	13.5	QPSK	5,6,7,8					

Table C.21. RMSA solution for the CONUS 30 optical network with BER= 10^{-3} .

Appendix C *Complementary material used in Chapter 4*

Blocked Demands	<p>[1-3], [1-4], [1-6], [1-7], [1-8], [1-9], [1-10], [1-11], [1-12], [1-13], [1-14], [1-15], [1-17], [1-20], [1-21], [1-22], [1-23], [1-24], [1-25], [1-26], [1-27], [1-28], [1-29], [2-6], [2-7], [2-8], [2-9], [2-10], [2-12], [2-13], [2-14], [2-15], [2-17], [2-20], [2-21], [2-22], [2-23], [2-24], [2-25], [2-26], [2-27], [2-28], [2-29], [3-4], [3-7], [3-8], [3-9], [3-10], [3-11], [3-12], [3-13], [3-14], [3-15], [3-17], [3-20], [3-21], [3-22], [3-23], [3-24], [3-25], [3-26], [3-27], [3-28], [3-29], [4-5], [4-7], [4-8], [4-9], [4-10], [4-13], [4-14], [4-15], [4-17], [4-18], [4-19], [4-20], [4-21], [4-22], [4-23], [4-24], [4-25], [4-27], [4-28], [4-29], [5-6], [5-7], [5-8], [5-9], [5-10], [5-11], [5-12], [5-13], [5-14], [5-17], [5-20], [5-21], [5-22], [5-23], [5-24], [5-25], [5-26], [5-27], [5-28], [5-29], [6-7], [6-8], [6-9], [6-10], [6-12], [6-13], [6-14], [6-15], [6-16], [6-17], [6-18], [6-19], [6-20], [6-21], [6-22], [6-23], [6-24], [6-25], [6-27], [6-28], [6-29], [6-30], [7-8], [7-9], [7-11], [7-13], [7-14], [7-15], [7-16], [7-18], [7-19], [7-20], [7-21], [7-22], [7-24], [7-25], [7-26], [7-27], [7-28], [7-29], [7-30], [8-10], [8-11], [8-13], [8-14], [8-15], [8-16], [8-17], [8-18], [8-19], [8-20], [8-21], [8-23], [8-24], [8-25], [8-26], [8-27], [8-28], [8-29], [8-30], [9-11], [9-12], [9-15], [9-16], [9-17], [9-18], [9-19], [9-21], [9-22], [9-24], [9-25], [9-26], [9-27], [9-28], [9-29], [9-30], [10-11], [10-12], [10-13], [10-14], [10-15], [10-16], [10-18], [10-19], [10-20], [10-21], [10-22], [10-24], [10-25], [10-26], [10-27], [10-28], [10-30], [11-13], [11-14], [11-15], [11-17], [11-20], [11-21], [11-22], [11-23], [11-24], [11-25], [11-27], [11-28], [11-29], [12-13], [12-14], [12-15], [12-16], [12-17], [12-18], [12-19], [12-20], [12-21], [12-22], [12-23], [12-24], [12-25], [12-27], [12-28], [12-29], [12-30], [13-15], [13-16], [13-17], [13-18], [13-19], [13-22], [13-23], [13-26], [13-27], [13-28], [13-29], [13-30], [14-15], [14-16], [14-17], [14-18], [14-19], [14-21], [14-23], [14-24], [14-25], [14-26], [14-27], [14-28], [14-29], [14-30], [15-16], [15-18], [15-19], [15-20], [15-21], [15-22], [15-23], [15-24], [15-25], [15-26], [15-27], [15-30], [16-17], [16-20], [16-21], [16-22], [16-23], [16-24], [16-25], [16-27], [16-28], [16-29], [17-18], [17-19], [17-20], [17-21], [17-22], [17-24], [17-25], [17-26], [17-27], [17-30], [18-20], [18-21], [18-22], [18-23], [18-24], [18-25], [18-26], [18-27], [18-28], [18-29], [19-20], [19-21], [19-22], [19-23], [19-24], [19-25], [19-26], [19-27], [19-28], [19-29], [20-21], [20-23], [20-26], [20-27], [20-28], [20-29], [20-30], [21-23], [21-26], [21-27], [21-28], [21-29], [21-30], [22-23], [22-26], [22-27], [22-28], [22-29], [22-30], [23-24], [23-25], [23-26], [23-27], [23-28], [23-29], [23-30], [24-26], [24-27], [24-28], [24-29], [24-30], [25-26], [25-27], [25-28], [25-29], [25-30], [26-27], [26-28], [26-29], [26-30], [27-28], [27-29], [27-30], [28-30], [29-30]</p>
-----------------	--

Table C.22. Blocked demands in the RMSA solution for the CONUS 30 optical network with BER= 10^{-3} .

Scientific contributions

Impact of Network Physical Topology on Planning Multiband Optical Networks Aware of Physical Layer Impairments

Margarida Vaz[†], Luís Cancela^{*†}, João Rebola^{*†}

^{*}*Optical Communications and Photonics Group, Instituto de Telecomunicações, Lisboa, Portugal*

[†]*Department of Science and Information Technology, Iscte-Instituto Universitário de Lisboa, Lisboa, Portugal*

E-mail: micvz@iscte-iul.pt, luis.cancela@iscte-iul.pt, joao.rebola@iscte-iul.pt.

Abstract—Nowadays, with the increase in traffic demands due to, the growth of cloud-based and 5G applications, emerging solutions are arising to improve optical networks spectrum efficiency and transmission capacity. The promising multiband solution improves the fiber capacity by expanding the optical spectrum beyond the C-band. So, efficient multiband planning tools are paramount to explore network resources efficiently. The planning tool developed in this work solves the routing, modulation format and spectrum assignment (RMSA) in a static network scenario. Using this tool, we discuss the influence of the network physical topology on several parameters, such as, on the number of paths utilized in the most used link or on the number of frequency slots assigned, considering four optical networks, different target bit error rates (BERs) and transmission capacities. We conclude that, using lower BERs and higher information bit rates, lead to greater percentage of blocked demands, due to decrease of the maximum reach, which, limits the maximum hops between nodes, specially, in networks with longer links. It is also concluded that for higher request scenarios, networks with more demands require more spectrum capacity, and the flexible grid utilizes the network resources more efficiently than the fixed grid.

Index Terms—Flexible grid, multiband transmission, optical networks, physical layer impairments, RMSA.

I. INTRODUCTION

The need for more capacity in the optical transport network, due to, for example, the growth of cloud-based and 5G applications demands, nowadays, new solutions [1]. The implementation of spatial division multiplexing (SDM) techniques in optical domain [2] is seen as a long term solution, whereas the exploitation of the unused bands on the widely deployed G.652.D fibers, called multiband solution, is seen as a near term solution [2].

Several authors have already studied the signal transmission on these multiband systems, and it is well known that some physical layer impairments (PLIs) are more pronounced than in C-band only systems. For example, the effect of the stimulated Raman scattering (SRS), that causes a power transfer from higher to lower frequency signals, can be neglected on C-band only systems, but must be considered in multiband systems [1].

The capacity increase given by the multiband solution in comparison with C-band only systems needs to be used in the most efficient way, so that a cost effective solution could be attained. In this way, well designed multiband planning

tools are of paramount importance in optimizing the transport capacity. This optimization is typically performed in a two-step procedure, first the routes for the demands having in mind the PLIs are found and the signal modulation format is chosen, and then the spectrum assignment is performed, i.e., a given number of frequency slots (FSs) is assigned to a particular demand. This two-step procedure is called a routing, modulation format and spectrum assignment (RMSA) problem. Some authors, [2], [3] have already developed, both heuristic and integer linear programming (ILP) tools for solving this RMSA problem.

In this work, a C+L multiband heuristic planning tool is designed for solving RMSA problems. This tool is used in four network topologies (COST 239, NSFNET, UBN and CONUS 30) considering three different request scenarios. The first scenario uses the common 100 Gbps bit rate and a detailed analysis is performed, in particular the percentage of blocked demands, the number of FSs used, as well as parameters like the path with the highest and lowest optical signal-to-noise ratio (OSNR), and the usage of the different types of modulation formats are discussed. Moreover, we discuss the influence of the network physical topology on the various parameters analyzed, like the number of paths that utilize the most used link, an analysis that has not been done in [2] and [3], that consider only a single network topology, the German network in [2] and the British network in [3].

This work is organized in four sections. Section II presents the multiband planning tool used to solve the RMSA problem aware of PLIs. Section III shows the results of the RMSA problem for several network topologies, and discusses them, considering requests for different bit rates (100, 200 and 400 Gbps), in terms, for example, of the number of FSs used and blocked demands percentage. A comparison between the flexible and fixed grid scenarios is also presented. Finally, in section IV, the conclusions of this work are drawn.

II. MULTIBAND NETWORK PLANNING TOOL

In this section, we present and explain our C+L multiband network planning tool aware of the PLIs. We start by highlighting the lightpath OSNR evaluation procedure and then explain the flowchart of the developed multiband network simulator used to solve the RMSA problem.

A. Lighpath OSNR evaluation

The total OSNR in the lightpath p in a C+L multiband scenario can be given by [4],

$$\frac{1}{\text{OSNR}_{\text{tot},p}} = \sum_{i=1}^{m_{\text{links}}} \left(\frac{1}{\text{OSNR}_{\text{NLI},i}} + \frac{1}{\text{OSNR}_{\text{pos},i}} + \frac{1}{\text{OSNR}_{\text{pre},i}} + \sum_{j=1}^{N_{\text{in},i}} \frac{1}{\text{OSNR}_{\text{in},i,j}} \right) \quad (1)$$

where m_{links} is the number of links in path p , $N_{\text{in},i}$ is the number of in-line amplifiers in link i , osnr_k with $k=\text{pre},i$ or pos,i or in,i,j is the OSNR at the output of, respectively, the pre-amplifier, pos-amplifier and in-line amplifiers in link i , and $\text{osnr}_{\text{NLI},i}$ is the OSNR due to the nonlinear interference noise (NLI) in link i . The osnr_k can be given by,

$$\text{osnr}_k = \frac{p_m}{2p_{\text{ASE},k}} \quad k = \text{pre},i, \text{ or } \text{pos},i, \text{ or } \text{in},i,j. \quad (2)$$

where $p_{\text{ase},k}$ is the amplified spontaneous emission (ASE) noise introduced by each type of amplifier (pre, in-line or post amplifier) and p_m is optical power of channel m . The Erbium-Doped Fiber Amplifiers (EDFAs) used, have a maximum gain (G_{max}) of 25 dB and the noise figure (F_n) depends on the span loss and is estimated with a linear interpolation considering $F_n=5$ dB with the EDFA maximum gain and 7 dB for the 15 dB gain [4]. Likewise, the $\text{osnr}_{\text{NLI},i}$ is given by,

$$\text{osnr}_{\text{NLI},i} = \frac{p_m}{p_{\text{NLI},i}} \quad (3)$$

where the $p_{\text{NLI},i}$ is the NLI noise power introduced in link i . This NLI noise that includes the SRS effect is calculated with a closed-form formula based on the Gaussian noise (GN) model, that considers the impact of the modulation format, so that p_{NLI} can be given by [5],

$$p_{\text{NLI}} = (\eta_{\text{GN}} + \eta_{\text{corr}}) \cdot p_m^3 \quad (4)$$

where η_{GN} is the GN model contribution and η_{corr} is the modulation format correction.

B. Simulator flowchart

The C+L multiband network simulator was developed in Matlab and has two main steps in order to solve the RMSA problem, first routing and modulation format assignment and, then, spectrum assignment. The simulator inputs are the network physical topology, the traffic matrix, the number of candidate paths, the available bands, the total number of FSs per band, the bit error rate (BER) and the information bit rate.

The first step consists in computing the list of the k -th candidate paths for each demand (or request), as described in the flowchart shown in Fig. 1 a). These paths are computed with the Yen's k -shortest path algorithm [6]. After, the OSNR of each candidate path is calculated considering the ASE noise along the path and the NLI noise. The following simplifications are assumed in the OSNR calculation:

- 1) the NLI noise at the end of a link is calculated considering that all FSs are being used in the C+L band;
- 2) the NLI noise accumulates incoherently [5], which means that the NLI noise is calculated at the end of each link independently of the NLI noises calculated for the other links of a given path;
- 3) the channel launch power is optimized for the longest candidate path in the network [3] for each modulation format and is used in all channels across the network that use that specific modulation format;
- 4) the NLI noise and corresponding OSNR are calculated for the center channel, since there is no knowledge of how the spectrum will be assigned.

Then, it is checked, starting from the highest to the lowest modulation format (64-Quadrature-amplitude modulation (QAM), 16-QAM and Quaternary phase-shift keying (QPSK)), if the required OSNR (ROSNR) is achieved. If none of the modulation formats meets the ROSNR, the corresponding candidate path is not used. Moreover, if no candidate paths for the demand satisfy the ROSNR, that demand is blocked. After calculating the OSNR for all demands and candidate paths and assigning the modulation format, the paths are sorted based on the OSNR in descending order, for each demand.

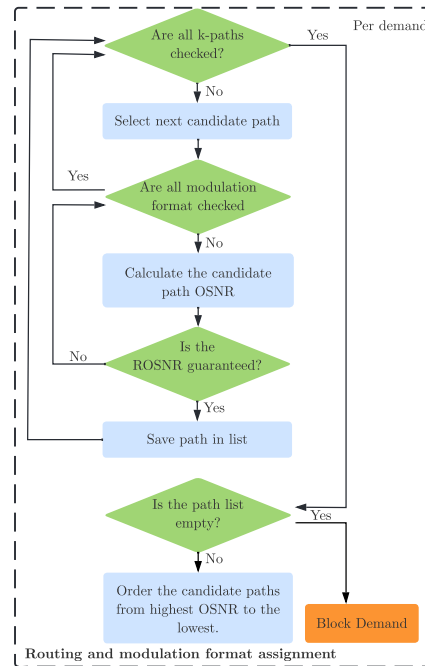


Fig. 1 a). Flowchart of the Matlab simulator for the routing and modulation format assignment.

In the second step, the path list just built is used by the spectrum assignment algorithm to assign the FSs using the First-Fit (FF) algorithm, as shown in Fig. 1 b). It starts with the candidate path with the highest OSNR, and tries different candidate paths in descending order of OSNRs. Since we are considering a flexible grid scenario, the FSs assigned to each demand must be contiguous, and must be the same in every link of a specific optical path [2]. The number of FSs allocated for each demand depends on the symbol rate, which depends on the modulation format used in the candidate path [2]. Therefore, depending on the modulation format, the FF algorithm tries to assign the corresponding FSs. If those FSs cannot be assigned in the whole C+L band, then another candidate path from the list is chosen. If the FSs are not assigned to any of the candidate paths corresponding to a specific demand, then that demand is blocked, as represented in Fig. 1 b).

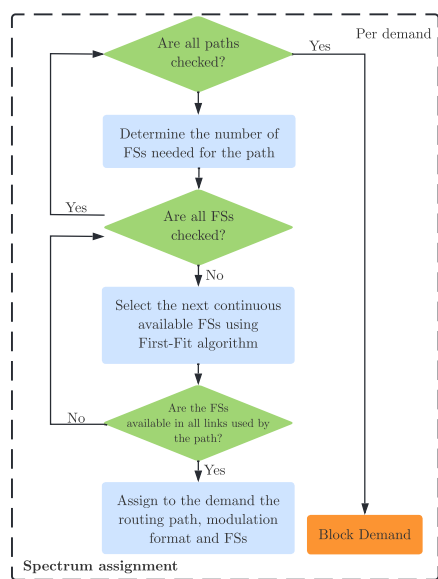


Fig. 1 b). Flowchart of the Matlab simulator for the spectrum assignment.

III. RESULTS AND DISCUSSION

In this section, we are going to use the multiband planning tool presented in section II in several network topologies scenarios - COST 239, NSFNET, UBN and CONUS 30 [7] - considering a static traffic matrix and a full mesh logical topology. In particular, we solve the RMSA problem for each one of the network topologies studied considering three BER values (4×10^{-2} , 1×10^{-2} and 1×10^{-3}) for 100, 200, and 400 Gbps requests. A detailed analysis for the 100 Gbps requests case is given in subsection A, whereas in subsection B the

200 and 400 Gbps scenarios are considered. In subsection C, a comparison between the fixed and flexible grids scenario is performed. Table I presents some physical (number of nodes, number of links, average node degree, average link length) and logical (number of demand requests for full mesh topology) parameters of the network topologies considered.

TABLE I
PHYSICAL AND LOGICAL FEATURES OF THE NETWORK TOPOLOGIES.

Network	#Demands	#Nodes	#Links	Average node degree	Average link length [km]
COST 239	55	11	26	4.73	463
NSFNET	91	14	21	3	1081
UBN	276	24	43	3.58	996
CONUS 30	435	30	36	2.40	696

As can be observed in Table I, the network with more nodes is the CONUS 30, and therefore, this is the network that has more traffic demands, while the network with the longest links in average is the NSFNET network. The network that presents nodes with an higher degree is the COST 239, which is the smallest size network. Table II presents the ROSNR for the three BER values and for the three modulation formats considered in this study - QPSK, 16-QAM and 64-QAM, as in [2]. Table III shows the system and network parameters considered in this section.

TABLE II
ROSNR FOR THE DIFFERENT BERS.

BER	ROSNR [dB]		
	64-QAM	16-QAM	QPSK
4×10^{-2}	18.9	13.3	7.1
1×10^{-2}	21.9	16.1	9.5
1×10^{-3}	24.8	18.6	12

TABLE III
SYSTEM PARAMETERS USED TO SOLVE THE RMSA PROBLEM.

Parameters	Values
Number of candidate paths k	5
Total number of FSs in the C+L band	862
Frequency slot width	12.5 GHz
Amplifier maximum gain G_{max}	25 dB
Fiber attenuation coefficient α	0.25 dB/km
Fiber effective area A_{eff}	$80 \mu\text{m}^2$
Dispersion D_{λ_0}	17 ps/nm/km
Dispersion slope S_0	67 fs/nm ² /km
Reference wavelength λ_0	1550 nm
Raman gain slope C_r	0.028 1/W/km/THz
Nonlinear refractive index \bar{n}_2	$2.6 \times 10^{-20} \text{ m}^2/\text{W}$
Coherent factor ε	0

A. 100 Gbps requests scenario

In this subsection, the 100 Gbps requests scenario is analyzed. Table IV shows the transmitted signal features that depend on the chosen modulation format and the required FSs to transmit 100 Gbps requests including one FS used as a guard-band between channels.

The solution for the RMSA problem considering 100 Gbps requests is given in Table V for the four network topologies

TABLE IV
SYSTEM PARAMETERS USED TO CALCULATE THE OSNR FOR 100 GBPS.

Parameters	64-QAM	16-QAM	QPSK
Channel Spacing	25 GHz	37.5 GHz	50 GHz
Symbol rate	10.67 Gbaud	16 Gbaud	32 Gbaud
#FSs allocated	2	3	4

and three BER values. In particular, Table V shows the number of blocked demands, the number of allocated FSs, the highest and lowest OSNR values, the path with the longest distance served, the number of unused links and the usage of the different modulation formats in the whole network.

As observed in Table V, the COST 239 network is the only network that successfully serves all demands, i.e. the blocked demands percentage is zero. In this network, as the BER decreases, slightly more FSs are allocated, since lower BERs demand higher ROSNRs (see Table II), resulting on the assignment of lower modulation formats that require more FSs. For the other three networks, the number of FSs allocated decreases for lower BERs, since the number of blocked demands increases, being the QPSK format predominant in the successful demands. In the CONUS 30 and UBN networks, more than half of the demands are blocked for $\text{BER}=10^{-2}$ or lower. The UBN network has the higher number of blocked demands, with a maximum of demands blocked of 84% for the lowest BER. Also observed in Table V, none of the networks use more than 40% of the multiband spectrum, despite the existence of blocked demands for NSFNET, UBN and CONUS 30 topologies. The reason for blocking the demands is the insufficient OSNR, and not the unavailability of FSs. The maximum spectrum allocated is in the CONUS 30 network with 40.6%, which corresponds to 350 FSs of the 862 available in the C+L multiband. This network is the only one that assigns FSs in the L-band using only 5 FSs in this band.

We have checked that the highest OSNR estimated presented in Table V is always obtained for the same demand in the networks considered, independently of the BER, whereas the lowest OSNR can be reached with different demands. Moreover, the highest OSNR is obtained in all four networks in the direct path that uses the shortest link in the network. On the other hand, the lowest OSNR is obtained in one of the longest paths in the network, that has not been blocked due to not fulfilling the ROSNR. In the three larger networks, the path reach is similar for all BERs, the maximum distance with $\text{BER}=4 \times 10^{-2}$ is around 4000 km, for $\text{BER}=10^{-2}$ is about 2500 km, and around 1500 km for $\text{BER}=10^{-3}$. This maximum reach limits the number of hops in networks with longer links, like in the UBN network where the average link length is 996 km (see Table I). This means that, in this network, for $\text{BER}=4 \times 10^{-2}$, where the maximum range is 4000 km in average, the source and destination nodes can have at most four links between them for a demand to be served, without resorting to the more expensive regeneration solution [4].

From Table V, it can also be observed that, in general, the number of paths utilized in the most used link is higher for

higher BERs, since other paths with lower OSNRs tend to be blocked (i.e. the ROSNR is not achieved) when the BER is lower. The link with the most paths assigned, in general, is also the one with the most FSs allocated. Generally, the number of unused links increases for lower BERs, since the unused links are some of the longest in the network, experience higher OSNR degradation and do not meet the ROSNR. In networks with higher average node degree, like the COST 239 and UBN network, (see Table I) some links are never used, since these links lead to an enhanced performance degradation due to PLIs in the network, but as these nodes are more interconnected the demands can be routed using a different link.

Finally, in Table V, it can be observed that the QPSK format is the most used format, except for the COST 239 network for $\text{BER}=4 \times 10^{-2}$ and 10^{-2} , where the 16-QAM format is the most used modulation format. The only scenario where the QPSK format is not used in the COST 239 network occurs when $\text{BER}=4 \times 10^{-2}$, which is also the scenario where the 64-QAM modulation format is assigned more times, corresponding to 36.4% of the assigned optical paths. The CONUS 30 network is the only network where the 64-QAM format is assigned when the $\text{BER}=10^{-3}$. In this case, the two paths with 64-QAM are direct links that do not require in-line amplification.

B. Higher than 100 Gbps requests scenario

In this subsection, the RMSA planning tool is used for studying higher than 100 Gbps requests, in particular, 200 and 400 Gbps requests are considered. In Table VI, the channel spacing, symbol rate and number of FSs allocated are shown, for the three modulation formats.

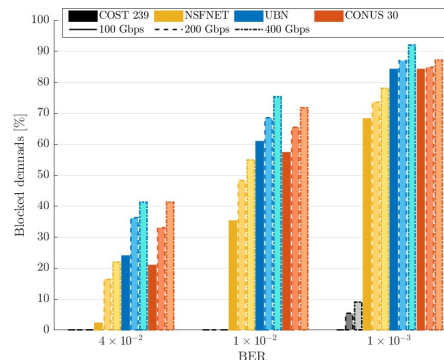


Fig. 2. Blocked demands percentage for three BERs, 4×10^{-2} , 10^{-2} , and 10^{-3} considering three bit rate request scenarios (100, 200 and 400 Gbps) and four network topologies.

In Fig. 2, the blocked demands percentage for three BER values, considering three bit rate request scenarios (100, 200 and 400 Gbps) and four network topologies (COST 239, NSFNET, UBN and CONUS 30) is represented. As it can be observed in Fig. 2, the percentage of blocked demands

TABLE V
RMSA SOLUTION FOR THE COST 239, NSFNET, UBN, AND CONUS 30 TOPOLOGIES CONSIDERING THREE DIFFERENT BERS FOR 100 GBPS REQUEST.

Network	BER	#Blocked demands	#FSs allocated	Highest OSNR	Lowest OSNR	Longest path served	Higher #paths assigned to link	Higher #FSs allocated to link	#Unused links	#Paths using 64-QAM format	#Paths using 16-QAM format	#Paths using QPSK format
COST 239	4×10^{-2}	0 (0%)	62 (7.2%)	24.0 dB (64-QAM)	14.1 dB (16-QAM)	1452 km	18 paths (32.7%)	50 FSs (5.8%)	4	20 paths (36.4%)	35 paths (63.6%)	0 paths (0%)
	1×10^{-2}	0 (0%)	62 (7.2%)	24.0 dB (64-QAM)	12.4 dB (QPSK)	1452 km	18 paths (32.7%)	62 FSs (7.2%)	4	10 paths (10.9%)	32 paths (58.2%)	17 paths (30.9%)
	1×10^{-3}	0 (0%)	70 (8.1%)	23.6 dB (64-QAM)	14.1 dB (QPSK)	1452 km	18 paths (32.7%)	68 FSs (7.9%)	4	0 paths (0%)	20 paths (36.4%)	35 paths (63.6%)
NSFNET	4×10^{-2}	2 (2.2%)	114 (13.2%)	22.8 dB (64-QAM)	7.2 dB (QPSK)	4467 km	30 paths (33.0%)	113 FSs (13.1%)	-	4 paths (4.5%)	28 paths (31.5%)	57 paths (64%)
	1×10^{-2}	32 (35.2%)	71 (8.2%)	22.8 dB (64-QAM)	9.6 dB (QPSK)	2885 km	18 paths (19.8%)	71 FSs (8.2%)	1	1 path (1.7%)	12 paths (20.3%)	46 paths (78%)
	1×10^{-3}	62 (68.1%)	28 (3.2%)	22.6 dB (16-QAM)	12.3 dB (QPSK)	1545 km	6 paths (6.6%)	15 FSs (1.7%)	6	0 paths (0%)	4 paths (13.8%)	25 paths (86.2%)
UBN	4×10^{-2}	66 (23.9%)	133 (15.4%)	22.6 dB (64-QAM)	7.1 dB (QPSK)	4150 km	33 paths (12.0%)	131 FSs (15.2%)	3	2 paths (1%)	46 paths (21.9%)	162 paths (77.1%)
	1×10^{-2}	168 (60.9%)	44 (5.1%)	22.8 dB (64-QAM)	9.5 dB (QPSK)	2300 km	10 paths (3.6%)	39 FSs (4.5%)	3	1 path (0.9%)	9 paths (8.3%)	98 paths (90.9%)
	1×10^{-3}	232 (84.1%)	16 (1.9%)	22.5 dB (16-QAM)	12.0 dB (QPSK)	1300 km	4 paths (1.4%)	15 FSs (1.7%)	5	0 paths (0%)	2 paths (4.5%)	42 paths (95.5%)
CONUS 30	4×10^{-2}	91 (20.9%)	350 (40.6%)	27.9 dB (64-QAM)	7.6 dB (QPSK)	4850 km	75 paths (17.2%)	289 FSs (33.5%)	-	19 paths (5.5%)	73 paths (21.2%)	252 paths (73.3%)
	1×10^{-2}	249 (57.2%)	156 (18.1%)	27.9 dB (64-QAM)	9.5 dB (QPSK)	2835 km	35 paths (8.0%)	132 FSs (15.3%)	-	7 paths (3.8%)	35 paths (18.8%)	144 paths (77.4%)
	1×10^{-3}	350 (80.5%)	73 (8.5%)	27.9 dB (64-QAM)	12.0 dB (QPSK)	1602 km	19 paths (4.4%)	71 FSs (8.23%)	3	2 paths (2.4%)	17 paths (20%)	66 paths (77.6%)

TABLE VI
SYSTEM PARAMETERS USED TO CALCULATE THE OSNR FOR 200 AND 400 GBPS REQUESTS.

Information bit rate	Channel Spacing [GHz]		
	64-QAM	16-QAM	QPSK
200 Gbps	37.5	50	87.5
400 Gbps	62.4	87.5	150
Symbol Rate [Gbaud]			
200 Gbps	21.3	32	64
400 Gbps	42.7	64	128
#FSs allocated			
200 Gbps	3	4	7
400 Gbps	5	7	12

increases with the increase of the information bit rate and as the BER lowers. The highest percentage increase (14.3%) of blocked demands is observed in the NSFNET network, when $BER=4 \times 10^{-2}$, and we replace the 100 Gbps requests by 200 Gbps requests. This can be explained, since the maximum reach is around 3000 km for the 200 Gbps requests (1000 km less than with 100 Gbps requests), limiting the distance between nodes so paths with longer distances are blocked. From the four topologies analyzed, the UBN network has the highest percentage of blocked demands - 92% for $BER=10^{-3}$ and 400 Gbps requests- since the maximum reach served in this network is 959 km, which is shorter than the average link (996 km, see Table I). This is also the scenario where the COST 239 network exhibits a non zero blocked demand percentage - 9.1% of blocked demands -, due to shorter path reach.

In Fig. 3, the allocated FSs percentage for three BER values, considering three bit rate request scenarios (100, 200 and 400 Gbps) and four network topologies (COST 239, NSFNET, UBN and CONUS 30) is represented. From Fig. 3, it can be observed that the higher the information bit rate, more percentage of FSs is allocated, as the BER increases, even though

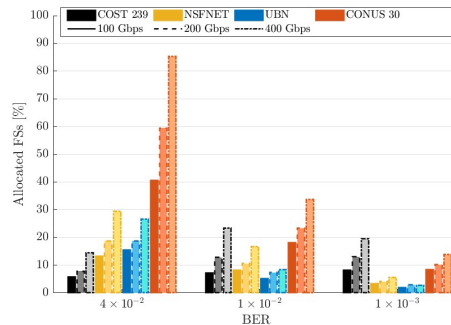


Fig. 3. Allocated FSs percentage for three BERs, 4×10^{-2} , 10^{-2} , and 10^{-3} considering three bit rate request scenarios (100, 200 and 400 Gbps) and four network topologies.

more demands are blocked than in the 100 Gbps requests (see Fig. 2), since these information bit rates, need higher symbol rates, resulting in more allocated FSs. Only for the COST 239 network, the percentage of FSs allocated increases from $BER=4 \times 10^{-2}$ to $BER=10^{-3}$ and then decreases from $BER=10^{-2}$ to $BER=10^{-3}$, since, for this last scenario, the percentage of demands served is no longer 100%, as observed in Fig. 2. Likewise in 100 Gbps scenario request, the CONUS 30 topology continues to be the only topology that assigns spectrum in the L-band. For $BER=4 \times 10^{-2}$ and 400 Gbps requests, 85% of the available multiband spectrum is assigned, which corresponds to 735 FSs of the 862 available.

C. Comparison between the fixed and flexible grid scenarios

In this subsection, the spectrum allocation in the flexible and fixed grids scenarios, for $BER=4 \times 10^{-2}$, is compared considering the three information bit rates used previously

(100, 200 and 400 Gbps). Table VII shows some transmitted signal features that depend on the modulation format.

TABLE VII
SYSTEM PARAMETERS USED TO CALCULATE THE OSNR WITH FIXED GRID FOR 100, 200 AND 400 GBPS REQUESTS.

Information bit rate	Channel Spacing [GHz]		
	64-QAM	16-QAM	QPSK
100 Gbps	50	50	50
200 Gbps	50	50	100
400 Gbps	100	100	200
#FSs allocated			
100 Gbps	4	4	4
200 Gbps	4	4	8
400 Gbps	8	8	16

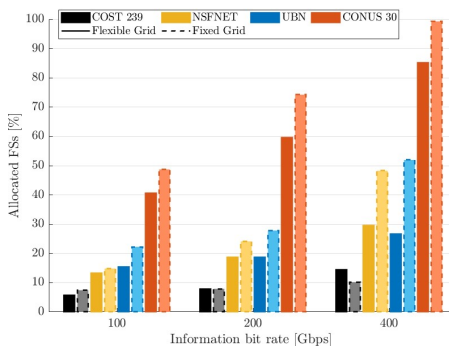


Fig. 4. Allocated FSs percentage in the fixed and flexible grids when $BER=4 \times 10^{-2}$ for three information bit rates, 100 Gbps, 200 Gbps, and 400 Gbps.

In Fig. 4, the percentage of FSs allocated as a function of the information bit rate, for the four network topologies considering the fixed and flexible grid scenarios is shown. As observed in Fig. 4, in general, the percentage of allocated FSs grows with the increase of the information bit rate. Also, from Fig. 4 it can be observed that in the fixed grid scenario the percentage of allocated FSs is higher than in the flexible grid scenario. This can be explained since with the fixed grid the estimated OSNR is higher, due to a larger channel spacing and, consequently, less interfering from other channels. This results in less blocked demands due to the paths not satisfying the ROSNR and also because more FSs are required to transmit requests with this grid. However, in the COST 239 network case less FSs are allocated with the fixed grid than with the flexible grid for the 400 Gbps request scenario, since higher modulation formats, that require less FSs, are assigned in fixed grid, due to higher estimated OSNR.

We have also checked that in the fixed grid scenario NSFNET, UBN and CONUS 30 topologies fill all the C-band spectrum and also assign spectrum in the L-band for the 400 Gbps requests case. In particular, for 400 Gbps requests, in the CONUS 30 topology only 6 FSs are not allocated,

which corresponds to a FSs allocated percentage of 99.3%, nevertheless there are 32 blocked demands due to spectrum unavailability.

IV. CONCLUSIONS

In this work, we studied the influence of the network physical topology on the planning of multiband C+L optical networks. For that, we have developed a RMSA tool to explore several network parameters: number of blocked demands, FSs allocated and unused links, dominant modulation format and longest paths served, as a function of the network considered. The RMSA tool has been applied to four optical networks, considering different target BERs and bit rates.

For 100 Gbps transmission, with full mesh logical topologies networks with more nodes and longer links, as the BER decreases, the number of blocked demands grows, and, consequently, less FSs are allocated and lower order modulation formats are predominant. The COST 239 network, which has shorter links in average and less nodes, serves all demands for the BERs considered, and the QPSK format reaches a spectral occupation of 63.6% of the available FSs, for the $BER=4 \times 10^{-2}$.

For higher bit rates, that require more FSs to transmit the signal, we have also shown that the number of blocked demands increases, reaching a maximum of 14.3%, for networks with longer links due to lower maximum reach for higher request scenarios.

The flexible grid, for networks with more demands, allocate the network resources more efficiently than the fixed grid. With this grid, for 400 Gbps request, 7.4% of the demands in the CONUS 30 network are blocked, due to spectrum unavailability.

ACKNOWLEDGMENT

This work was supported under the project of Instituto de Telecomunicações UIDB/50008/2020.

REFERENCES

- [1] R. Sadeghi, B. Correia, A. Souza, N. Costa, J. Pedro, A. Napoli, and V. Curri, "Transparent vs translucent multi-band optical networking: Capacity and energy analyses," *Journal of Lightwave Technology*, vol. 40, no. 11, pp. 3486–3498, 2022.
- [2] M. Mehrabi, H. Beyranvand, and M. Emadi, "Multi-band elastic optical networks: Inter-channel stimulated Raman scattering-aware routing, modulation level and spectrum assignment," *Journal of Lightwave Technology*, vol. 39, pp. 3360–3370, 2021.
- [3] D. Uzunidis, E. Kosmatos, C. Matrakidis, A. Stavdas, and A. Lord, "Strategies for upgrading an operator's backbone network beyond the c-band: Towards multi-band optical networks," *IEEE Photonics Journal*, vol. 13, no. 2, pp. 1–18, 2021.
- [4] J. Pedro, "Designing transparent flexible-grid optical networks for maximum spectral efficiency," *Journal of Optical Communications and Networking*, vol. 9, pp. C35–C44, 2017.
- [5] D. Semrau, E. Sillekens, R. I. Killey, and P. Bayvel, "A modulation format correction formula for the gaussian noise model in the presence of inter-channel stimulated raman scattering," *Journal of Lightwave Technology*, vol. 37, no. 19, pp. 5122–5131, 2019.
- [6] E. Amir, "K-shortest paths in a graph represented by a sparse matrix (Yen's algorithm)," <https://www.mathworks.com/matlabcentral/fileexchange/35397-k-shortest-paths-in-a-graph-represented-by-a-sparse-matrix-yen-s-algorithm>, 2012.
- [7] J. Simmons, *Optical Network Design and Planning*. Optical Networks, Springer International Publishing, 2nd ed., 2014.